UNCLASSIFIED

SECURITY CLASSIFICATION OF THIS PAGE

REPORT DOCUMENTATION PAGE

1a REPORT SECURITY CLASSIFICATION UNCLASSIFIED	1b RESTRICTIVE MARKINGS
2a SECURITY CLASSIFICATION AUTHORITY	3 DISTRIBUTION / AVAILABILITY OF REPORT Approved for public release; distribution is unlimited
2b DECLASSIFICATION / DOWNGRADING SCHEDULE	
4 PERFORMING ORGANIZATION REPORT NUMBER(S) NRSCTR-6.	5. MONITORING ORGANIZATION REPORT NUMBER(S) CR 88-10
6a. NAME OF PERFORMING ORGANIZATION Nansen Remote Sensing Center, Norway.	6b OFFICE SYMBOL (*If applicable*)
7a. NAME OF MONITORING ORGANIZATION Naval Environmental Prediction Research Facility	
6c. ADDRESS (*City, State, and ZIP Code*) Edvard Griegsvei 3 a, N-5037 Solheimsvik, Norway	7b. ADDRESS (*City, State, and ZIP Code*) Monterey, CA 93943-5006
8a. NAME OF FUNDING / SPONSORING ORGANIZATION Naval Air Systems Command	8b. OFFICE SYMBOL (*If applicable*) (AIR-3301)
9. PROCUREMENT INSTRUMENT IDENTIFICATION NUMBER N00014-80-G-0003	
8c. ADDRESS (*City, State, and ZIP Code*) Washington, DC 20361	10. SOURCE OF FUNDING NUMBERS

PROGRAM ELEMENT NO.	PROJECT NO.	TASK NO.	WORK UNIT ACCESSION NO.
62759N	WF59-553		DN657763

11 TITLE: NOAA AVHRR Observations During the Marginal Ice Zone Experiment, Between Spitzbergen and Greenland, June 7 to July 18, 1984 (U)

12 PERSONAL AUTHOR(S): Skagseth, Øystein; with K. Kloster, K. Barthel, O. Johannessen

13a. TYPE OF REPORT	13b. TIME COVERED	14. DATE OF REPORT (*Year, Month, Day*)	15. PAGE COUNT
Final	FROM 6/7/84 TO 7/18/84	1988, June	137

16 SUPPLEMENTARY NOTATION

17 COSATI CODES			18. SUBJECT TERMS (*Continue on reverse if necessary and identify by block number*)
FIELD	GROUP	SUB-GROUP	MIZEX Mesoscale eddies
04	02		AVHRR Marginal ice zone
			Arctic Satellite meteorology

19. ABSTRACT (*Continue on reverse if necessary and identify by block number*)

The marginal ice zone (MIZ) is the region in which the polar air, ice and water masses interact with the temperate air and ocean masses. During MIZEX-84 an intensive effort was made to obtain an integrated data set including meteorology, oceanography and glaciology, using remote sensing as well as conventional in situ observation methods, in the MIZ between Spitzbergen and Greenland from 7 June to 18 July 1984.

This report gives NOAA AVHRR (Advanced Very High Resolution Radiometer) satellite imagery near-visual and infrared overviews of the Fram Strait and the large-scale surrounding area. For near-visual imagery phenomena of particular interest, e.g., mesoscale vortices, the focus of attention is on off- and on-ice air circulation, island lee effects and synoptic low development. Features of special interest are noted, and important small scale phenomena are enlarged if they are not prominent on the overview images.

An appendix provides satellite images and surface charts showing day to day development over the MIZEX-84 area 7 June-18 July.

20 DISTRIBUTION / AVAILABILITY OF ABSTRACT	21. ABSTRACT SECURITY CLASSIFICATION
XX UNCLASSIFIED/UNLIMITED ☐ SAME AS RPT ☐ DTIC USERS	UNCLASSIFIED

22a NAME OF RESPONSIBLE INDIVIDUAL	22b. TELEPHONE (*Include Area Code*)	22c. OFFICE SYMBOL
Fett, Robert W., contract monitor	(408) 647-4728	NEPRF WU 6.2-9 (85)

DD FORM 1473, 84 MAR — 83 APR edition may be used until exhausted. All other editions are obsolete.

SECURITY CLASSIFICATION OF THIS PAGE

UNCLASSIFIED

AN (1) AD-A204 911
FG (2) 040200
FG (2) 080300
FG (2) 081200
CI (3) (U)
CA (5) NANSEN REMOTE SENSING CENTER SOLHEIMSVIK (NORWAY)
TI (6) NOAA (National Oceanic and Atmospheric Administration) AVHRR (Advanced Very High Resolution Radiometer) Observations during the Marginal Ice Zone Experiment, between Spitzbergen and Greenland, June 7 to 18 July 1984.
TC (8) (U)
DN (9) Final rept.,
AU (10) Skagseth, Oeastein
AU (10) Kloster, K.
AU (10) Barthel, K.
AU (10) Johannessen, O.
RD (11) Jun 1988
PG (12) 130p
RS (14) NRSCTR-6
CT (15) N00014-80-G-0003
PJ (16) F59553
RN (18) NEPRF-CR-88-10
RC (20) Unclassified report
NO (21) Original contains color plates: All DTIC and NTIS reproductions will be in black and white.
DE (23) *RADIOMETRY, *AIR WATER INTERACTIONS, AIR, AIR MASS ANALYSIS, AIR FLOW, ARCTIC REGIONS, ARCTIC OCEAN ISLANDS, ARTIFICIAL SATELLITES, CHARTS, CIRCULATION, GLACIOLOGY, GREENLAND, HIGH RESOLUTION, ICE, OPTICAL IMAGES, INFRARED SPECTRA, VISIBLE SPECTRA, STRAITS, VORTICES, EDDIES(FLUID MECHANICS), INTEGRATED SYSTEMS, ISLANDS, METEOROLOGICAL DATA, METEOROLOGICAL SATELLITES, OBSERVATION, OCEANOGRAPHIC DATA, POLAR REGIONS, SEA ICE, REMOTE DETECTORS, SURFACES, TEMPERATE REGIONS, WATER MASSES.
DC (24) (U)
ID (25) AVHRR(Advanced Very High Resolution Radiometers), Marginal ice zones, Fram Strait, PE62759N, WUDN657763.
IC (26) (U)
AB (27) The marginal ice zone (MIZ) is the region in which the polar air, ice and water masses interact with the temperate air and ocean masses. During MIZEX-84 an intensive effort was made to obtain an integrated data set including meteorology, oceanography and glaciology, using remote sensing as well as conventional in situ observation methods, in the MIZ between Spitzbergen and Greenland from 7 June to 18 July 1984. This report gives NOAA AVHRR (Advanced Very High Resolution Radiometer) satellite imagery near-visual and infrared overviews of the Fram Strait and the large-scale surrounding area. For near-visual imagery phenomena of

particular interest, e.g., mesoscale vortices, the focus of attention is on off- and on-air circulation, island lee effects and synoptic low development. Features of special interest are noted and important small scale phenomena are enlarged if they are not prominent on the overview images. An appendix provides

satellite images and surface charts showing day to day development over the MIZEX-84 area 7 June-18 July. Keywords: Arctic regions; Mesoscale eddies; Air water interactions; Satellite meteorology. (edc)
AC (28) (U)
DL (33) 01
SE (34) F
CC (35) 420052

Naval Environmental Prediction Research Facility .
Monterey, CA 93943-5006

ntractor Report CR 88-10. June 1988 .

NOAA AVHRR OBSERVATIONS DURING THE MARGINAL ICE ZONE EXPERIMENT, BETWEEN SPITZBERGEN AND GREENLAND, JUNE 7 TO JULY 18, 1984.

CONTENTS

FOREWORD

This contractor report was assembled under the direction of the Naval Environmental Prediction Research Facility to document, in high resolution satellite imagery, the atmospheric structure over the marginal ice zone (MIZ) in the Greenland/Norwegian and Barents Seas during June and July 1984.

The Polar regions have assumed increasing economic and military importance in the past decade. The meteorology of these areas is poorly understood, however, and until recently had received only casual attention in terms of active research that used vessels and aircraft to obtain ground, air and sea truth.

The Marginal Ice Zone Experiment (MIZEX) of 1984 was an important step in gaining new information about weather and oceanographic phenomena in the Fram Strait region. The value of the experiment is greatly enhanced, furthermore, by the addition of the high resolution satellite data.

The purpose of this report is to display these data as documentation of weather events that occurred during MIZEX-84, and possibly to stimulate additional research concerning the wide variety of phenomena that actually occurred.

W.L. Shutt
Commander, U.S. Navy
Commanding Officer,
Naval Environmental Prediction
Research Facility, Monterey, CA

1. Introduction

The experiment MIZEX-84 was carried out in the marginal ice zone (MIZ) between Spitzbergen and Greenland from 7 June to 18 July 1984.

Imagery from the NOAA satellites 6, 7 and 8 has been collected for every day during this experiment. The images have been processed and studied with the aim of detecting various atmospheric and oceanic features. These features are described in the two following chapters;

- description of meteorological processes in polar regions that are occuring during MIZEX-84,
- description of the ice edge eddy formation.

The meteorological part uses overview images made in the near-visual channel (0.7μ - 1.1μ) of the Advanced Very High Resolution Radiometer (AVHRR) on the satellites. Features of special interest have been focused upon by enlarging the images by use of an image processing system.

The images are mostly presented in a grey scale from black to white, where black is equivalent to low albedo and white to high albedo. The width of the scale is chosen to give a reasonable grey scale compared to the feature that is focused upon. The interpretation of the images is aided by the synoptic surface pressure charts also presented. Different atmospheric circulation characteristics during the MIZEX-84 period are listed in Table 1 with respect to day of occurence.

The ice edge eddy part is mainly concentrated to the period from 26 June to 4 July. In this clear weather period it was possible to follow the development of the eddies in the ice edge area with reasonable time intervals. Realistic surface temperatures were retrieved through the thermal infrared channel (10.5μ - 11.5μ) of the AVHRR instrument. On these grey scale infrared images light and dark corresponds to cold and warm respectively.

Some of these images are presented in colours, as this gives a better signal resolution, which is needed to detect features where the temperature or albedo contrasts are small.

All images are found in the appendix, containing visual imagery and weather charts used mainly for the meteorological interpretations (chapter 2), and thermal infrared imagery used mainly for the ice edge eddy surface temperature interpretations (chapter 3). Figures 1 - 42 are in order of increasing day number from 7 June, and the letter following the figure number has the following coding;

a for visual imagery in original (Tromsö Telemetry Station) format
b for surface pressure charts
c for visual imagery, enhanced and/or enlarged on our image processing system
d for thermal imagery

Figures 43 -47 are various images and figures such as SAR imagery and time-sequences related to chapter 3.

The original AVHRR imagery (quick-look-images) has been supplied by Tromsö Telemetry Station.

The processed AVHRR imagery has been obtained at the image processing system CMI-BILD at Christian Michelsen Institute in Bergen, using digital tape from Tromsö as input. The processing includes enhancement, gridding, enlargement and the choice of suitable greyscale or colour scale.

2. Polar Meteorology

Lack of data has hindered the study of the intense dynamics of the air-ocean-ice interactive processes taking place in the polar regions. During MIZEX-84 a great effort to collect air, sea and ice data from the area between Spitzbergen and Greenland was made. The aim was to map mesoscale vortices, off- and on-ice air circulation phenomena, island lee effects and synoptic lows development. Polar lows are mostly confined to the winter season, therefore the mapping of polar lows was not expected during MIZEX-84 (which went on in the summer season.)

In the following a short description of the different atmospheric circulation patterns encountered during the MIZEX-84 program is given. Detailed explanation are associated with each figure.

Mesoscale vortices.

Mesoscale vortices are not resolved on a weather map because of their small scale and often short duration. Different kinds of instabilities of the flow, such as baroclinic, barotropic and convective instability can be the reason for the generation of these vortices. Vortex shedding in the lee of mountains are quite common. Mesoscale vortices can be rather energetic and cause severe damage. On the satellite images from the MIZEX-84 period mesoscale vortices were spotted twelve times (see table 1.) That on 25 June could possibly be defined as a polar low (figure 19), bearing some characteristics of this penomenon.

Off-ice circulation.

Like the land-sea-breeze circulation the off-ice wind results from the differential heating of the airmasses over ice and sea. This is also a mesoscale phenomenon. (The off-ice wind can of course as well be a result of the large scale atmospheric pressure distribution giving a geostrophic wind with an off-ice component.)

A column of air crossing the ice edge will be heated from below (both latent and sensible heat transport will take place) and the thickness and the potential temperature of its planetary boundary layer will increase very quickly. (In the planetary boundary layer the potential temperature and the water vapor mixing ratio is assumed to be constant with height.) As the air column moves over the warmer sea, its temperature will continue to increase, and after a certain distance downstream from the ice edge clouds are generated on the top of the planetary boundary layer. The clouds can form streets parallel to the wind direction as seen for instance in figure 3 for 9 June.

On-ice circulation.

When the geostrophic wind has an on-ice component, the common situation is that warm air from the sea is advected into the domain of the cold airmass over the ice. The mixing of warm moist air with cold dry air results in saturation, and fog and cloud formation. The static stability of an air column will increase by the cooling from below and the clouds will often be of the stratiform type. A typical situation is seen on figure 36d for 12 July.

On figure 22 for 28 June another effect of on-ice circulation is seen. The static stability distribution of the atmosphere favours the generation of gravity waves as the warm air flows northwards and becomes lifted over the cold arctic air.

Circulation patterns generated by topography.

The satellite images show several features where the air flow is influenced by topography. Figure 1 for 7 June shows both short mountain waves and lee subsidence generated by the Spitzbergen topography. Figure 17 for 23 June shows a wavy lane of clouds generated in the air flow over Jan Mayen. Figure 25 for 1 July shows lee cyclogenesis on different scales; a synoptic low generated to the lee of Greenland, and a mesoscale vortex off the westcoast of Spitzbergen.

Depending on the static stability and the vertical shear of the horizontal wind, short mountain waves can be generated, made visible through the condensation and cloud formation at the wave tops. If the static stability is not too large and the vertical shear of the wind is sufficiently large, waves can be generated with wavelength of the same order as the thickness of the shear layer. The mountain waves can be trapped in a horizontal layer giving a long wavetrain downwind from the mountain. Or they can have a vertical component of propagation. This depends also on the wind shear and the static stability.

Clear sky regions downwind from islands is connected with lee subsidence. The descending motion is dependent on the variation of the static stability with height. If the lower atmosphere is very stable, the subsidence is strong.

Isolated mountains produce a different circulation pattern than mountain ridges. The pattern produced by a ridge can be looked at as two-dimensional, while that from an isolated mountain has three dimensions. The wavy cloud lane generated at Jan Mayen 23 June 1984 (figure 17) is a feature that has been discussed by Gjevik and Marthinsen(1978). The feature is appearing when a shallow layer with large static stability is intersecting the mountain. Vortex shedding is common during such conditions.

Large scale mountain ranges like Greenland can favour lee cyclogenesis of synoptic scale. Conservation of potential vorticity will lead to increased relative vorticity by vortex stretching to the lee of the mountain range. The same effect produces mesoscale lee vortices when the mountain range is smaller.

These various atmospheric circulation patterns both influence and are influenced by the position and configuration of the ice edge. The ice edge can be a marked borderline between areas of strong and none convective heating. Along this line air masses lying close to each other can have large differences in temperature, humidity and static stability. The observational network needed to cover these small scales of large gradients has to be dense and comprehensive. The combination of in situ observation and remote sensing by aircraft and satellite made during MIZEX-84 succeeded in gathering a large data set of the marginal ice zone. However, the experiment went on in the summer season, so that the seasonal variation of the conditions in the ice zone was not observed. Therefore the next experiment, MIZEX-87, covered a period of late winter.

Off-ice wind	On-ice wind	Topographic effects	Mesoscale convergence lines	Mesoscale vortices
7 June	14 June	7 June	9 June	11 June
8 June	15 June	8 June	11 June	12 June
9 June	28 June	9 June	26 June	18 June
11 June	12 July	11 June		20 June
13 June	14 July	19 June		22 June
17 June	16 July	22 June		25 June
19 June	17 July	23 June		1 July
20 June	18 July	24 June		4 July
21 June		25 June		5 July
23 June		27 June		10 July
28 June		1 July		13 July
2 July		4 July		18 July
4 July		5 July		
6 July		6 July		
7 July		7July		
8 July		8 July		
		9 July		
		10 July		
		12 July		
		15 July		
		17 July		

Table 1.
Occurence of typical atmospheric circulation patterns during the MIZEX-84 period.

3. Ice edge eddies in the Fram Strait MIZ

Introduction.

One objective of MIZEX-84 is to better understand the physics of mesoscale eddies along an ice edge and the role that eddies play in the process of mass and heat exchange and in controlling the position of the ice edge. Previous studies in the Fram Strait marginal ice zone (MIZ) have established the existence of eddies at the ice edge with scales that range from 5 to 15 km north of Spitzbergen to 50 to 60 km in the western part of the Fram Strait. Barotropic and baroclinic instability have been suggested as generating mechanisms. In the central part of the Fram Strait the topography is so complex that topographic steering and trapping also seems to be important factors. Also, due to the different drag conditions over ice and water, the wind can generate ocean eddies. This part of the report describes a dedicated eddy investigation during the summer of 1984 between 77°N and 79°N along the ice edge of the Fram Strait. The study used remote sensing; conductivity, temperature, and depth (CTD) observations; and ice-drifting satellite tracked buoys that were suspended with current meters.

Observations.

Remote sensing observations were used in near real-time mode for locating eddies and for guiding the research vessels into the eddy region. For example, the high resolution aperture radar (SAR) mosaic on 5 July (figure 45) clearly shows detailed surface structure of an elliptically shaped eddy E1 on the scale of about 30km. Since the wind was light, the floe-size distribution of 50-500 m reflected the upper ocean circulation. The orbital motion was cyclonic and the ice concentration was more than 80% at the center of the eddy. This implies that there was convergence and that ageostrophic effects must be included when modelling these eddies. A second eddy E2 was seen south of E1, centered at 78°05' N and 3° 55' W. Slicks and bands of ice were also identified that indicated internal wave activity. The area marked "Band of dead water" off the ice edge was a distinct meltwater zone (figure 46).

The abundance of eddies in this region is shown in the AVHRR images. Eddies E1 through E4 strongly interacted with the ice edge. Analyses of earlier AVHRR images showed that on 26 June E1 started to form at approximately 79°15'N and 1°30'W

(figure 43) and was fully developed by 29 June at 79°N and 2°15'W(figures 43 and 44). This suggested an upper layer spin-up time of the order of 3 days, during which time the mean southward advection of the eddy, deduced from the images, was approximately 10 km/day. From 30 June to 1 July E1 moved slowly eastward. The spin-up of E2, which was then 50 km southwest of E1, occured during 1 to 4 July.

After 4 July, cloudiness precluded the continued use of the NOAA satellite monitoring the eddies. However, aircraft microwave observation continued to provide high-resolution monitoring of the eddies and demonstrated that radar observations were indispensable for the experiment. Sequential radar images through 16 July showed that E1 was nearly stationary. A northerly wind (2 days' duration, 15 m/sec) erased the clear ice convergence signature within the eddy but did not completely erase the boundary signature, and demonstrated that imaging radar can observe ice-ocean eddies even under high wind conditions. The ice convergence structure at the center reappeared when the wind

decreased. The remote sensing data showed that E1 had a lifetime of at least 20 days.

Extensive star pattern CTD sections of E1 obtained by the research vessels R.V. Haakon Mosby and R.V. Kvitbjørn during the period 10 to 14 July coupled with the remote sensing observations during the same period give a nearly synoptic three dimensional picture of the eddy. A CTD-section perpendicular to the ice edge (figure 47) near the center of E1 showed the doming and the surfacing of the isopycnals, and indicated cyclonic motion down to 500 m and confirmed the rotation that was seen on the radar image. Another section directed south-north showed that E1 was actually present at 800 to 1000m. Current velocity measurements within E1 (obtained with satellite tracked argos buoys with current meter) measured cyclonic orbital speeds of 30 to 40 cm/sec. The subsurface structures of E4 and E5 was also confirmed by CTD observations.

The thermodynamic importance of the eddies in determining the ice edge position could be estimated from the AVHRR images. The cyclonic motion of each eddy not only swept ice away from the main ice pack, but also transported warm Atlantic water (3 to 4°C) beneath the ice. Melt rates from the bottom of the ice tongue of E1 varied from 20 to 40 cm/day in contrast with rates of 2 to 3cm/day when the ice was in the colder Arctic water. To estimate eddy thermodynamics, assume that half of the eddy was covered by ice and that the ice was 1.5m thick; under such conditions the observed melt rates can easily account for the loss of approximately 350 km^2 of sea ice in 4 to 7 days. Hence at an eddy spacing of 50 km, these eddies alone could cause the ice edge to melt at a rate of 1 to 2 km/day. Such intense melting was observed from 1 to 6 July in the vicinity of E4. The warming and thinning of the ice augmented by the eddies also make the ice more susceptible to fracturing by waves and floe collisions.

All the eddies observed were cyclonic (during MIZEX-87 vortex pair, one cyclonic and one anticyclonic, was observed). They transferred heat from the Atlantic water to the ice and thus greatly enhanced the rates of ice melting. Eddies play an important role in transfer processes in the MIZ, and should be included in both long- and short term ice edge position forecasting. Further details of the MIZEX eddy studies are reported by Johannessen et. al. (1987).

Conclusion.

Five prominent ice edge eddies in the Fram Strait on the scale of 30 to 40 km were observed over deep water within 77°N to 79°N and 5°W to 3°E. The use of remote sensing, a satellite-tracked buoy, and in situ oceanographic measurements showed the presence of eddies with orbital speed of 30 to 40 centimeters per second and lifetimes of at least 20 days. Ice ablation measurements made within one of these ice-ocean eddies indicated that melting, which proceeded at rates of 20 to 40 centimeters per day, is an important process in determining the ice edge position. These studies give new insight on the formation, propagation, and dissipation of ice edge eddies.

Acknowledgment: This work was supported by ONR contract N00014-80-G-0003 with Mr. R.W.Fett as technical monitor.

References

Gjevik, B and T.Martinsen: Three dimensional lee-wave pattern. *Quart.J.R. Met Soc.* 1978, Vol. 104, No.442, 947-958.

Johannessen, J.A., O.M.Johannessen, E.Svendsen, R.Shuchman, T.Manley, W.J.Campbell, E.G.Josberger, S.Sandven, J.C.Gascard, T.Olaussen, K.Davidson, and J.Van Leer: Mesoscale Eddies in the Fram Strait Marginal Ice Zone During the 1983 and 1984 Marginal Ice Zone Experiments, *Journal of Geophysical Research* 1987, Vol 92, No. C7, 6754-6772 and 7199-7202.

Johannessen, O.M., J.A.Johannessen, E.Svendsen, R.A.Schuchman, W.J.Campbell, and E.Josberger : Ice-Edge Eddies in the Fram Strait Marginal Ice Zone, *Science* 1987, Vol 236, 427-429.

Kellogg, W.W. and P.F.Twitchell: Summary of the Workshop on Arctic Lows 9-10 May 1985, Boulder, Colorado. *Bulletin Am. Met. Soc.* 1986, Vol. 67, No. 2, 186-193.

Lindsay, R.W.: MIZEX-84 Integrated Surface Meteorological Data Set and Meterorological Atlas, Second Edition, Polar Science Center, University of Washington, 1985.

APPENDIX

DAY TO DAY DEVELOPMENT
7 JUNE - 18 JULY 1984

SATELLITE IMAGES AND SURFACE CHARTS

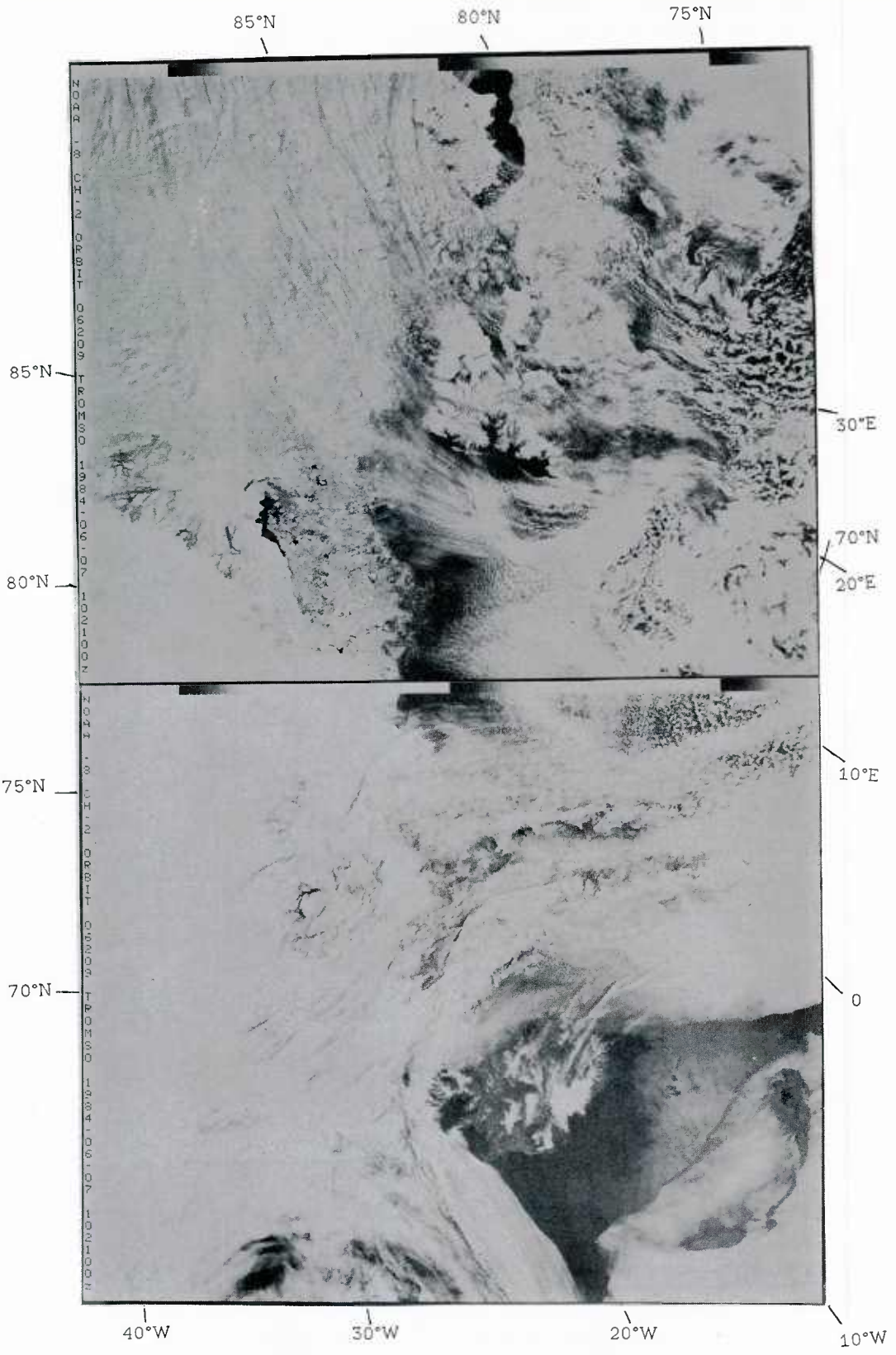

Figure 1a: NOAA-8 visual image 7 June 1984 1021 GMT.
It is off-ice wind in the Fram Strait MIZ area. As the dry and cold polar air becomes moistened and heated over ice-free water, cumulus clouds soon start to develop and grow with the distance downwind from the ice edge. Northeasterly winds over Spitzbergen generate mountain waves over the southern part of the island, and a subsidence area with its clear sky along the southwest coast is seen.

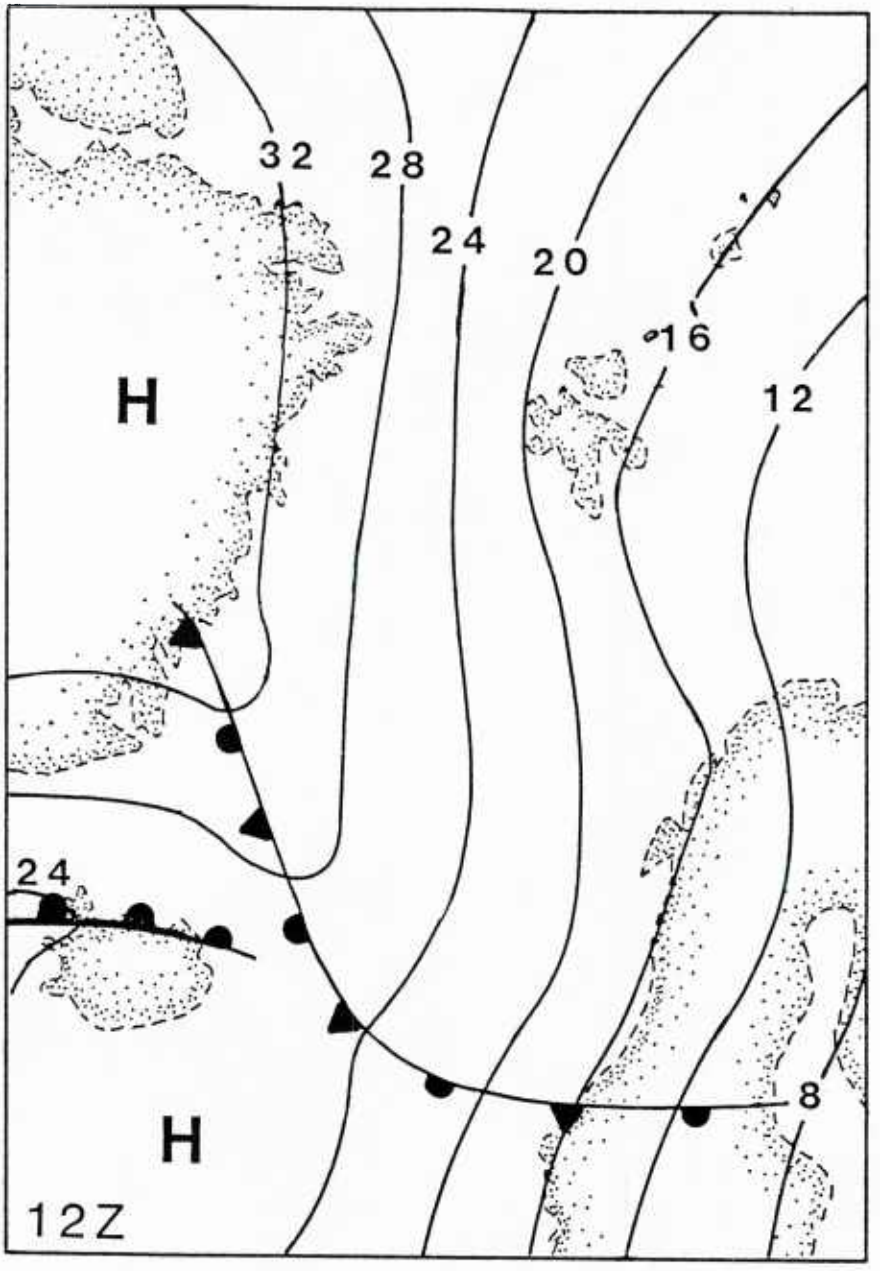

Figure 1b: Surface pressure chart 7 June 1984 1200 GMT.

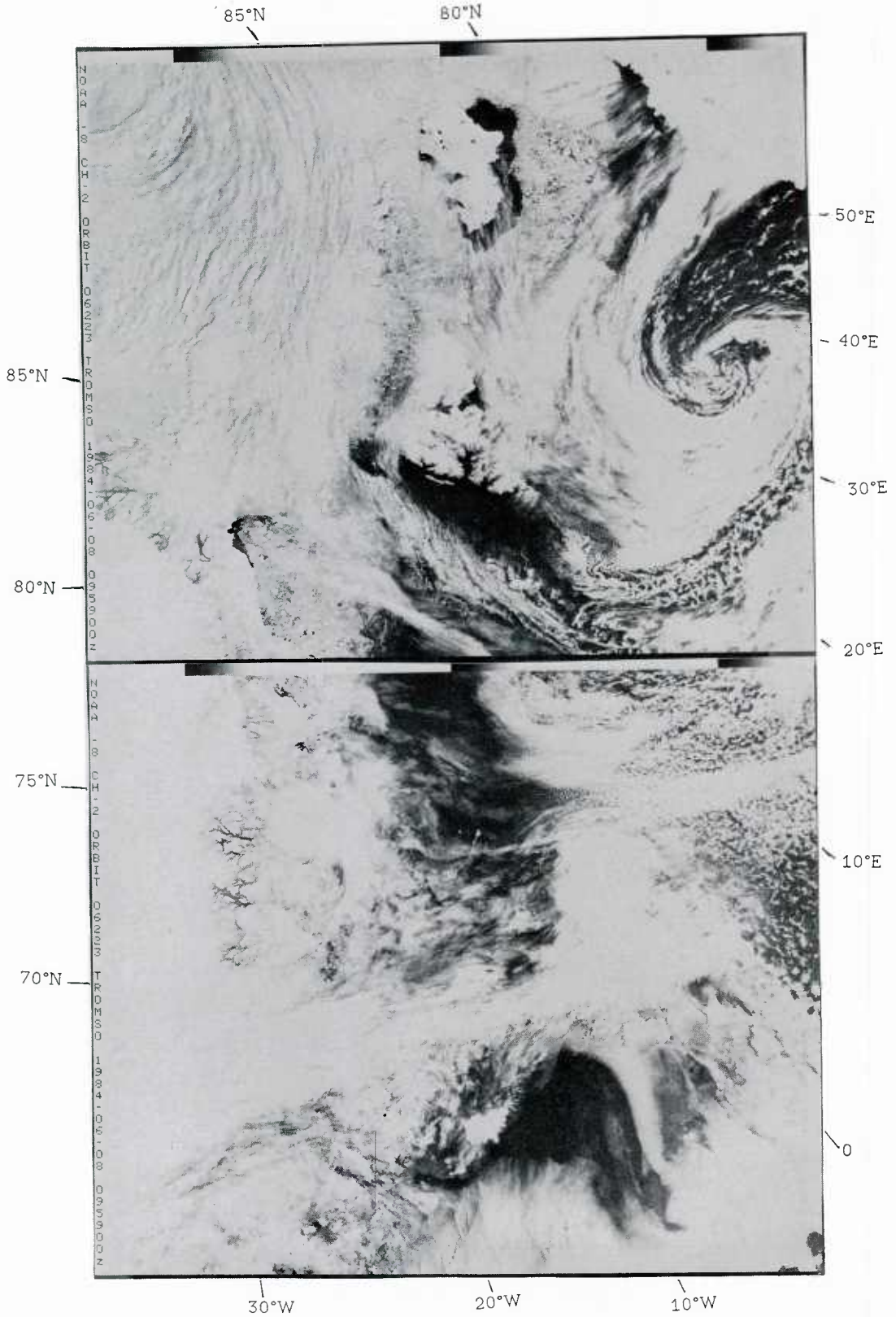

Figure 2a: NOAA-8 visual image 8 June 1984 0959 GMT.
Between the very deep low in the Barents Sea and the high over Greenland a ENE wind is blowing, giving lee subsidence along the western part of Spitzbergen. In the northern Fram Strait the wind is blowing along the ice edge, further south with an off-ice component.

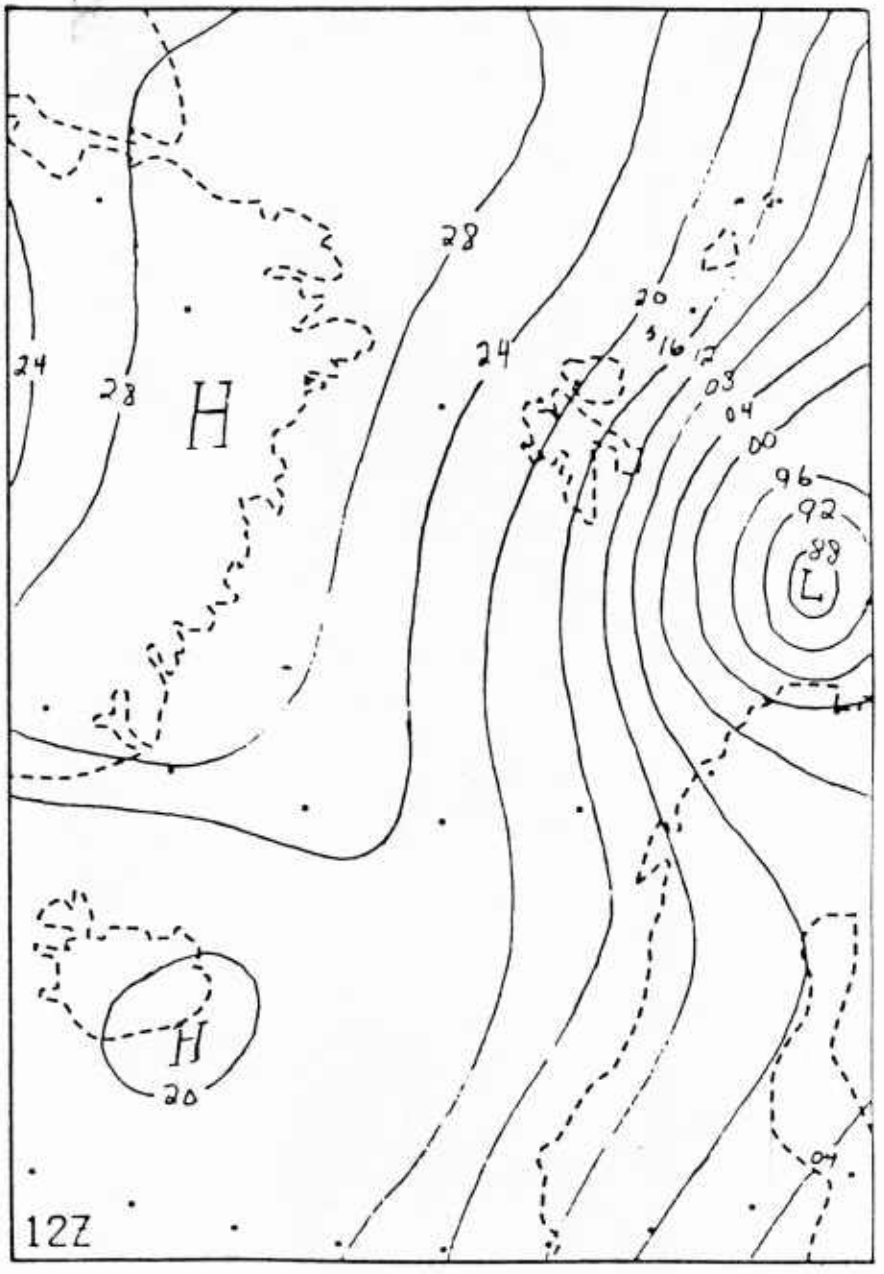

Figure 2b: Surface pressure chart 8 June 1984 1200 GMT.

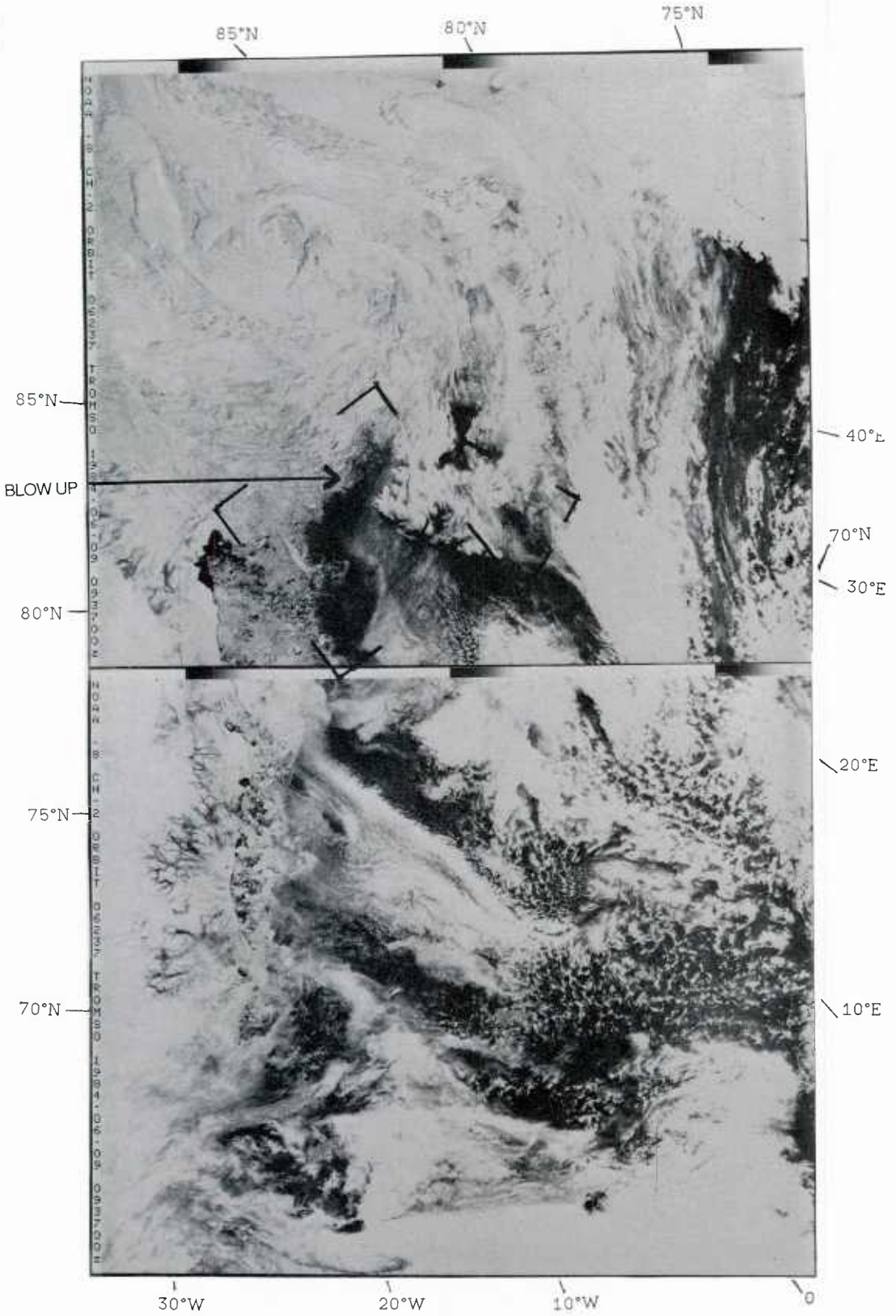

Figure 3a: NOAA-8 visual image 9 June 1984 0937 GMT.
The wind is blowing off-ice in the Fram Strait. Cloud streets forming at a certain distance downwind from the ice edge are seen. A strong convergence line at 0°E and between 70°N and 75°N is seen, curling up in a mesoscale cyclone at the southern end. In the Spitzbergen region northerly winds are generating mountain waves over the southern part of the islands.

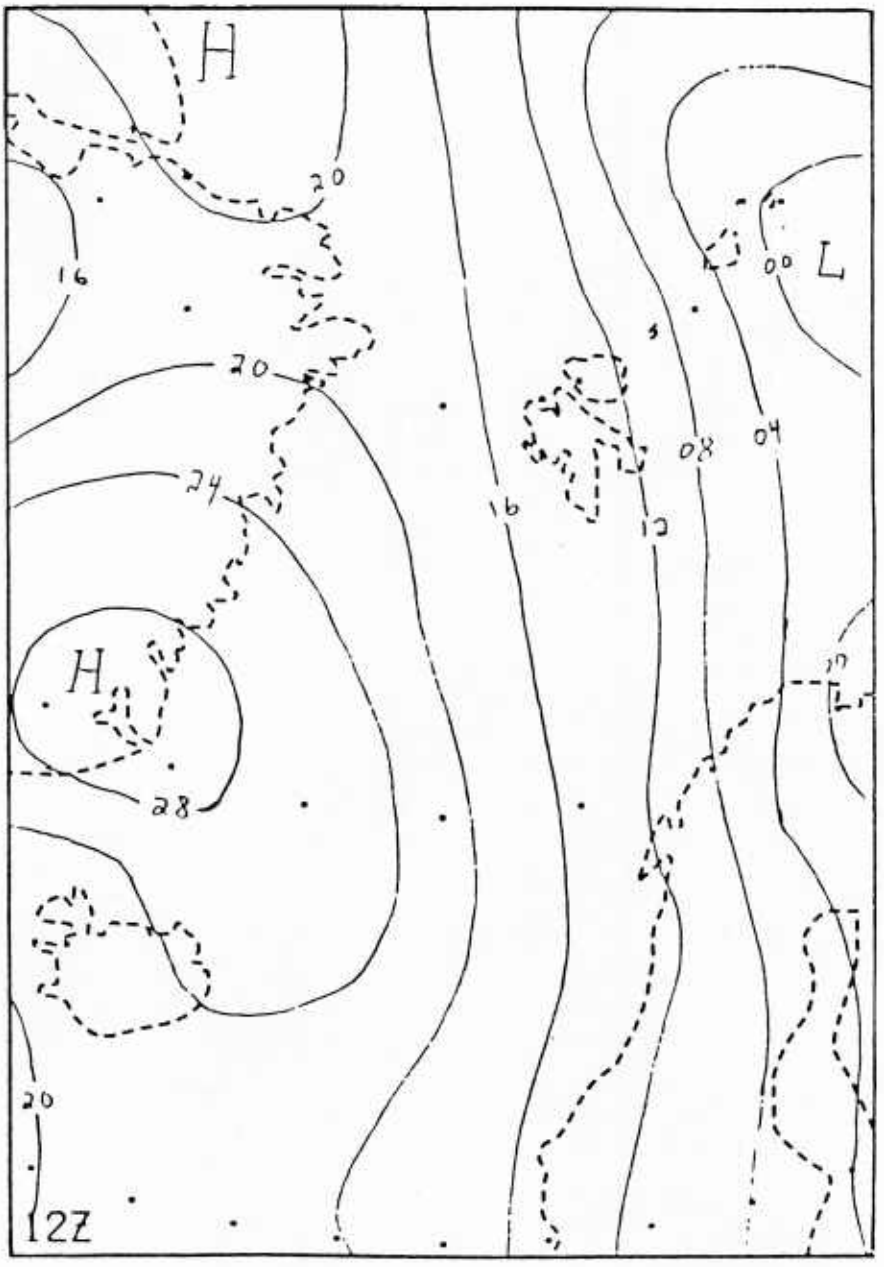

Figure 3b: Surface pressure chart 9 June 1984 1200 GMT.

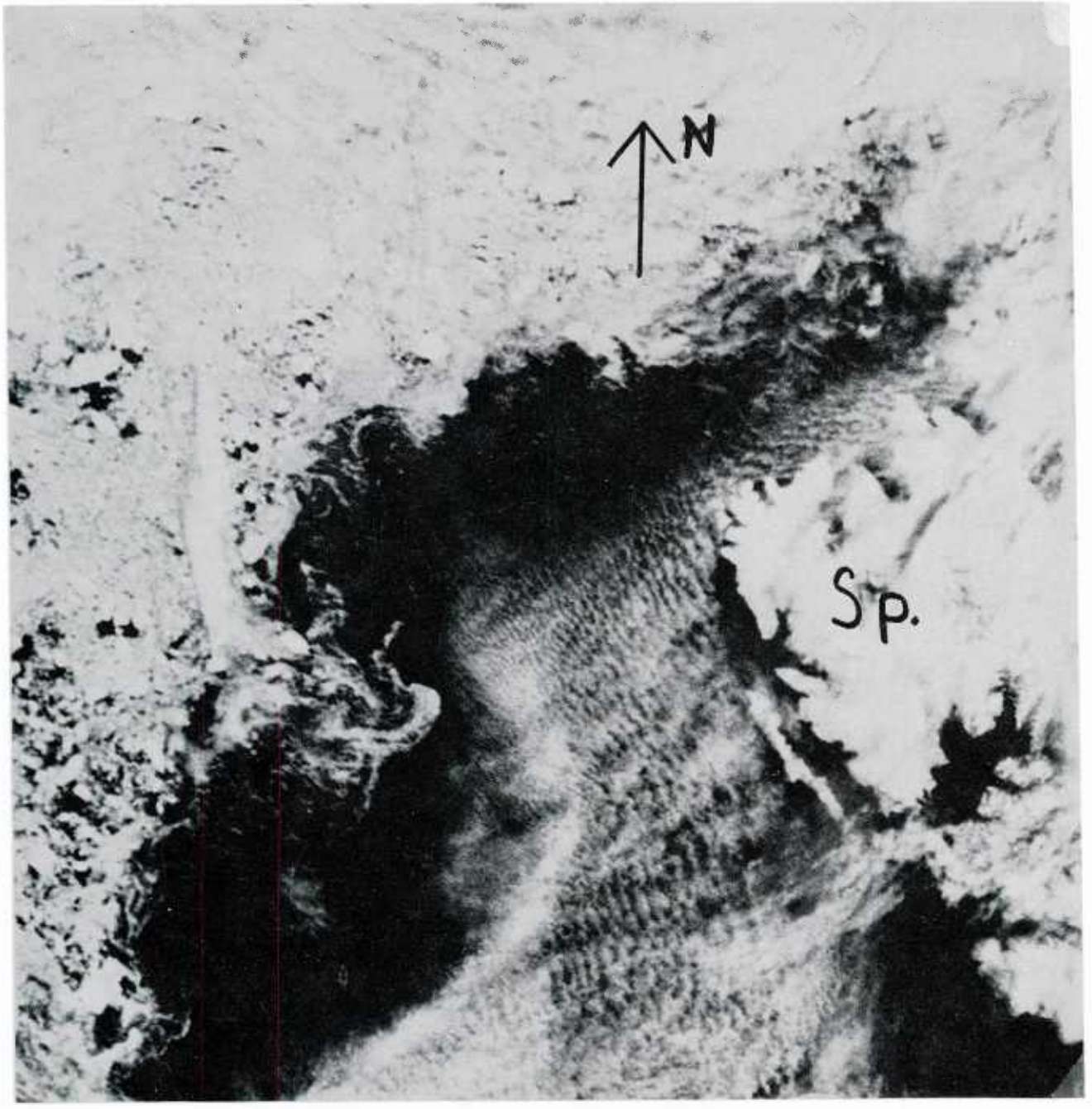

Figure 3c: NOAA-8 visual image 9 June 1984 0937 GMT.
The image shows a blow up of the cloud streets west of Spitzbergen. In the western part of the Fram Strait, the distance downwind from the ice edge to where the clouds start to form, is longer than in the eastern part. This is presumably connected with the distribution of the sea surface temperature, which has a strong easterly gradient in the Fram Strait.

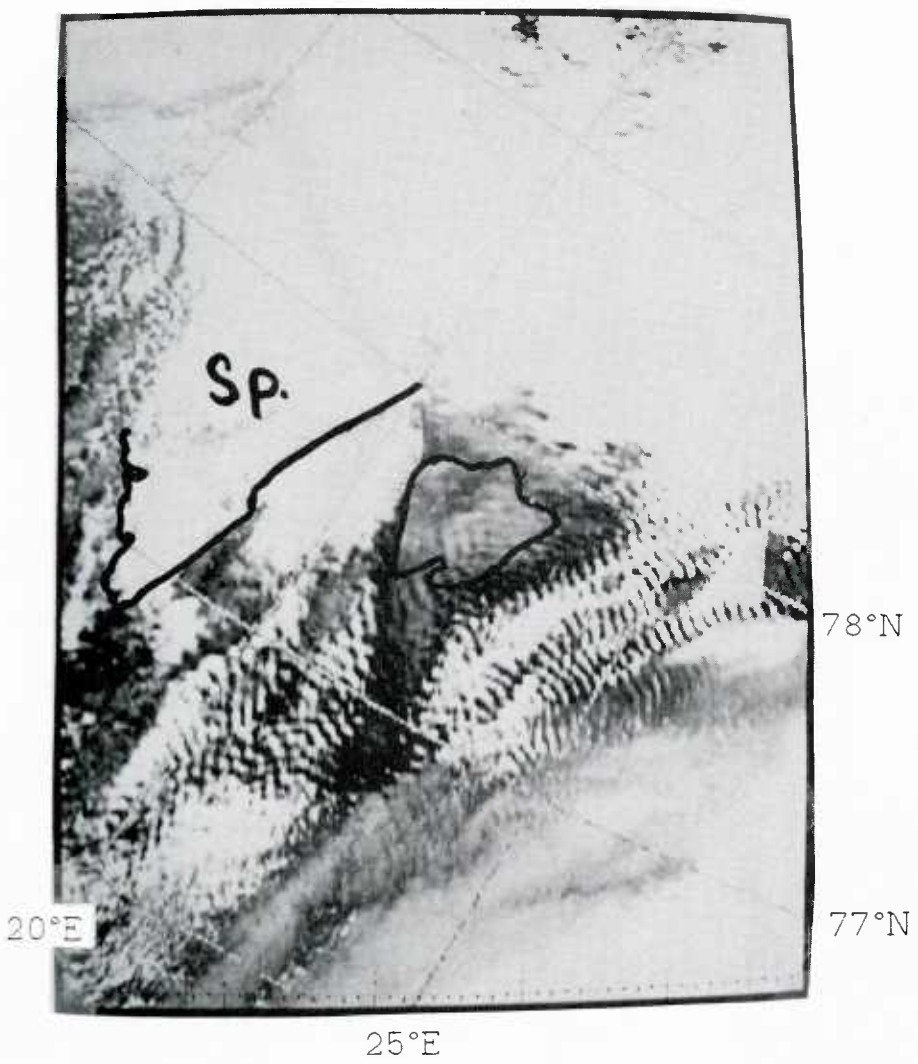

Figure 3d: NOAA-8 IR image 9 June 1984 0937 GMT.
The mountain wave clouds southeast of Spitzbergen are fairly well seen on the IR image. White means high cold clouds. Black colour is about 0°C. The wavelength of the lee-waves are approximately 5 km. If $\partial T/\partial z$=-5deg/km, g/c_p=9.8deg/km and T=250°K then the wind speed would be 10m/s, which is consistent with the geostrophic wind speed.

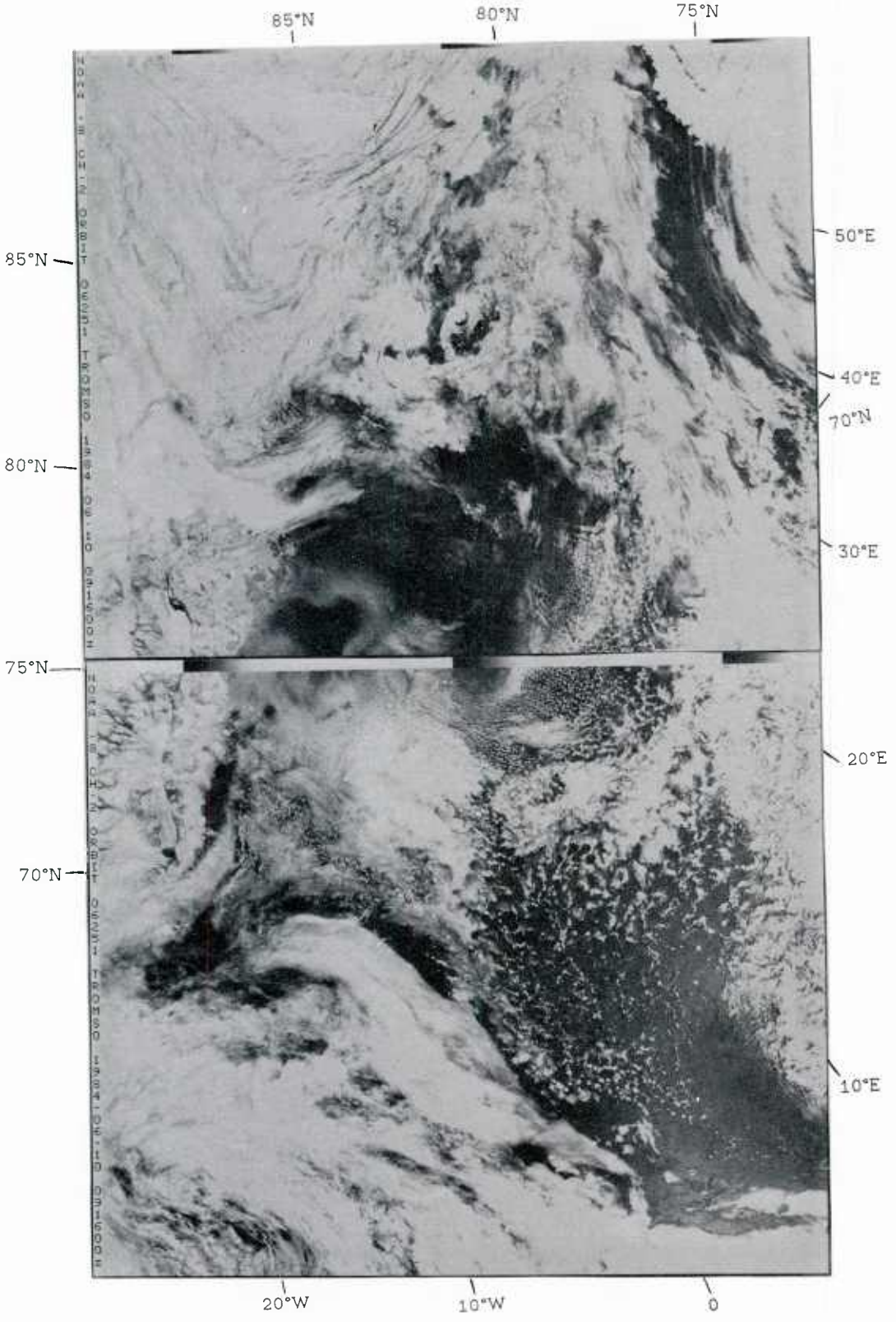

Figure 4a: NOAA-8 visual image 10 June 1984 0916 GMT.
Only weak winds in the Fram Strait blowing off-ice. Large parts of the southern MIZ area are influenced by the high pressure ridge over the Norwegian Sea, giving clear sky connected with subsidence.

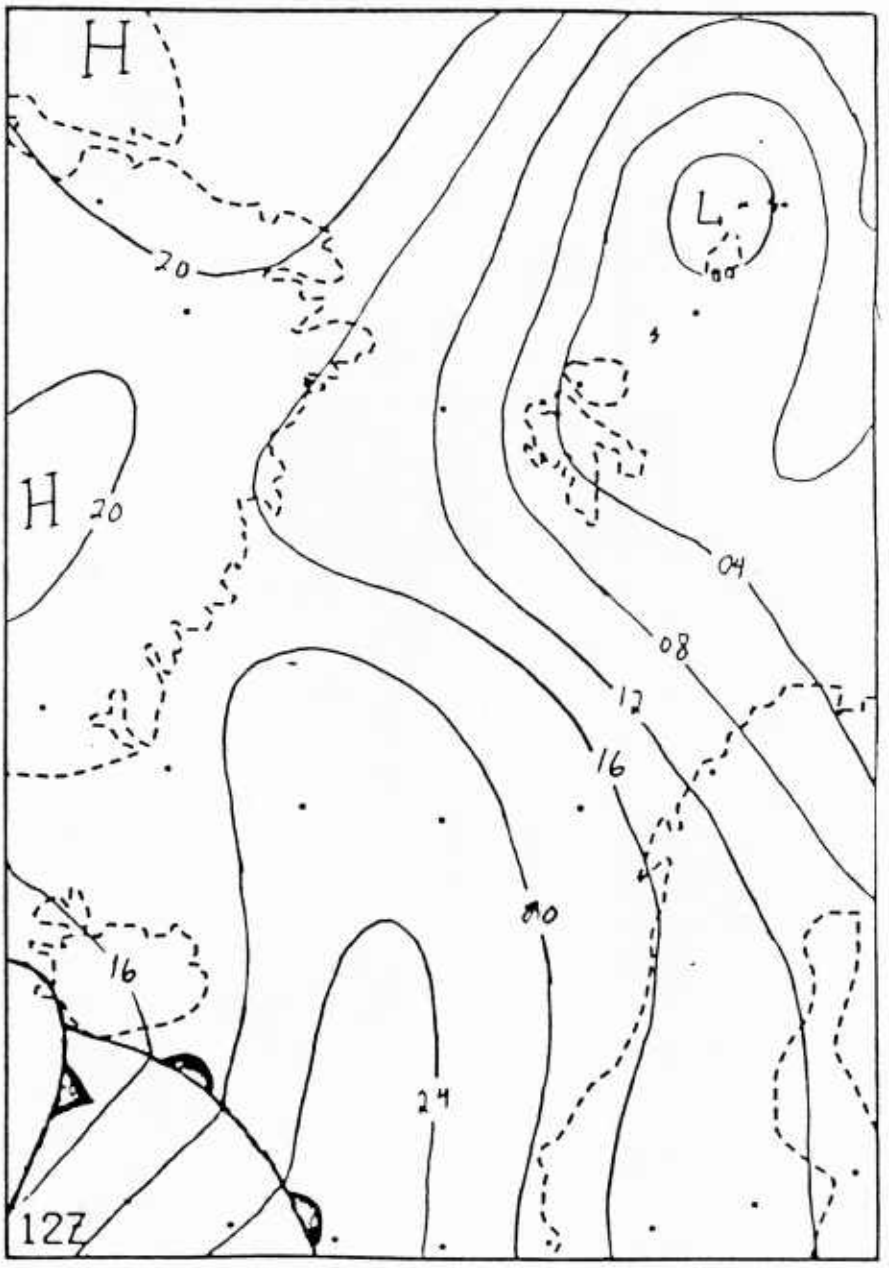

Figure 4b: Surface pressure chart 10 June 1984 1200 GMT.

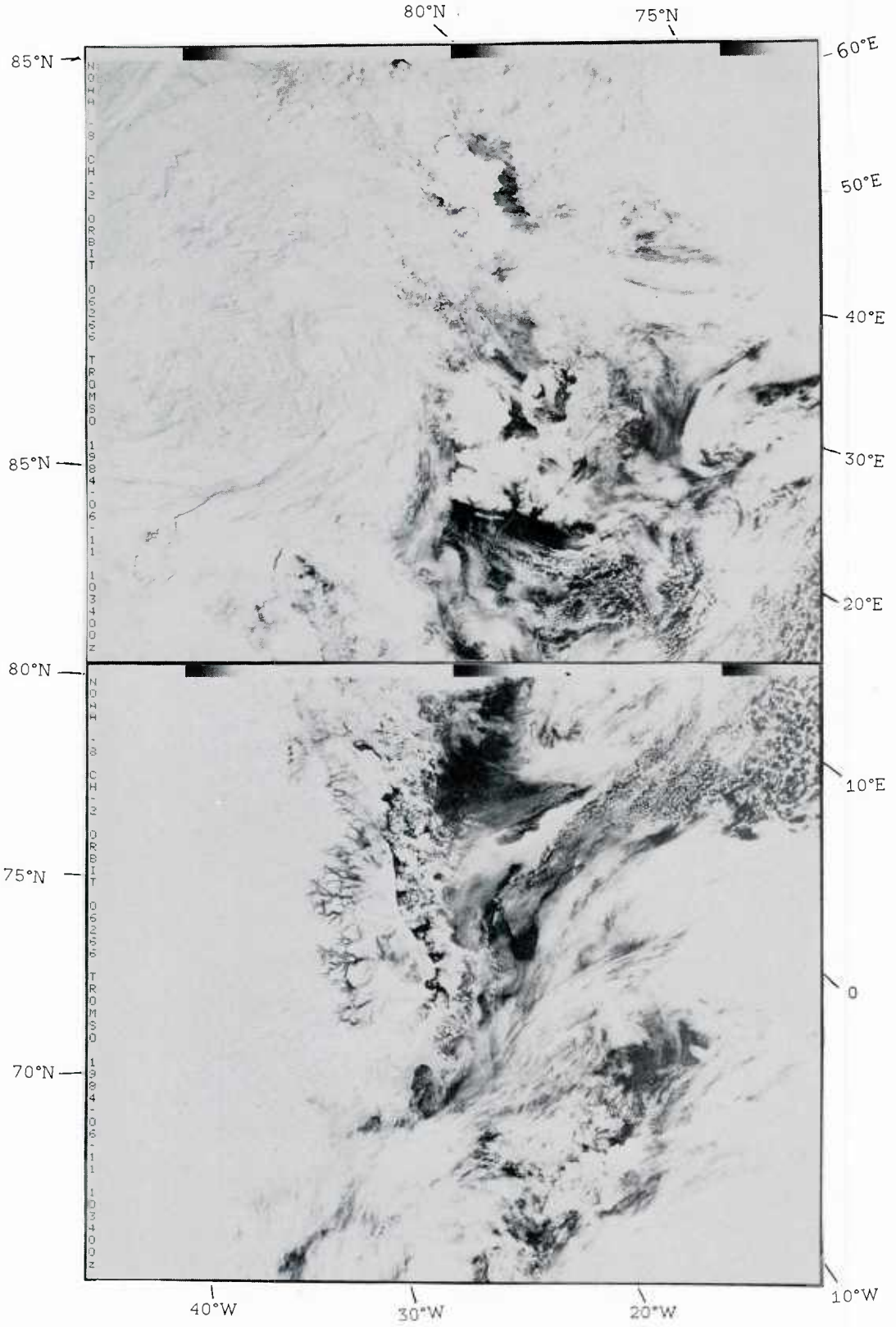

Figure 5a: NOAA-8 visual image 11 June 1984 1034 GMT.
A trough over the northern MIZ area sets up a WNW wind over the southern part. Strong subsidence east of Greenland gives a clear view of the ice zone. A longitudinal convergence line with strong convection is seen south of 75°N. The off-ice wind produces cumulus clouds in the Fram Strait, and some high level mesoscale vortices are spotted over the ice edge there.

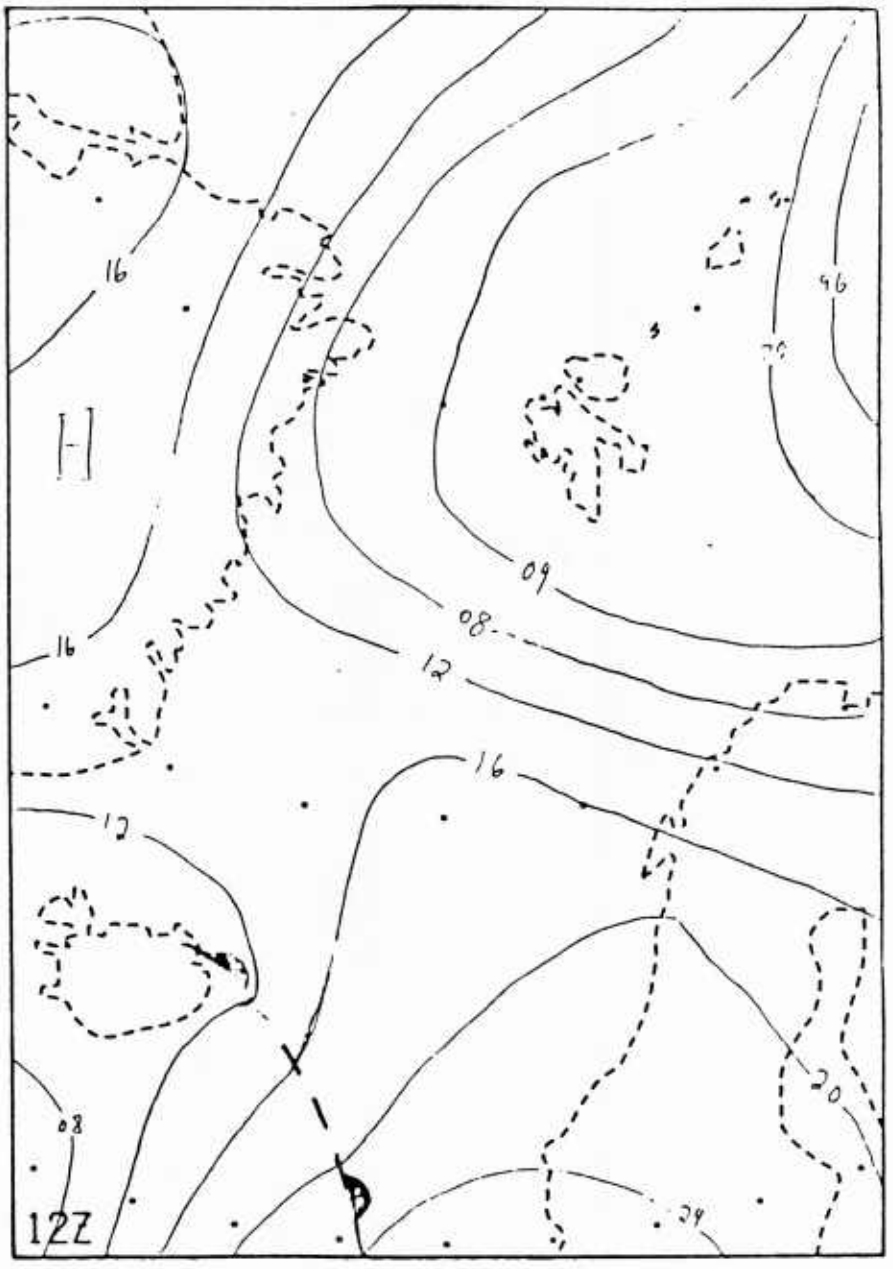

Figure 5b: Surface pressure chart 11 June 1984 1200 GMT.

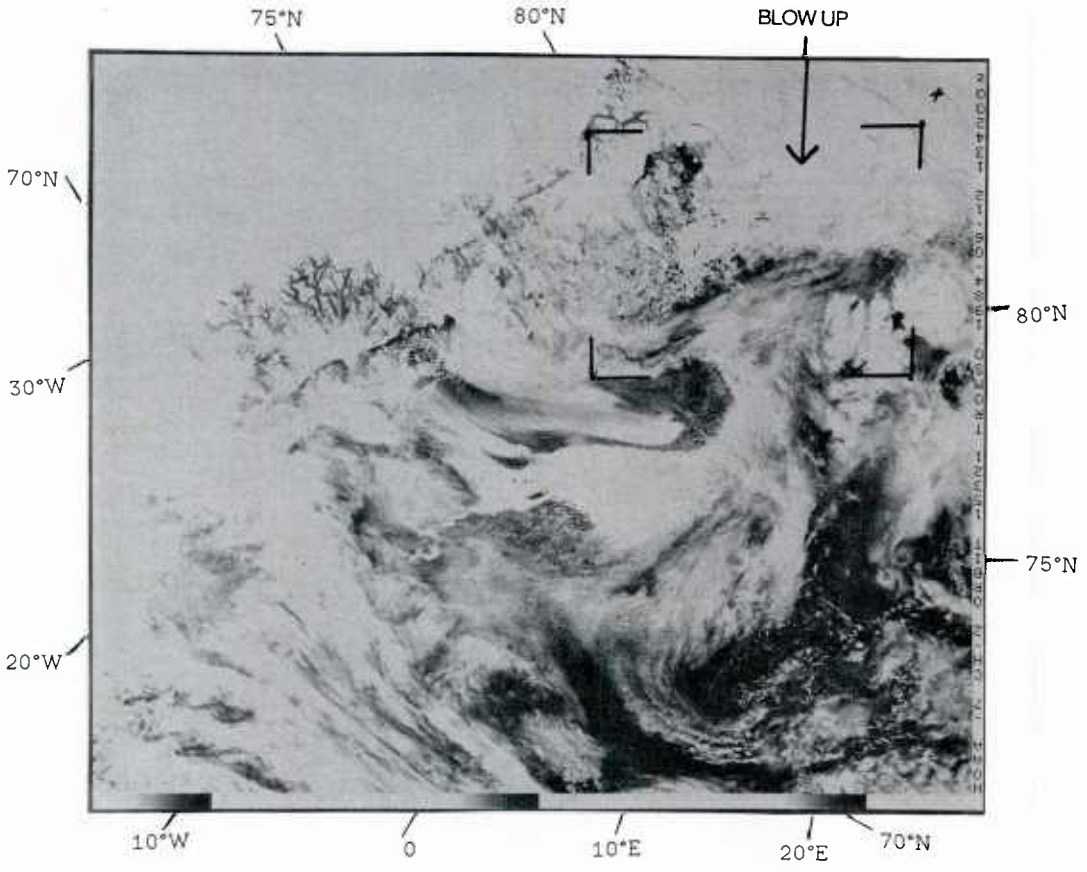

Figure 6a: NOAA-7 visual image 12 June 1984 1342 GMT.
There are weak surface winds in the MIZ area. The northern ice edge is clearly visible while the southern is obscured by some high level clouds. An interesting feature is the mesoscale vortex pair at 75°N, 22°E surrounded by mostly clear sky. They have the characteristics of the so-called comma-clouds, as reported by Kellogg et al. (1986).

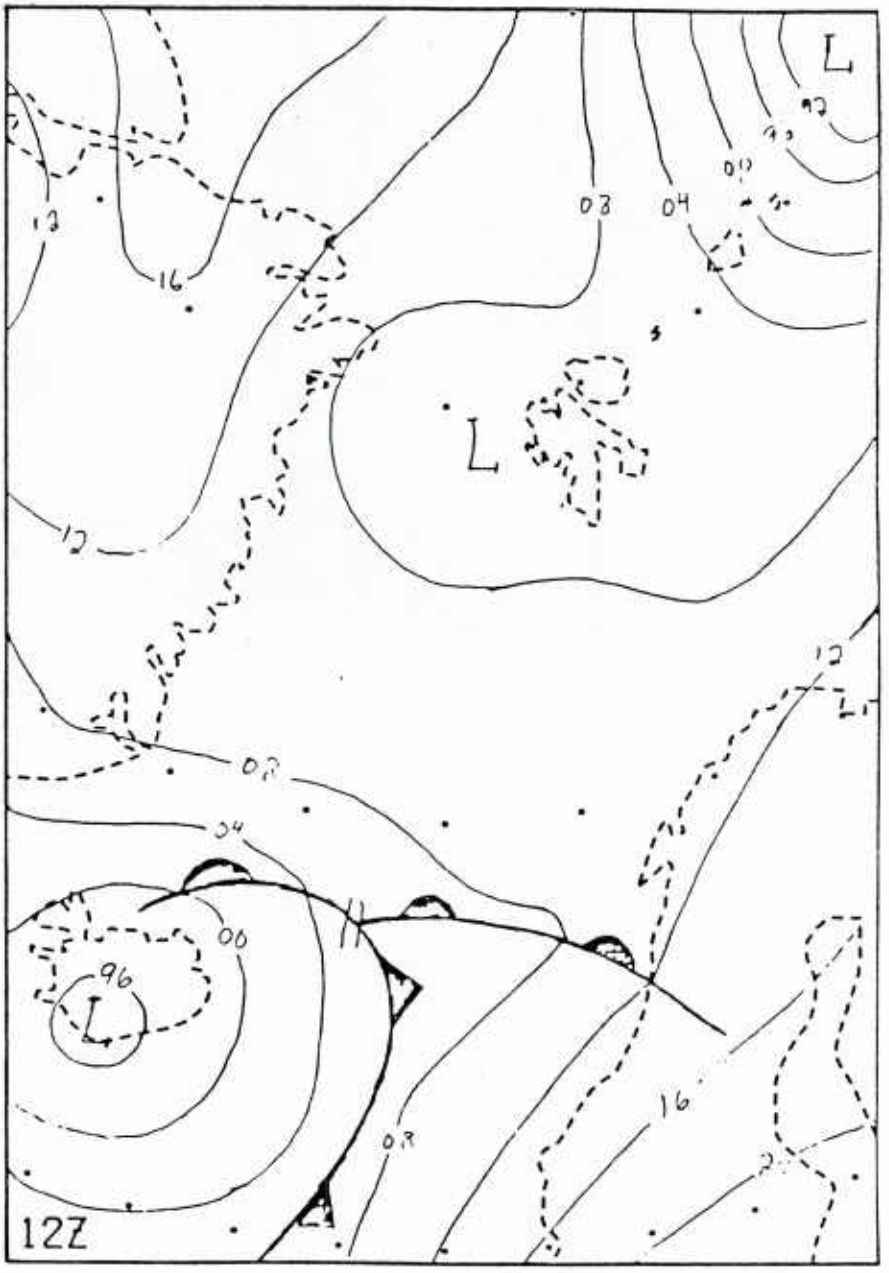

Figure 6b: Surface pressure chart 12 June 1984 1200 GMT.

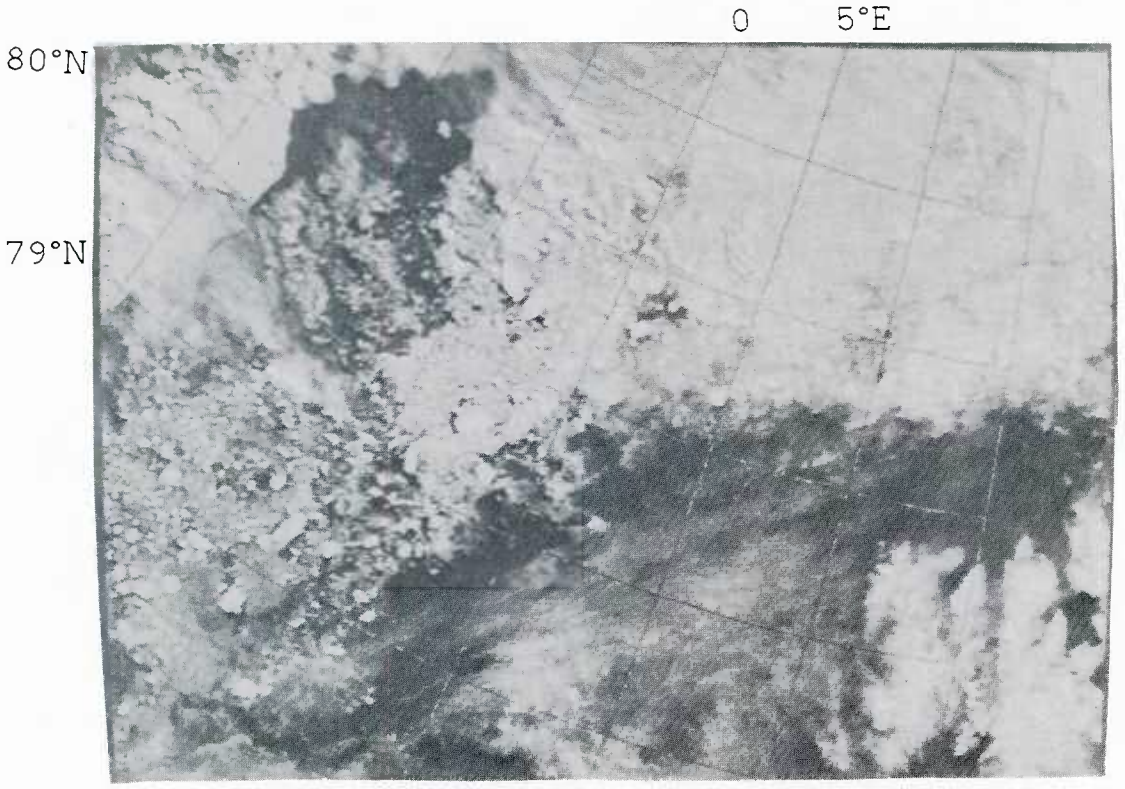

Figure 6c: NOAA-7 visual image 12 June 1984 1342 GMT.
The image shows the ice edge west of Svalbard. Signatures of ice edge eddies are seen.

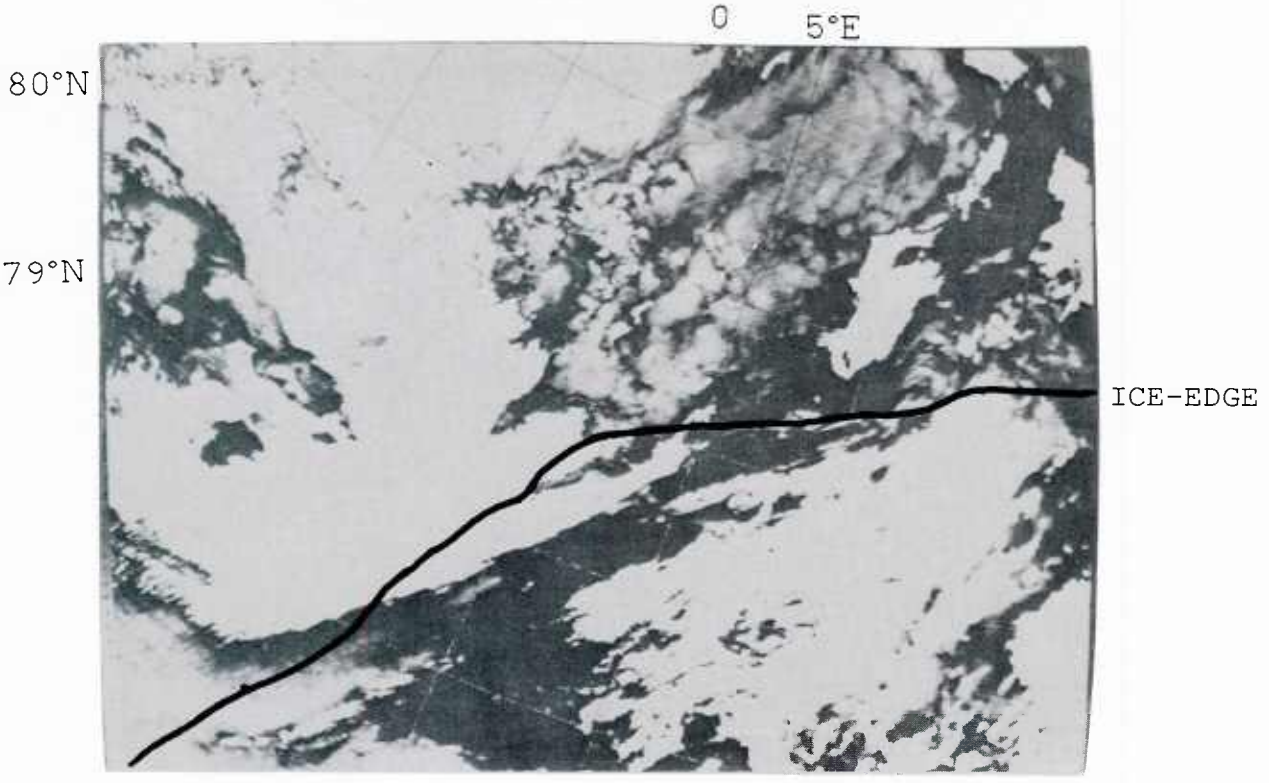

Figure 6d: NOAA-7 IR image 12 June 1984 1342 GMT.
Clouds, not seen on the visual channel, are detected on the IR channel. The ice edge as seen on the visual channel is marked with a black line.

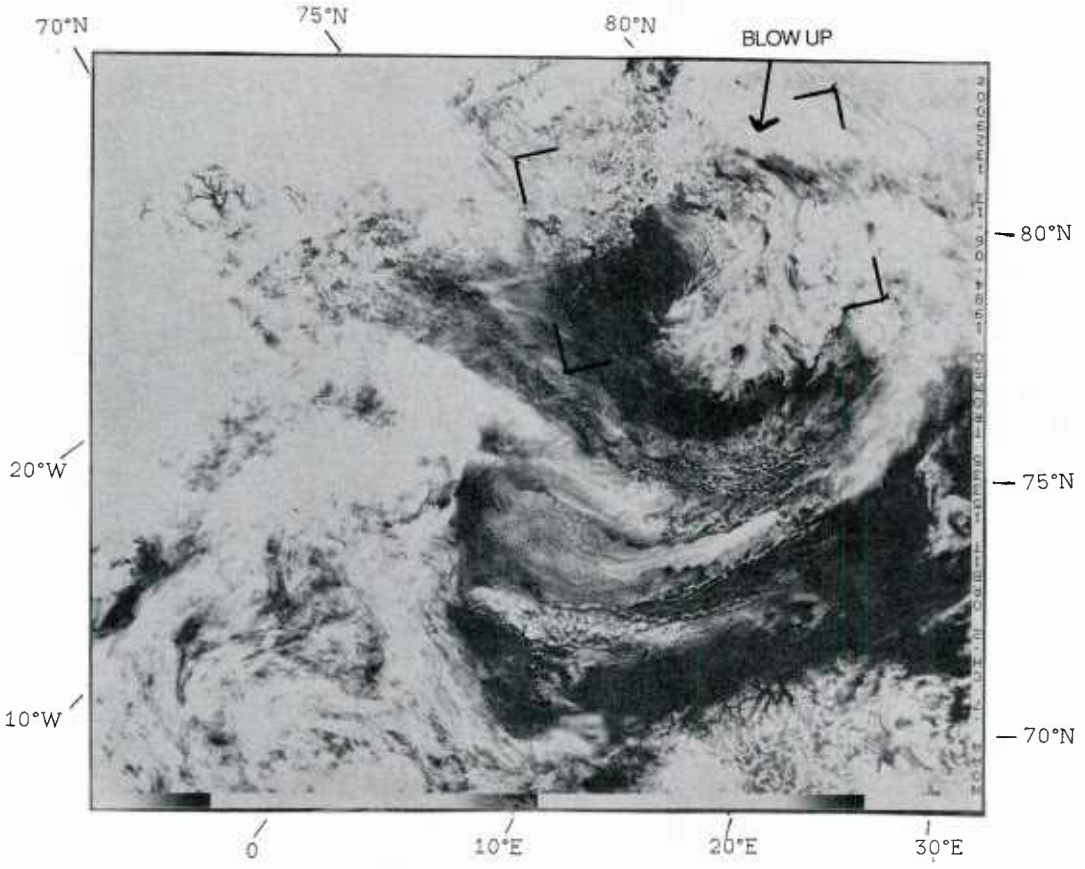

Figure 7a: NOAA-7 visual image 13 June 1984 1329 GMT.
The weather conditions in the MIZ area are rather calm. West of Spitzbergen the wind blows off-ice, and the ice edge in the Fram Strait is clearly seen.

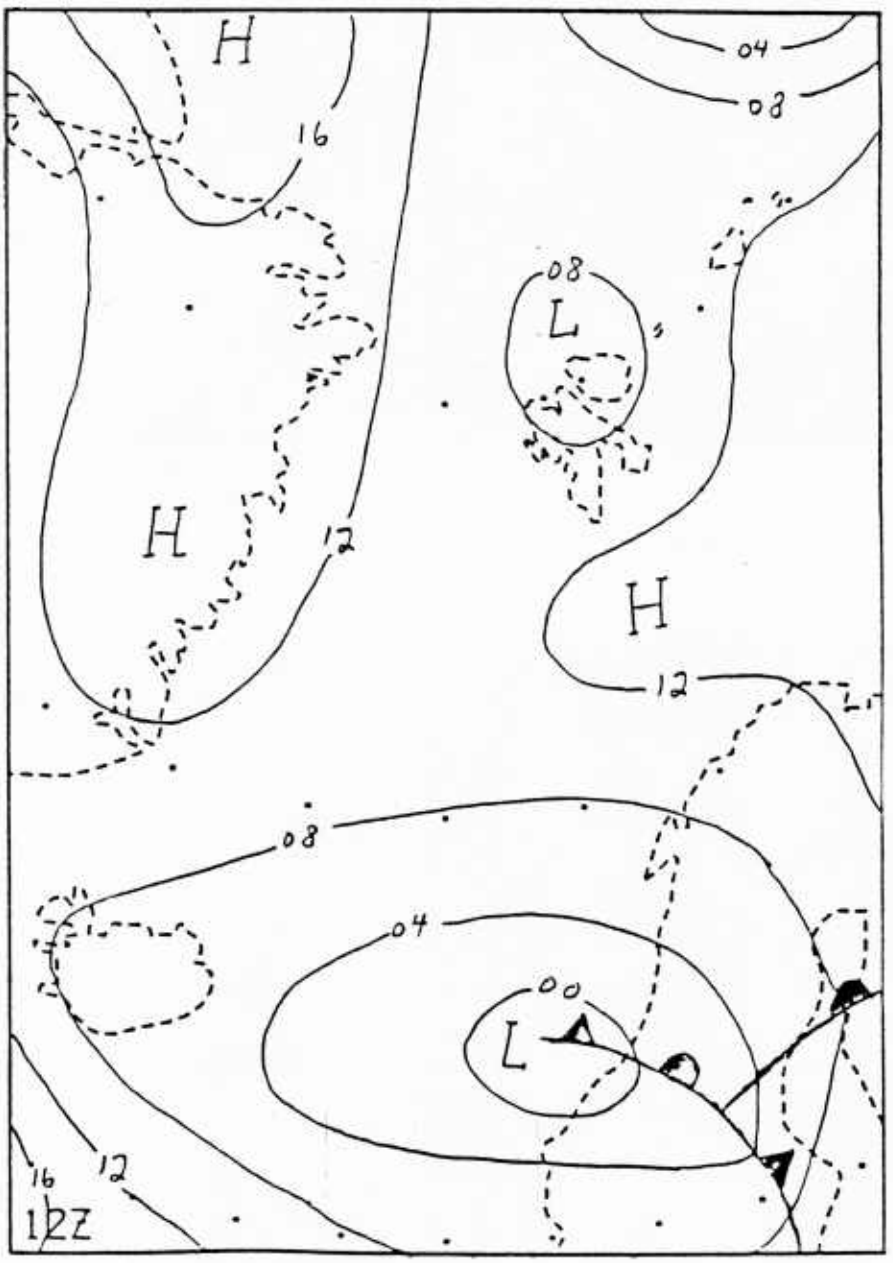

Figure 7b: Surface pressure chart 13 June 1984 1200 GMT.

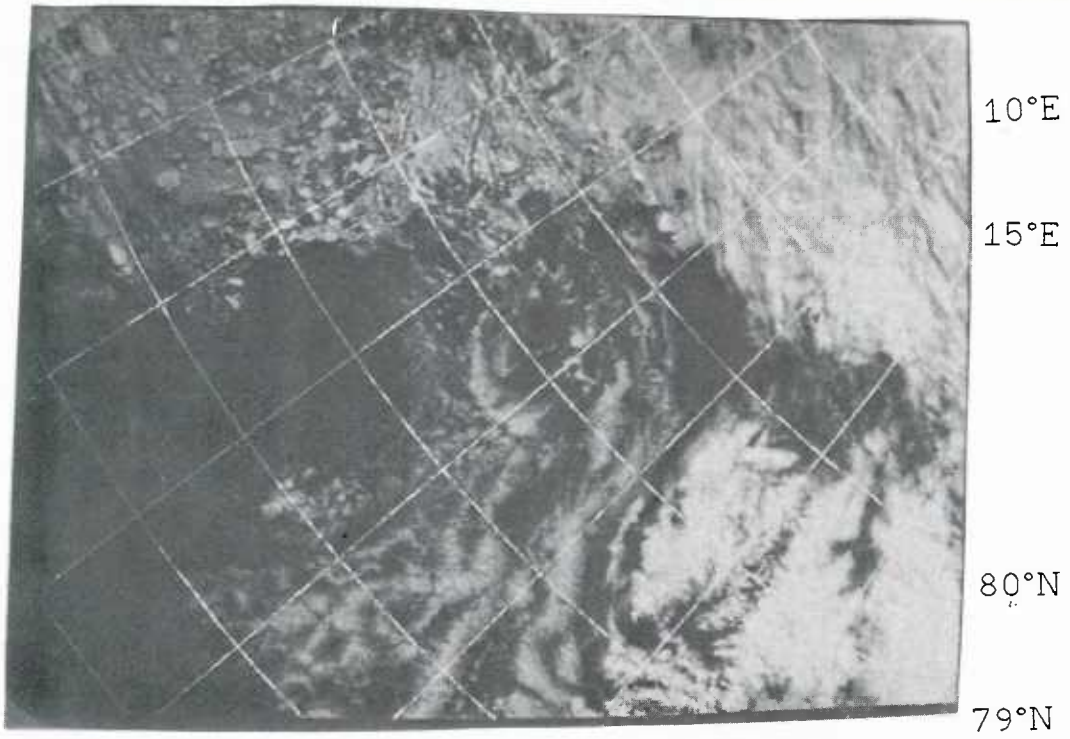

Figure 7c: NOAA-7 visual image 13 June 1984 1149 GMT.
The wind is blowing off-ice. Convective clouds are generated downstream from the ice edge.

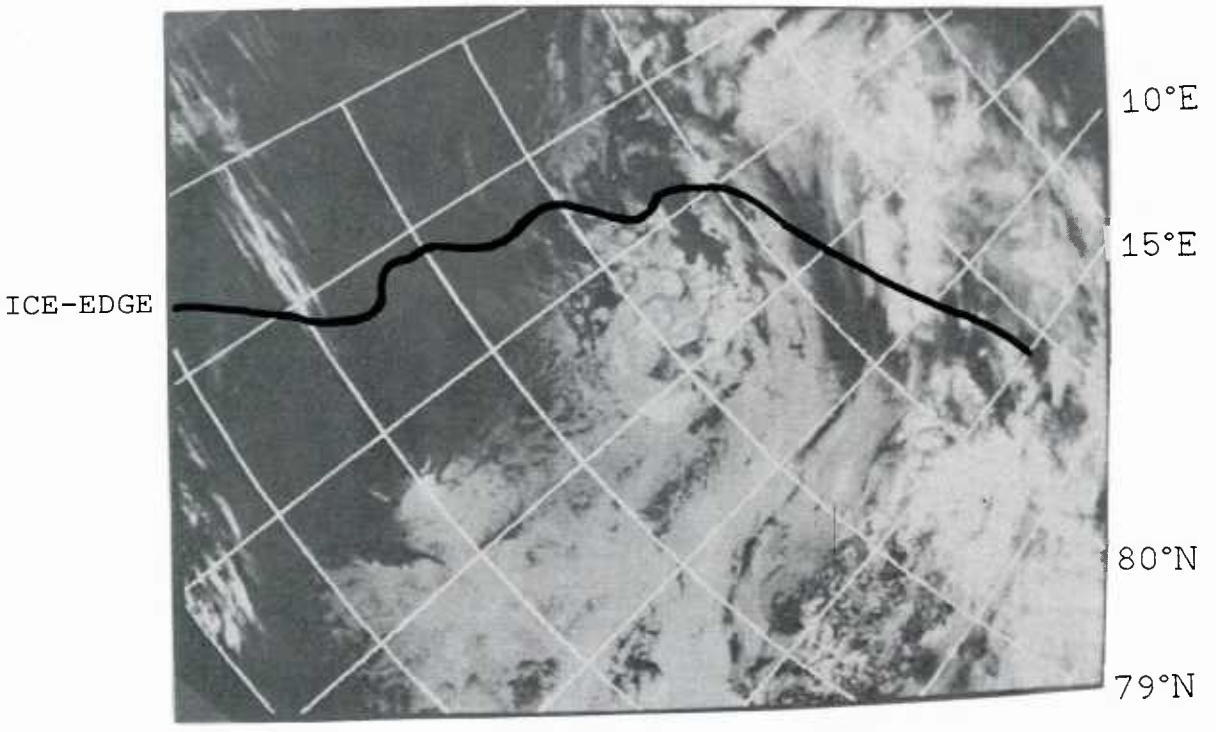

Figure 7d: NOAA-7 IR image 13 June 1984 1149 GMT.
The air-sea convection is clearly seen on the thermal image. The lack of contrast on the western half of the IR image shows that the temperature difference between the ice and the sea is small. The ice edge position is drawn on the image.

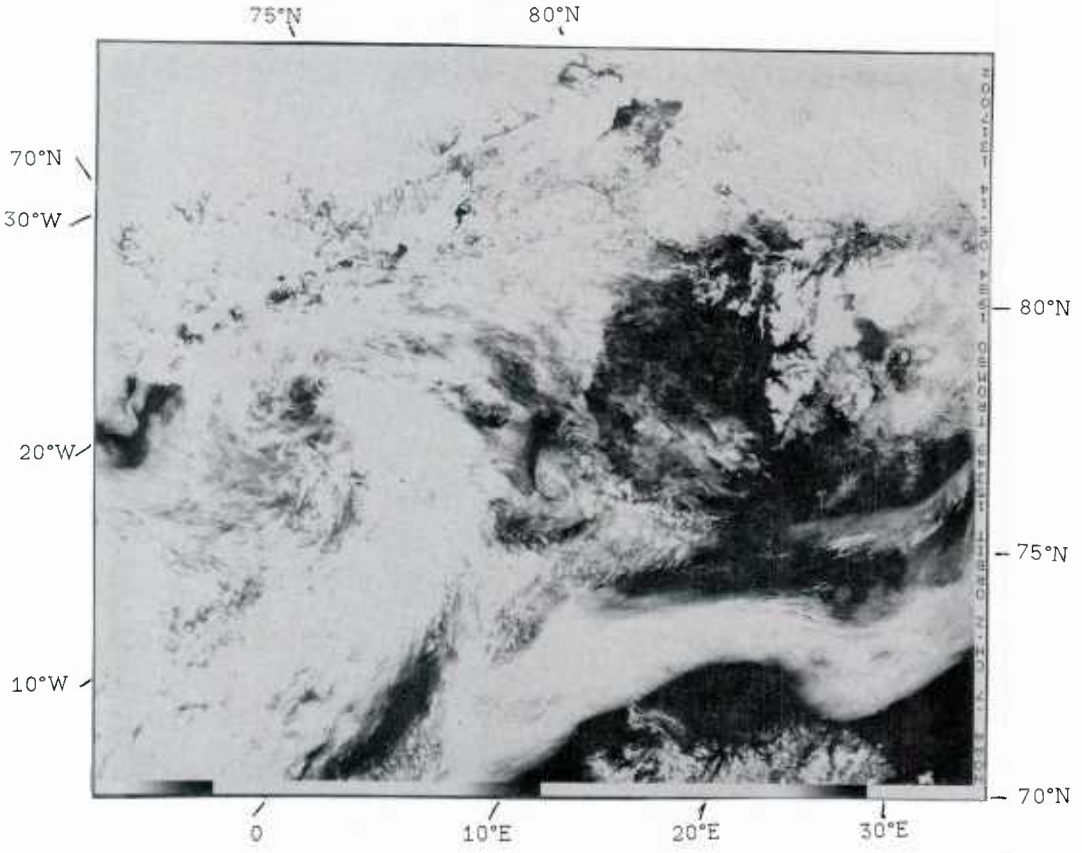

Figure 8a: NOAA-7 visual image 14 June 1984 1317 GMT.
The synoptic situation is dominated by a high over the Barents Sea and a high over Greenland and a low between Iceland and Spitzbergen. These pressure systems produce on-ice winds in the MIZ area.

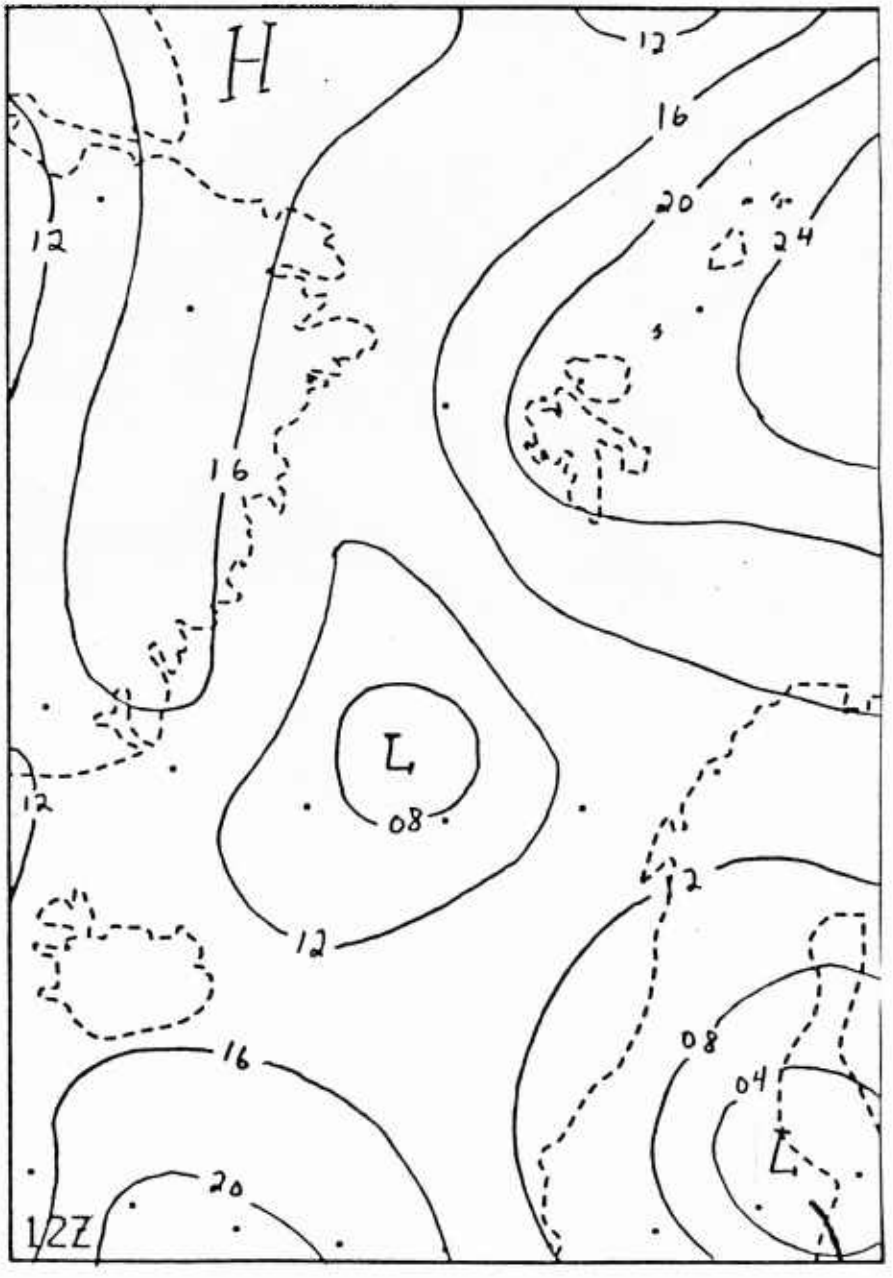

Figure 8b: Surface pressure chart 14 June 1984 1200 GMT.

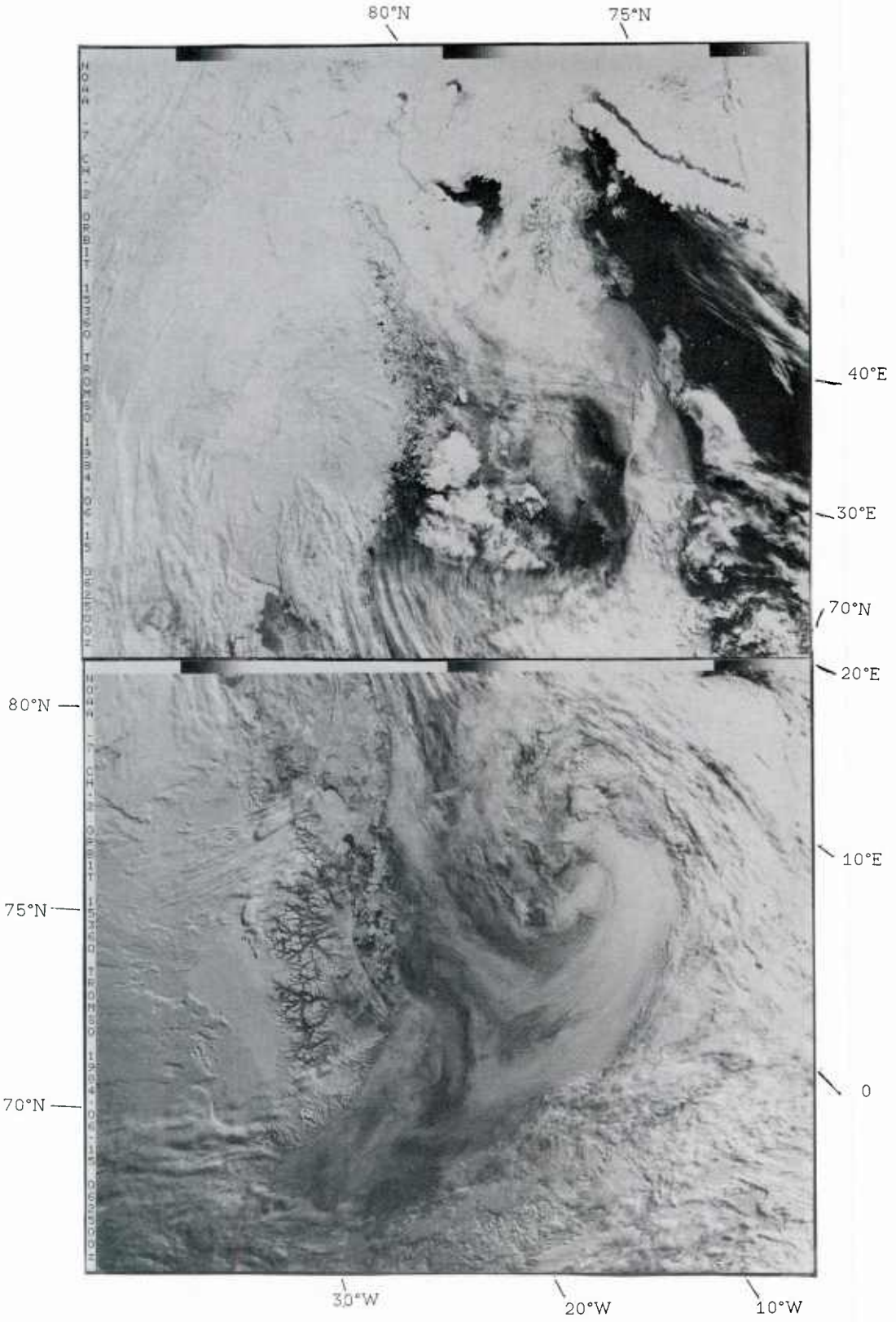

Figure 9a: NOAA-7 visual image 15 June 1984 0625 GMT.
The low pressure system from 14 June is still apparent, with a clearly defined vortex. It is centered at about 72°N and 0°E. North of Spitzbergen the wind is on-ice which usually gives a marginal ice zone convergence.

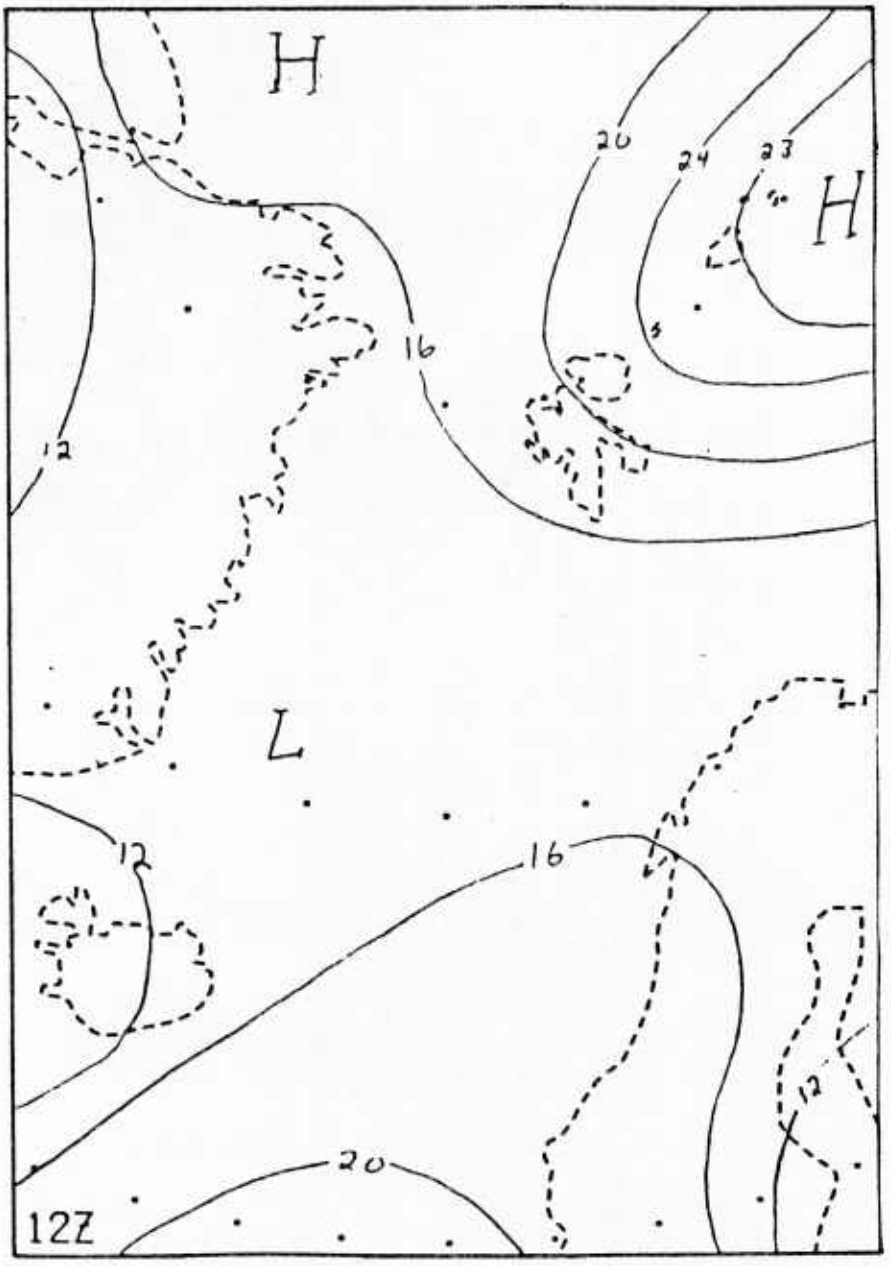

Figure 9b: Surface pressure chart 15 June 1984 1200 GMT.

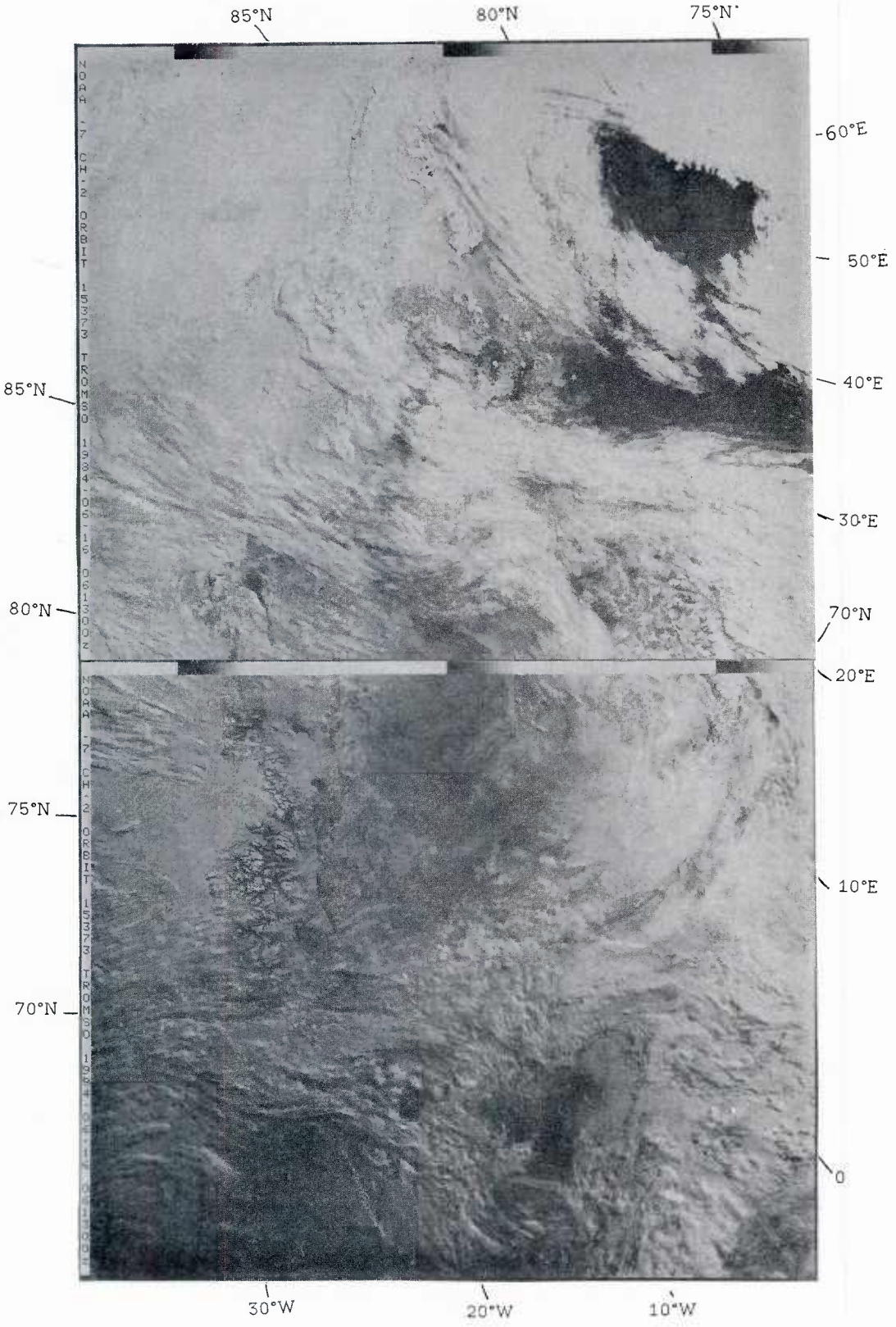

Figure 10a: NOAA-7 visual image 16 June 1984 0613 GMT.
The MIZ area is covered with clouds generated by cyclone activity over Spitzbergen and the Norwegian Sea, obscuring what happens at lower levels.

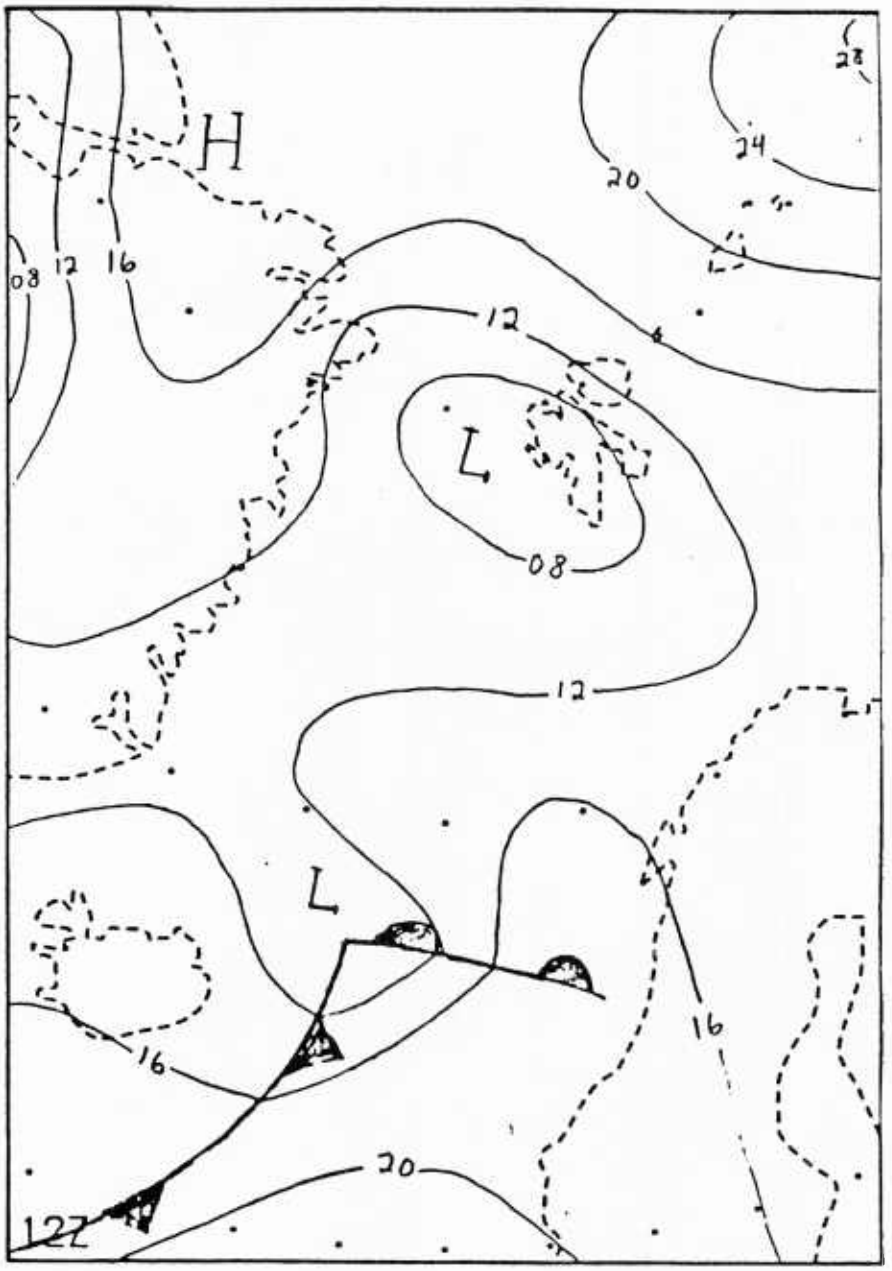

Figure 10b: Surface pressure chart 16 June 1984 1200 GMT.

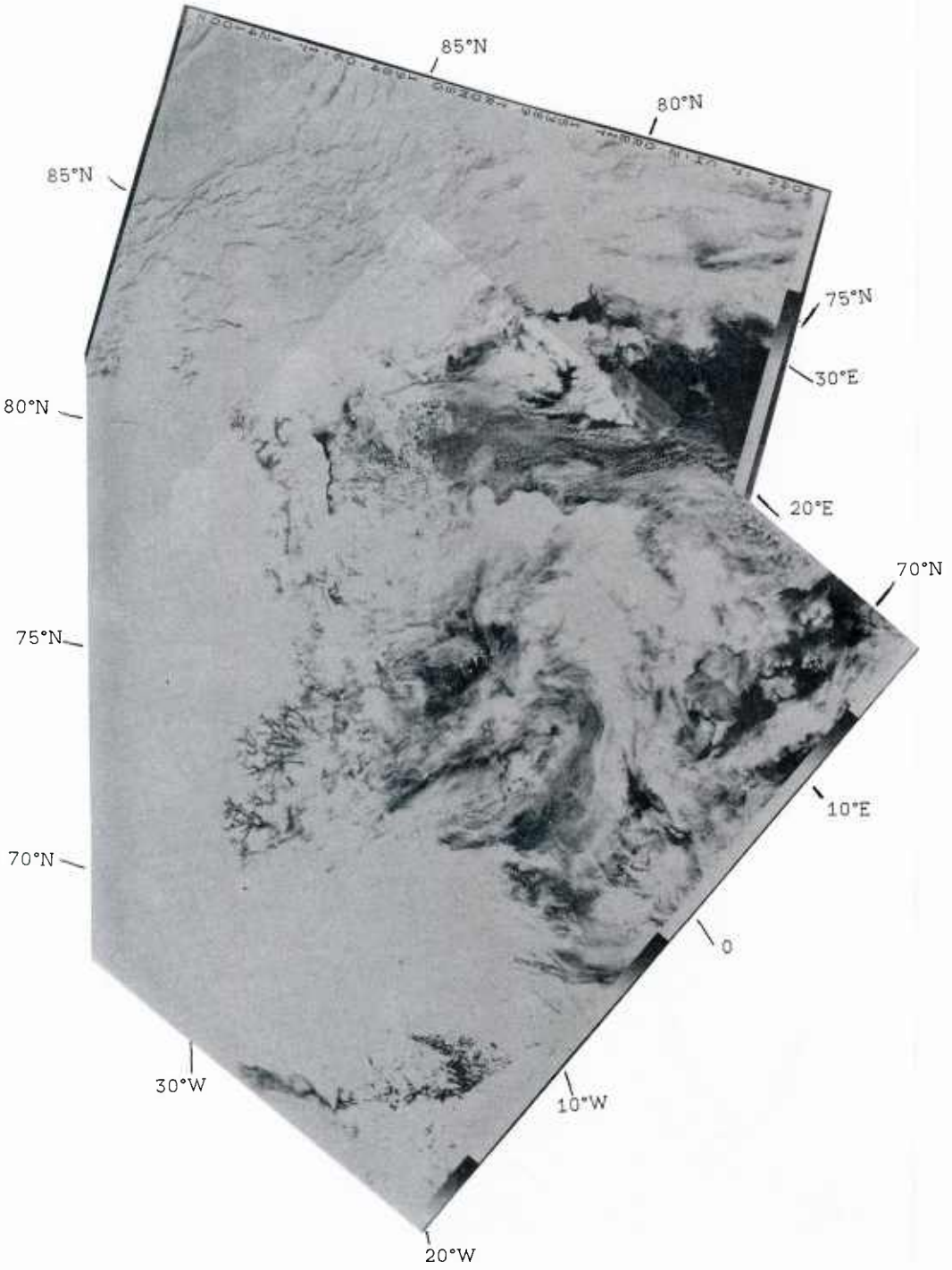

Figure 11a: NOAA-7 visual image 17 June 1984 1241 GMT.
The low from 14 June has now moved northwest of Spitzbergen. A warm high pressure ridge has moved into the southern MIZ area. There the warm midlatitude airmass meets the cold arctic air that is pumped southwards by the low northwest of Spitzbergen, resulting in strong rising motions generating clouds. The wind blows off-ice in the MIZ area, and in the eastern Fram Strait the typical cloud streets are visible.

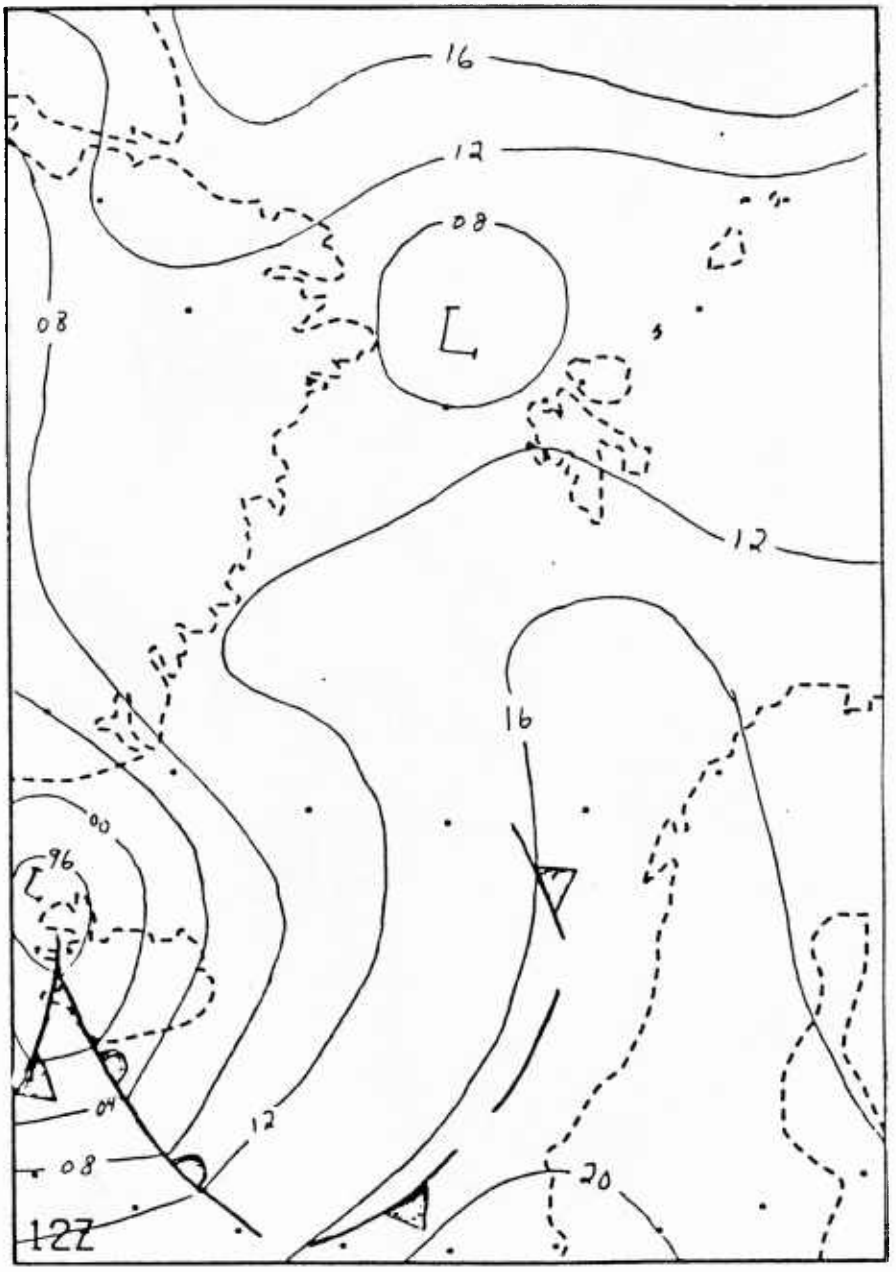

Figure 11b: Surface pressure chart 17 June 1984 1200 GMT.

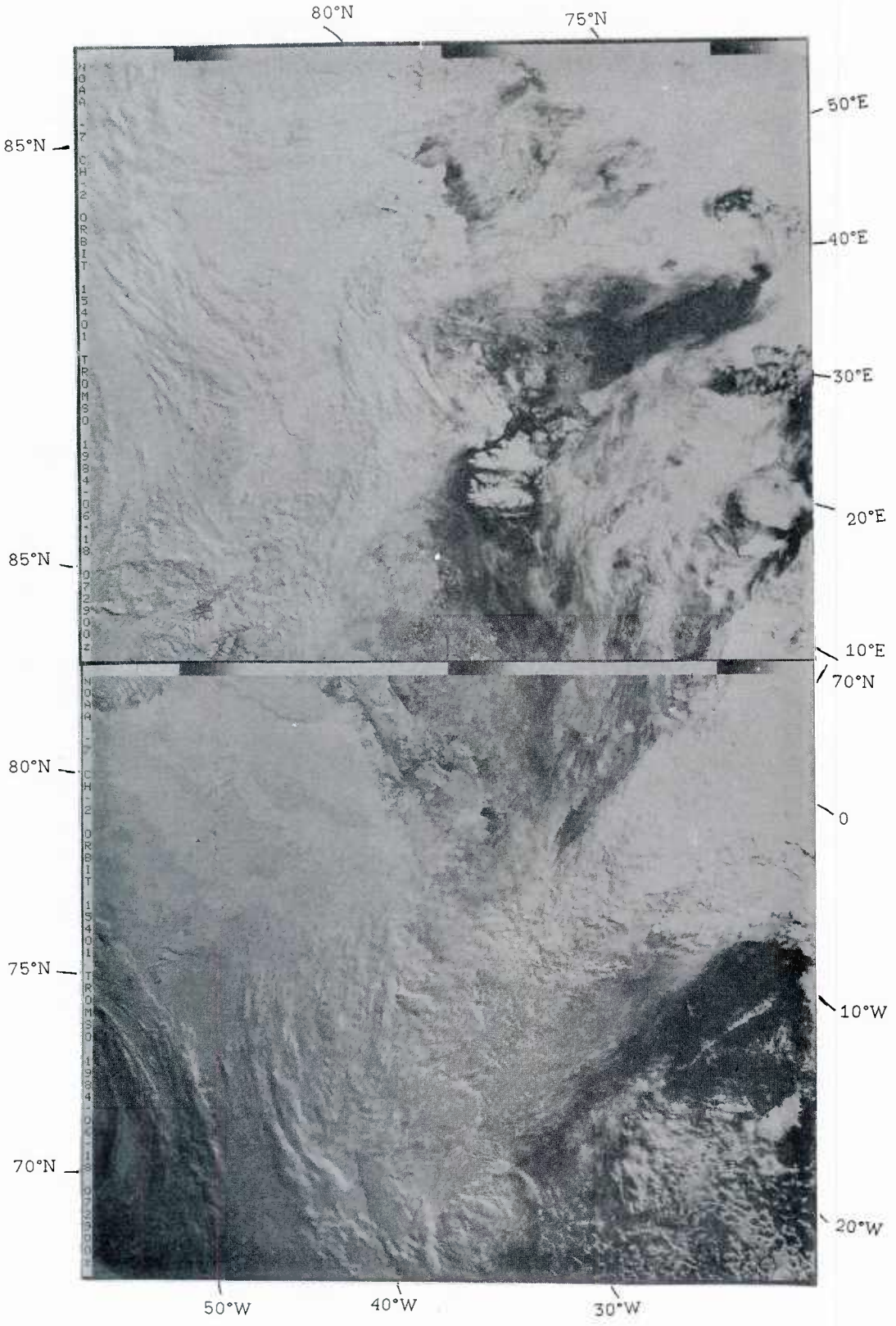

Figure 12a: NOAA-7 visual image 18 June 1984 0729 GMT.
There are only weak winds in the northern MIZ area, while the southern part is influenced by a deep low at Jan Mayen, that is generating heavy clouds. A mesoscale vortice is seen in the Barents Sea at about 75°N, 45°E.

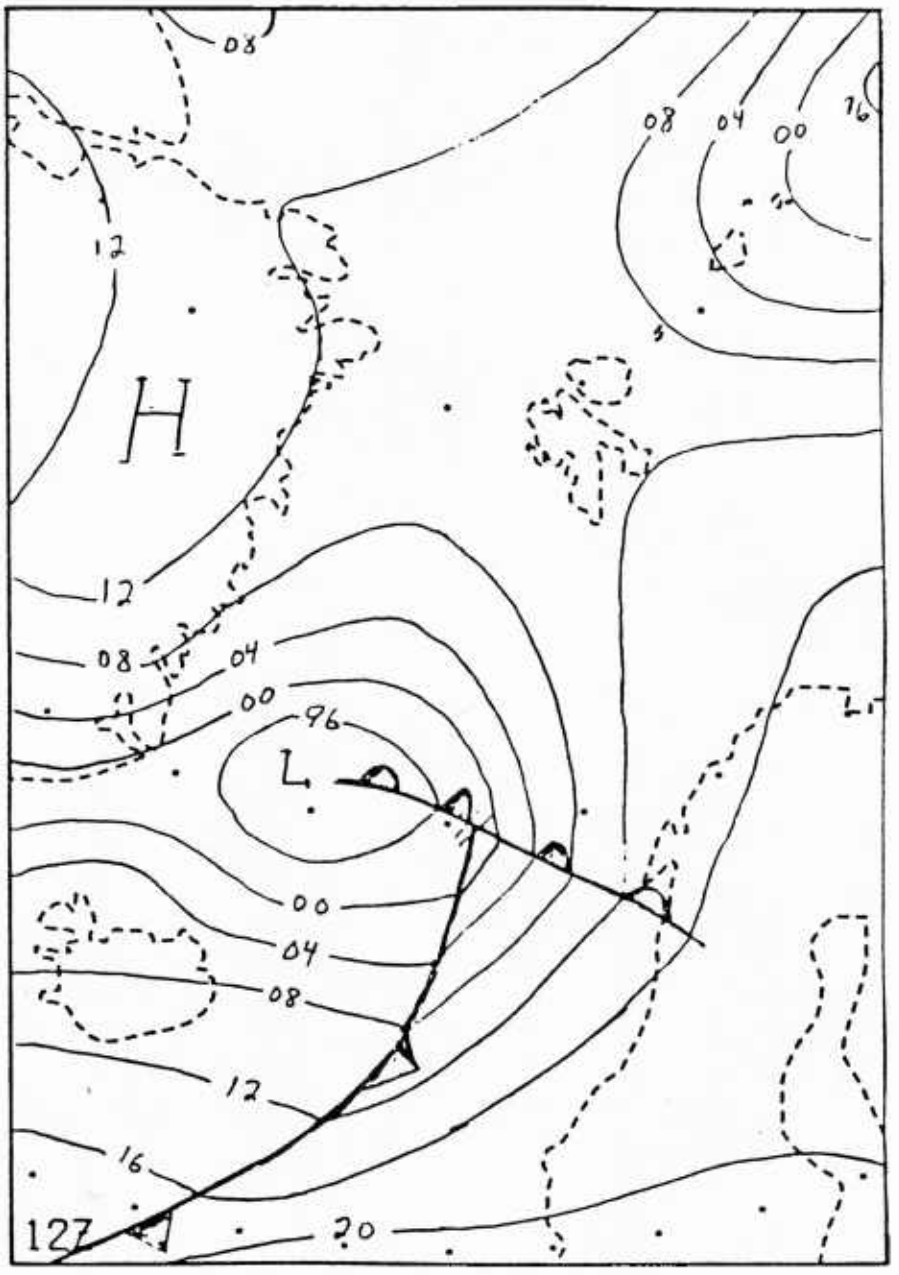

Figure 12b: Surface pressure chart 18 June 1984 1200 GMT.

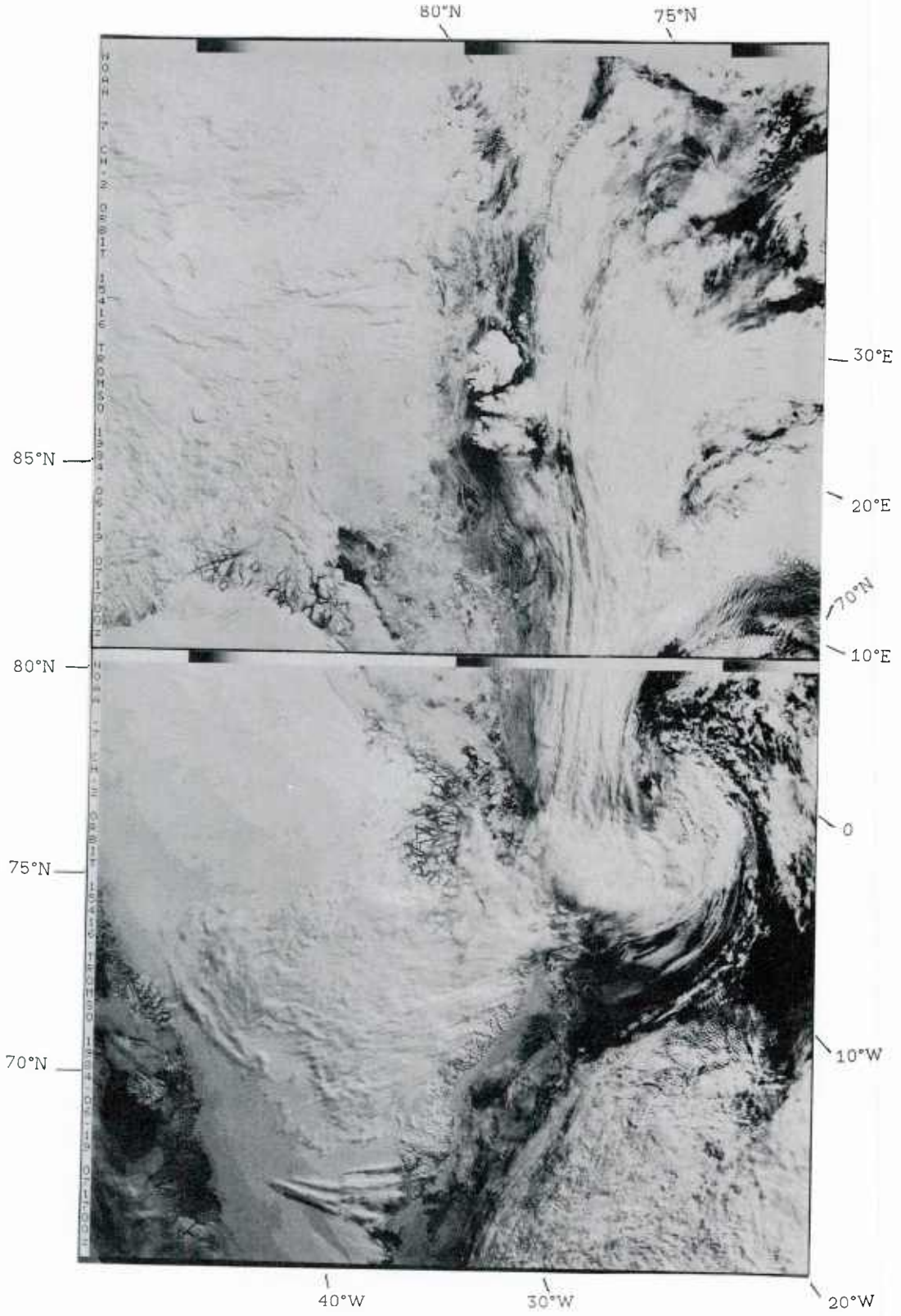

Figure 13a: NOAA-7 visual image 19 June 1984 0717 GMT.
The Jan Mayen low deepens and moves northeast. The winds in the MIZ area are strong, blowing from northeast. That is, off the northern ice edge, thereby generating the typical cloud streets seen along the northwestern ice edge in the Fram Strait. The Icelandic mountains generate high level mountain waves, clearly visible in the lower right of the image.

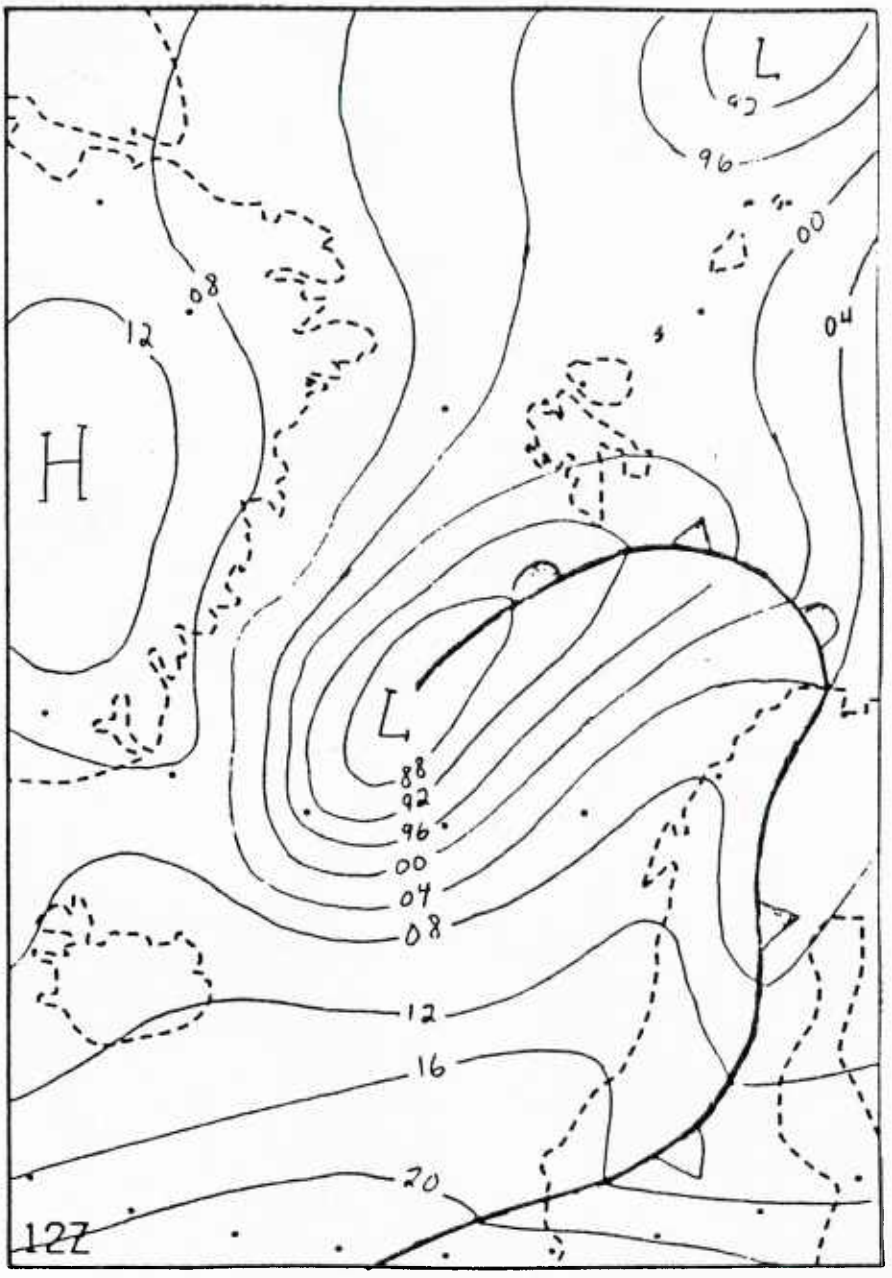

Figure 13b: Surface pressure chart 19 June 1984 1200 GMT.

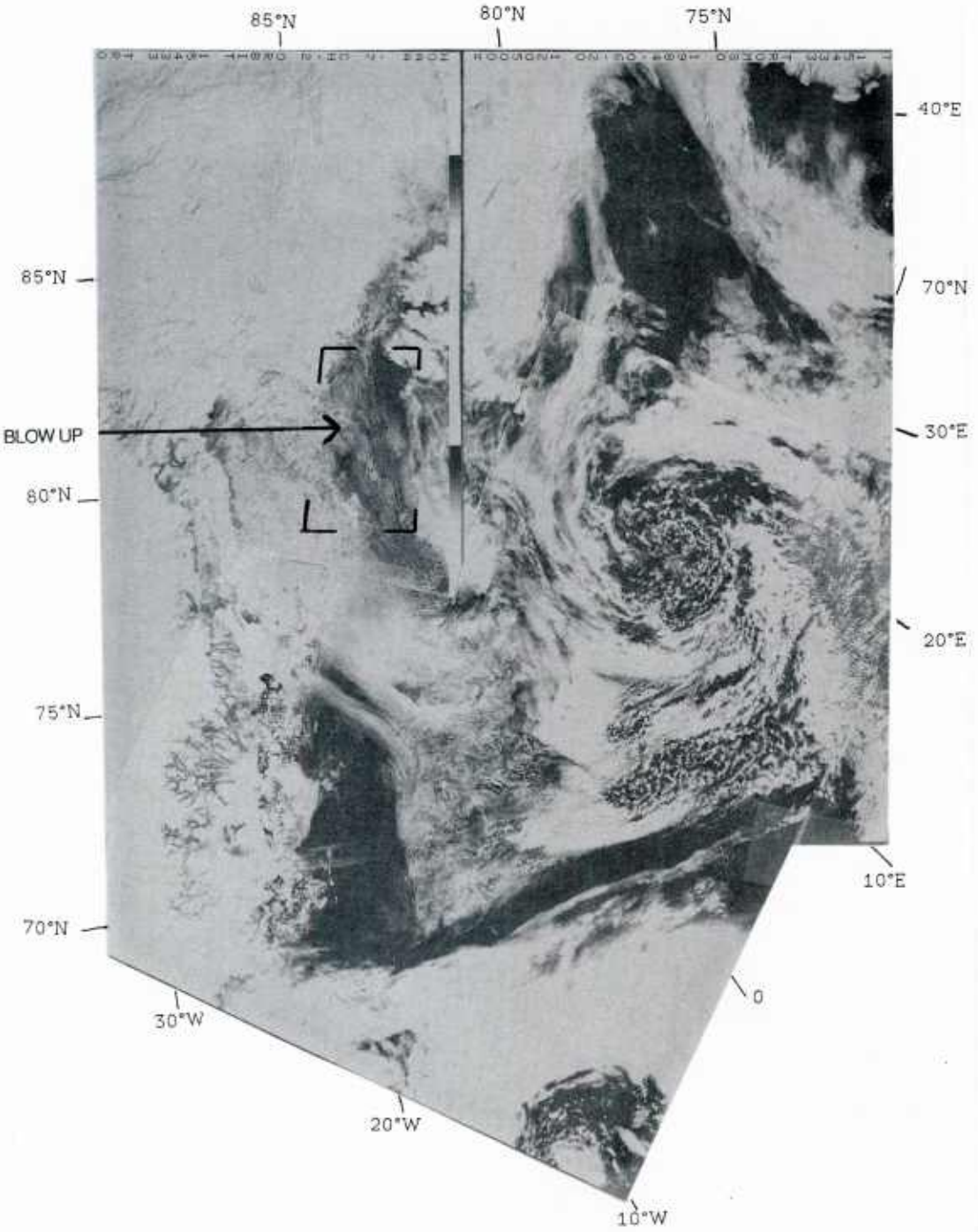

Figure 14a: NOAA-7 visual image 20 June 1984 1205 GMT.
The low looses a little power and has moved to a position south of Spitzbergen. (On the satellite image it is further east than on the surface chart.) There are off-ice winds along the Fram Strait ice edge, generating cloud streets downwind from it. Some mesoscale vortices are visible at 70°N, 10°W, nearby Jan Mayen.

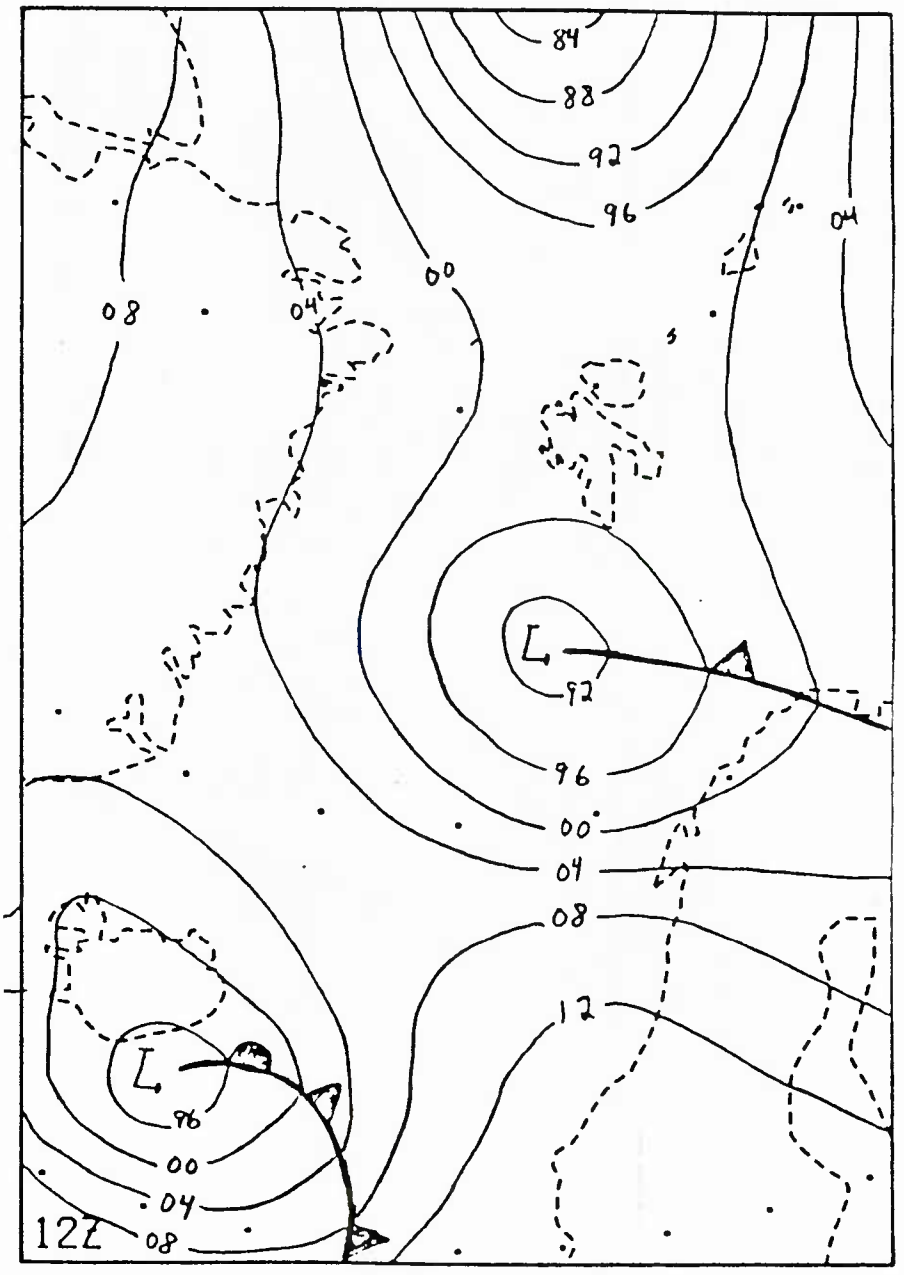

Figure 14b: Surface pressure chart 20 June 1984 1200 GMT.

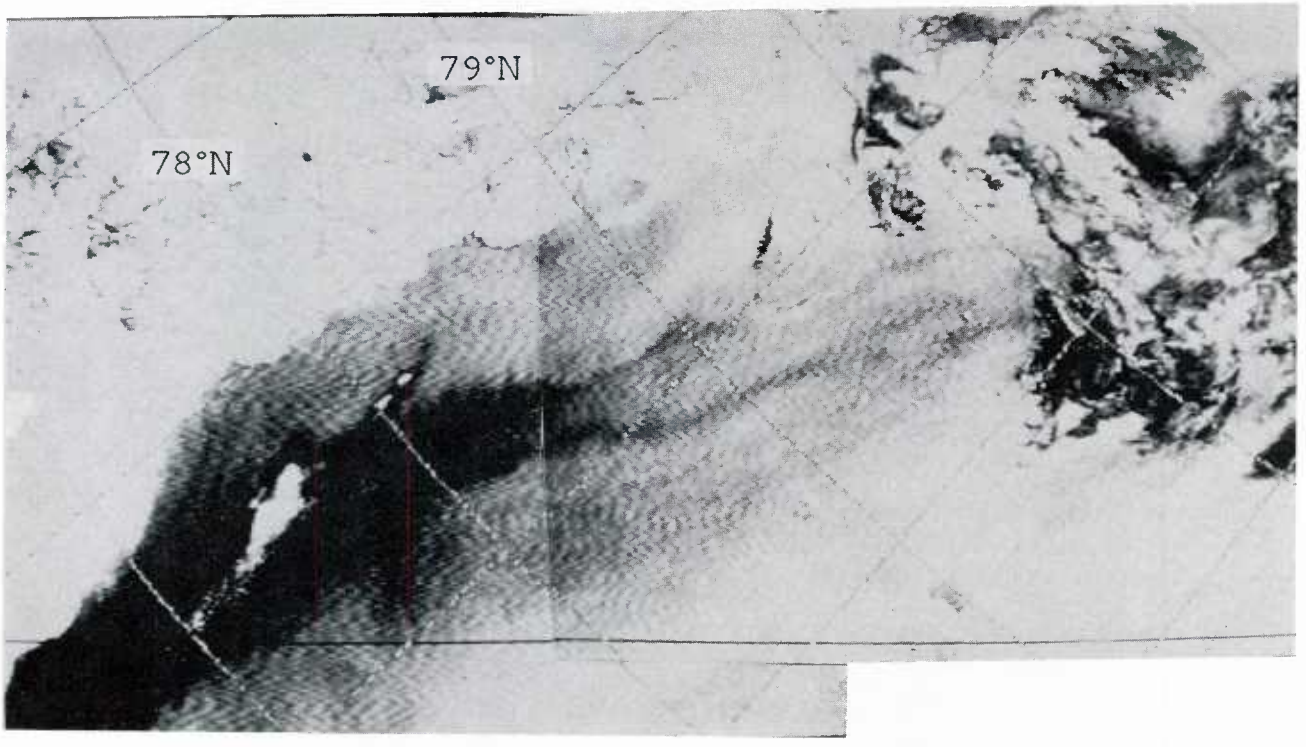

Figure 14c: NOAA-7 IR image 20 June 1984 1205 GMT.
The wind is blowing off-ice (5-10m/s) and the heat convection between the cold arctic air and the warmer ocean surface is clearly seen. There is a wave pattern in the convection clouds with a wavelength of ≈9 km.

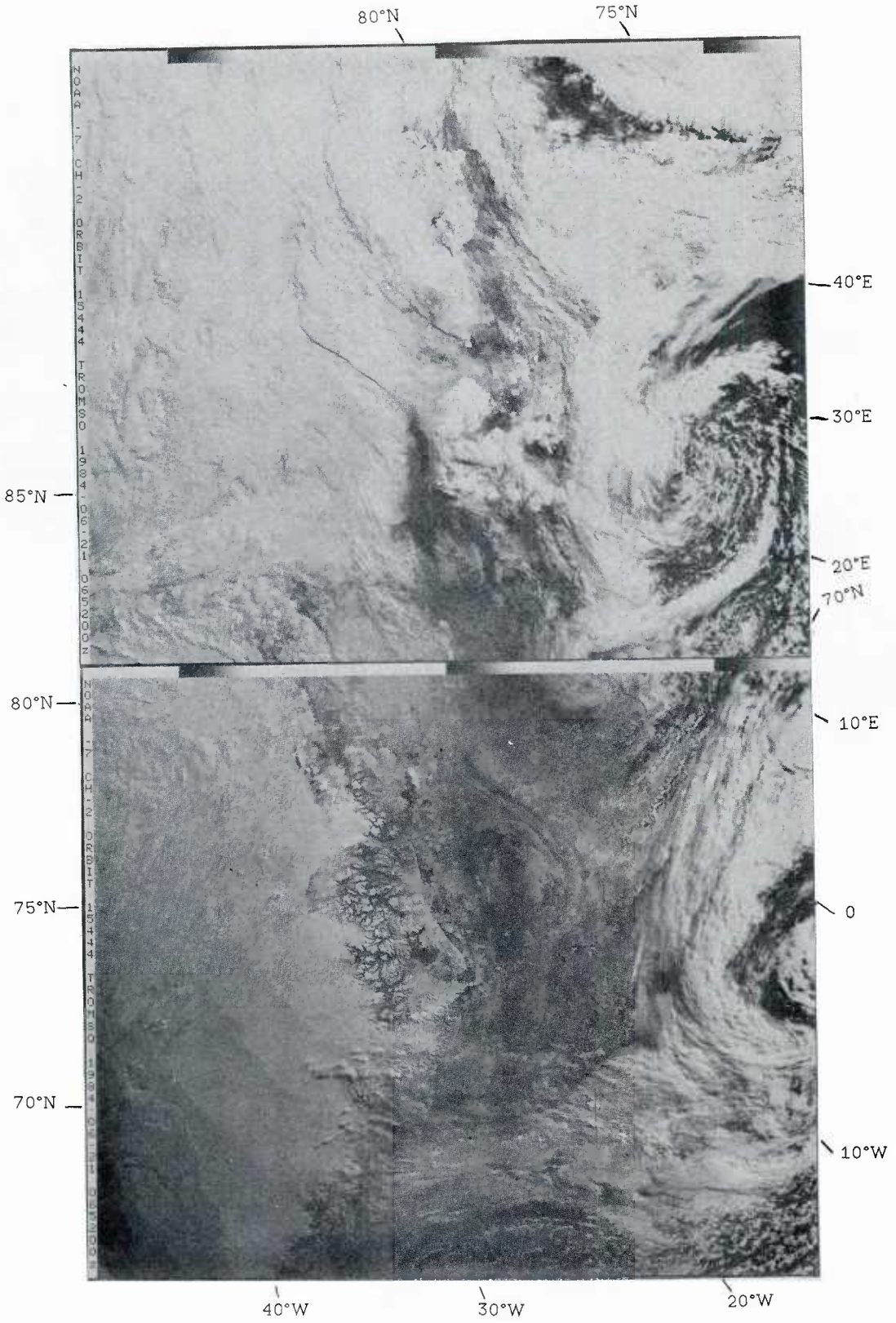

Figure 15a: NOAA-7 visual image 21 June 1984 0652 GMT.
The wind in the MIZ area is still blowing off-ice, but weakens as the low south of Spitzbergen moves eastwards.

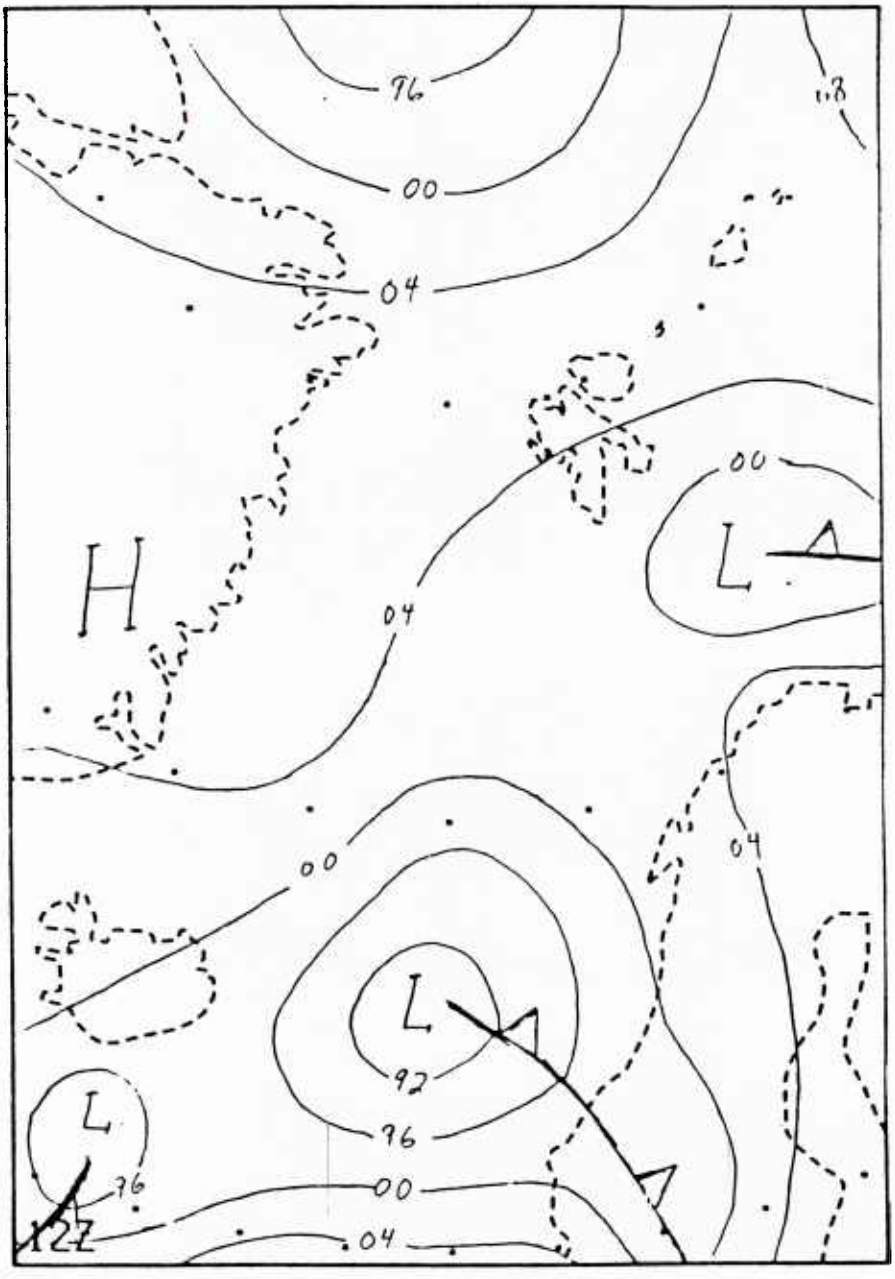

Figure 15b: Surface pressure chart 21 June 1984 1200 GMT.

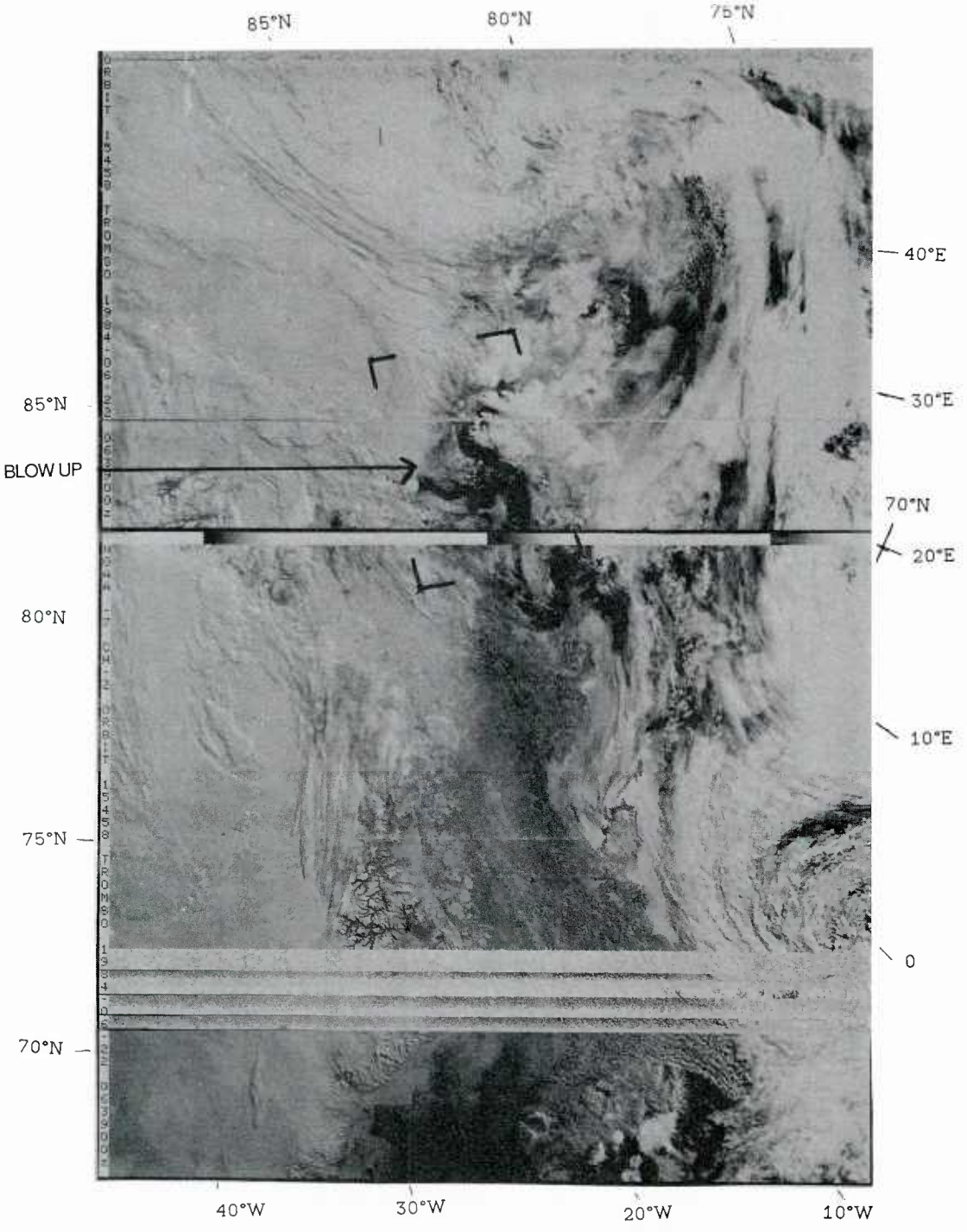

Figure 16a: NOAA-7 visual image 22 June 1984 0639 GMT. Weak winds prevail in the MIZ area. The surface chart shows a weak ridge with its axis directed WNW-ESE over Spitzbergen, giving subsidence in the eastern Fram Strait. Embedded in the large scale flow, there are some mesoscale vortices, probably generated by the topography of Spitzbergen.

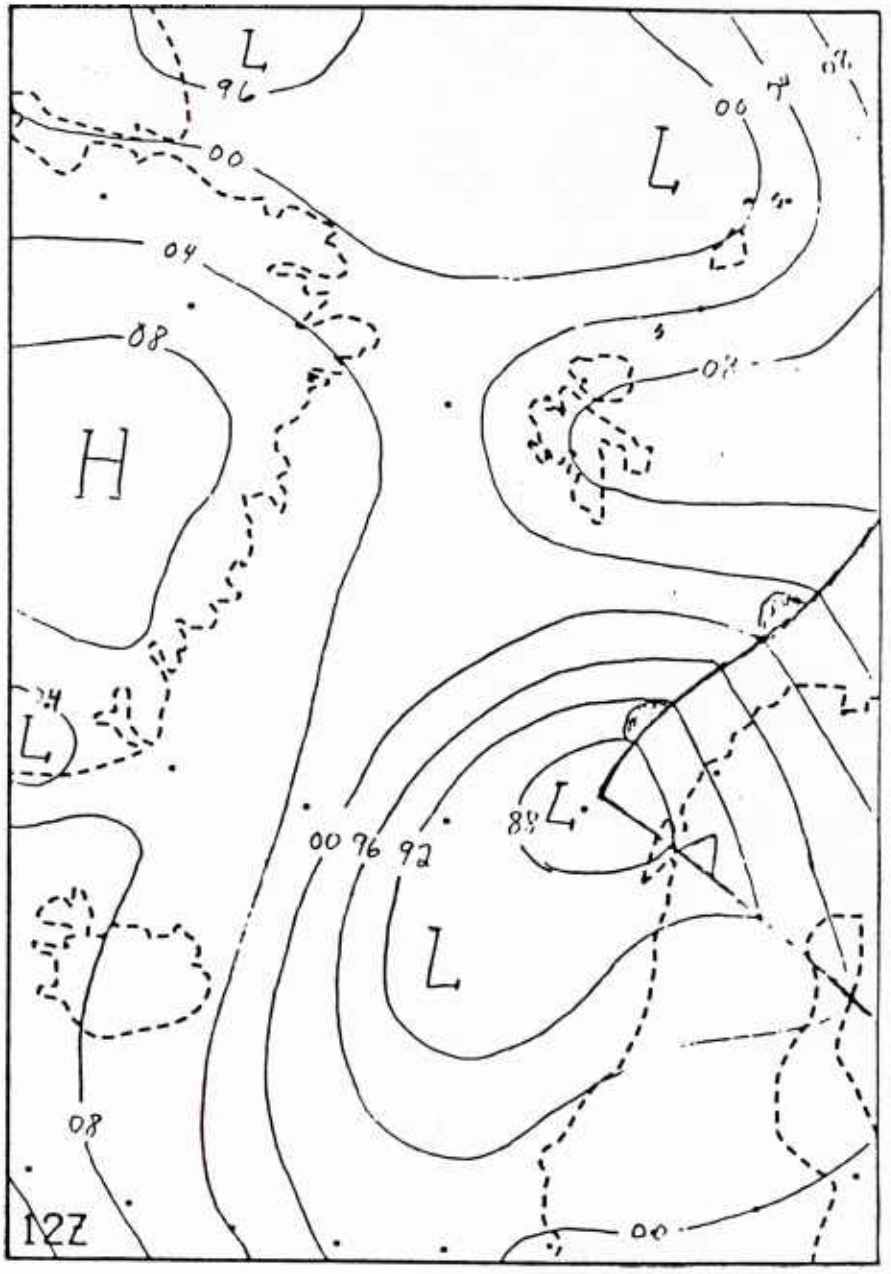

Figure 16b: Surface pressure chart 22 June 1984 1200 GMT.

Figure 16c: NOAA-7 visual image 22 June 1984 0639 GMT. Note the mesoscale vortex on the northwest coast of Spitzbergen. The generating mechanism could be the horizontal shear of the wind, resulting from the northerly mesoscale ice-sea breeze and the southerly geostrophic wind. The in situ observations from MIZEX-84 (Lindsay 1985) confirm this explanation.

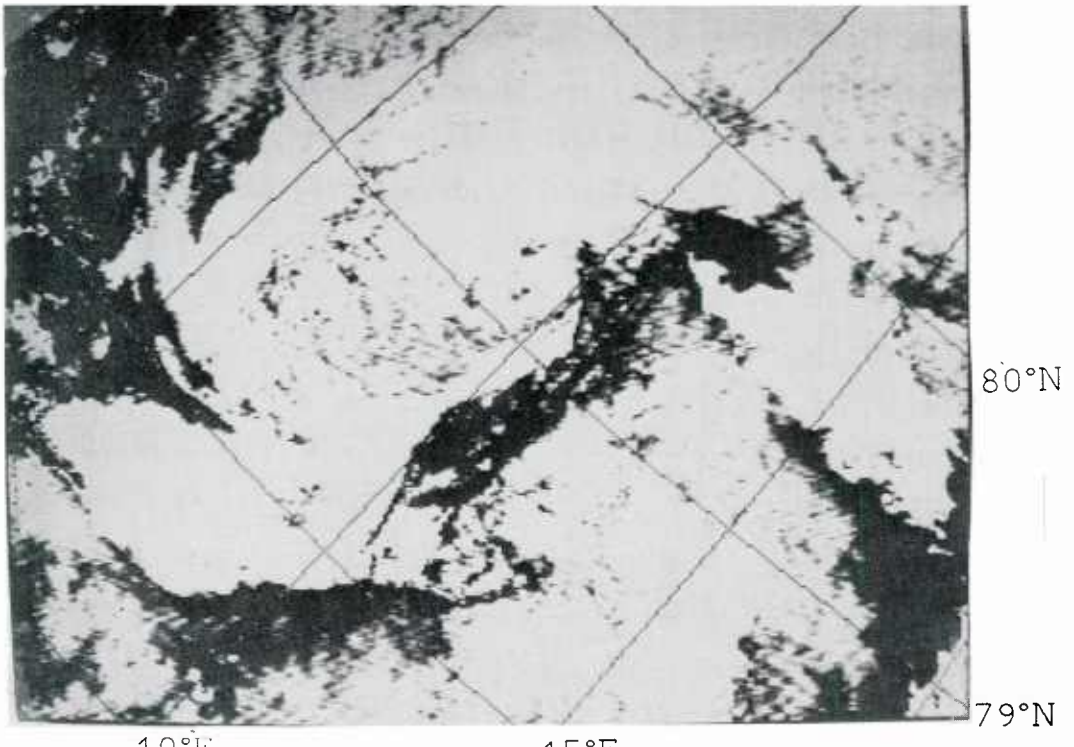

Figure 16d: NOAA-7 IR image 22 June 1984 0639 GMT. The thermal image does not show the same clear signature of the vortex, but shows a large temperature contrast in its area. This suggests that both barotropic and baroclinic effects are involved in the generation of the vortex.

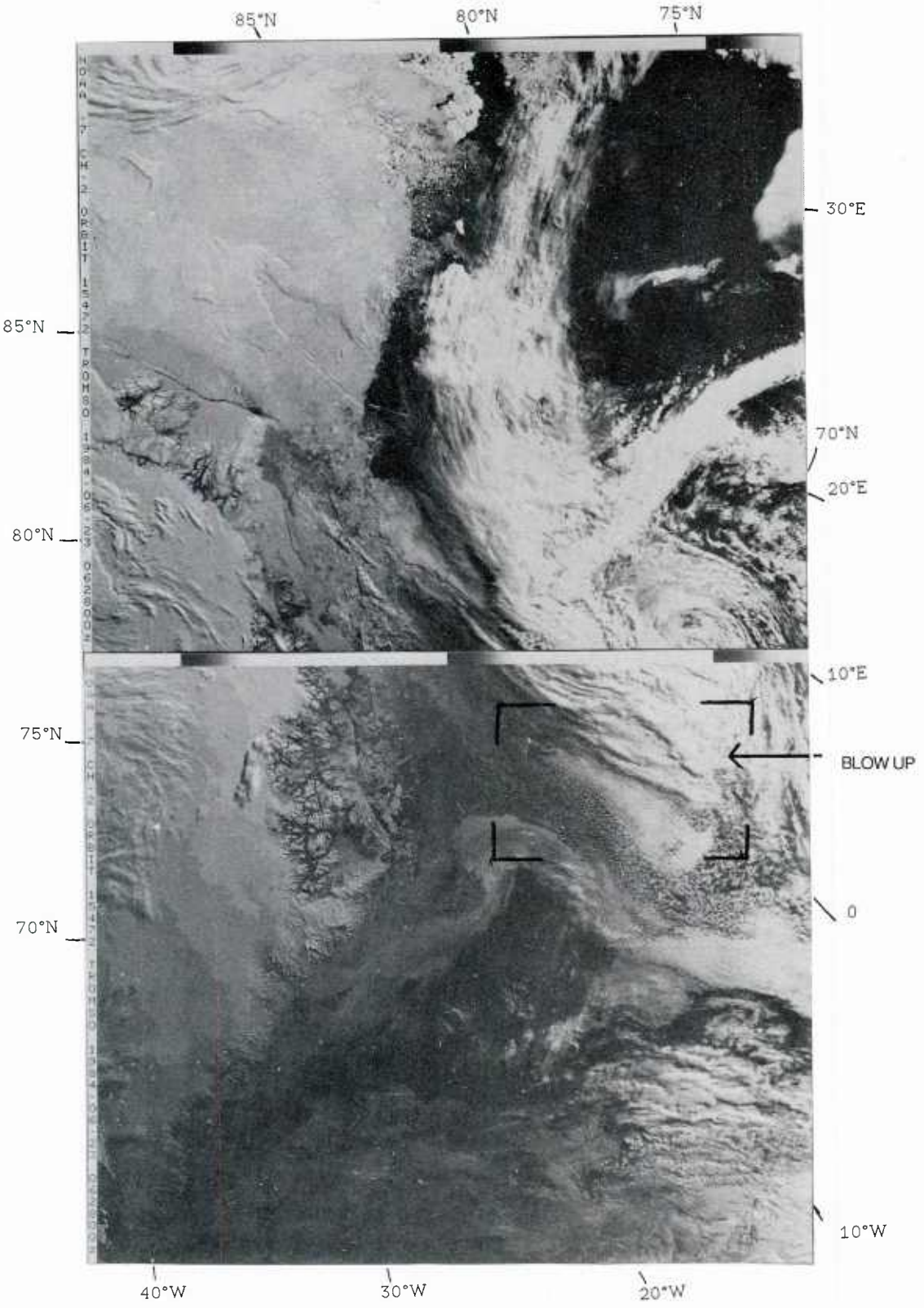

Figure 17a: NOAA-7 visual image 23 June 1984 0628 GMT. A well developed low in the Norwegian Sea creates a northwesterly wind over the Fram Strait. Some off-ice cloud streets are seen, but the most peculiar feature on the image is the wavy lane of clouds at Jan Mayen.

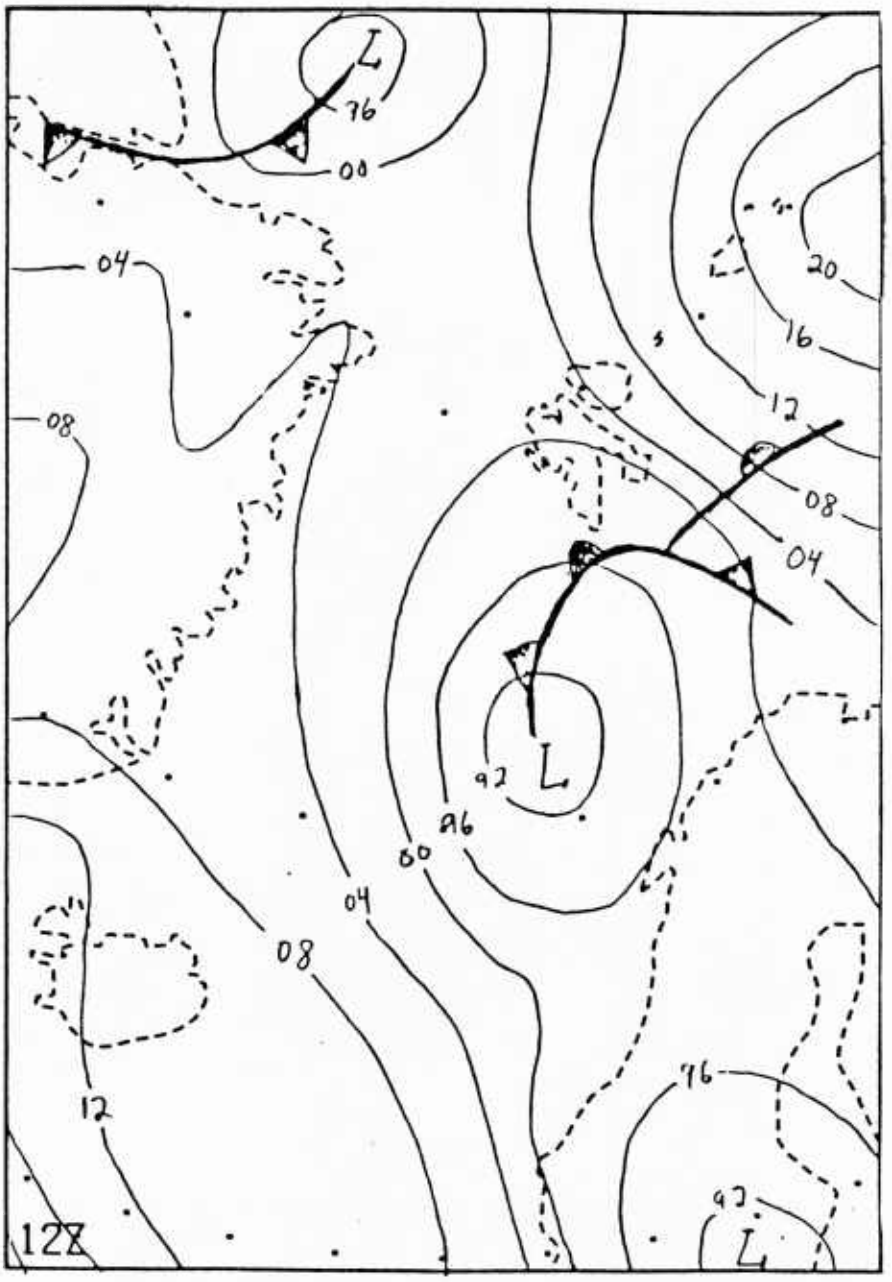

Figure 17b: Surface pressure chart 23 June 1984 1200 GMT.

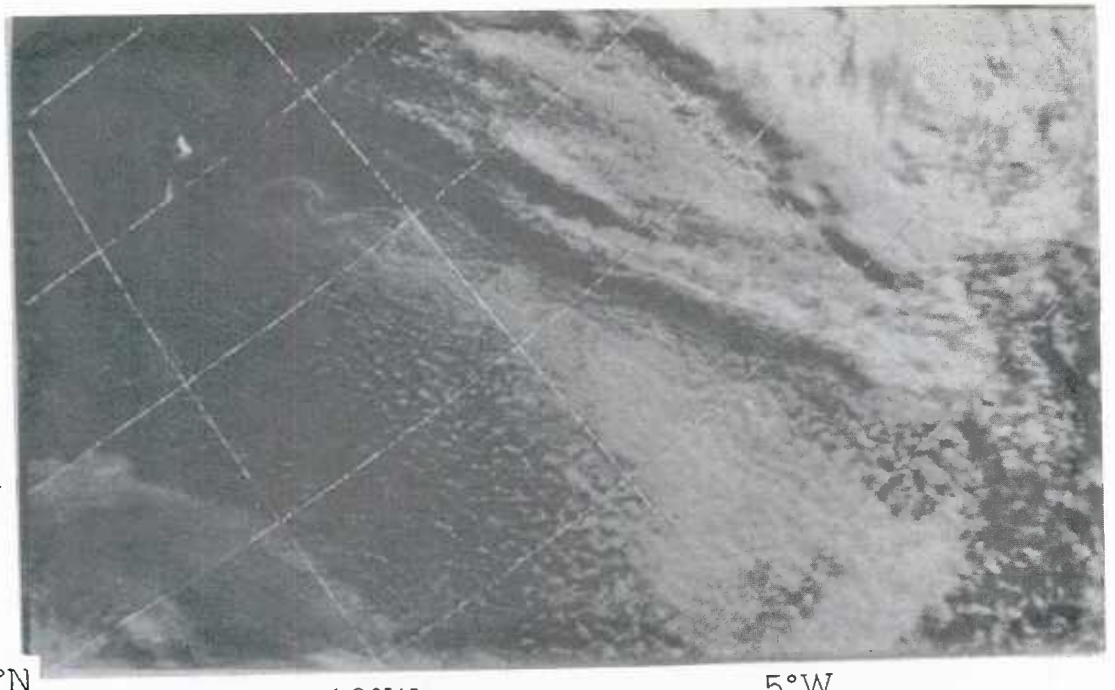

Figure 17c: NOAA-7 visual image 23 June 1984 0628 GMT.
The wave lane generated in the wake of Jan Mayen is clearly seen. The wavelength is estimated to be 55 km. The wave pattern indicates that the wake is unstable, and that atmospheric conditions are close to those which lead to vortex shedding (Gjevik and Marthinsen 1978).

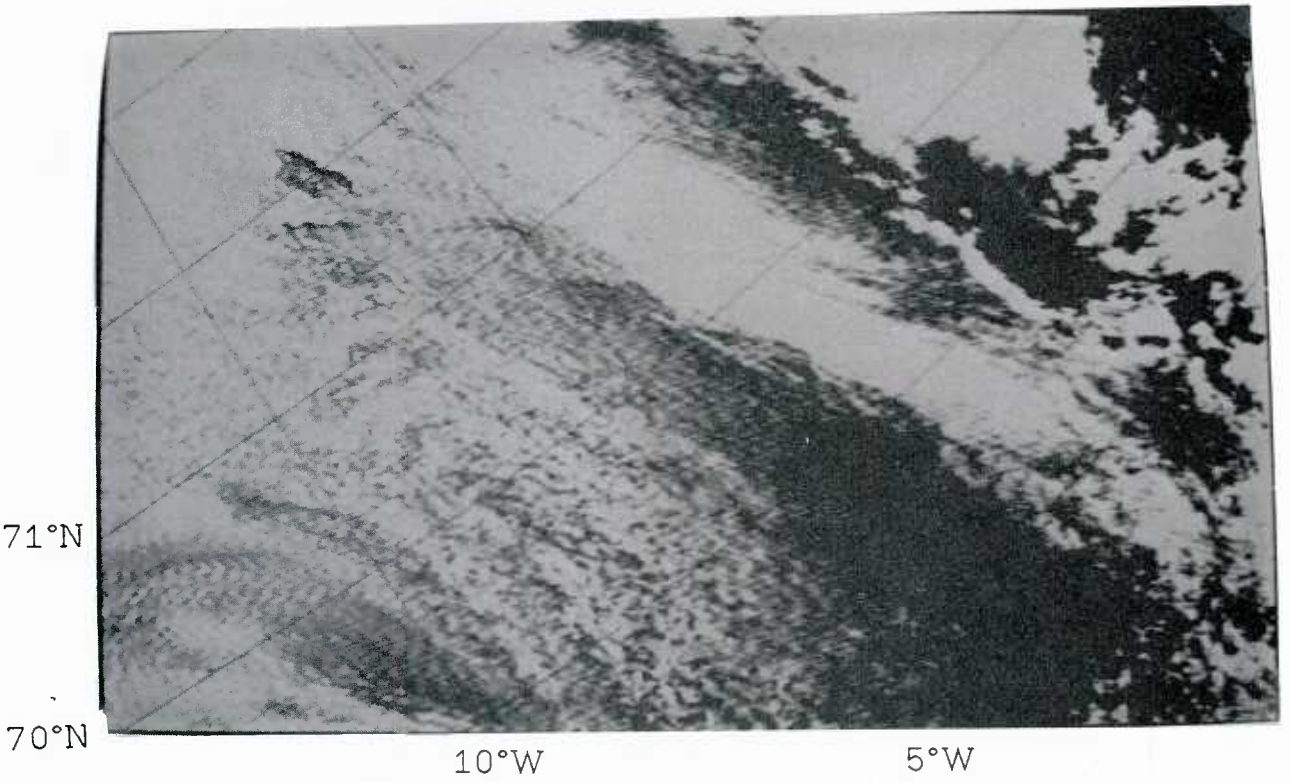

Figure 17d: NOAA-7 IR image 23 June 1984 0628 GMT.
The thermal image does not show the same clear signature of the wave lane.

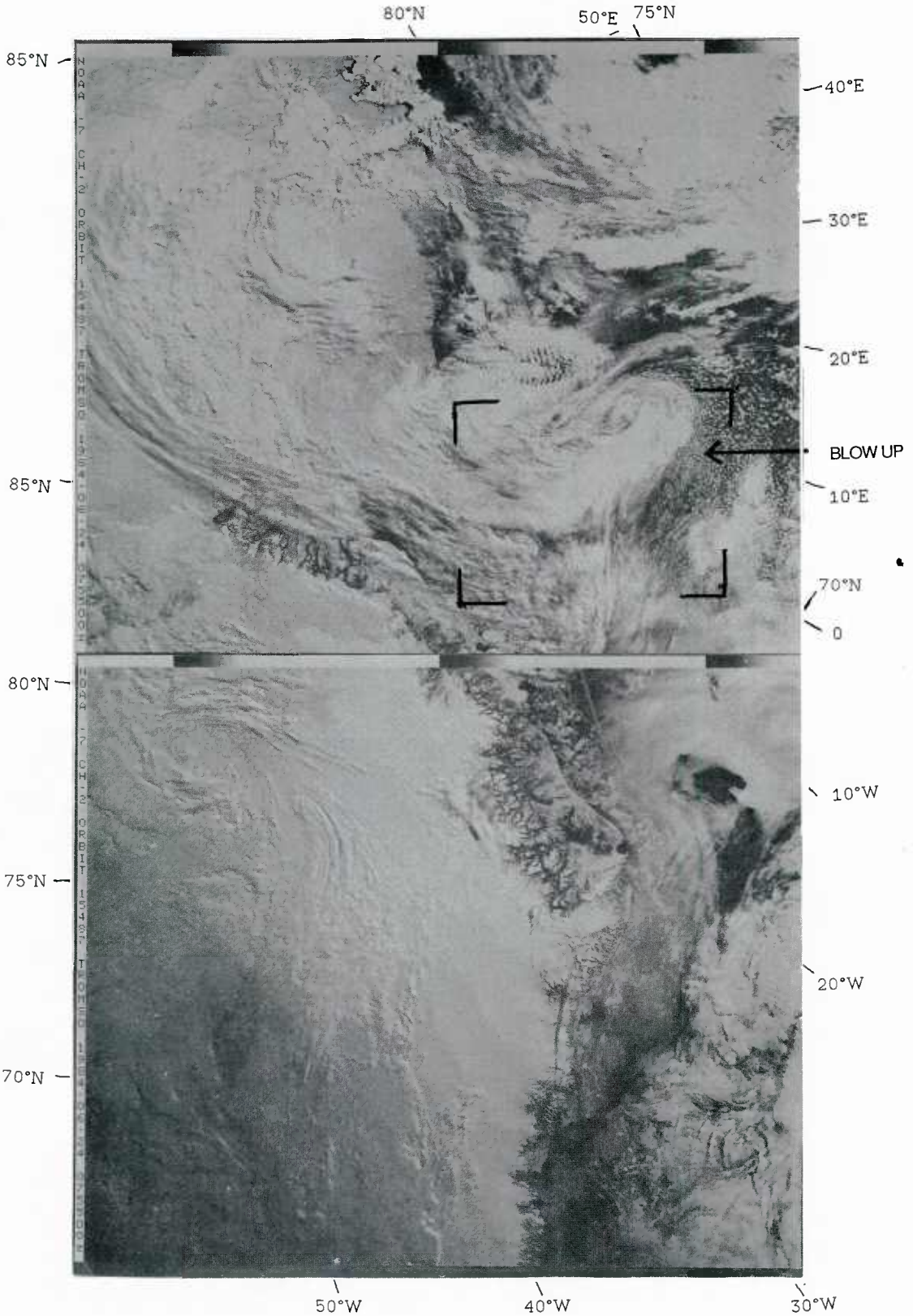

Figure 18a: NOAA-7 visual image 24 June 1984 0755 GMT. Southwest of Spitzbergen a cloud vortex is clearly seen. The point of convergence (76°N, 10°E) seen on the image coincides well with the location of the center of the low on the surface chart. Over Spitzbergen some mountain waves are seen.

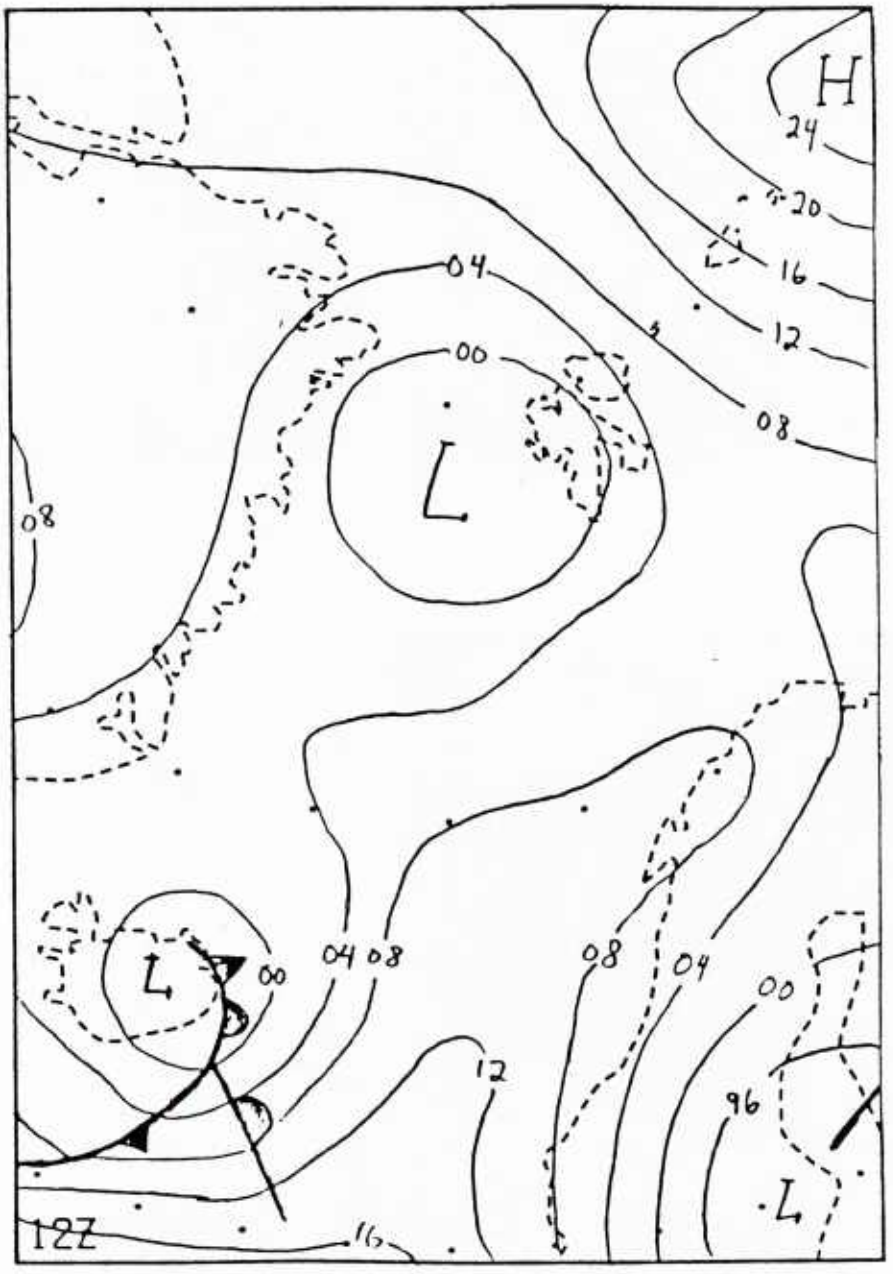

Figure 18b: Surface pressure chart 24 June 1984 1200 GMT.

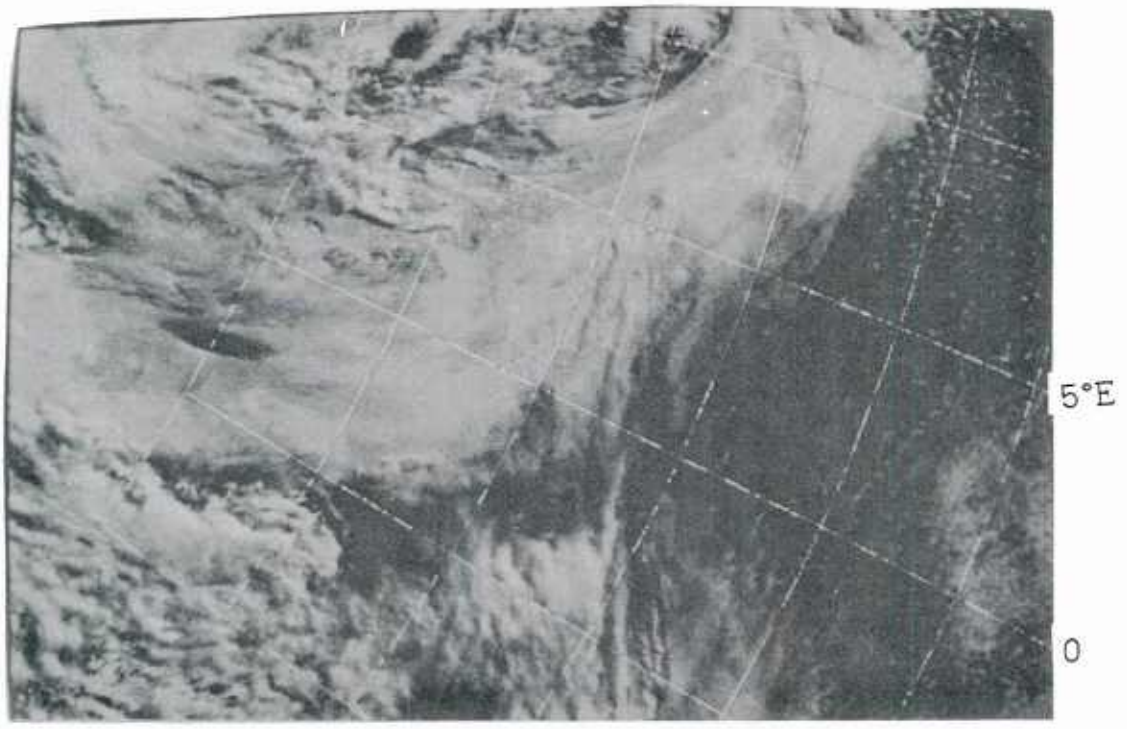

Figure 18c: NOAA-7 visual image 24 June 1984 0755 GMT.
The cloud vortex enlarged, the point of convergence is clearly seen at 76°N, 10°E. The MIZEX team observed winds of more than 15m/s in the region of the vortex.

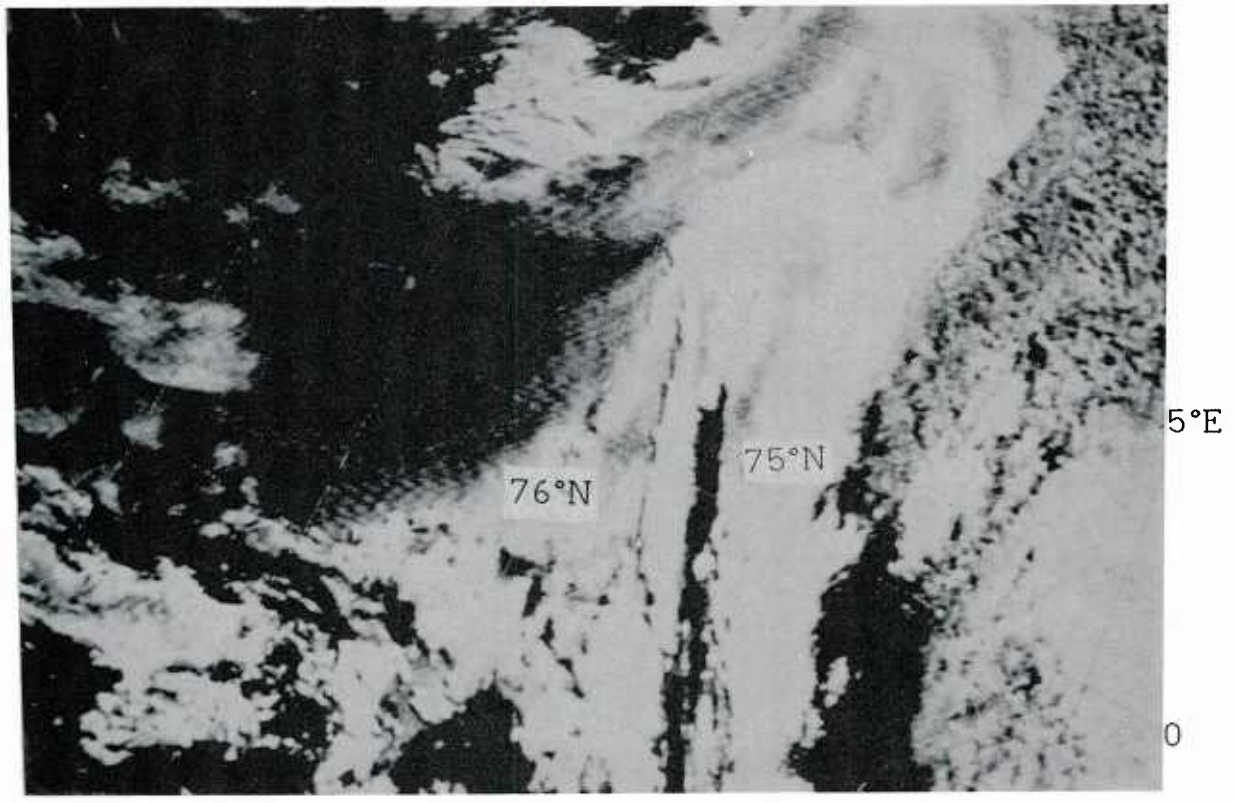

Figure 18d: NOAA-7 IR image 24 June 1984 0755 GMT.
The thermal image shows that the core is much warmer than the surroundings. The low temperature in the frontal zone (75°N) indicates that high clouds are present there.

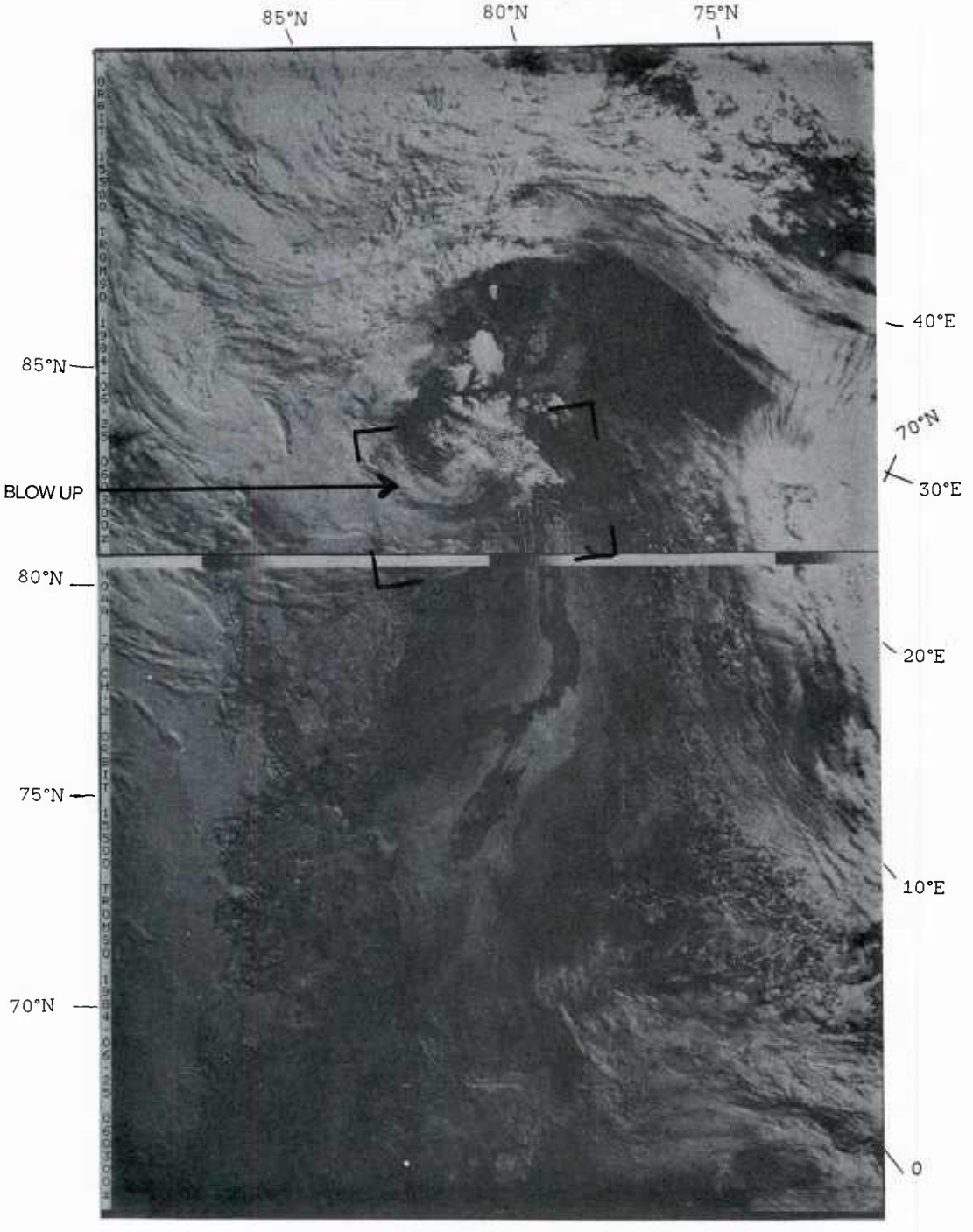

Figure 19a: NOAA-7 visual image 25 June 1984 0603 GMT. Embedded in the stream around the synoptic low over the northern Fram Strait is a quite energetic mesoscale low with its core near the westcoast of Spitzbergen. Over the islands mountain waves are seen.

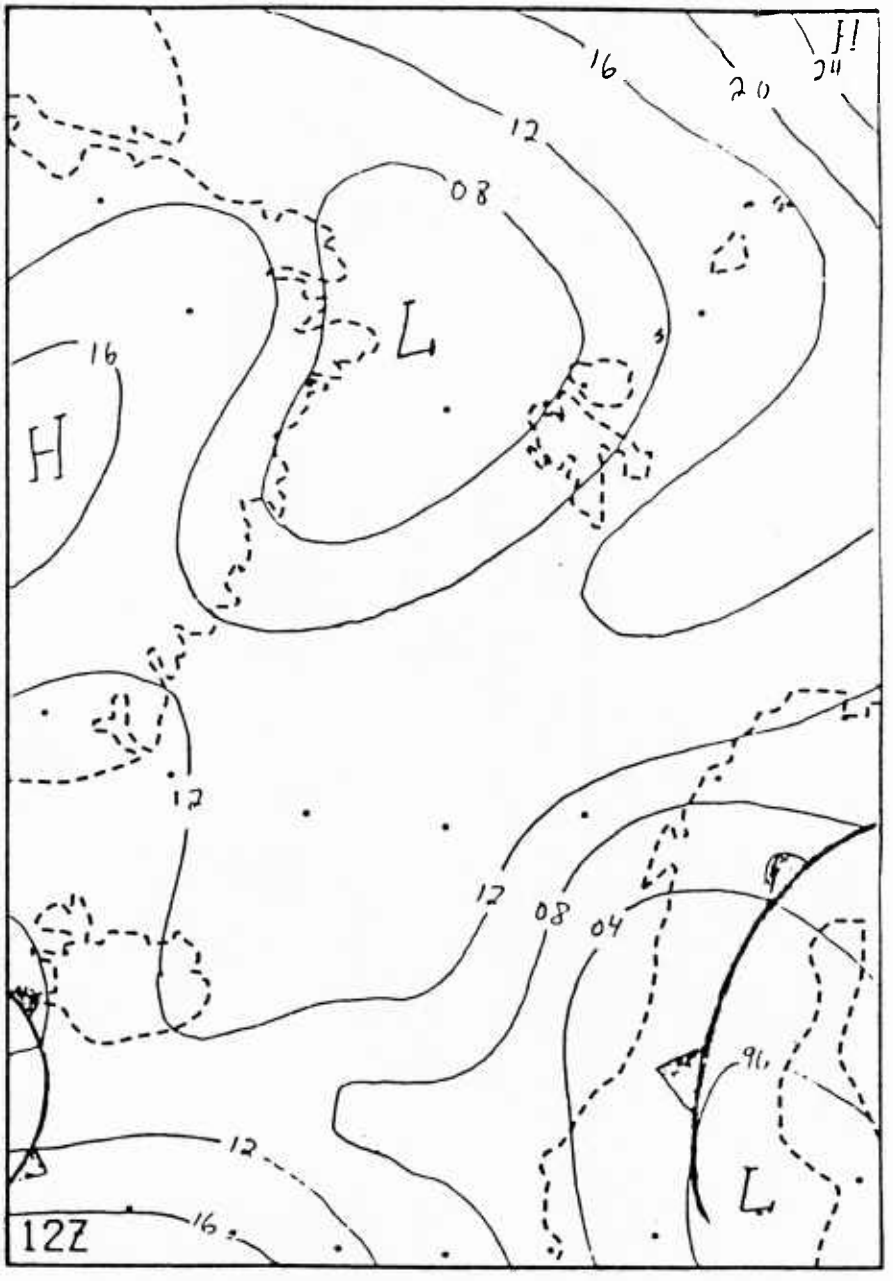

Figure 19b: Surface pressure chart 25 June 1984 1200 GMT.

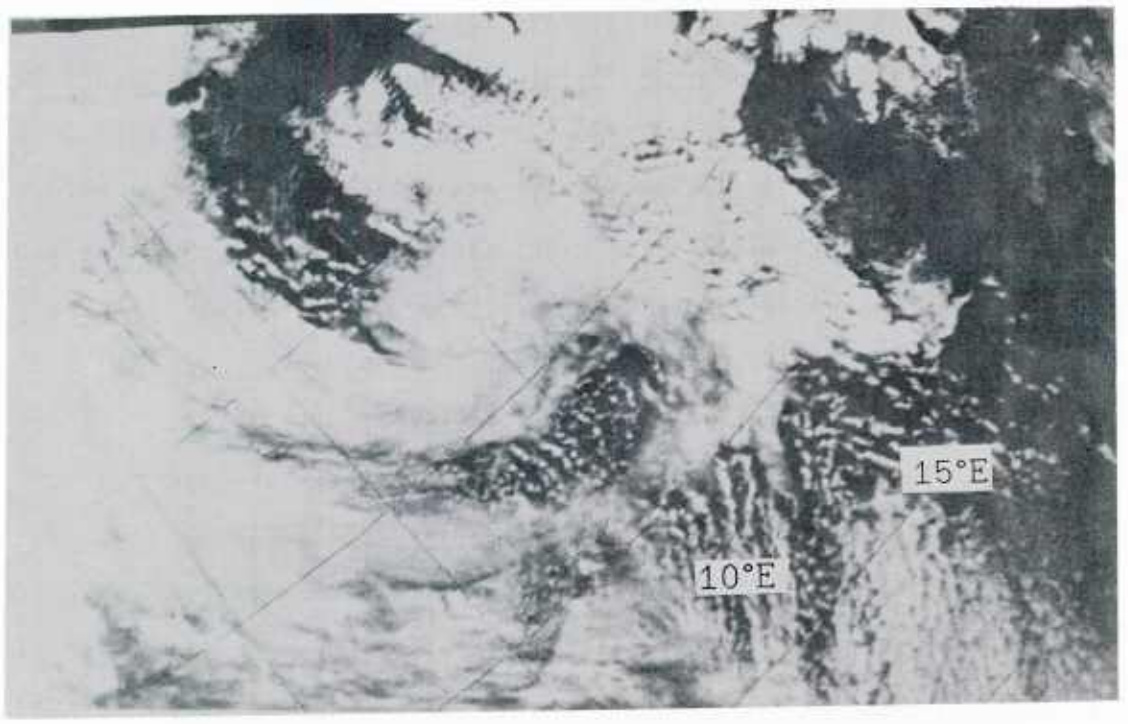

Figure 19c: NOAA-7 visual image 25 June 1984 0603 GMT. Enlarged image of the mesoscale low at the westcoast of Spitzbergen, and the mountain waves. The sharp transition between cloudy and clear air on the backside is a typical feature of polar lows.

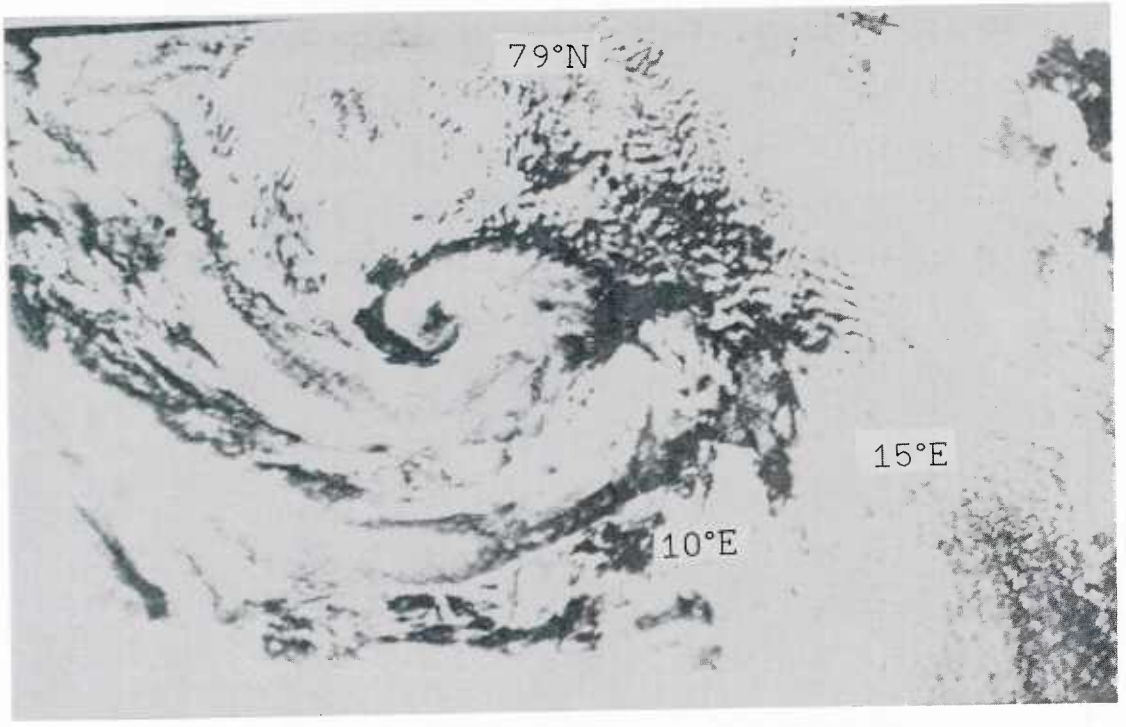

Figure 19d: NOAA-7 IR image 25 June 1984 0603 GMT. The thermal image shows that the core of the low has a temperature of about -20°C, while the surrounding cloud tops have temperatures below -40°C.

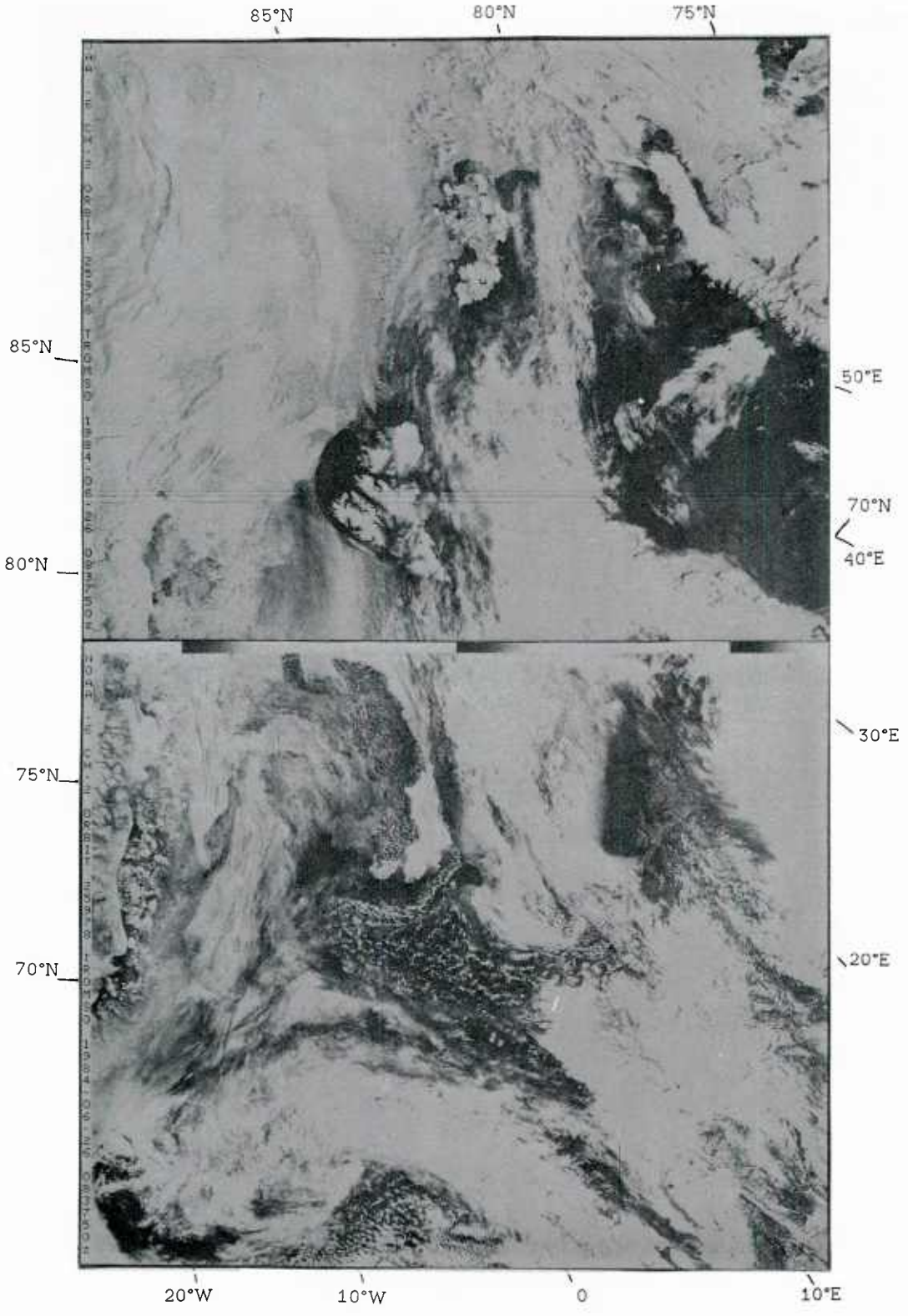

Figure 20a: NOAA-6 visual image 26 June 1984 0838 GMT.
Over Spitzbergen a narrow high pressure ridge with its axis directed SW-NE gives subsidence and clear sky over the islands. To the south heavy cloudmasses are flowing southwestwards. A sharp convergence line to the northwest of Spitzbergen is generated by the northwesterly wind and the opposing flow connected with the subsidence. Over the Fram Strait off-ice cloud streets are seen.

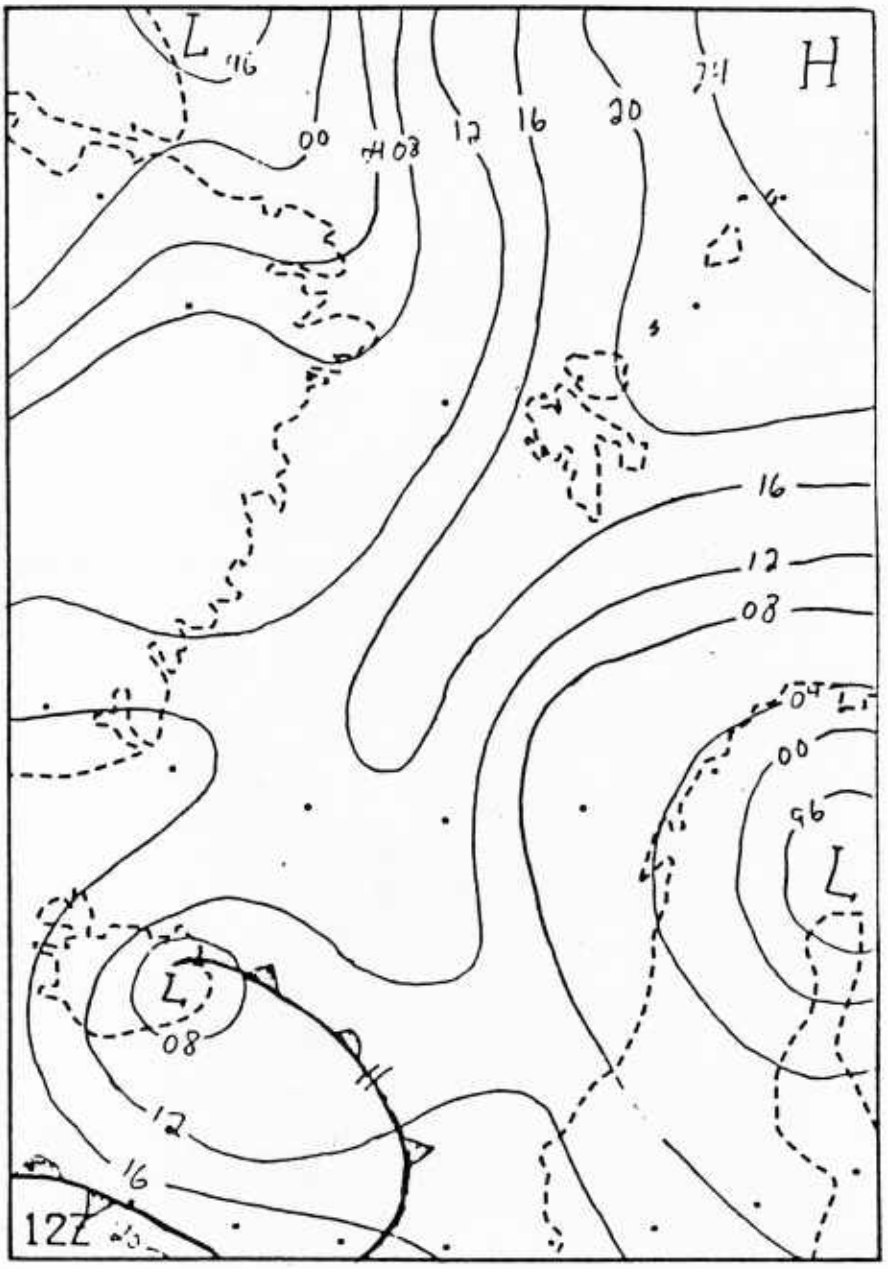

Figure 20b: Surface pressure chart 26 June 1984 1200 GMT.

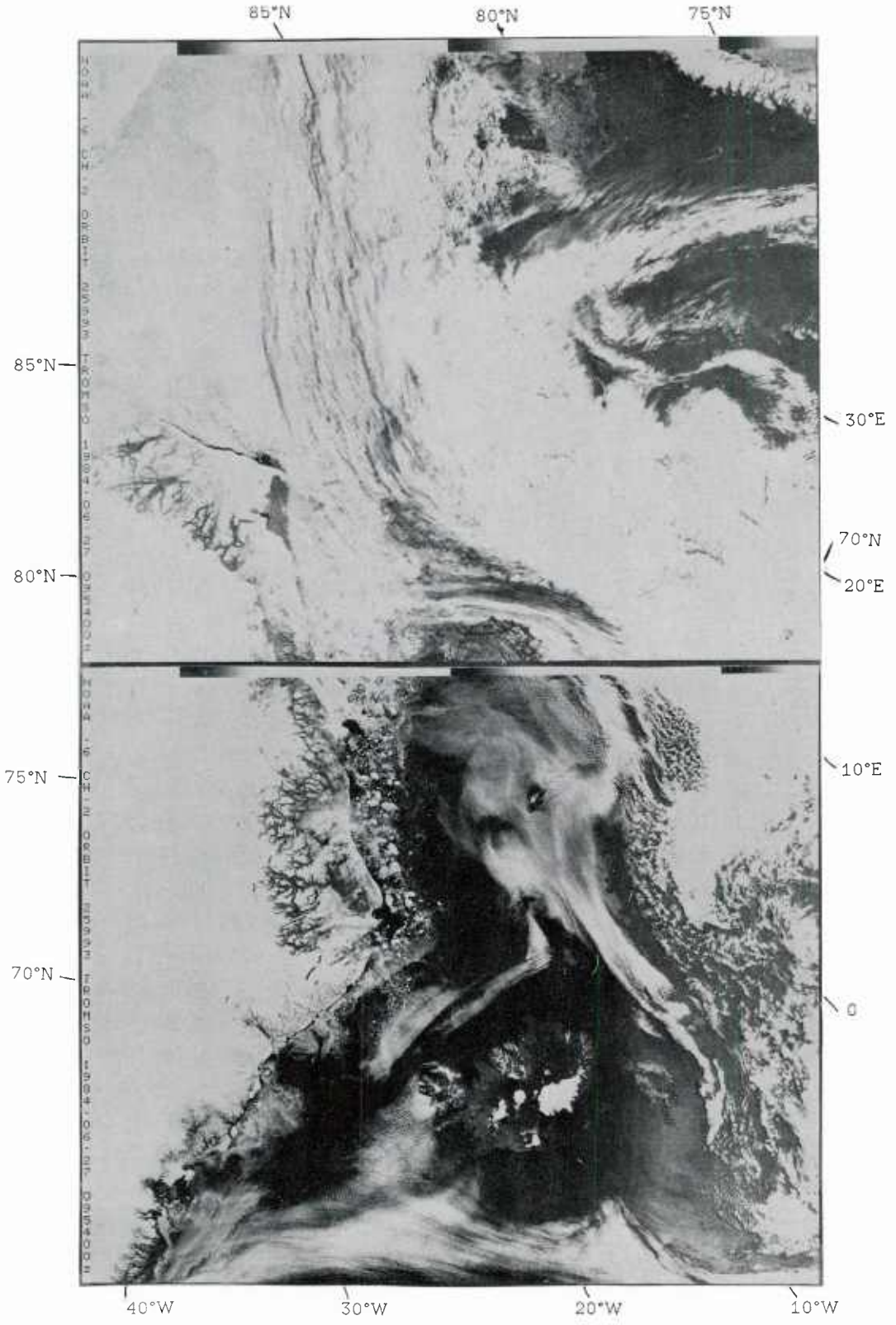

Figure 21a: NOAA-6 visual image 27 June 1984 0954 GMT.
A well developed low south of Spitzbergen generates northerly winds and heavy clouds over the Fram Strait. Ice streamlines are seen along the East-Greenland coast (south of 75°N) giving an estimate of the surface ocean currents in the area. At Jan Mayen a wavy cloud lane similar to that on figure 17a is seen.

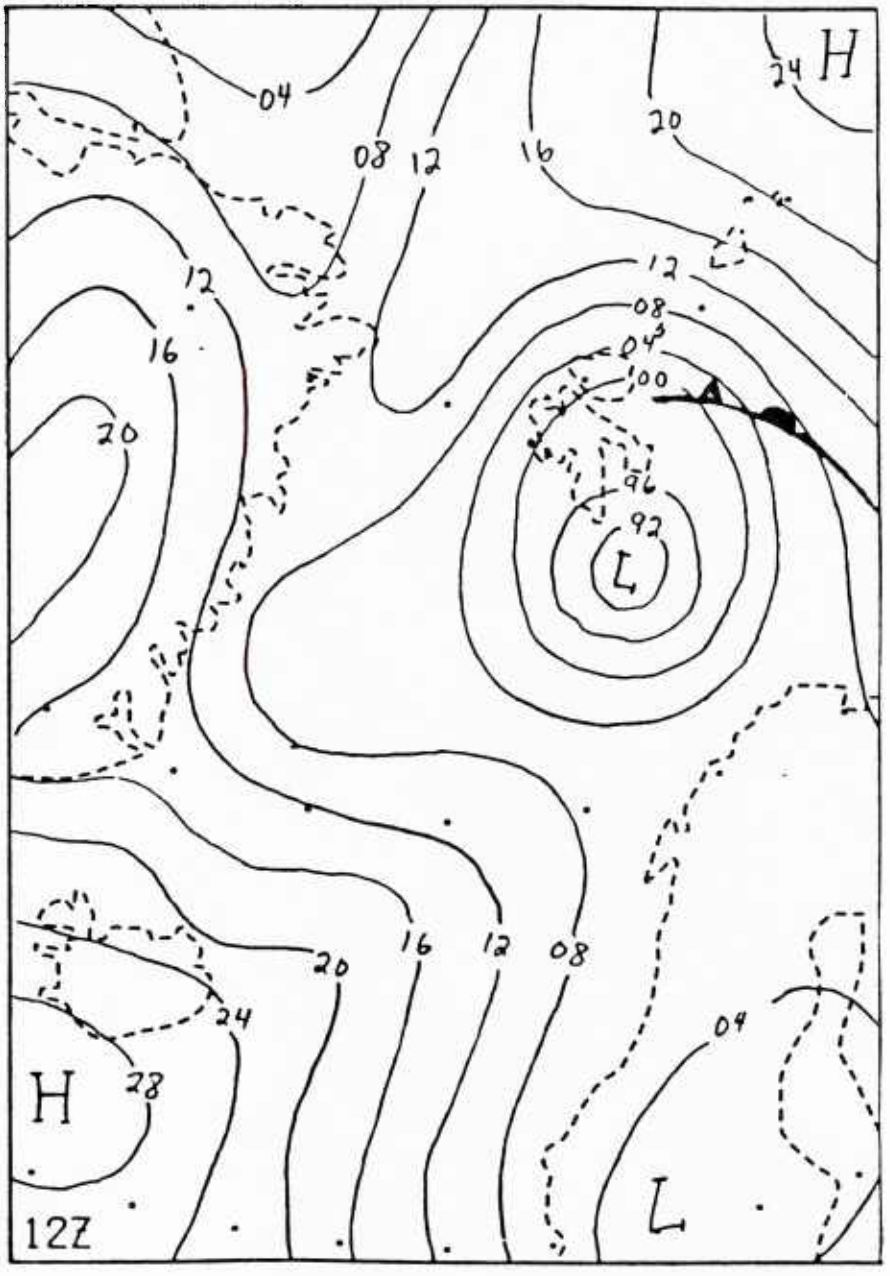

Figure 21b: Surface pressure chart 27 June 1984 1200 GMT.

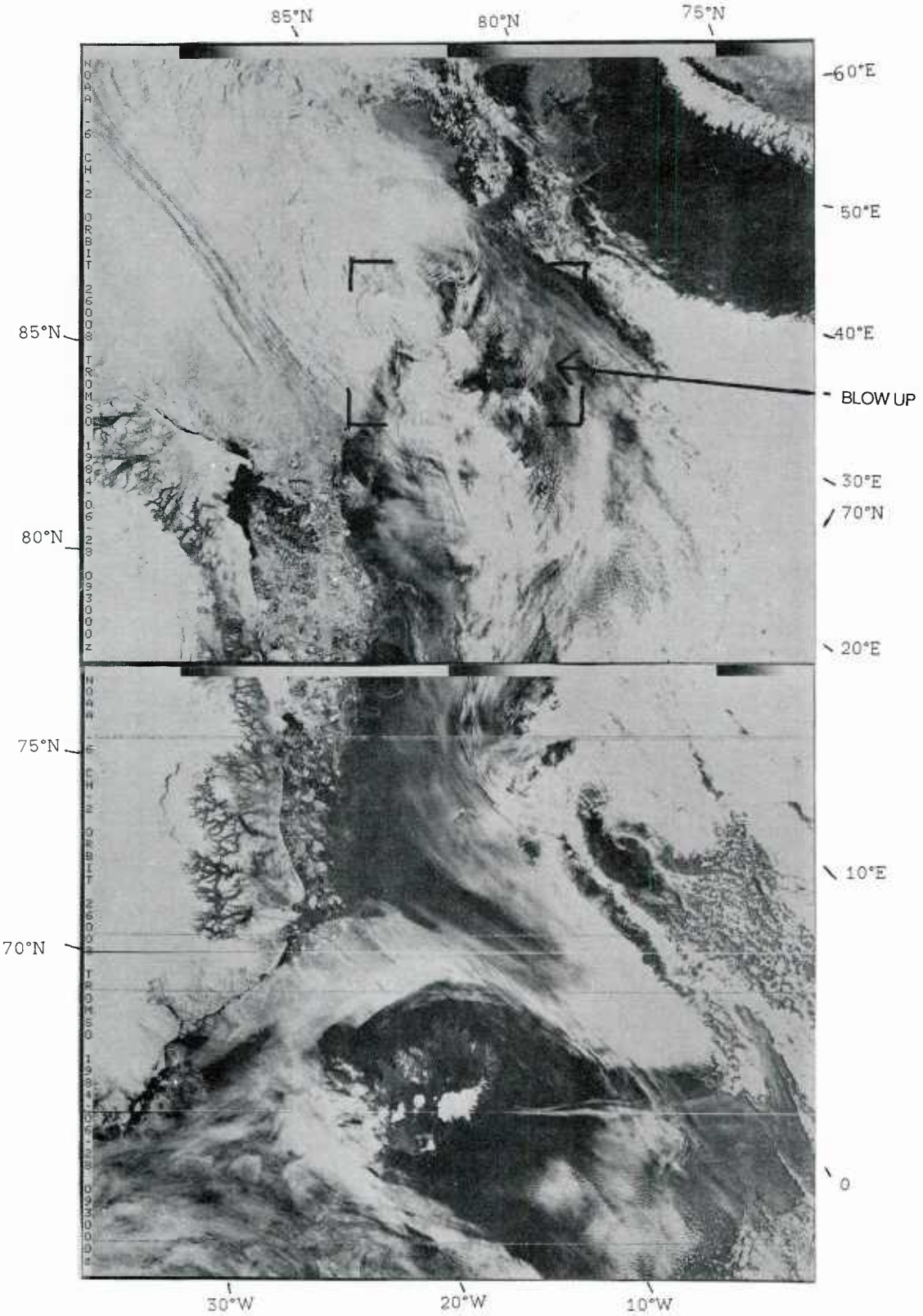

Figure 22a: NOAA-6 visual image 28 June 1984 0930 GMT.
The western part of the Fram Strait has clear weather with decreasing winds, blowing off-ice. The ice edge is clearly seen. East of Spitzbergen, where the wind is on-ice, some waves transverse to the flow are seen. They must be gravity waves, generated on the ice edge, rather than mountain waves. The bending of the wave fronts are due to the horizontal wind shear.

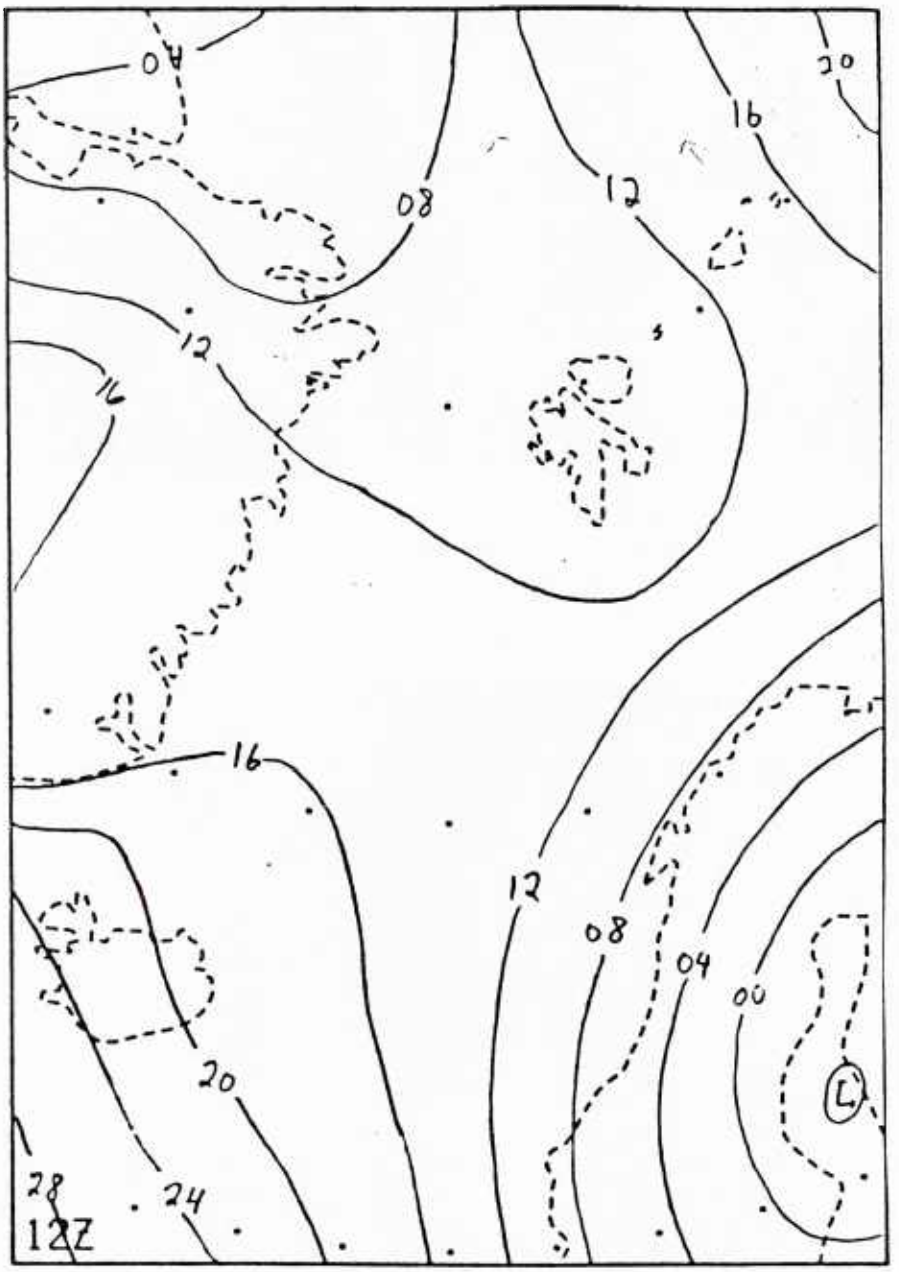

Figure 22b: Surface pressure chart 28 June 1984 1200 GMT.

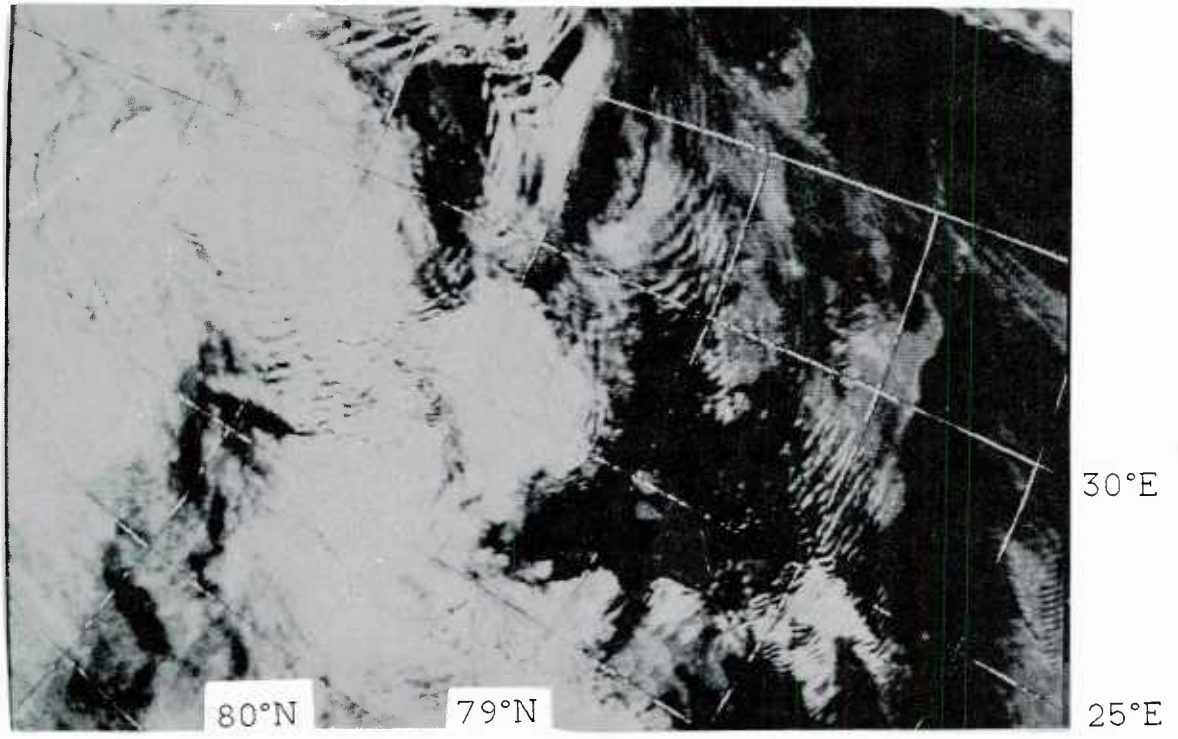

Figure 22c: NOAA-6 visual image 28 June 1984 0930 GMT.
The gravity waves east of Spitzbergen are clearly seen. The wind is southerly, and as the warm midlatitudinal air gets lifted over the cold arctic air, the waves are generated. The static stability distribution is crucial for the wave generation.

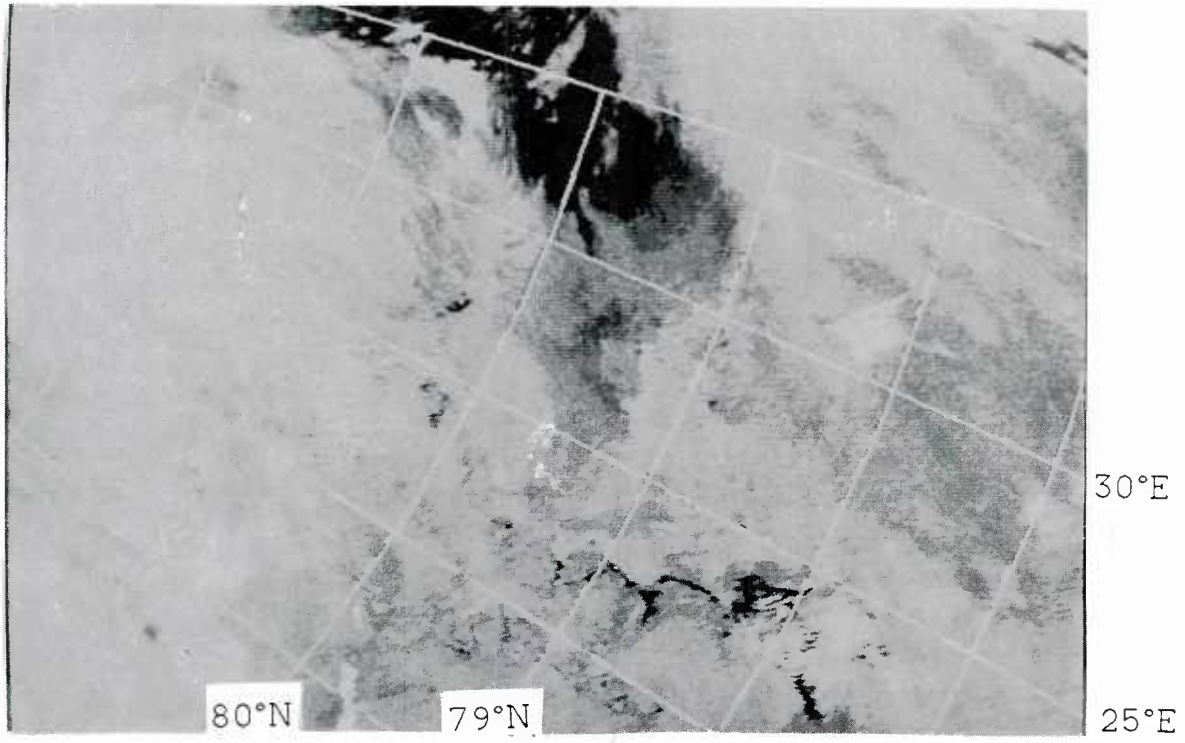

Figure 22d: NOAA-6 IR image 28 June 1984 0930 GMT.
Also on the thermal image the gravity waves are seen, but the signatures are less significant. The temperatures of the cloud tops in the waves are -15°C to −20°C.

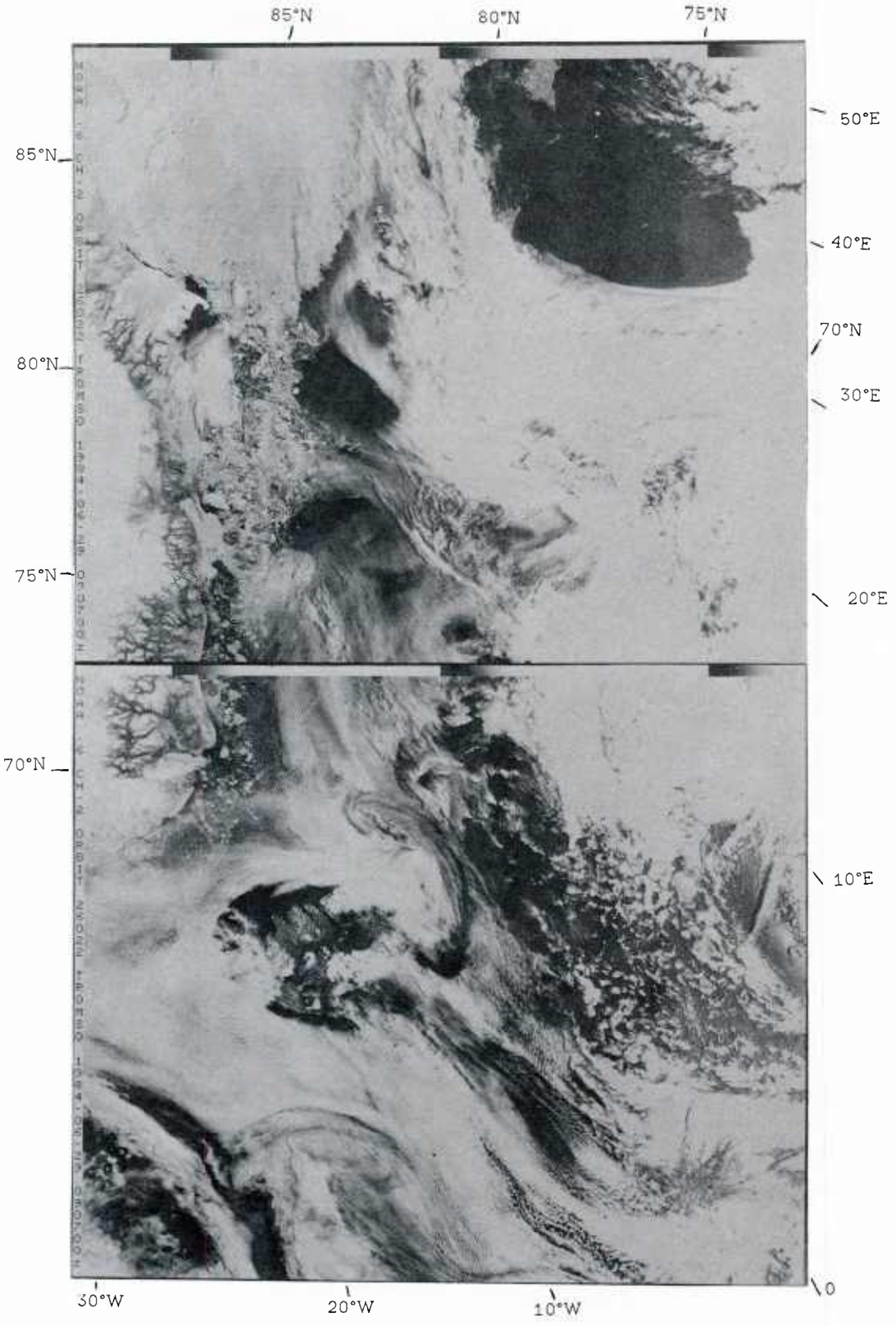

Figure 23a: NOAA-6 visual image 29 June 1984 0907 GMT.
The weather situation in the Fram Strait is dominated by a high pressure ridge from Spitzbergen to Iceland. The cloud cover along the ice-edge is rather thin.

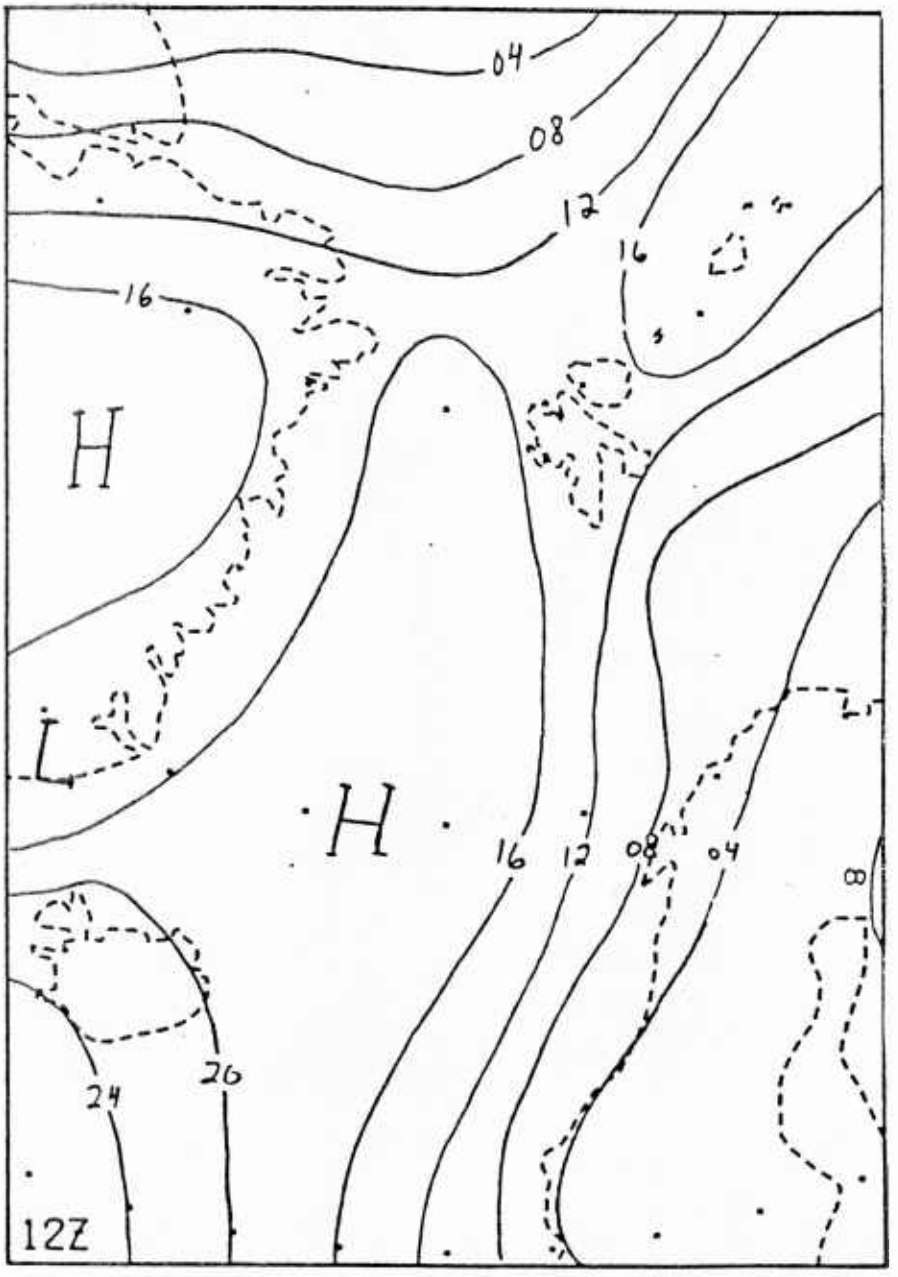

Figure 23b: Surface pressure chart 29 June 1984 1200 GMT.

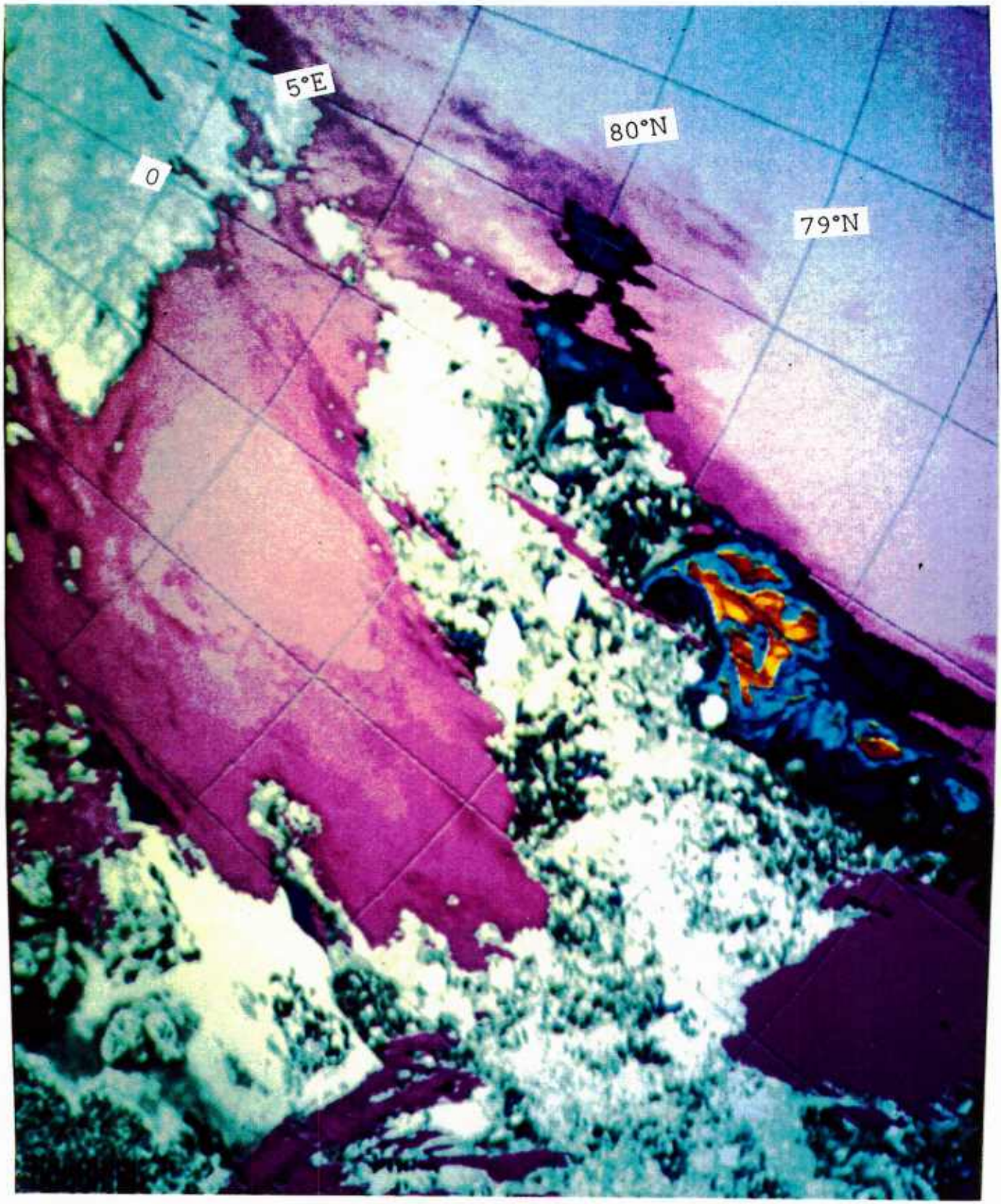

Figure 23c: NOAA-7 combination ch. 2 (visual) and ch. 4 (IR-temperature) image 29 June 1984 0907 GMT. Image shows sea surface temperature and ice and clouds albedo. Surface features separated and displayed as follows: cold temperatures taken as high clouds, shown in magenta; bright visual albedo taken as ice, shown in greyscale from black (10%) to white (40%) albedo; dark visual albedo taken as ocean, shown in temperature-coded colors from dark blue (0°C) to yellow (5°C).

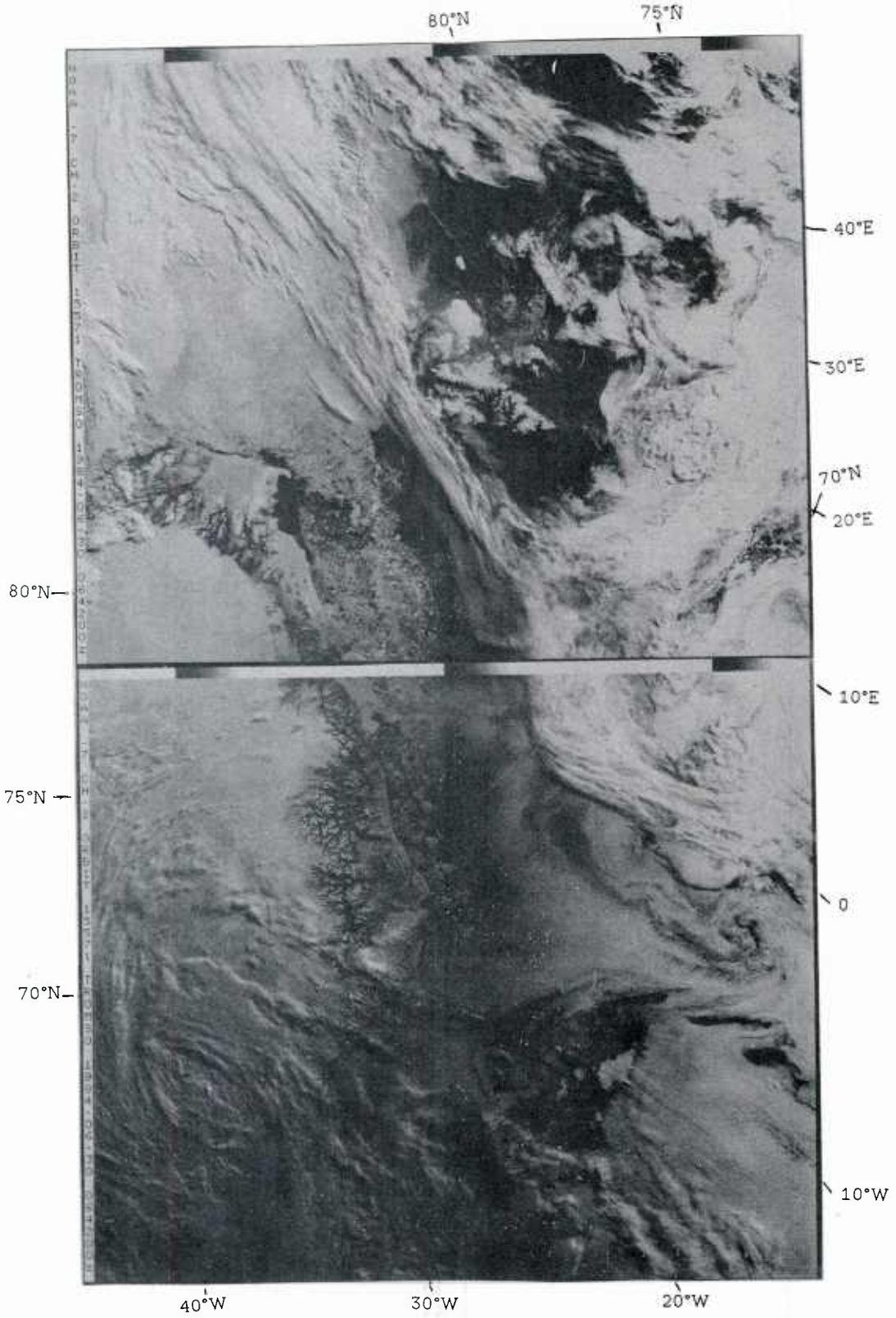

Figure 24a: NOAA-7 visual image 30 June 1984 0642 GMT.
The weather situation is much the same as on 29 June with a high pressure ridge along the marginal ice zone. The icefloes can be recocnized from orbit to orbit giving an estimate of the ice/ocean velocity. Note the high level cloudband extending southwards west of Spitzbergen.

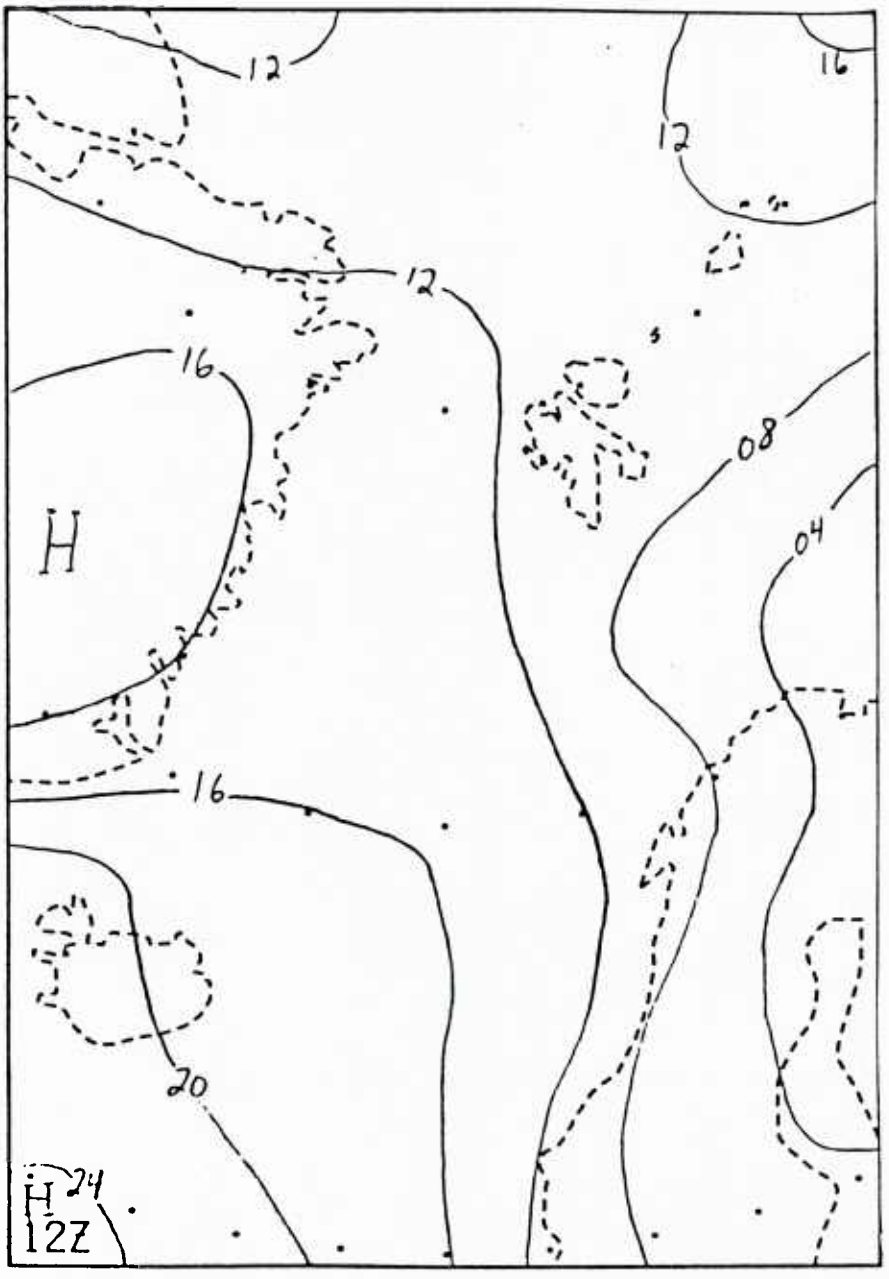

Figure 24b: Surface pressure chart 30 June 1984 1200 GMT.

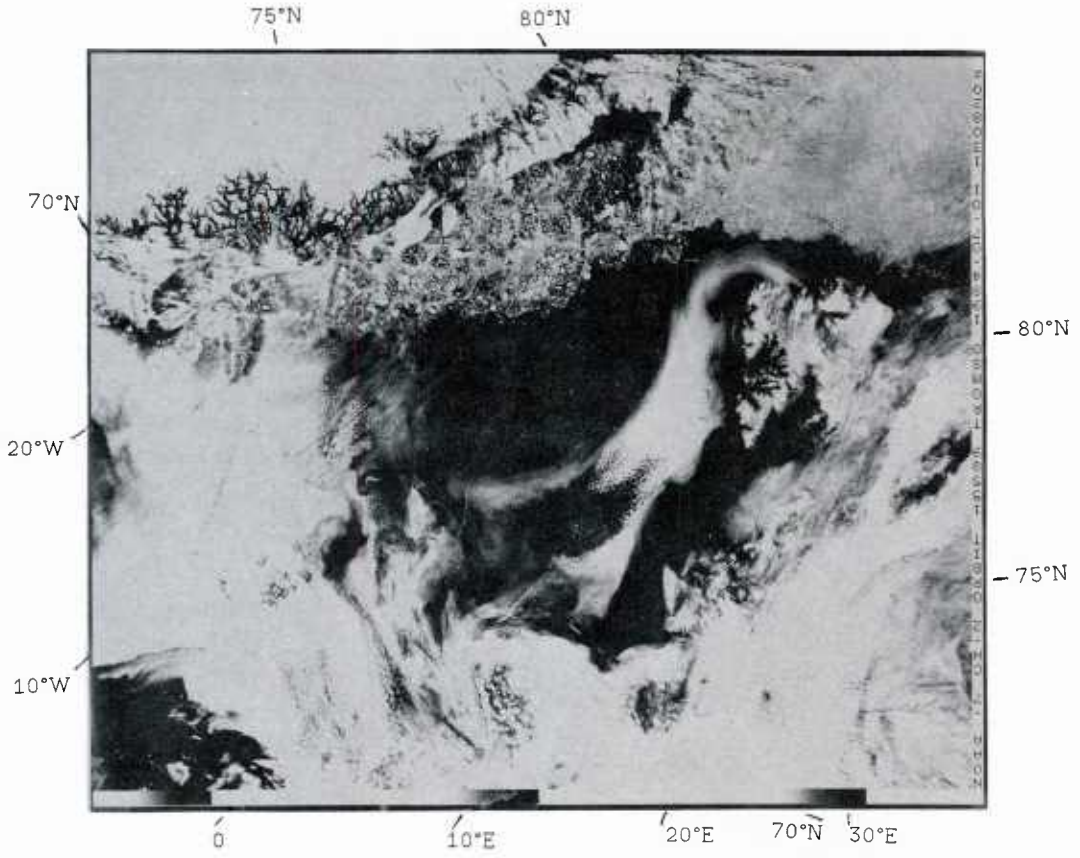

Figure 25a: NOAA-7 visual image 1 July 1984 1308 GMT.
It is still fair weather in the MIZ area, with calm winds fluctuating from off- to on-ice over a small area. A lee cyclone has developed on the East-Greenland coast, giving some overcasted sky in the southern MIZ area. Off the westcoast of Spitzbergen a mesoscale cyclone is seen.

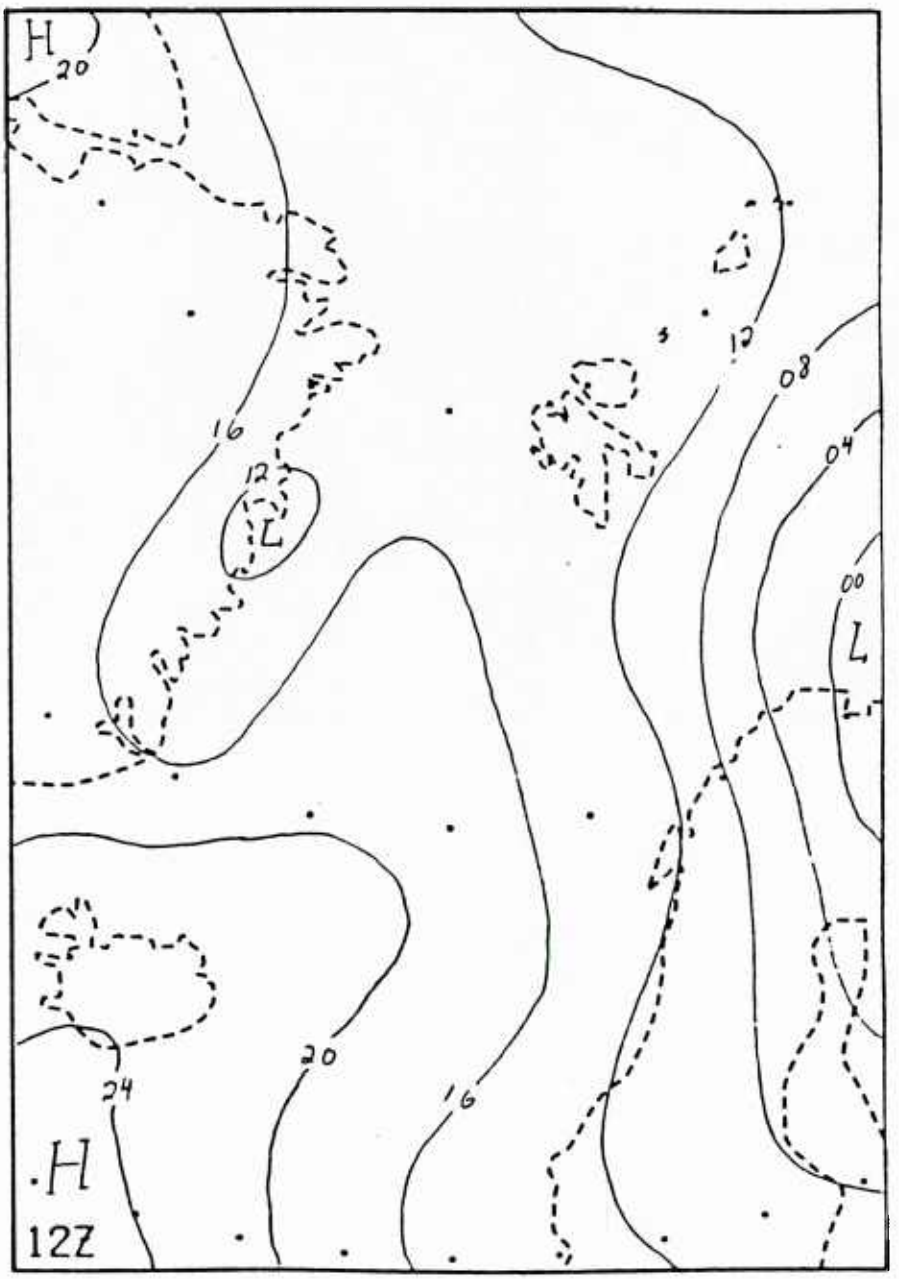

Figure 25b: Surface pressure chart 1 July 1984 1200 GMT.

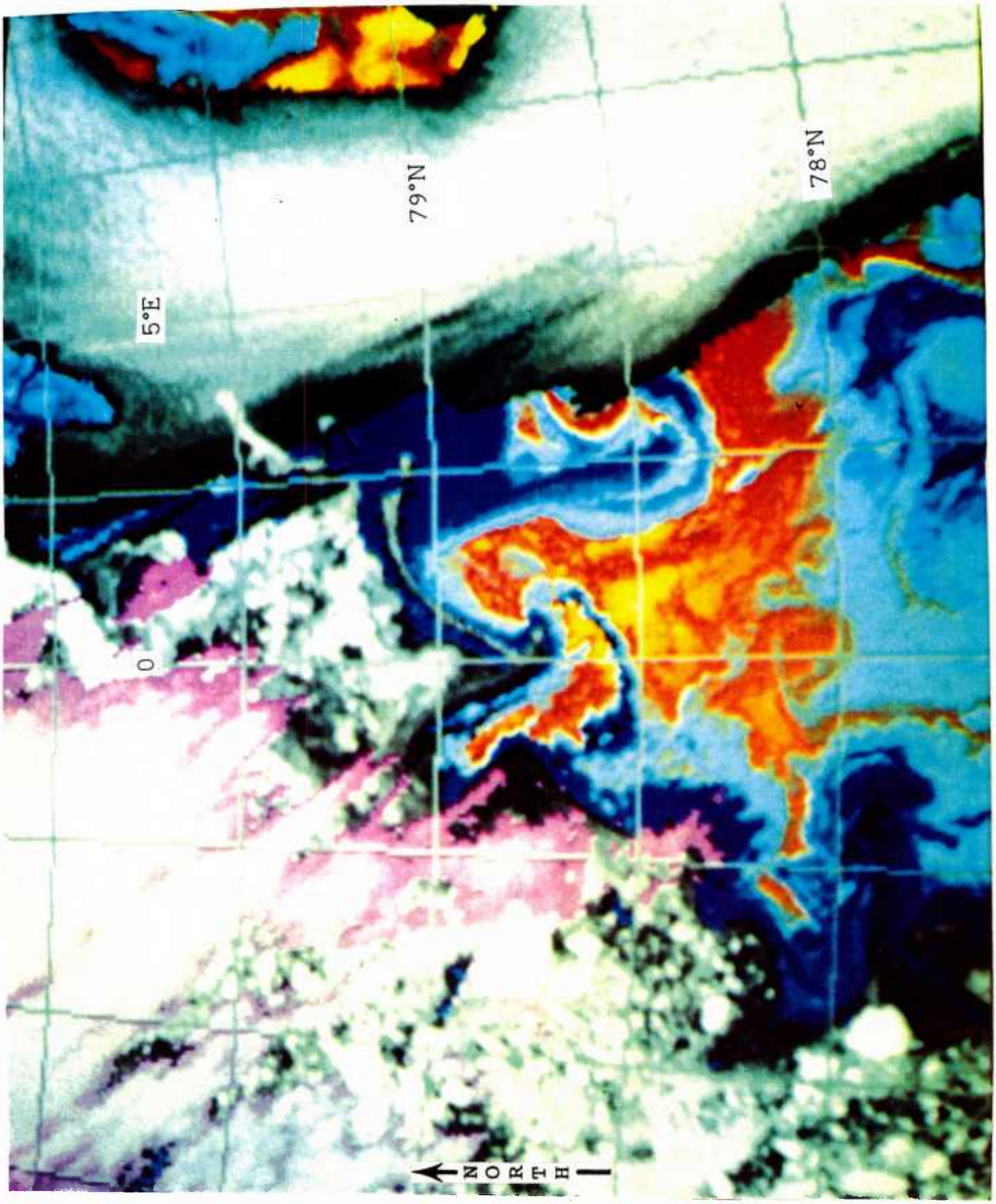

Figure 25c: NOAA-7 combination ch. 2 (visual) and ch. 4 (IR-temperature) image 1 July 1984 1308 GMT. Image shows sea surface temperature and ice and clouds albedo. Surface features separated and displayed as follows: cold temperatures taken as high clouds, shown in magenta; bright visual albedo taken as ice, shown in greyscale from black (10%) to white (40%) albedo; dark visual albedo taken as ocean, shown in temperature-coded colors from dark blue (0°C) to yellow (5°C).

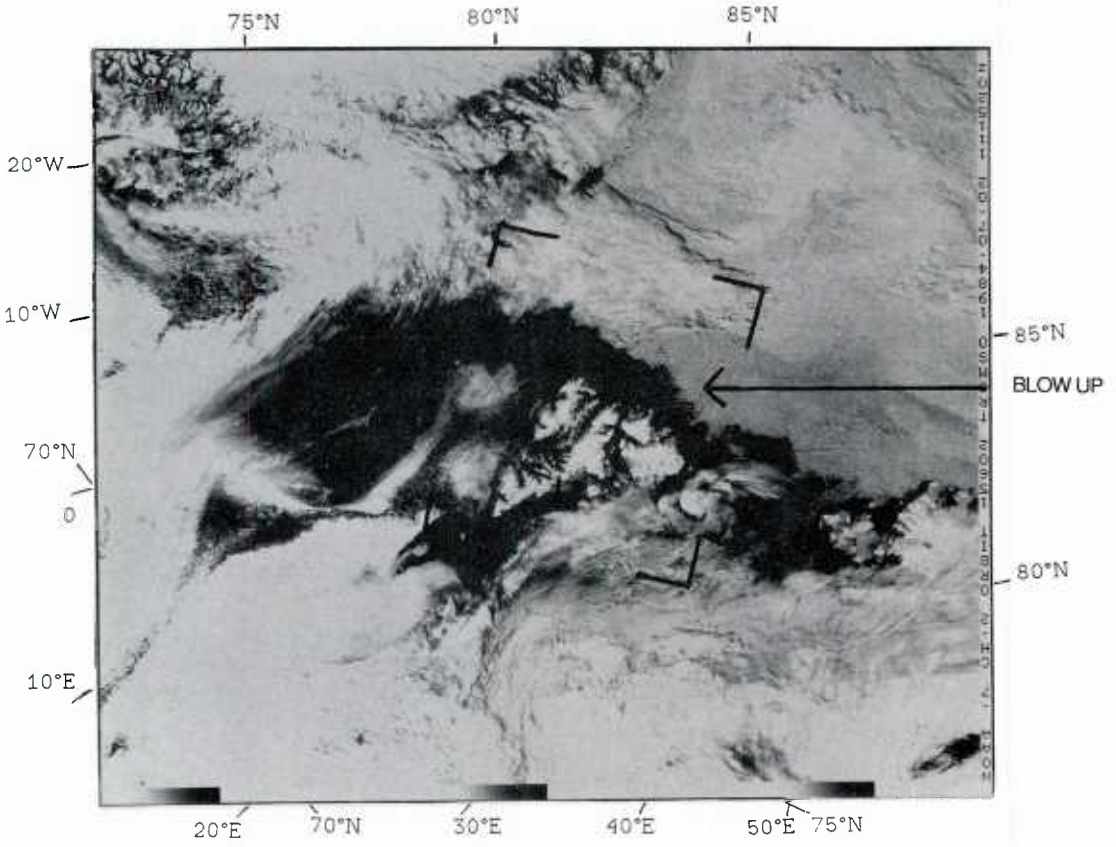

Figure 26a: NOAA-7 visual image 2 July 1984 1115 GMT. Northeasterly winds are blowing over the Fram Strait, the northern ice edge is clearly visible, lying in a region of atmospheric subsidence.

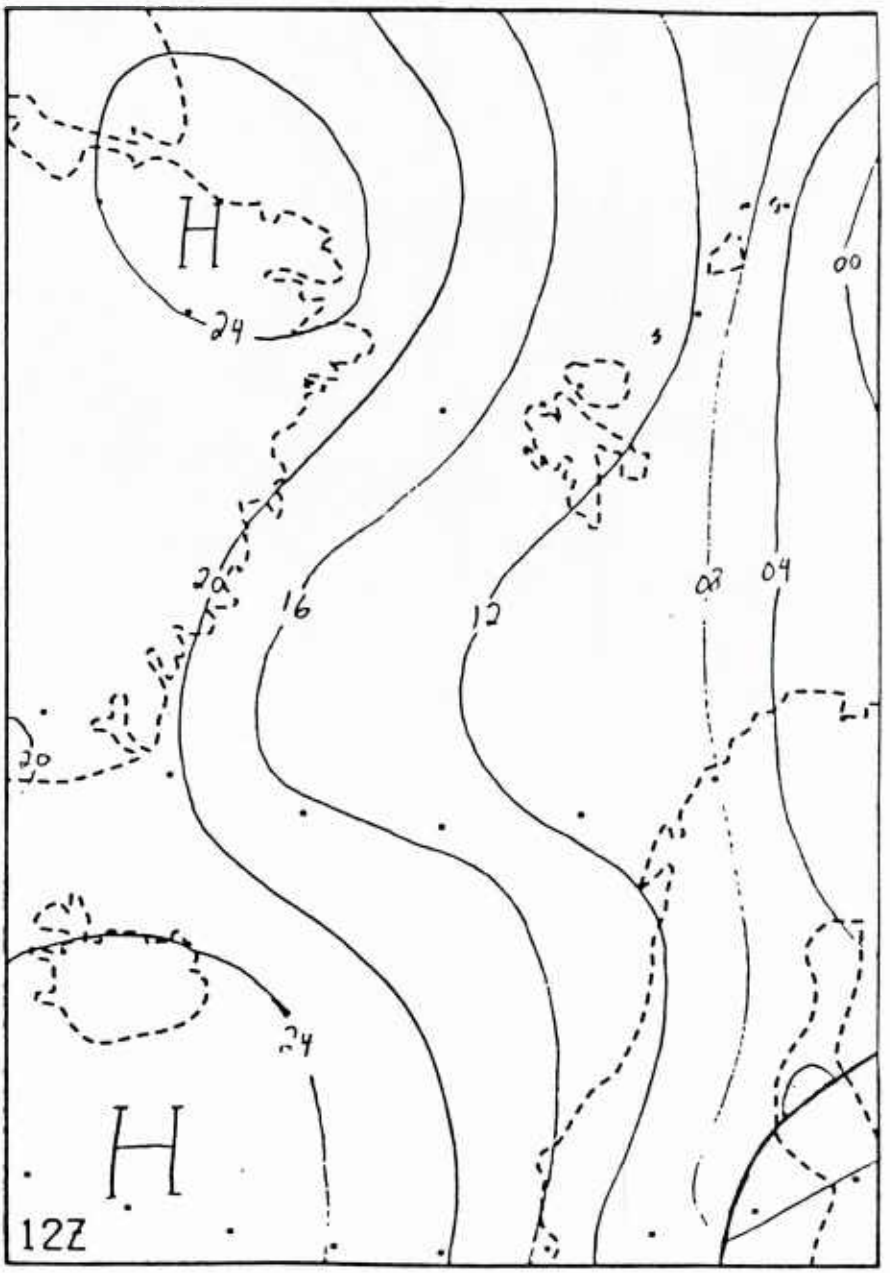

Figure 26b: Surface pressure chart 2 July 1984 1200 GMT.

Figure 26c: NOAA-7 visual image 2 July 1984 1115 GMT. Due to the large scale subsidence, the convective cloud streets are generated a considerable distance downwind from the ice edge.

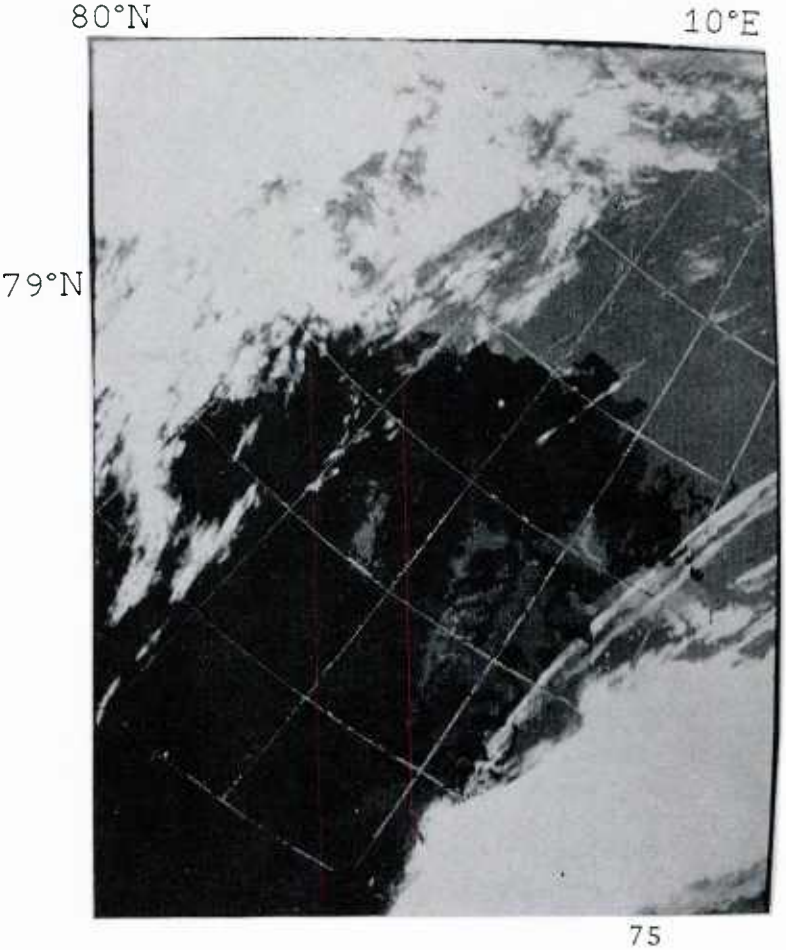

Figure 26d: NOAA-7 IR image 2 July 1984 1115 GMT. The thermal image shows the temperature contrast between the ice (grey) and the sea (black).

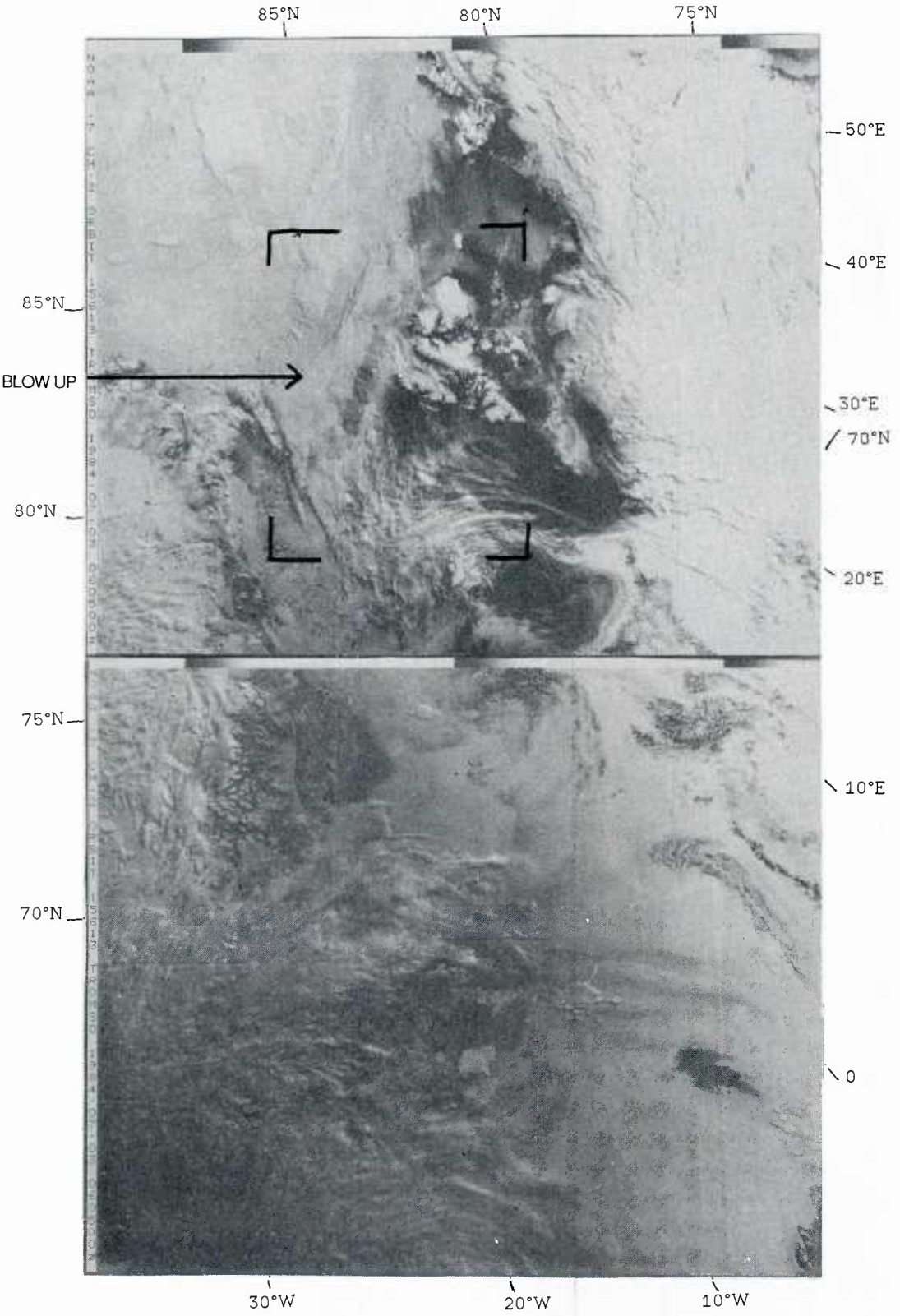

Figure 27a: NOAA-7 visual image 3 July 1984 0605 GMT. Northeasterly winds are blowing along the ice edge in the Fram Strait. The northern ice edge is covered by stratus.

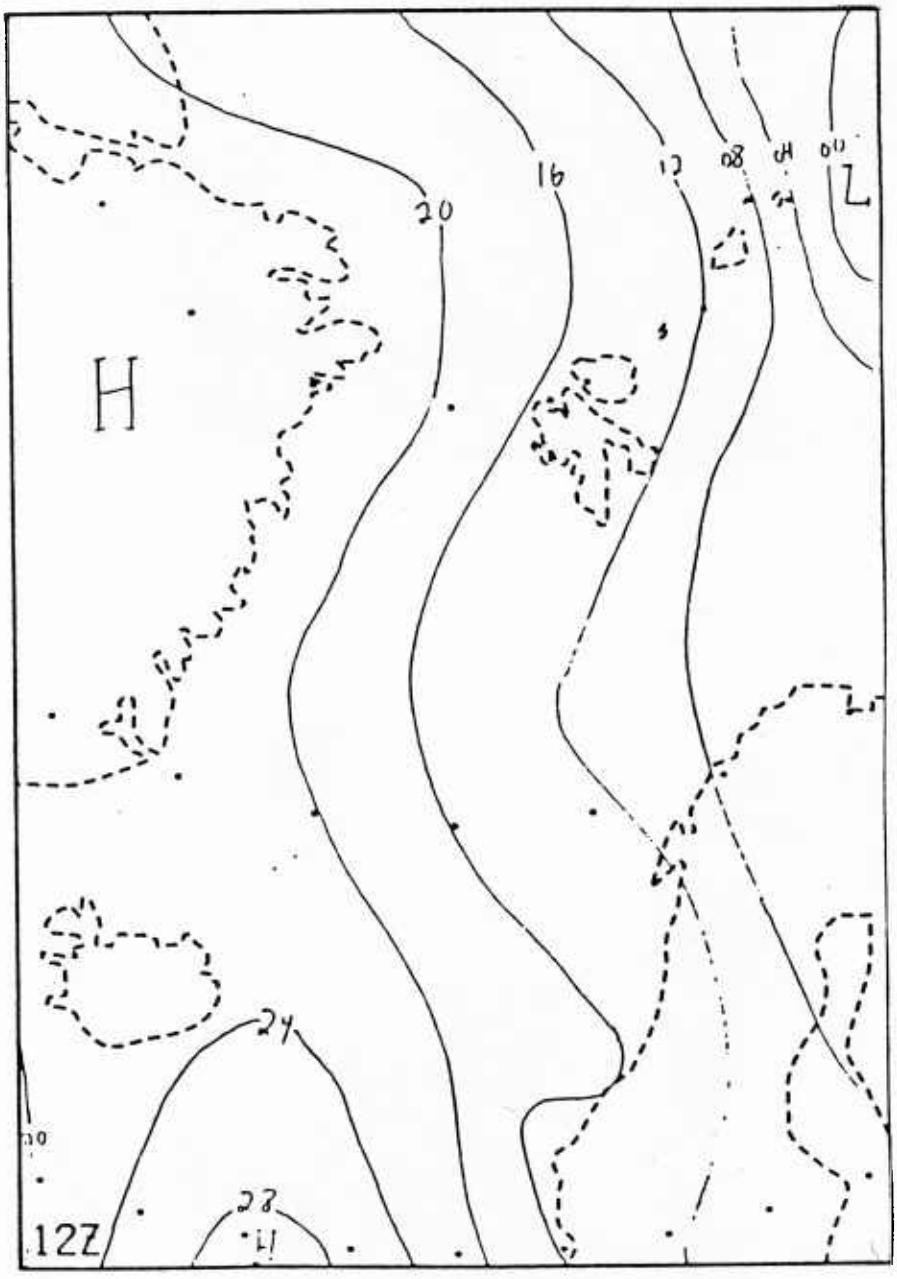

Figure 27b: Surface pressure chart 3 July 1984 1200 GMT.

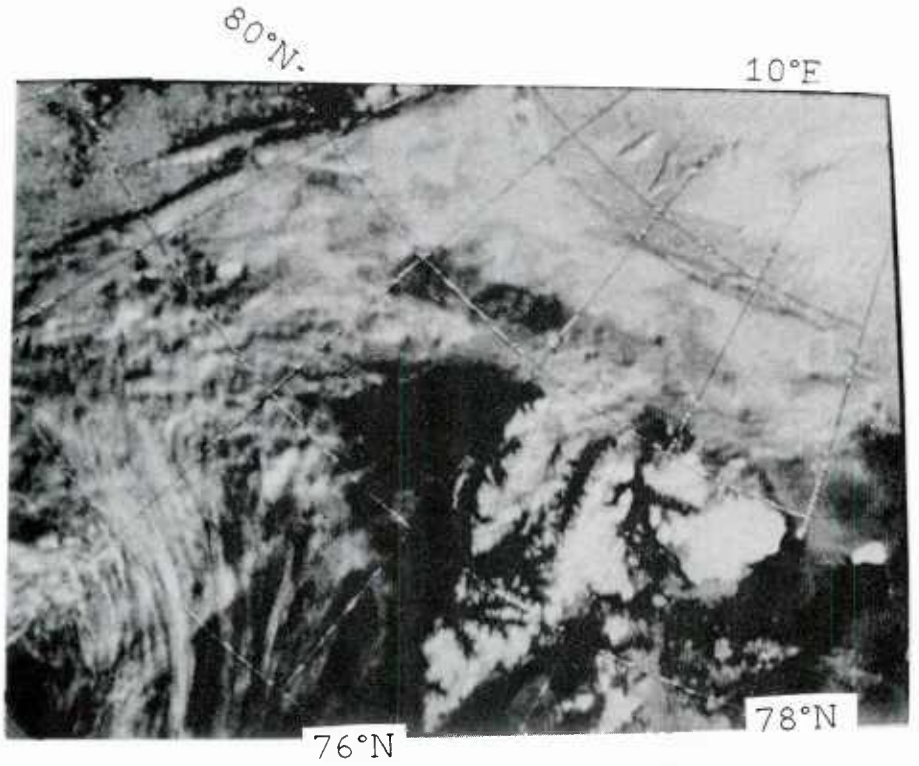

Figure 27c: NOAA-7 visual image 3 July 1984 0605 GMT.
The ice edge north and northwest of Spitzbergen is covered by a thick cloud mass with a very sharp transition to the clear sky region over the pack ice. These clouds are a result of the mixing of cold dry air with warm moist air.

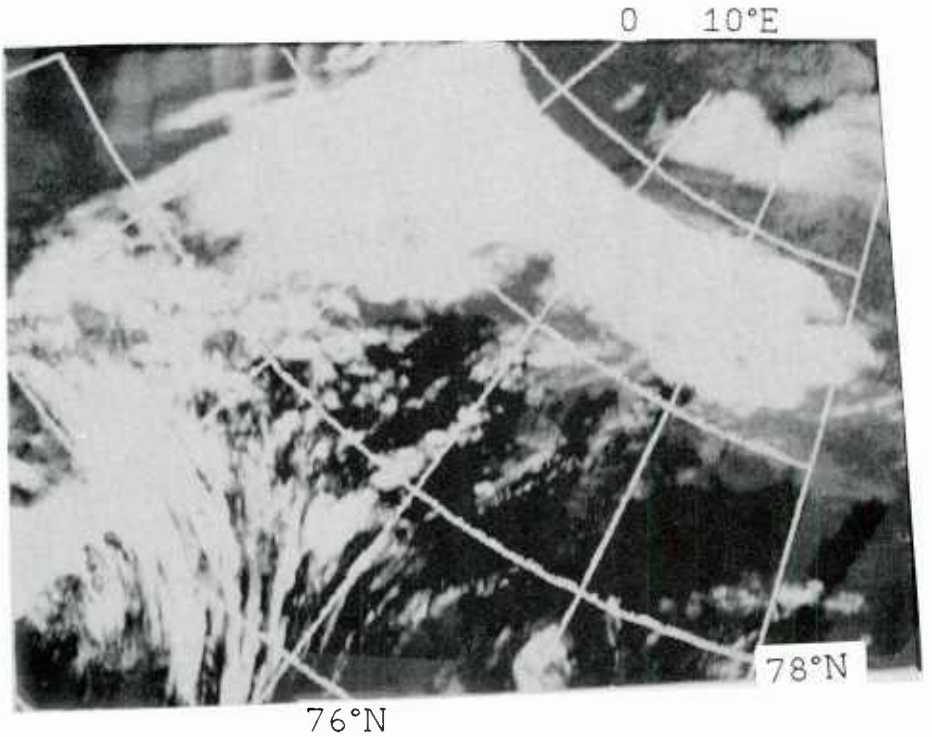

Figure 27d: NOAA-7 IR image 3 July 1984 0605 GMT.
The thermal image shows that the cloud cover over the ice edge is significantly colder than the ice, telling that the clouds reach high up in the troposphere where the temperature is low.

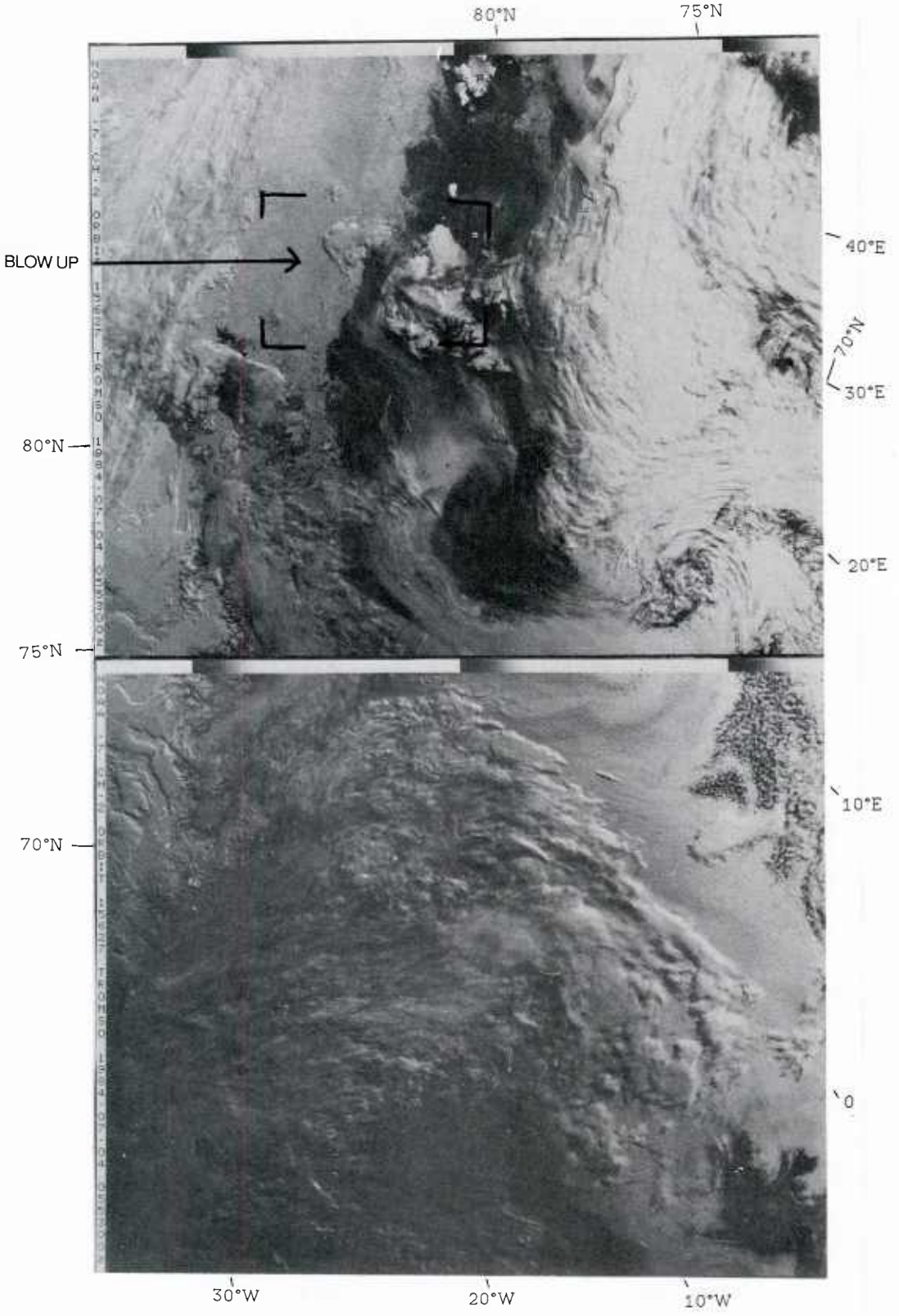

Figure 28a: NOAA-7 visual image 4 July 1984 0553 GMT.
A ridge over the Arctic ocean and a trough over the Barents Sea extending westwards over the MIZ area, gives an easterly wind over the northern parts of the region. A mesoscale low is seen north of Spitzbergen.

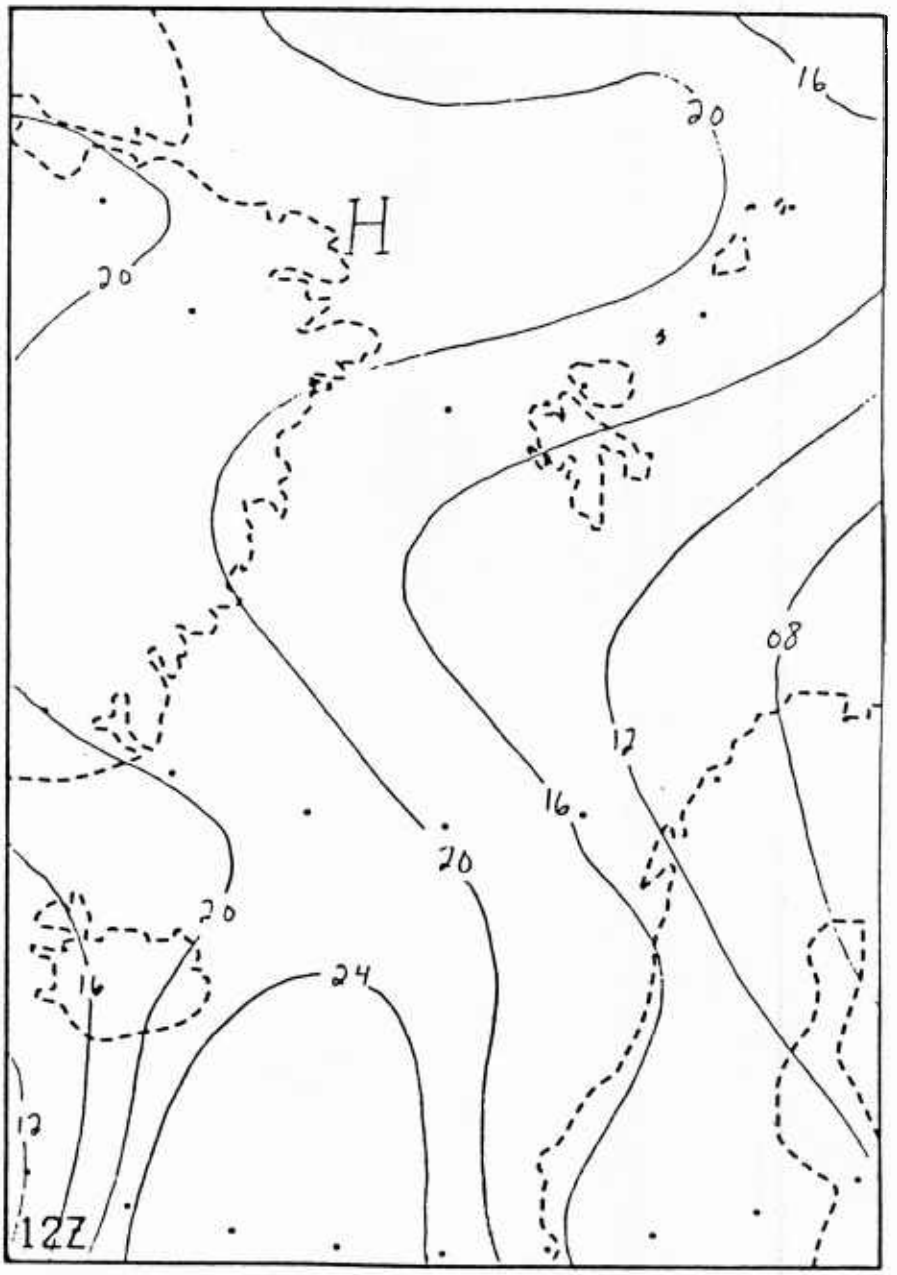

Figure 28b: Surface pressure chart 4 July 1984 1200 GMT.

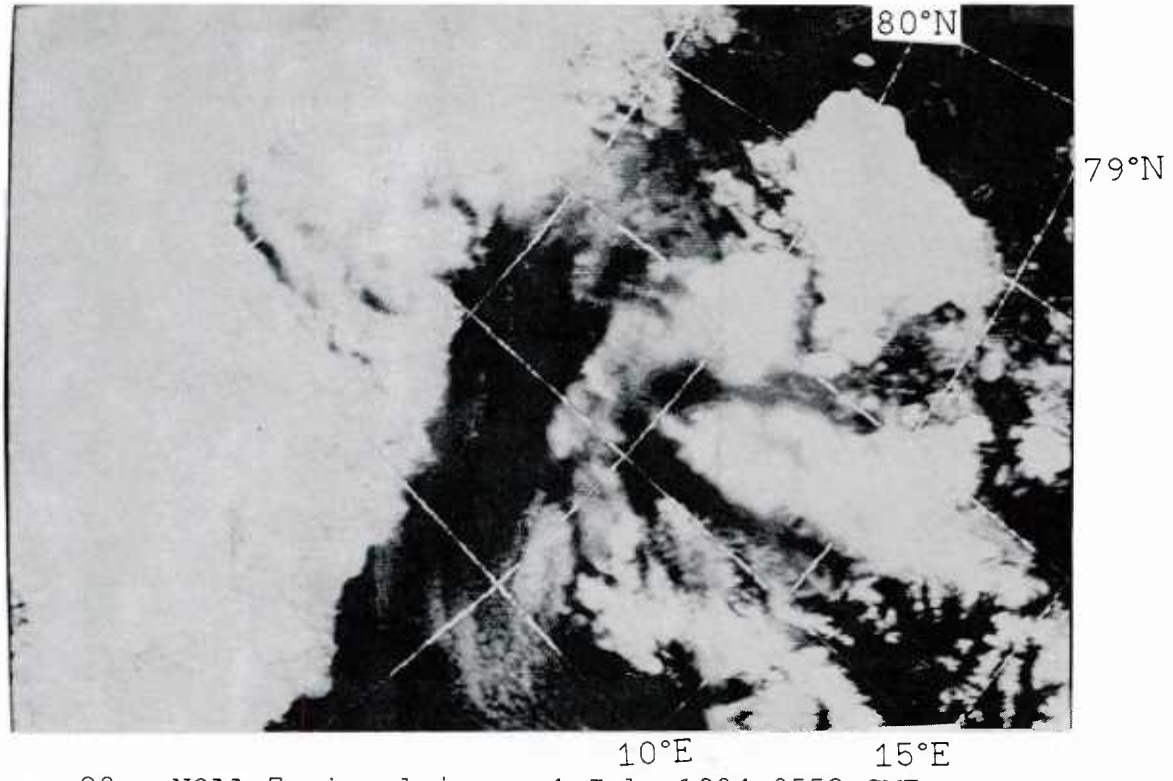

Figure 28c: NOAA-7 visual image 4 July 1984 0553 GMT.
The core of the mesoscale low lies over the ice edge. Both the topography and the horizontal temperature gradient in the region has played a role for the growth of the disturbance.

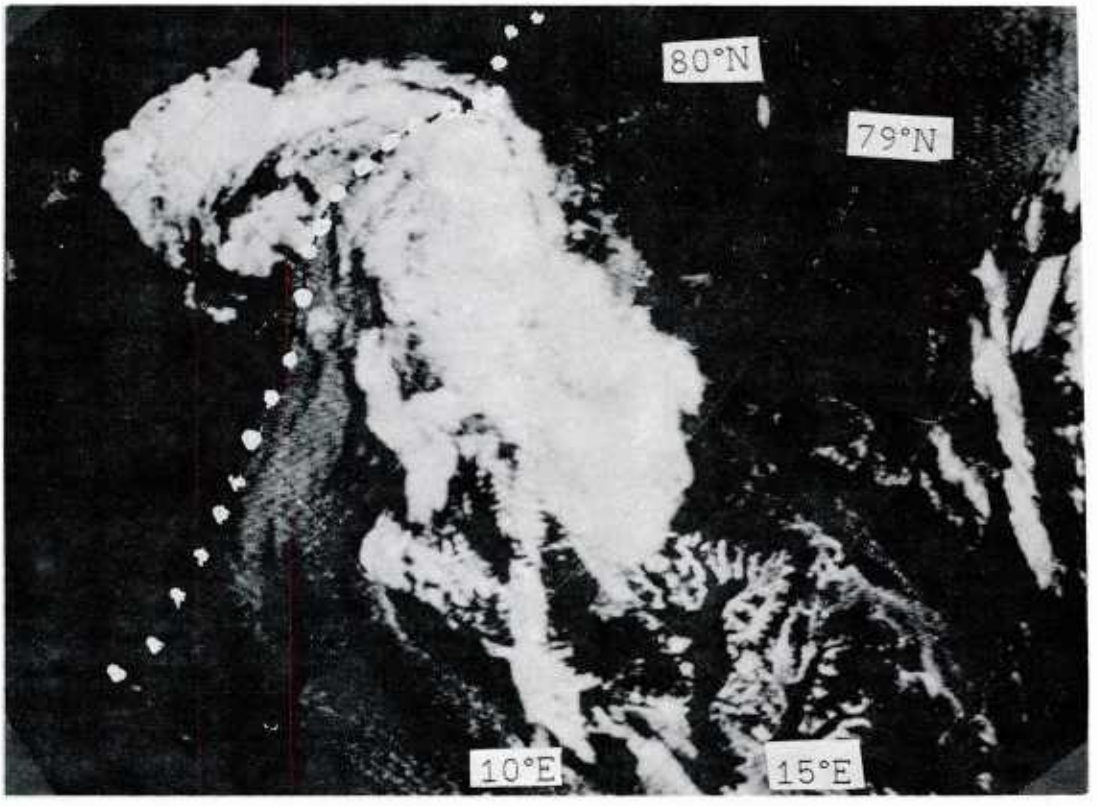

Figure 28d: NOAA-7 IR image 4 July 1984 0553 GMT.
The clouds of the vortex are extending to high levels where the temperatures are low. The ice edge is indicated by a dotted line. Some low level cloud streets formed downwind from the ice edge are seen bending around the northwest cape of Spitzbergen.

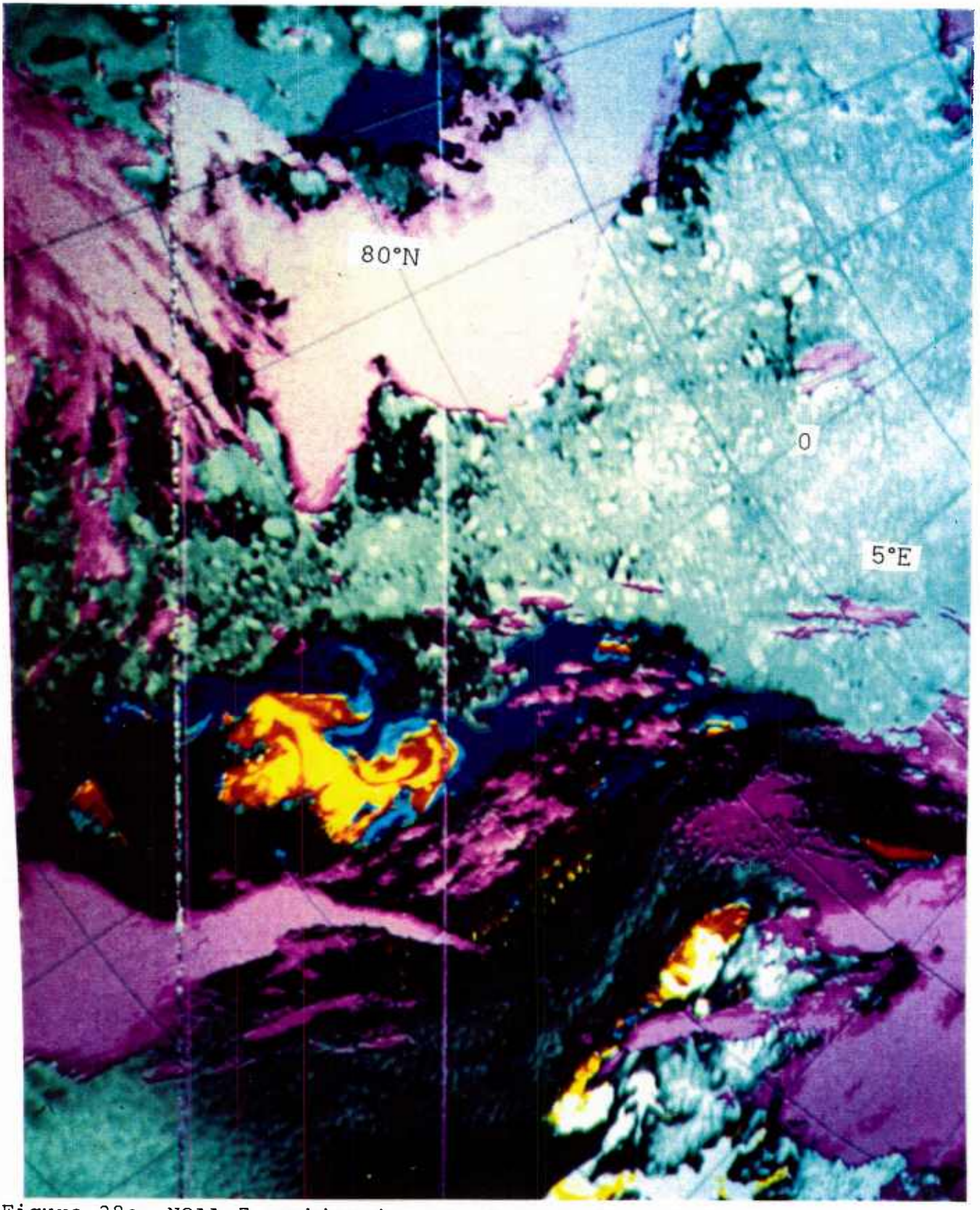

Figure 28e: NOAA-7 combination ch. 2 (visual) and ch. 4 (IR-temperature) image 4 July 1984 0553 GMT.. Image shows sea surface temperature and ice and clouds albedo. Surface features separated and displayed as follows: cold temperatures taken as high clouds, shown in magenta; bright visual albedo taken as ice, shown in greyscale from black (10%) to white (40%) albedo; dark visual albedo taken as ocean, shown in temperature-coded colors from dark blue (0°C) to yellow (5°C).

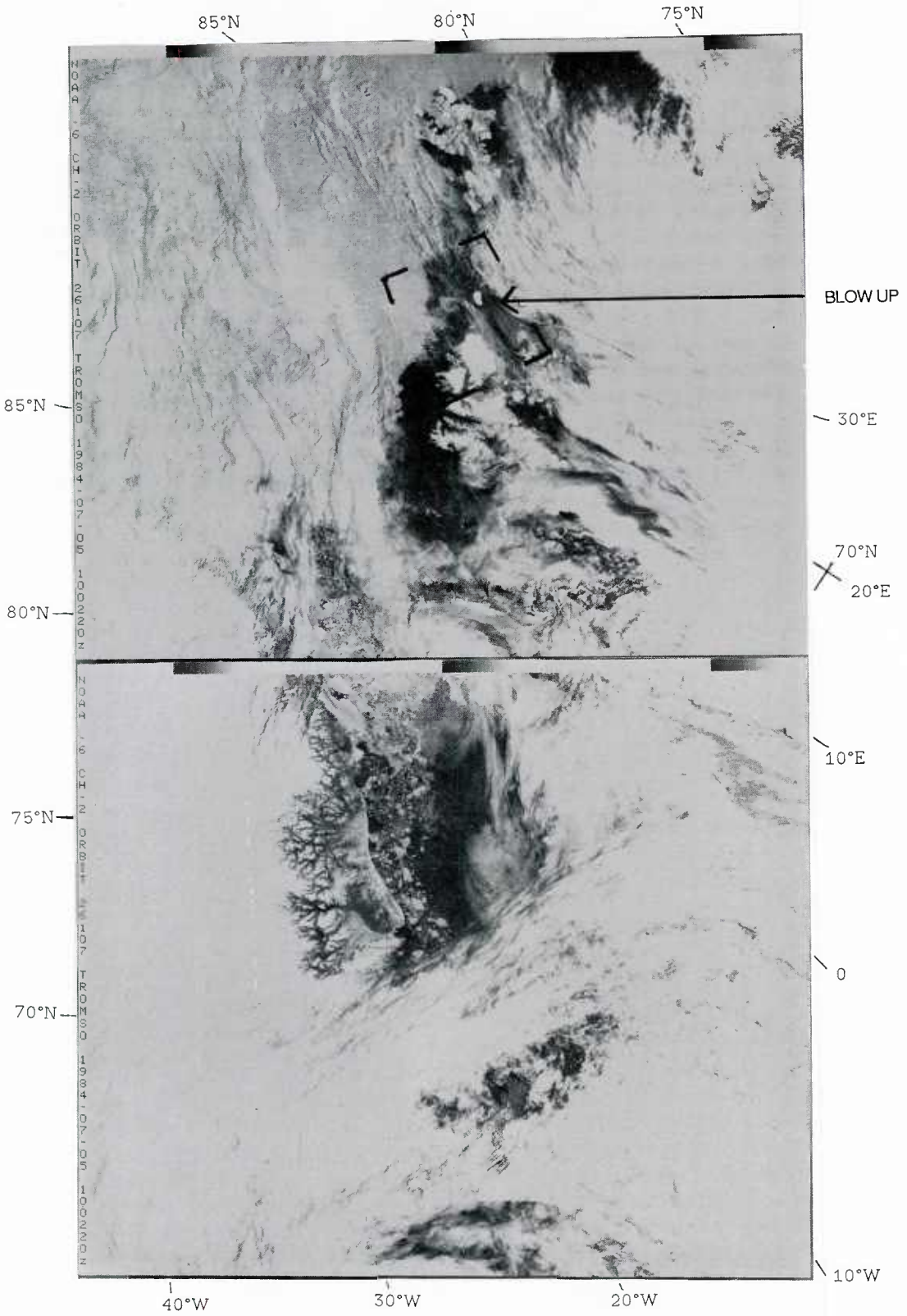

Figure 29a: NOAA-6 visual image 5 July 1984 1002 GMT.
A wide col is situated over the MIZ area. The mesoscale vortex north of Spitzbergen has moved eastwards by about 400 km and decays. Mesoscale vortices are also seen over the southern Fram Strait. South of Spitzbergen there is a wavy cloud pattern, presumably generated by the topography of the islands.

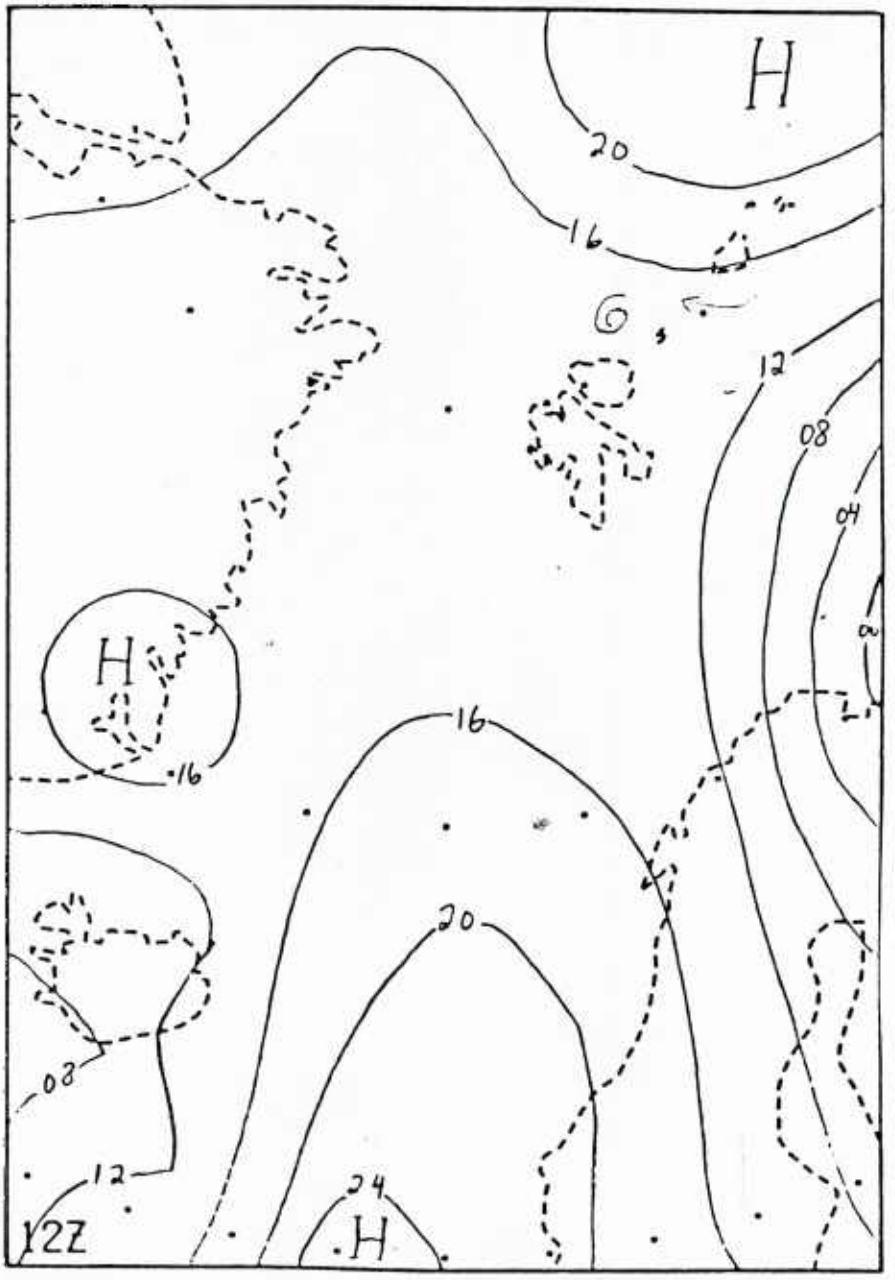

Figure 29b: Surface pressure chart 5 July 1984 1200 GMT.

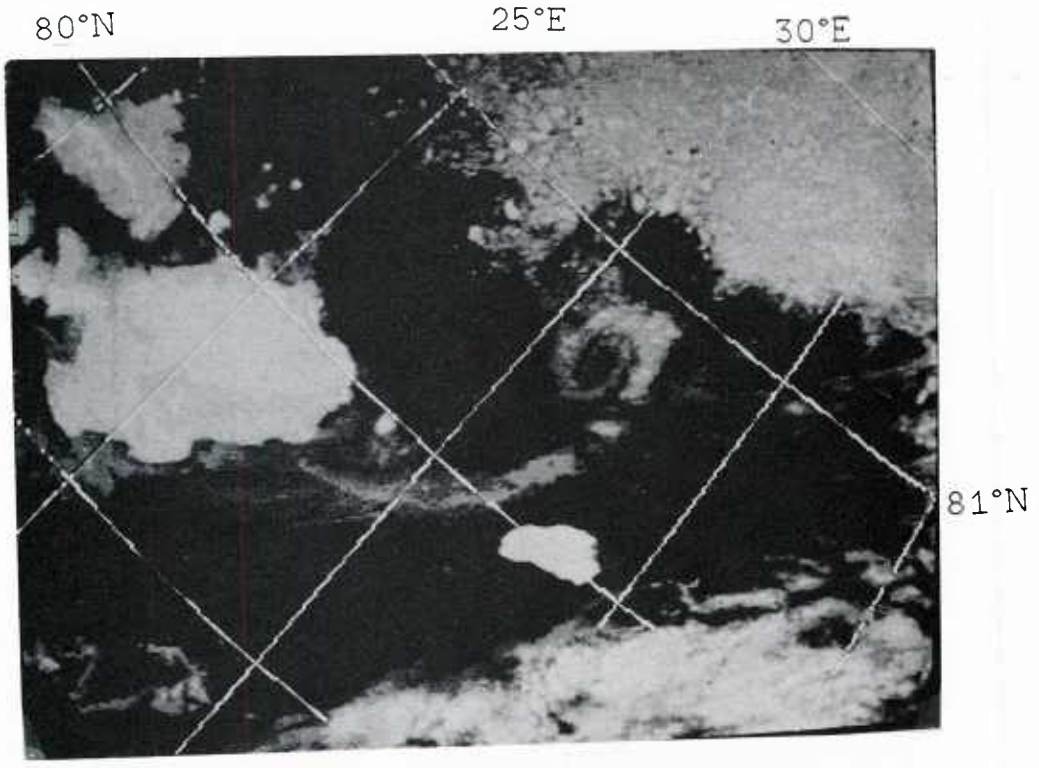

Figure 29c: NOAA-6 visual image 5 July 1984 1002 GMT.
The decay of the mesoscale vortex is seen by the smaller extent of its cloud mass (cf. figure 28c).

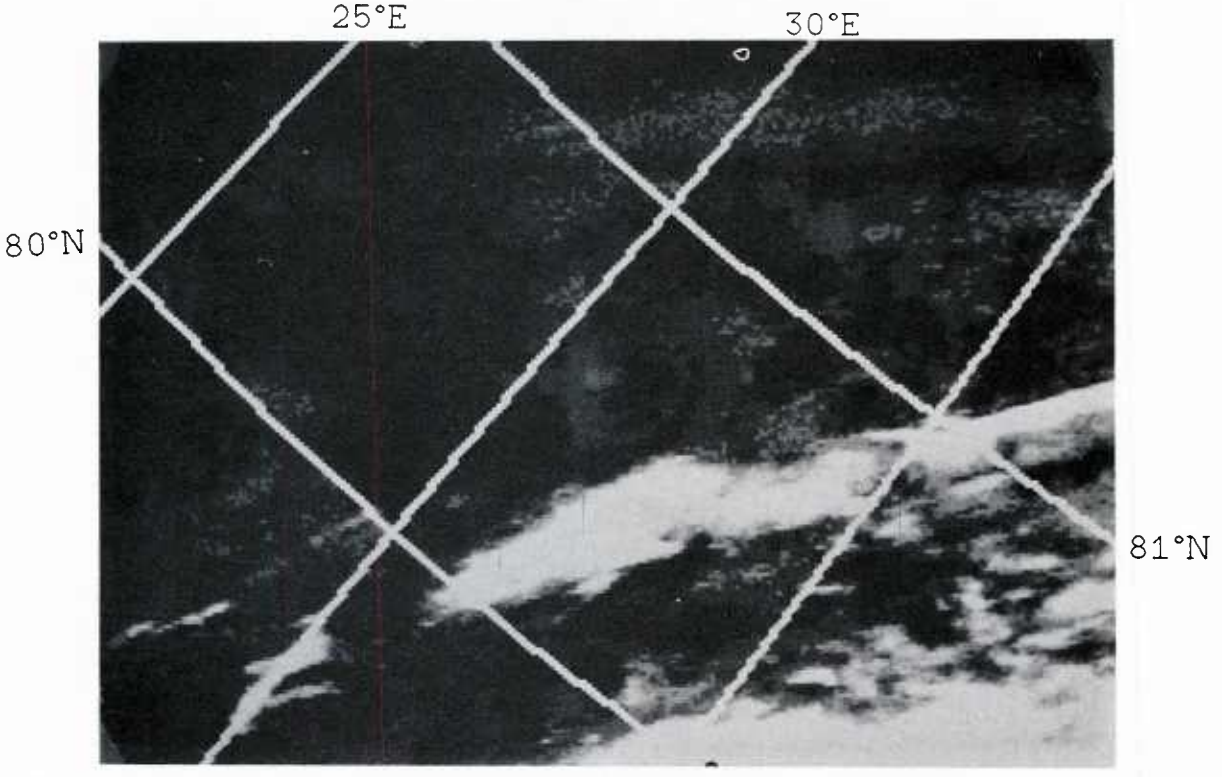

Figure 29d: NOAA-6 IR image 5 July 1984 1002 GMT.
The thermal image of the vortex shows that the top of its cloud mass does not reach as high as it did the day before (cf. figure 28d), the top being only about 5°C colder than the surface.

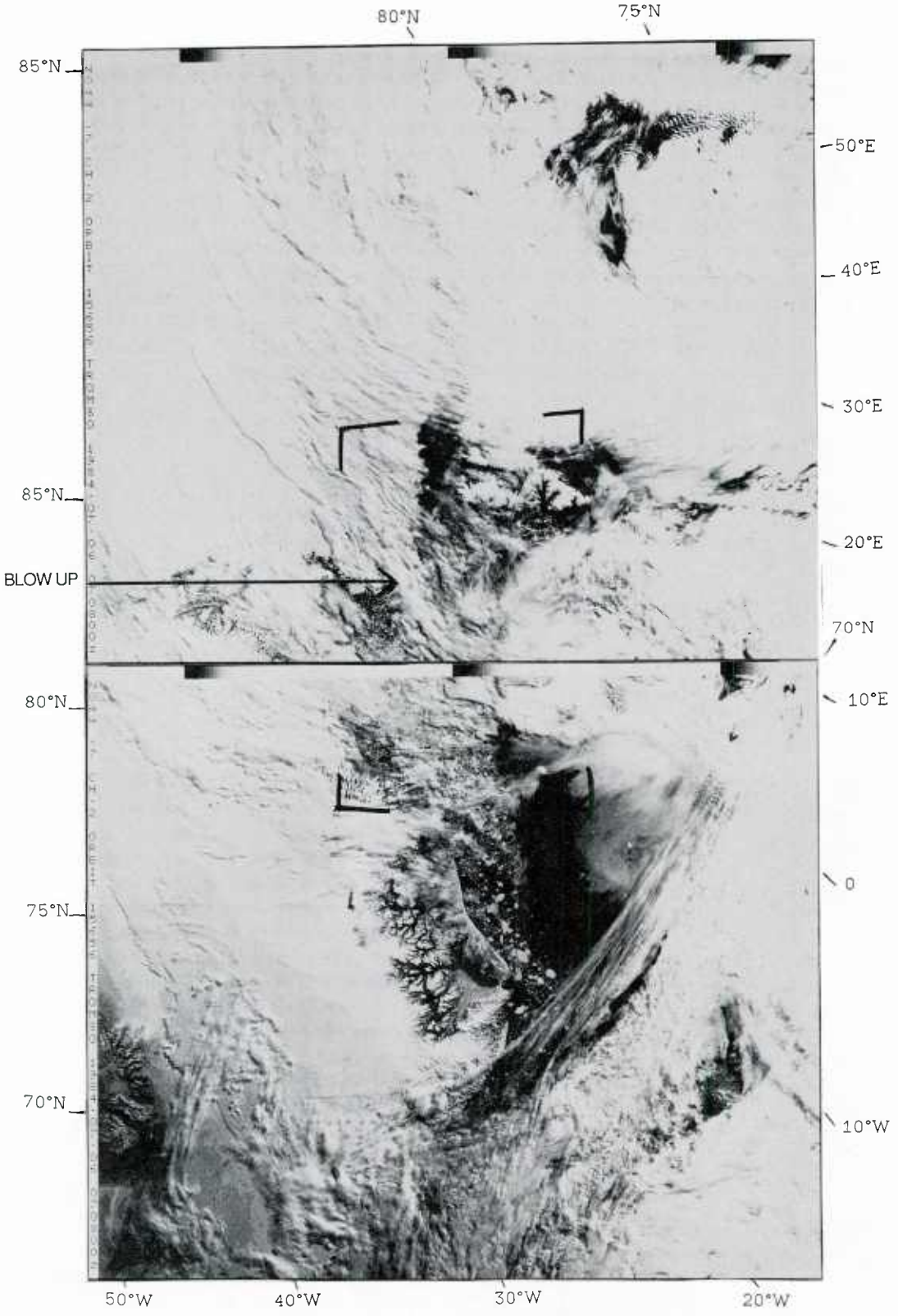

Figure 30a: NOAA-7 visual image 6 July 1984 0708 GMT.
This very dynamical scene gives a good impression of how warm air from the south moves north to meet the cold arctic air, and mixes together in the strong cyclone over the Barents Sea. Over the MIZ area the winds are blowing off-ice. The region is covered by high level clouds. Around Jan Mayen some fine structures of low level clouds are seen, for example a short wavy pattern in the lee of the island.

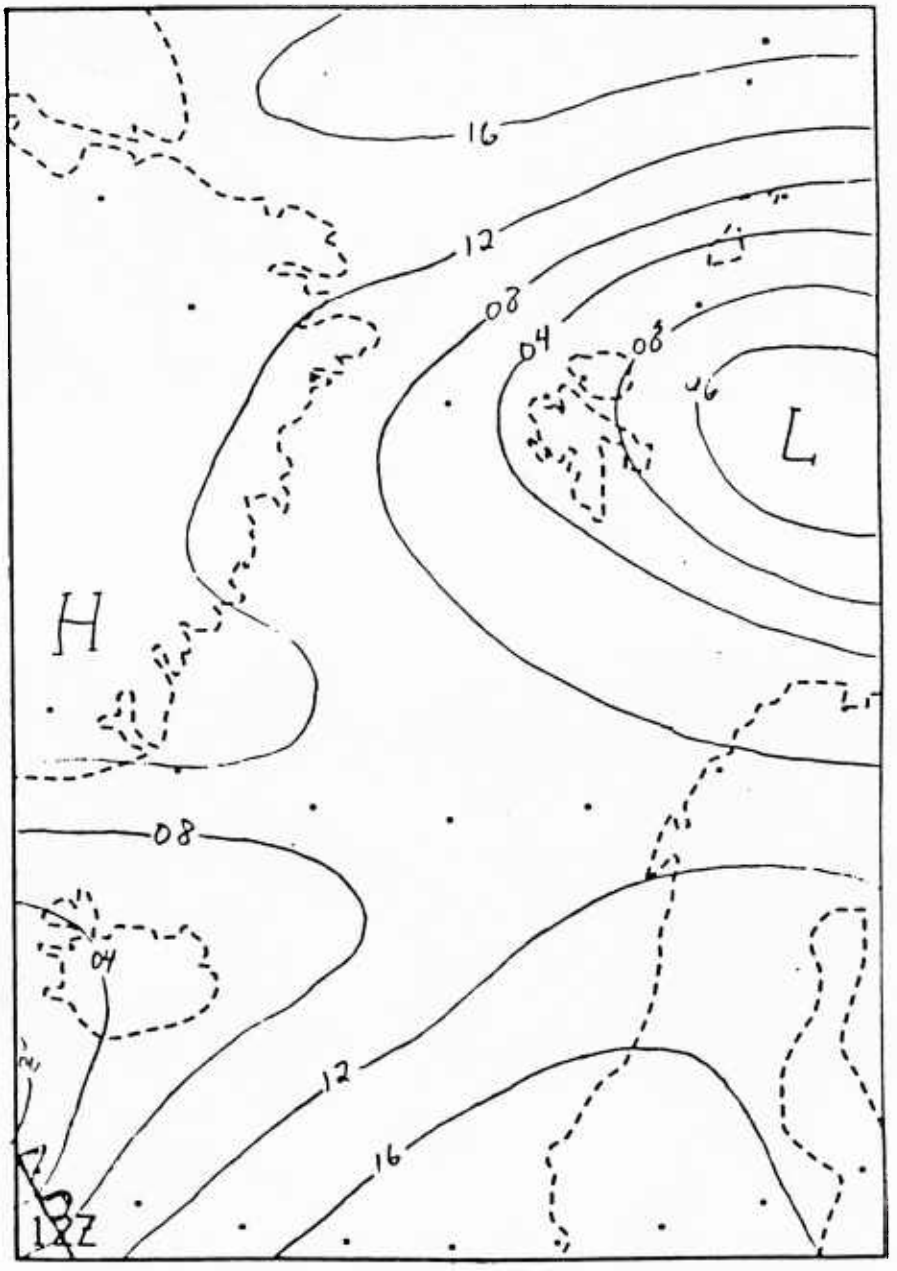

Figure 30b: Surface pressure chart 6 July 1984 1200 GMT.

Figure 30c: NOAA-7 visual image 6 July 1984 0708 GMT.
In the Fram Strait area the wind is off-ice and high level cloud streets following the streamlines of the air flow are seen. Some mountain waves generated over Greenland are visible (upper left corner of the image).

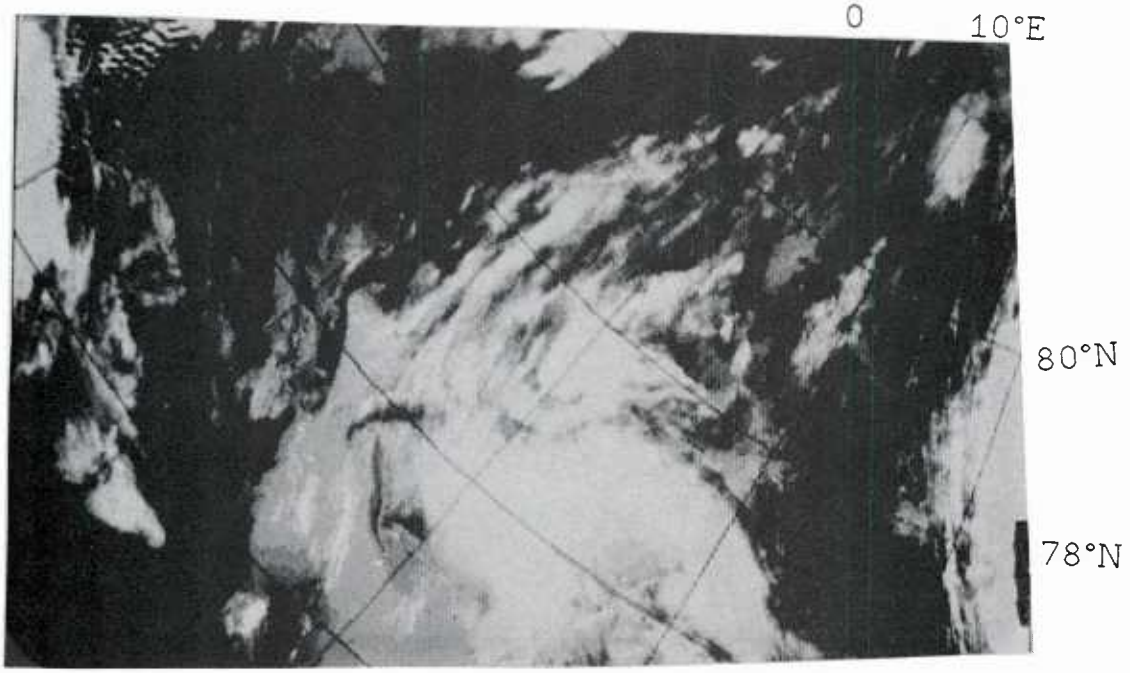

Figure 30d: NOAA-7 IR image 6 July 1984 0708 GMT.
The IR image indicates that the height of the cloud tops increases downwind. The mountain waves over Greenland are situated at a high level.

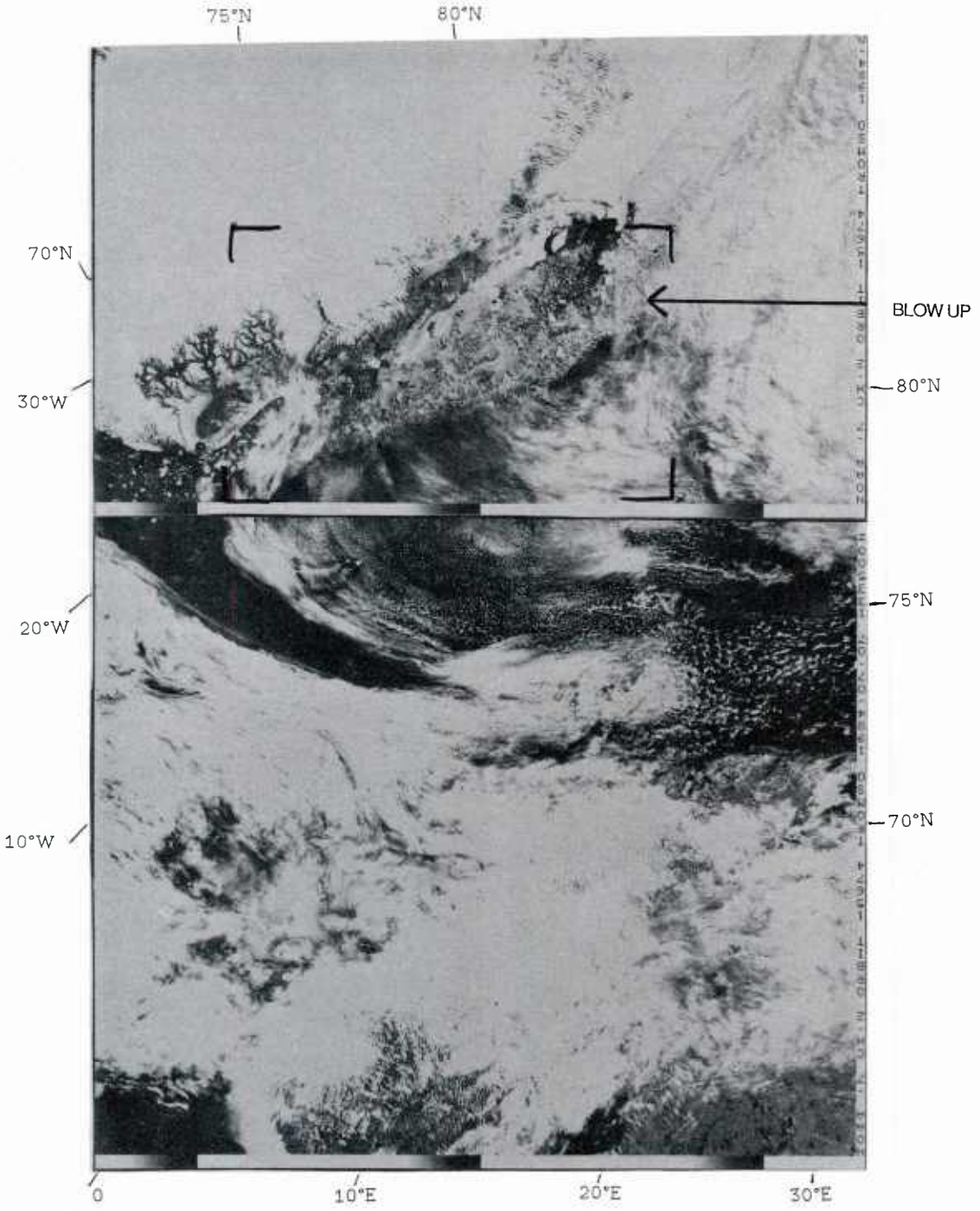

Figure 31a: NOAA-7 visual image 7 July 1984 1335 GMT.
The Barents Sea low is growing in intensity, and generates strong off-ice winds in the Fram Strait. The ice zone is clearly visible, lying in a region of atmospheric subsidence. Some mountain waves over the eastcoast of Greenland are seen.

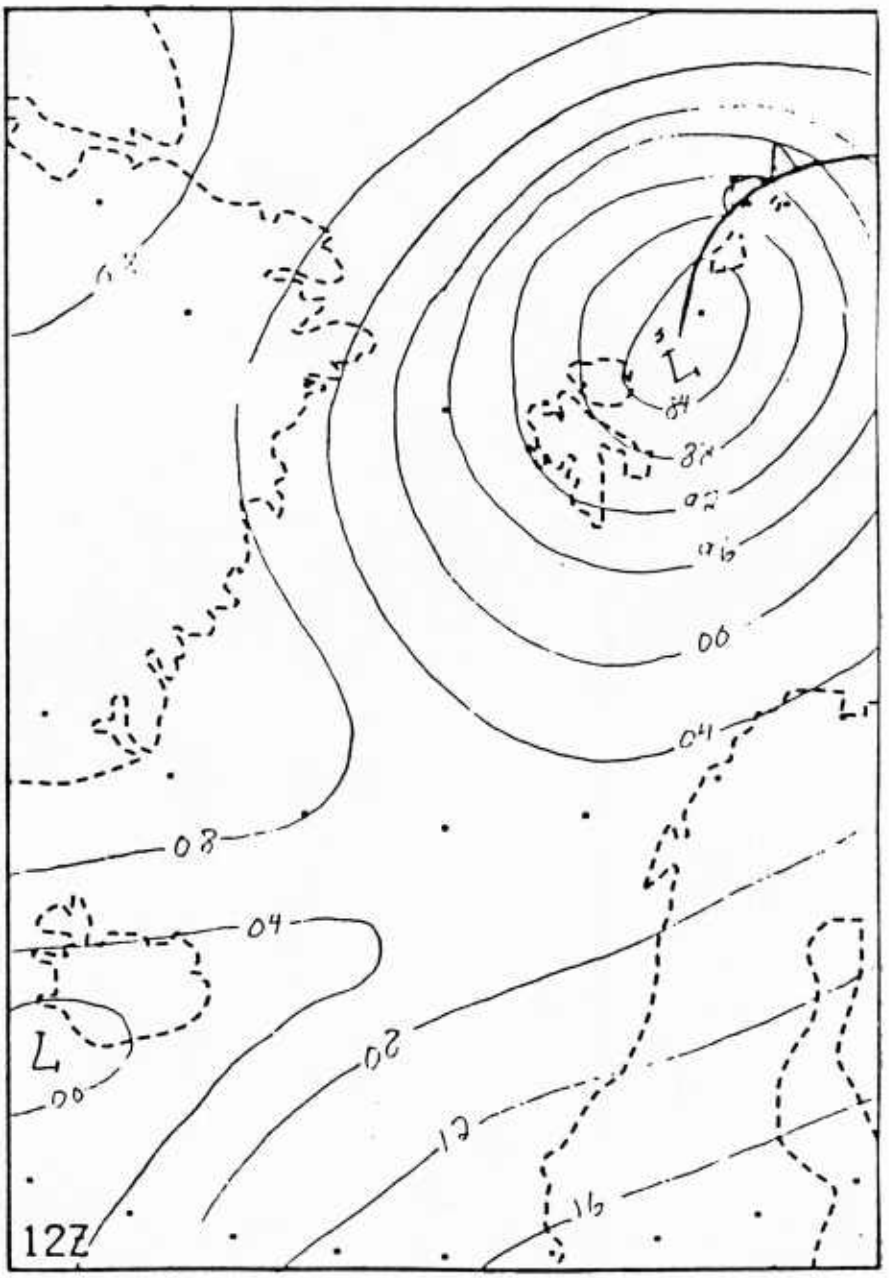

Figure 31b: Surface pressure chart 7 July 1984 1200 GMT.

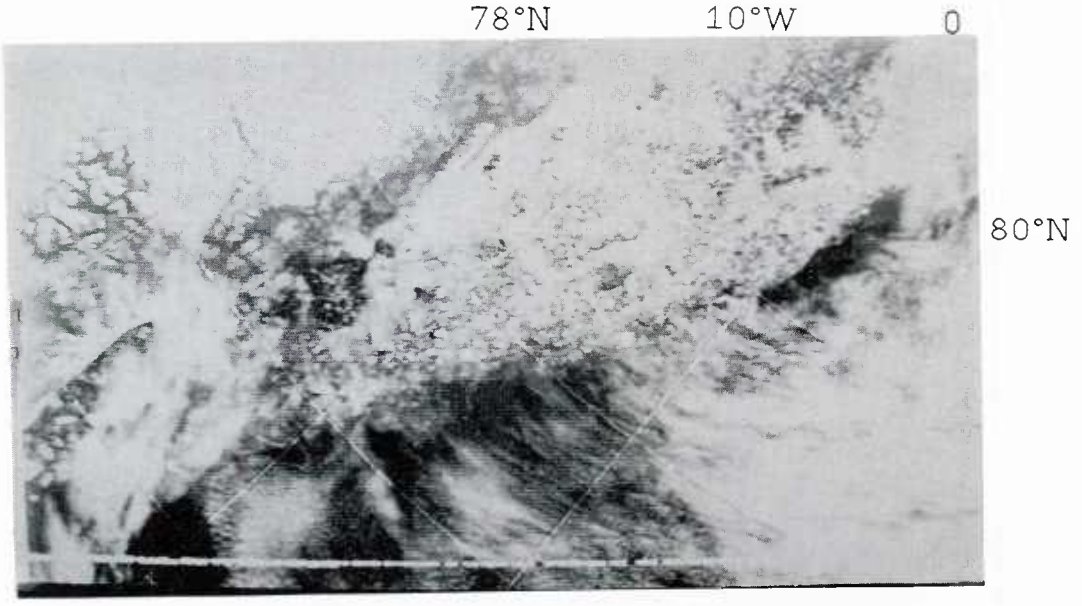

Figure 31c: NOAA-7 visual image 7 July 1984 1335 GMT.
Westerly winds prevail at higher levels over the MIZ area, indicated by the cloud streets seen on the image. The strong northwesterly surface wind stretches the ice edge and makes it rather diffuse.

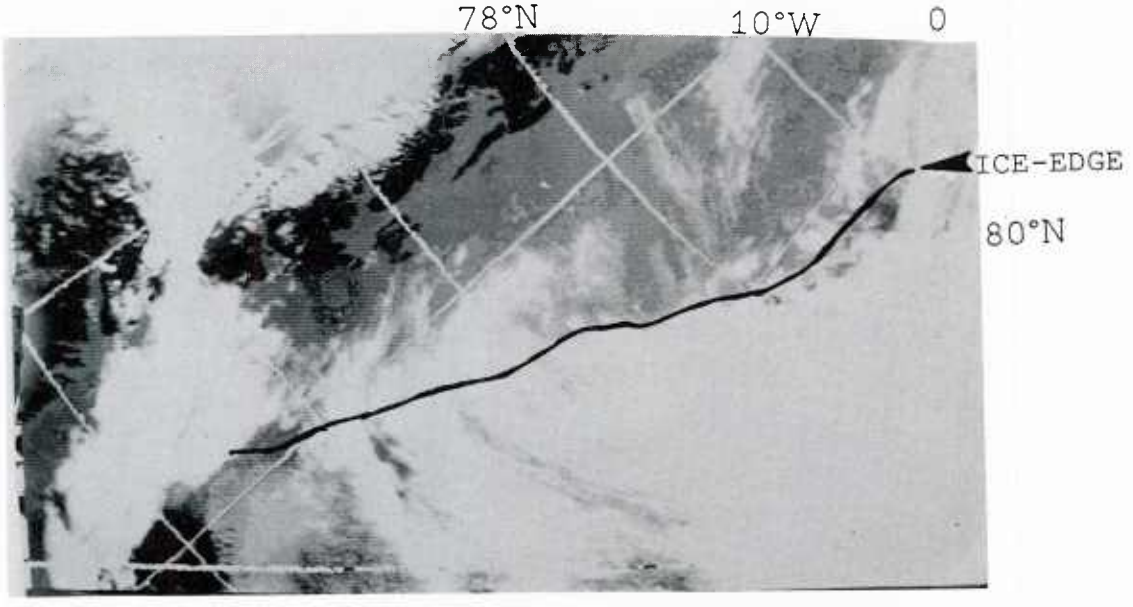

Figure 31d: NOAA-7 IR image 7 July 1984 1335 GMT.
The thermal image shows some open water areas closer to the shore far behind the ice edge. The cloud tops outside the ice edge are cold and high.

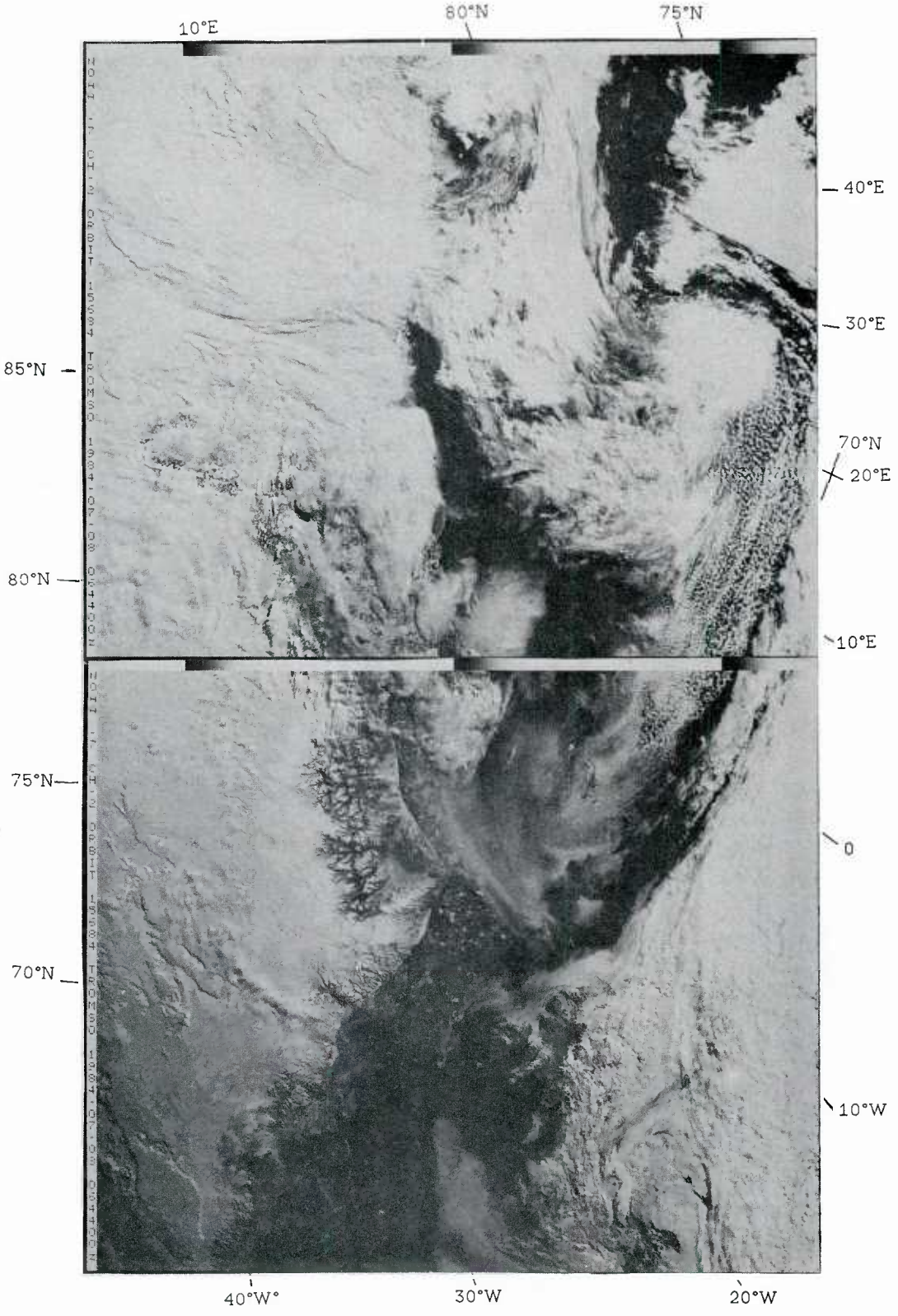

Figure 32a: NOAA-7 visual image 8 July 1984 0644 GMT.
The MIZ area is lying on the backside of the still intense low that has moved north of Frans-Josef-Land. The satellite image shows a second cyclone developing in the cold trough southeast of Spitzbergen. Mountain waves are seen over Spitzbergen. In the Fram Strait clouds cover the ice region, while the open sea region is only covered with light cirrus.

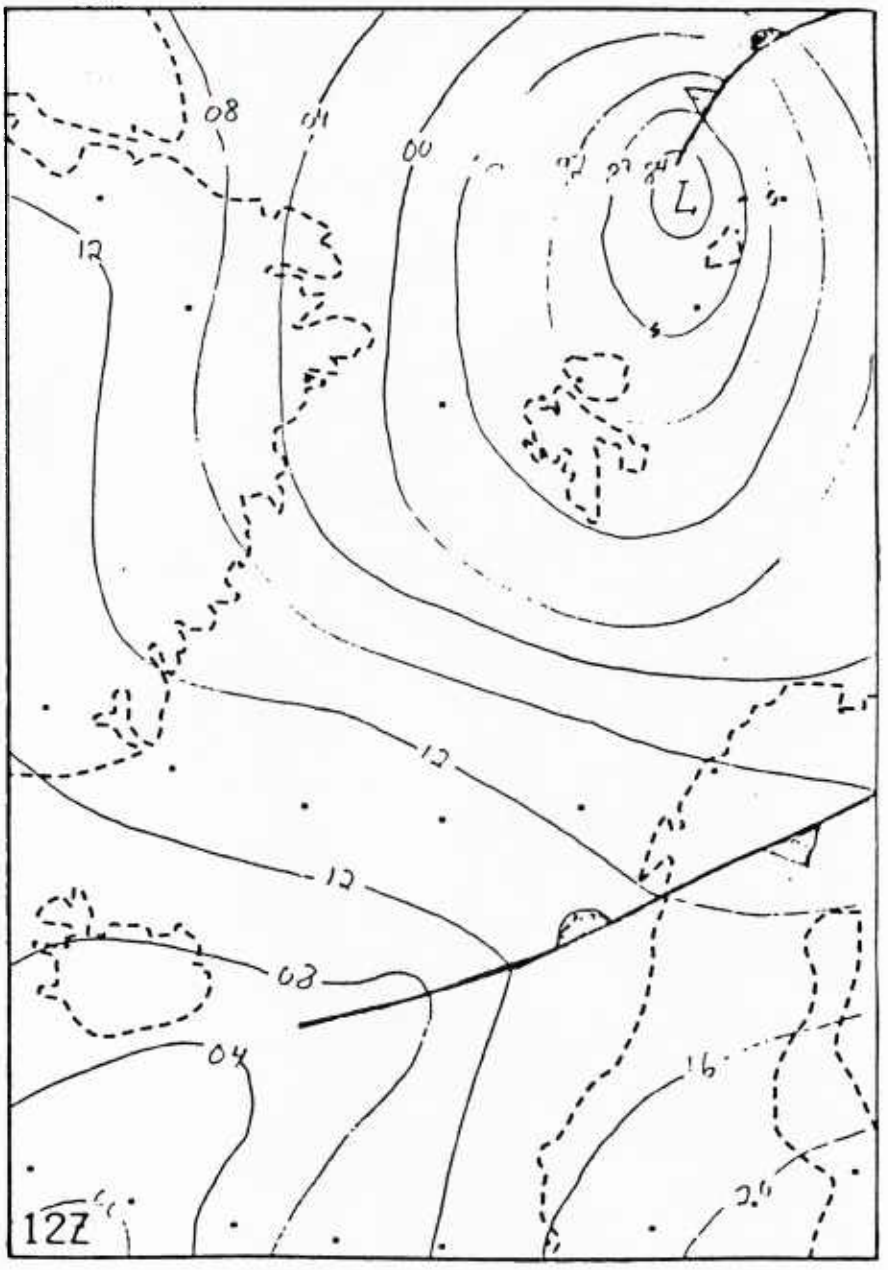

Figure 32b: Surface pressure chart 8 July 1984 1200 GMT.

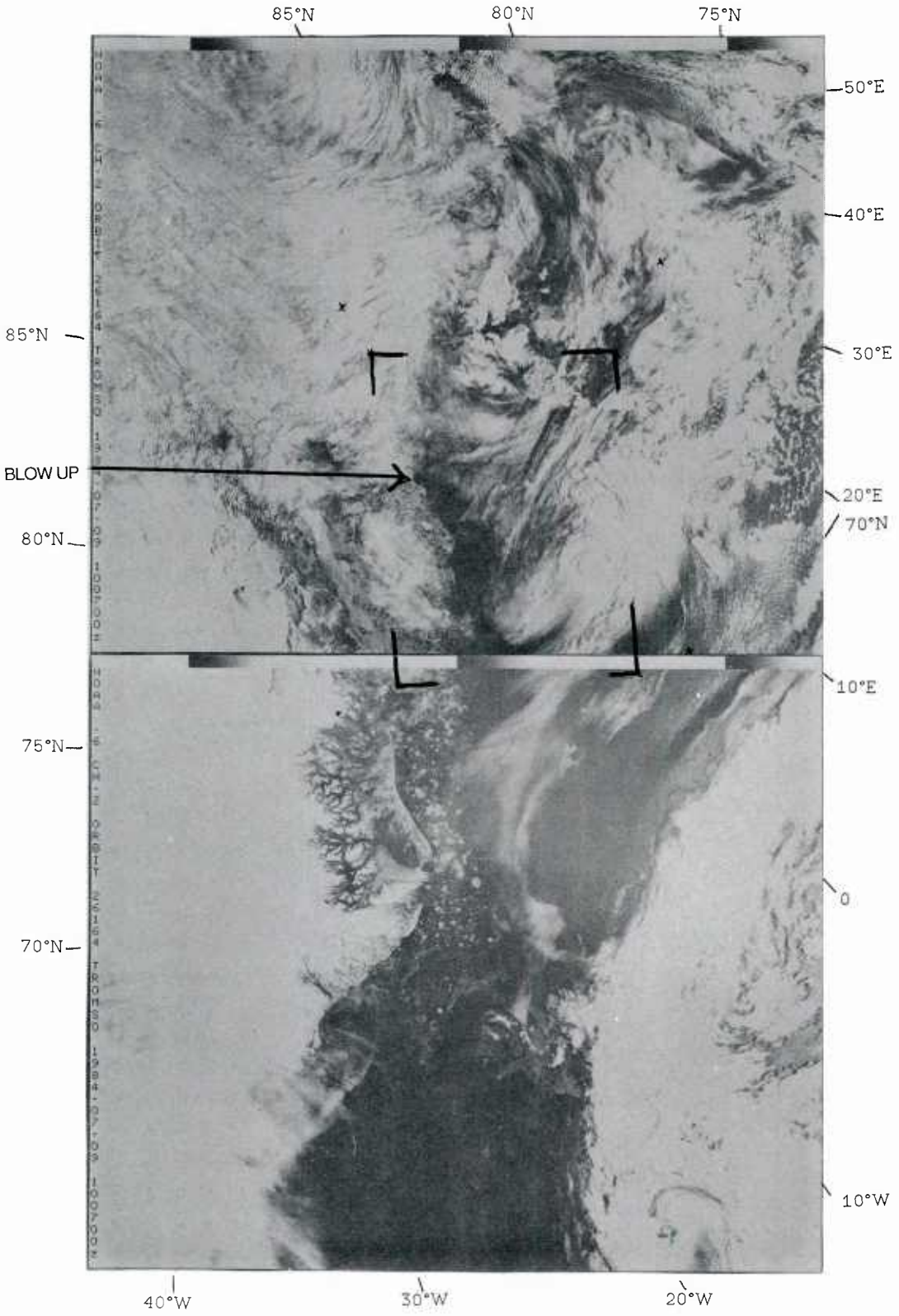

Figure 33a: NOAA-6 visual image 9 July 1984 1007 GMT.
The low north of Frans-Josef-Land has started to decay, but still influences the MIZ area. Strong off-ice winds blow along the whole ice edge, and some low level cloud streets are visible. Mountain waves are visible at several places, south of Spitzbergen, Frans-Josef-Land, and northeast of Greenland.

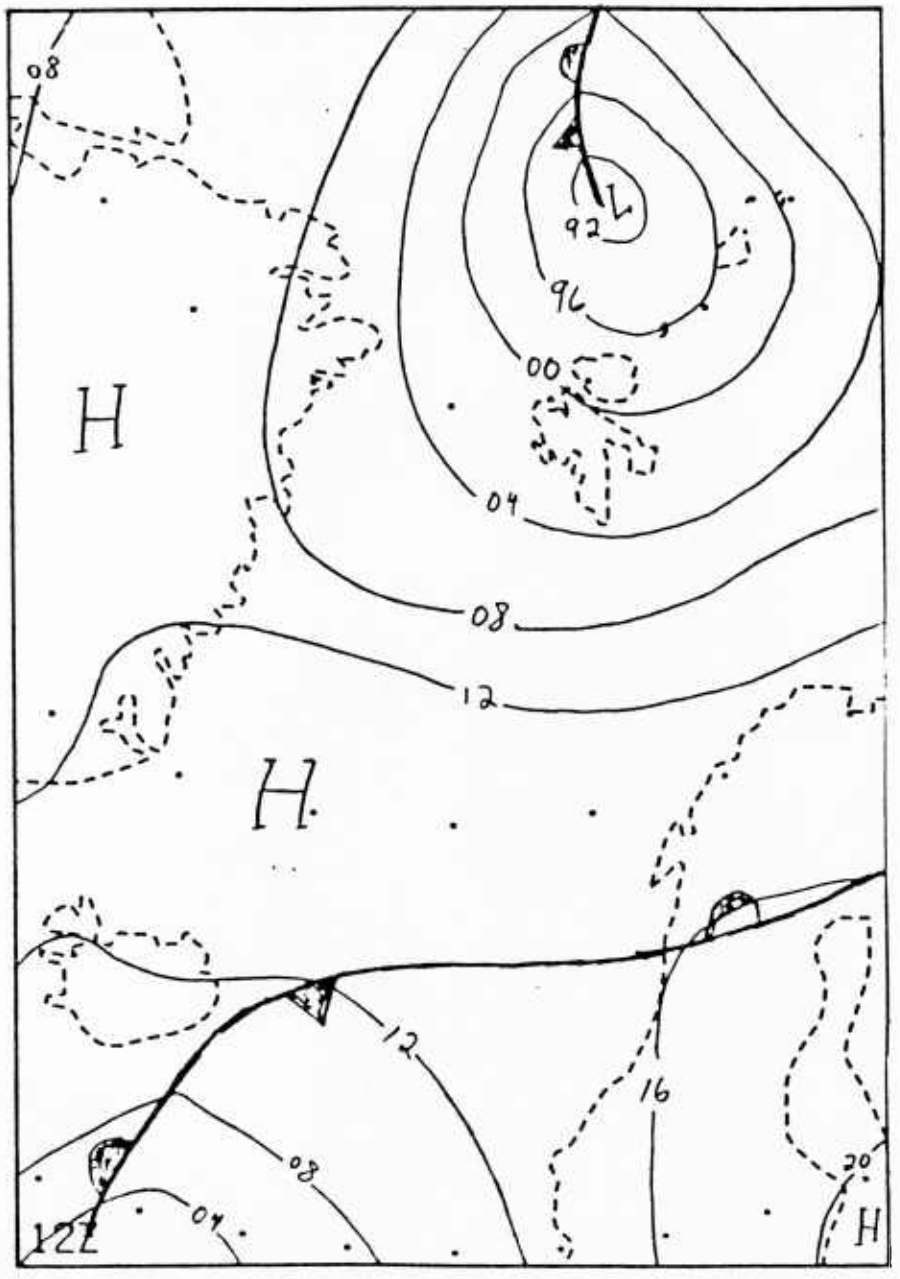

Figure 33b: Surface pressure chart 9 July 1984 1200 GMT.

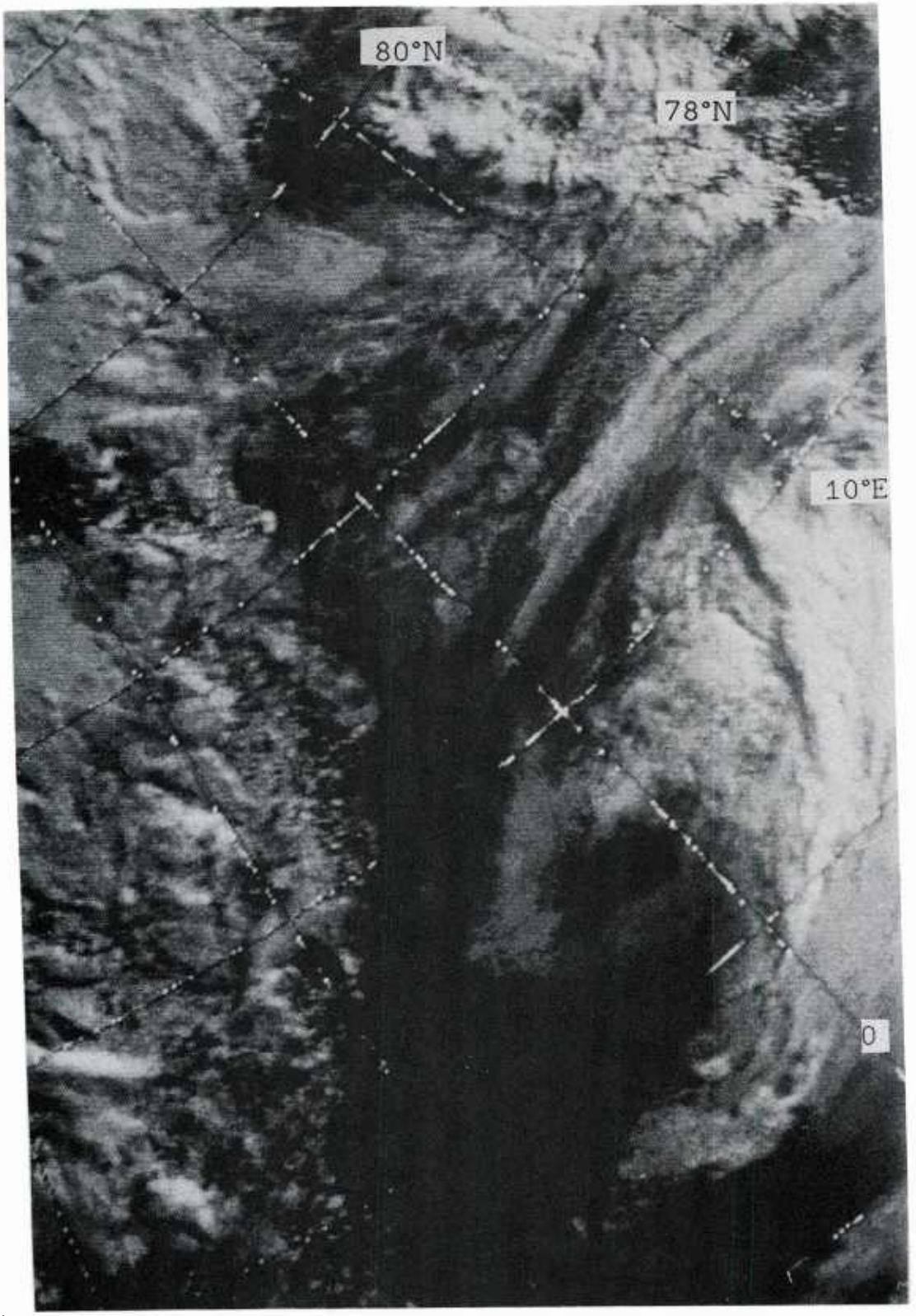

Figure 33a: NOAA-6 visual image 9 July 1984 1007 GMT.
After a long time with steady off-ice winds, the ice edge is rather diffuse. The heavy cloud formation on the middle right of the image reflects the convective activity along the cold trough protruding over the MIZ area from the Frans-Josef-Land low.

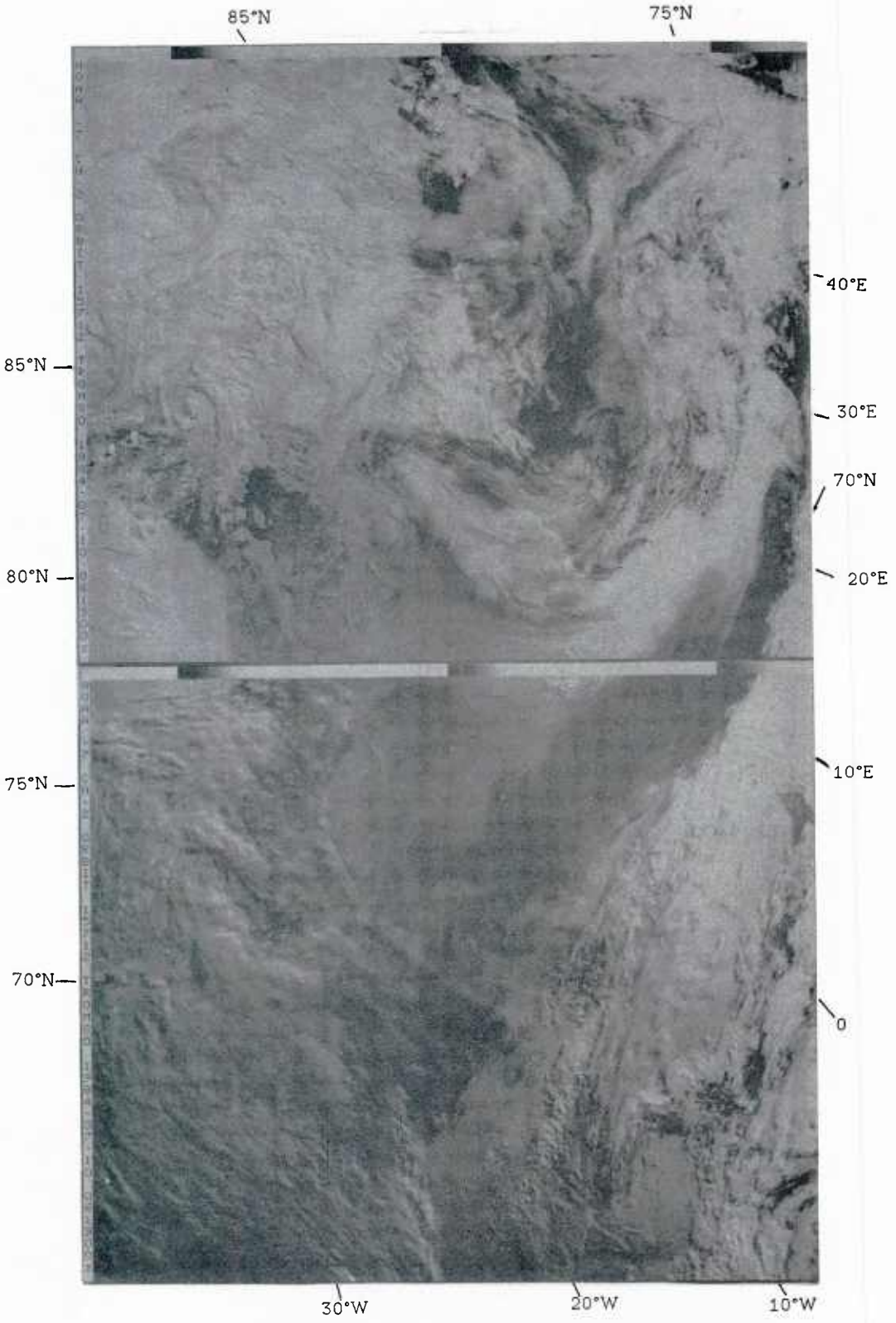

Figure 34a: NOAA-7 visual image 10 July 1984 0619 GMT.
A deep trough along the eastcoast of Greenland creates southwest winds over the MIZ area. At high levels the winds blow from west to northwest. In the large scale high level cloud veil around South-Spitzbergen, several mesoscale vortices are embedded. Mountain waves are seen over Spitzbergen.

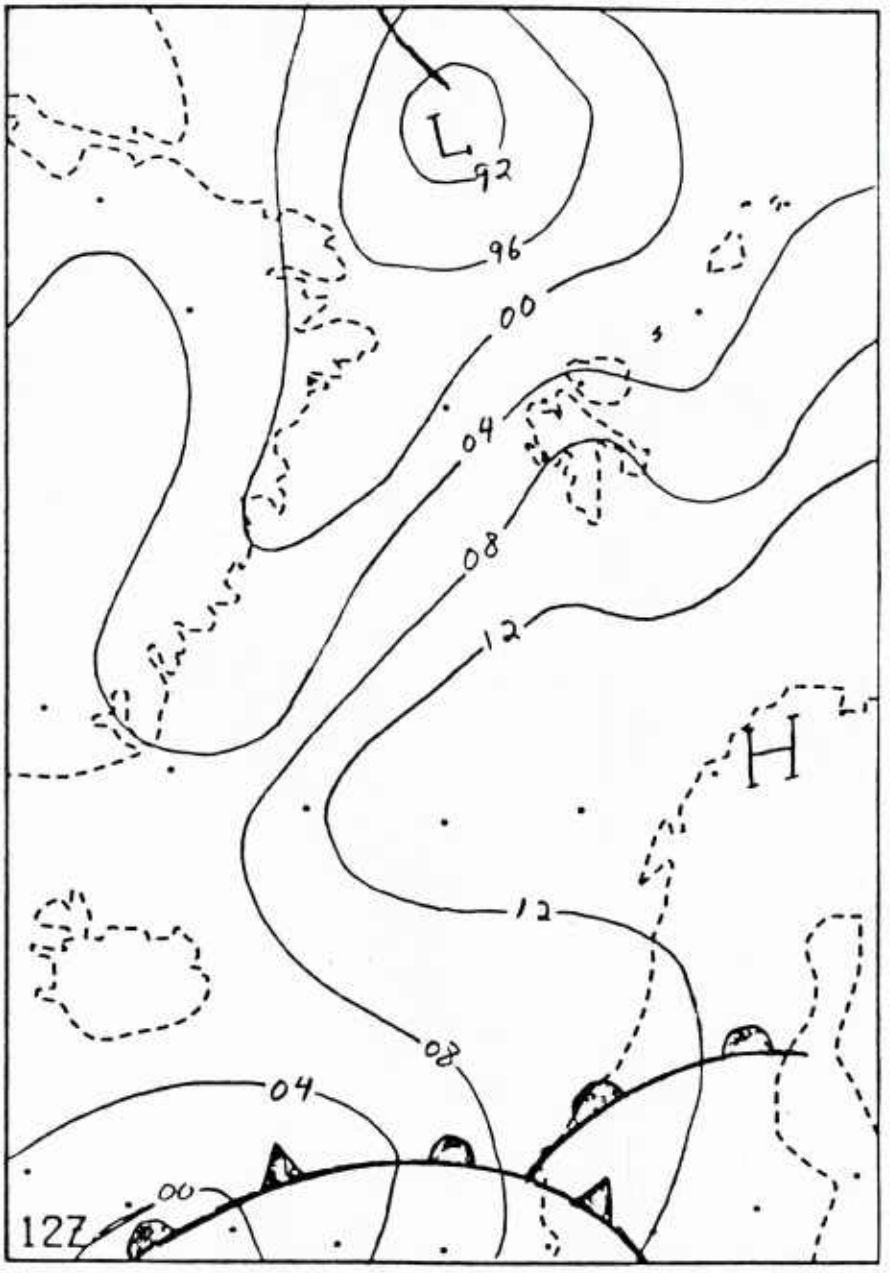

Figure 34b: Surface pressure chart 10 July 1984 1200 GMT.

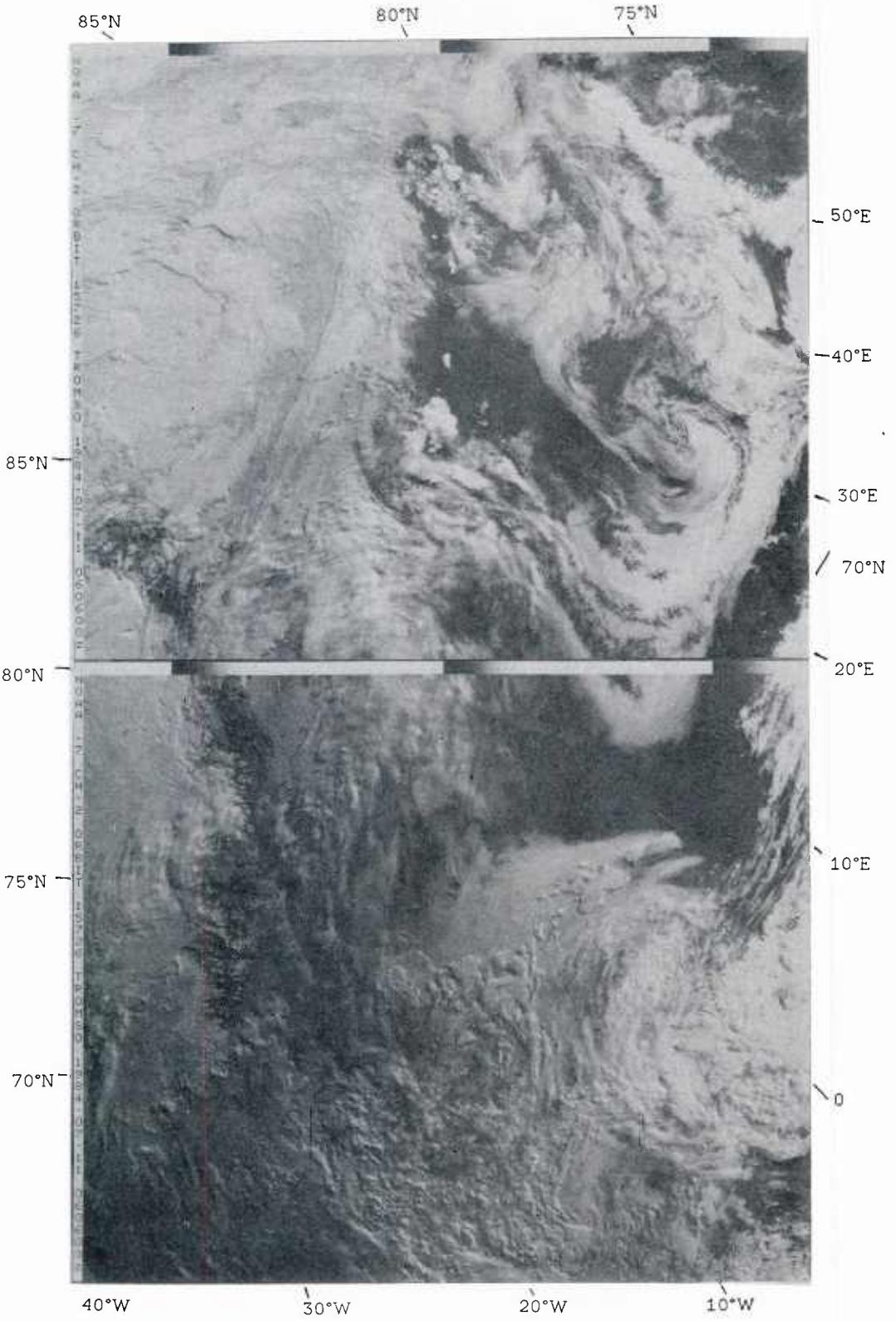

Figure 35a: NOAA-7 visual image 11 July 1984 0606 GMT.
The trough over the MIZ area has become filled, but a high over the Barents Sea has grown, so there are still strong southwesterly winds in the eastern Fram Strait. High level clouds obscure what is going on at lower levels in the MIZ area.

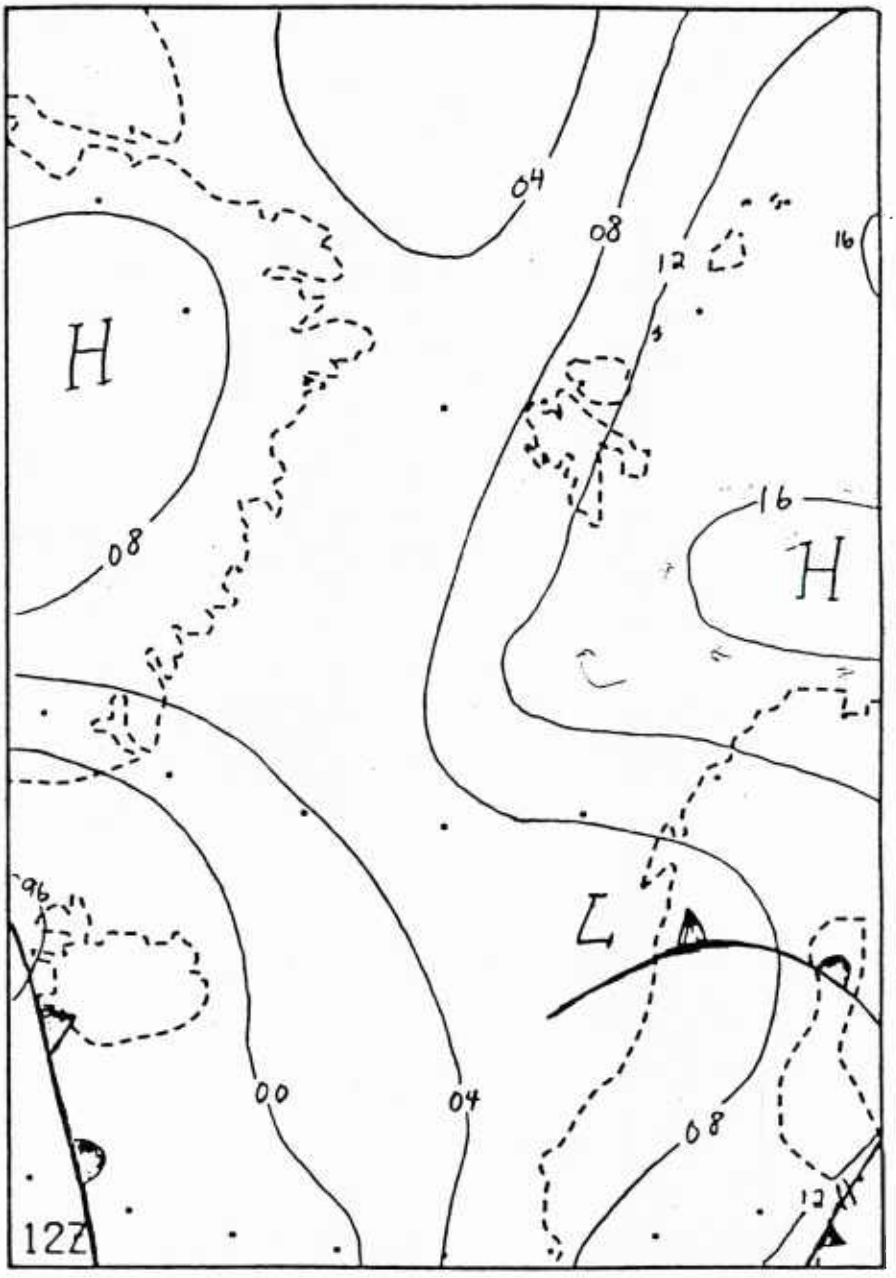

Figure 35b: Surface pressure chart 11 July 1984 1200 GMT.

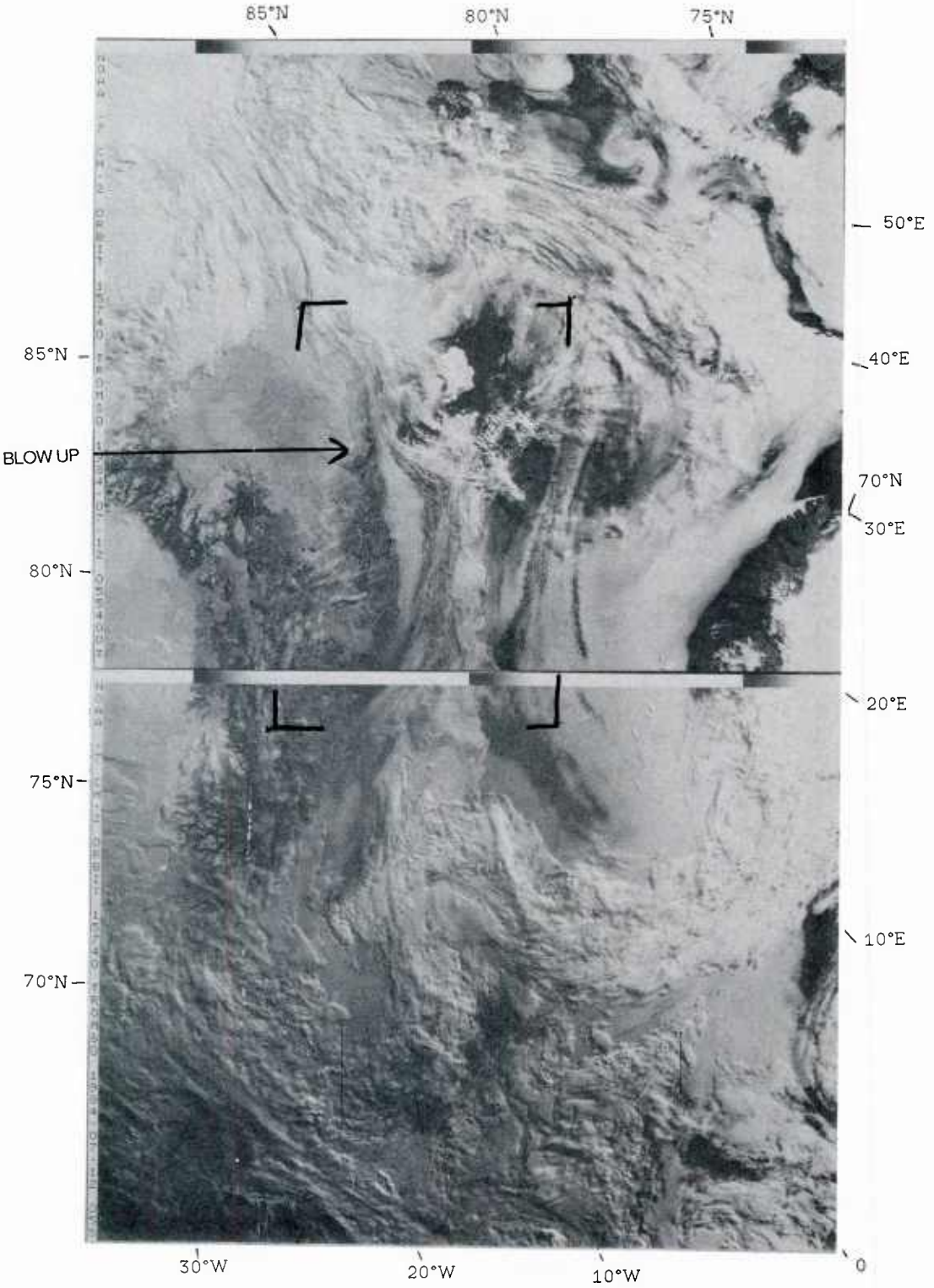

Figure 36a:NOAA-7 visual image 12 July 1984 0554 GMT.
The marginal ice zone is rather diffuse on the image, and covered with fog or layer clouds. The wind is light with an on-ice component. Mountain waves are seen over South-Spitzbergen.

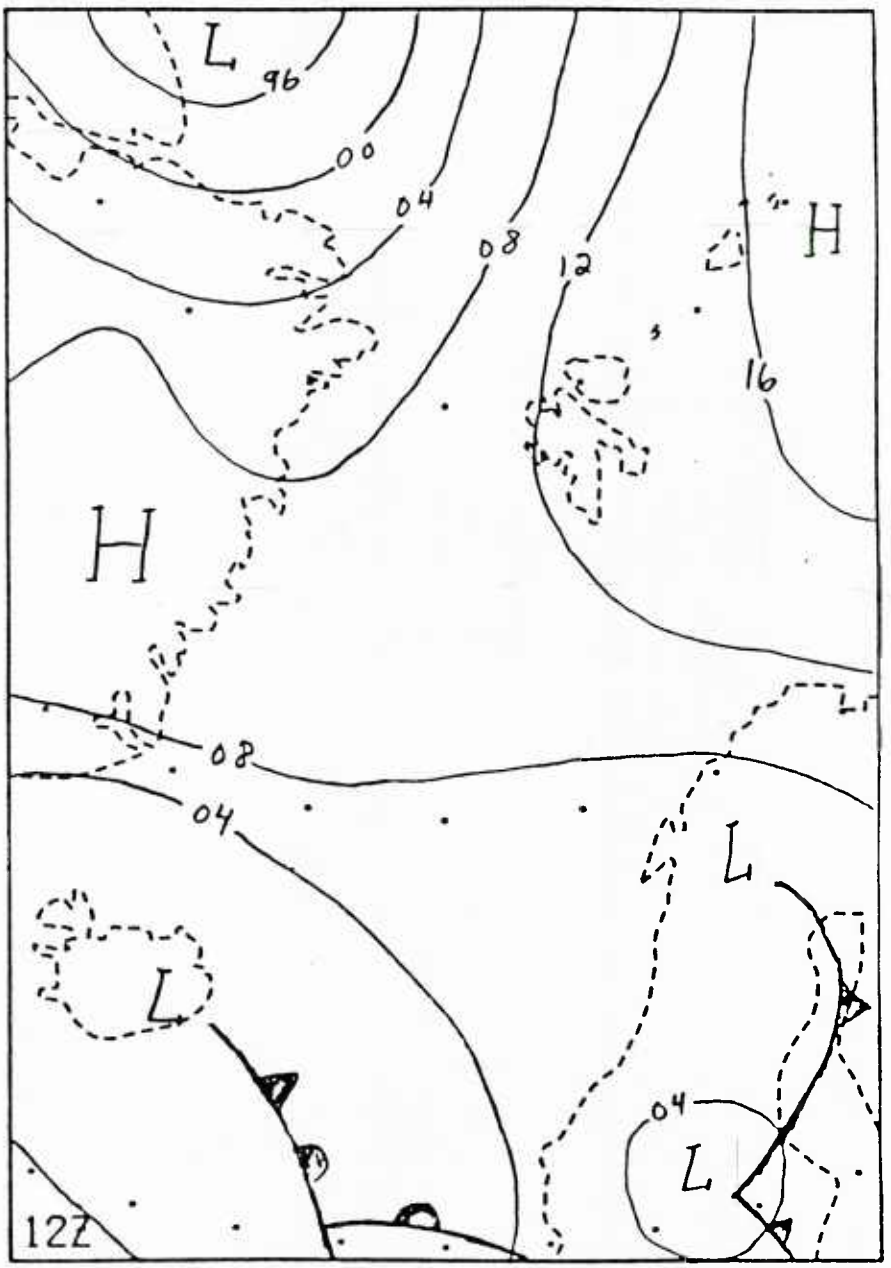

Figure 36b: Surface pressure chart 12 July 1984 1200 GMT.

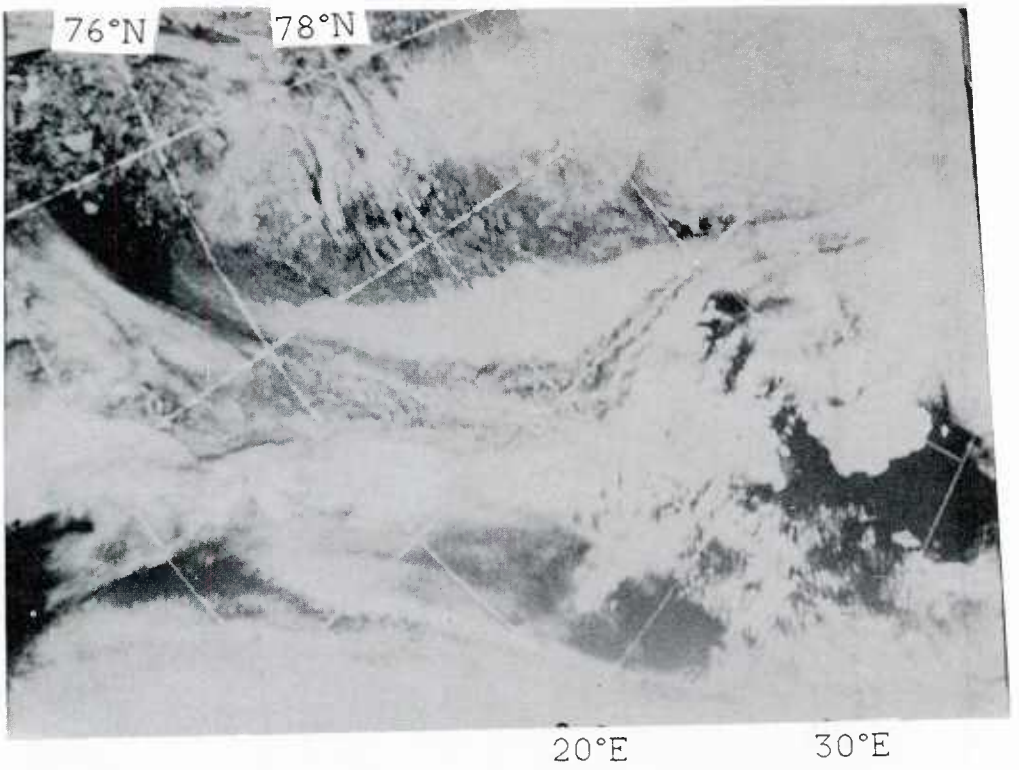

Figure 36c: NOAA-7 visual image 12 July 1984 0554 GMT. The MIZ area is covered by clouds and light on-ice winds prevail.

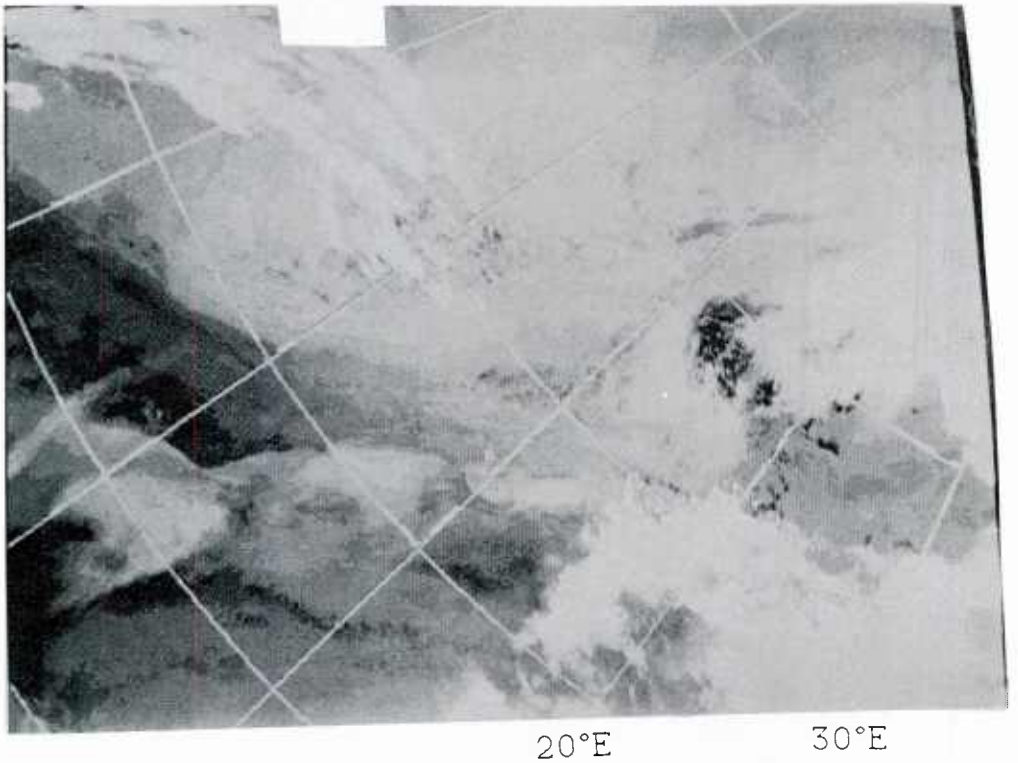

Figure 36d: NOAA-7 IR image 12 July 1984 0554 GMT. The thermal image shows that layer clouds are present at different heights. The temperatures range from 0°C (black) to -20°C (white).

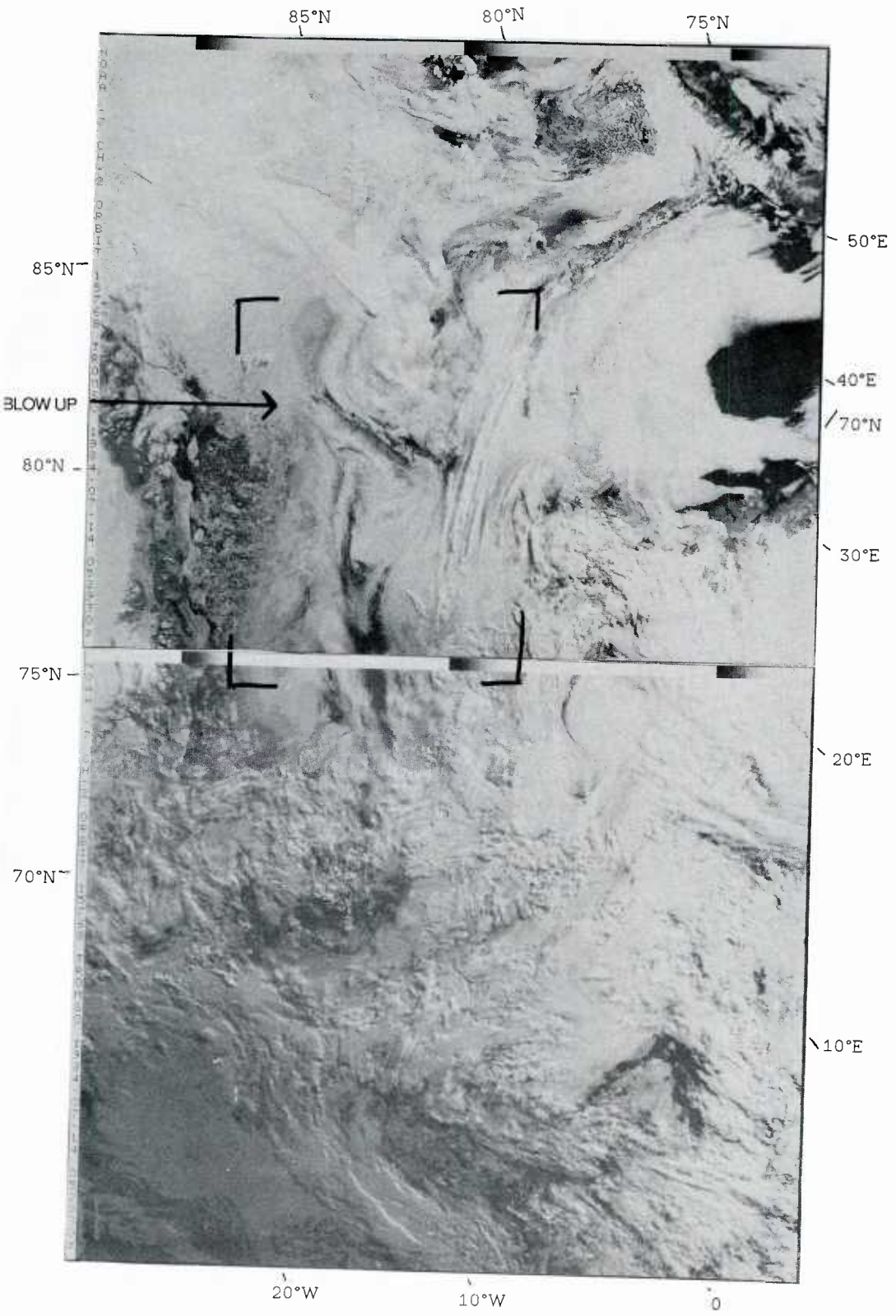

Figure 38a: NOAA-7 visual image 14 July 1984 0529 GMT.
The MIZ area is covered with stratiform clouds, and the wind conditions are calm with a weak on-ice component.

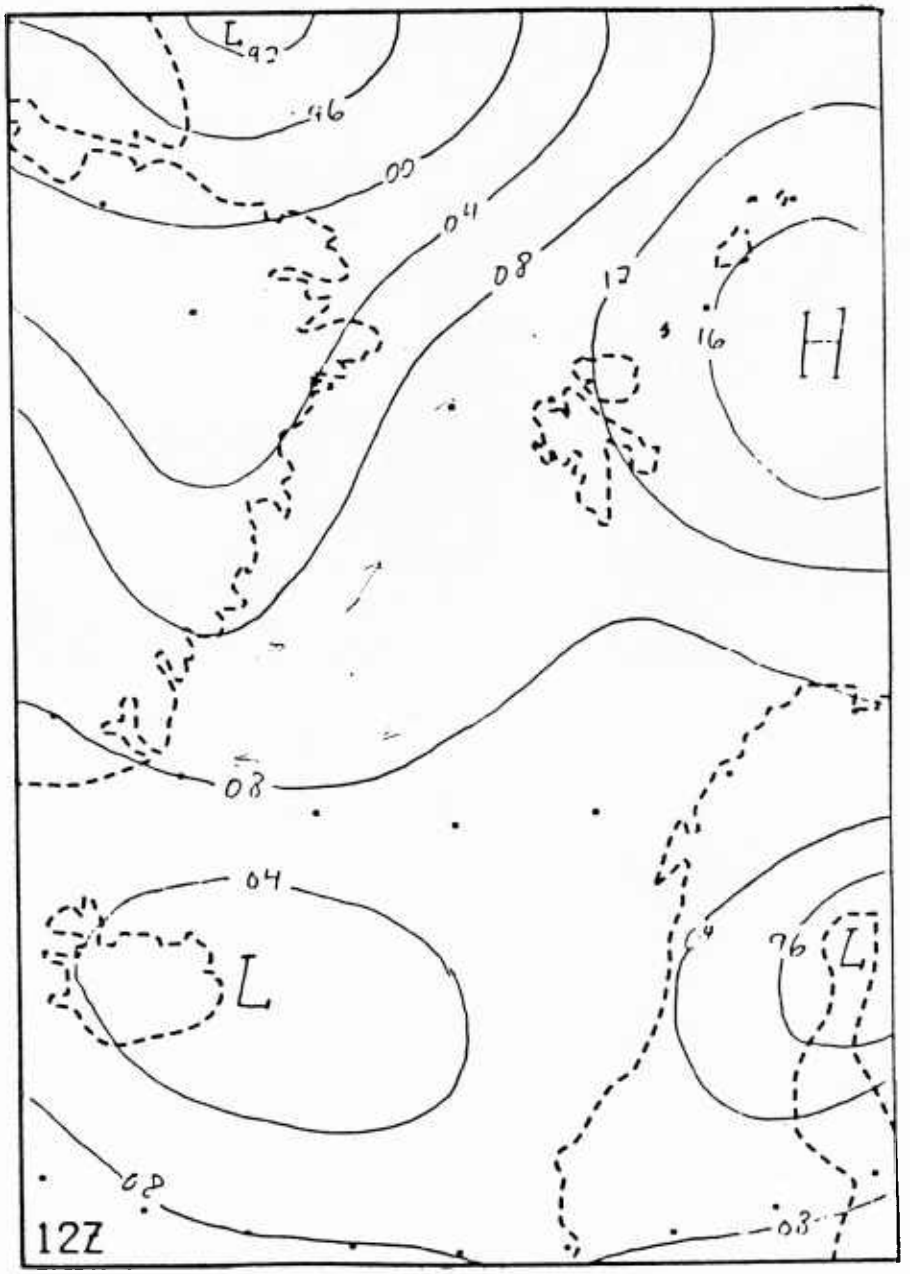

Figure 37b: Surface pressure chart 13 July 1984 1200 GMT.

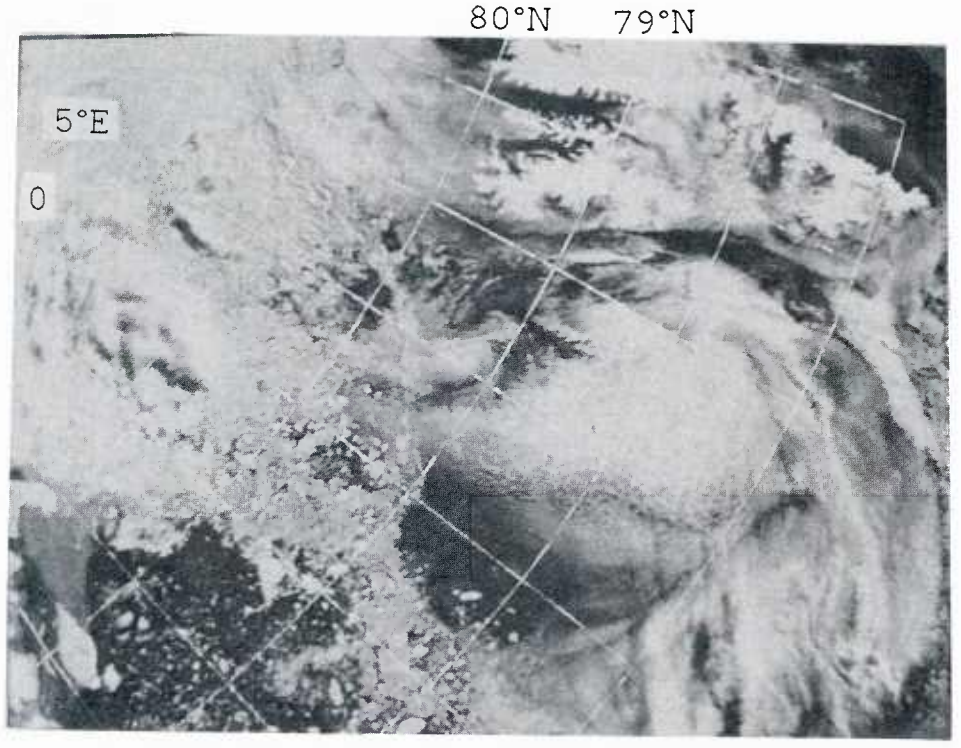

Figure 37c: NOAA-6 visual image 13 July 1984 0831 GMT.
The mesoscale vortex to the northwest of Spitzbergen is not as apparent on this enlarged image as on the standard image.
Note the very large ice-free areas behind the ice edge in the lower left of the image.

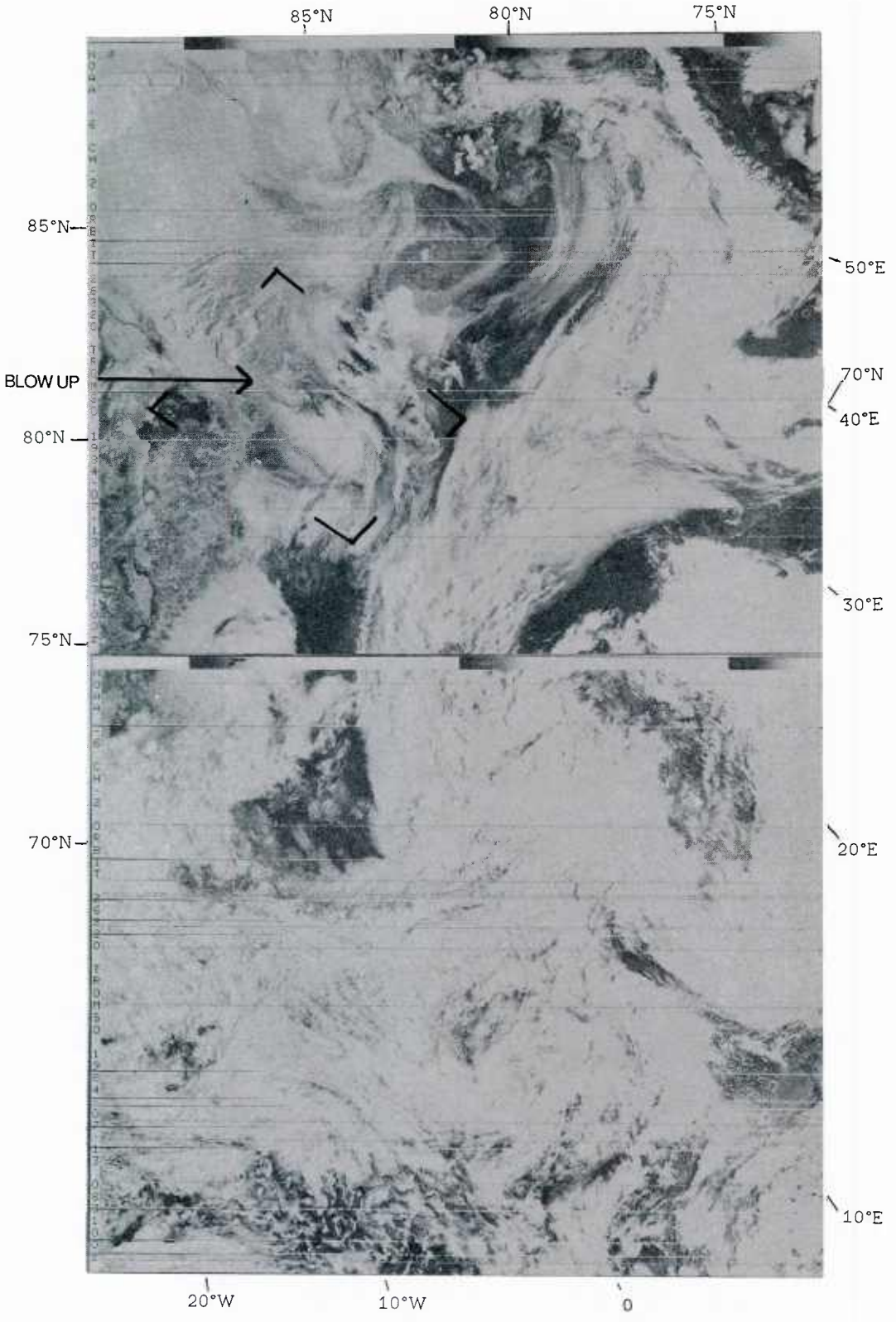

Figure 37a: NOAA-6 visual image 13 July 1984 0831 GMT. Southwesterly winds are blowing over the MIZ area. To the northwest of Spitzbergen is a mesoscale vortex.

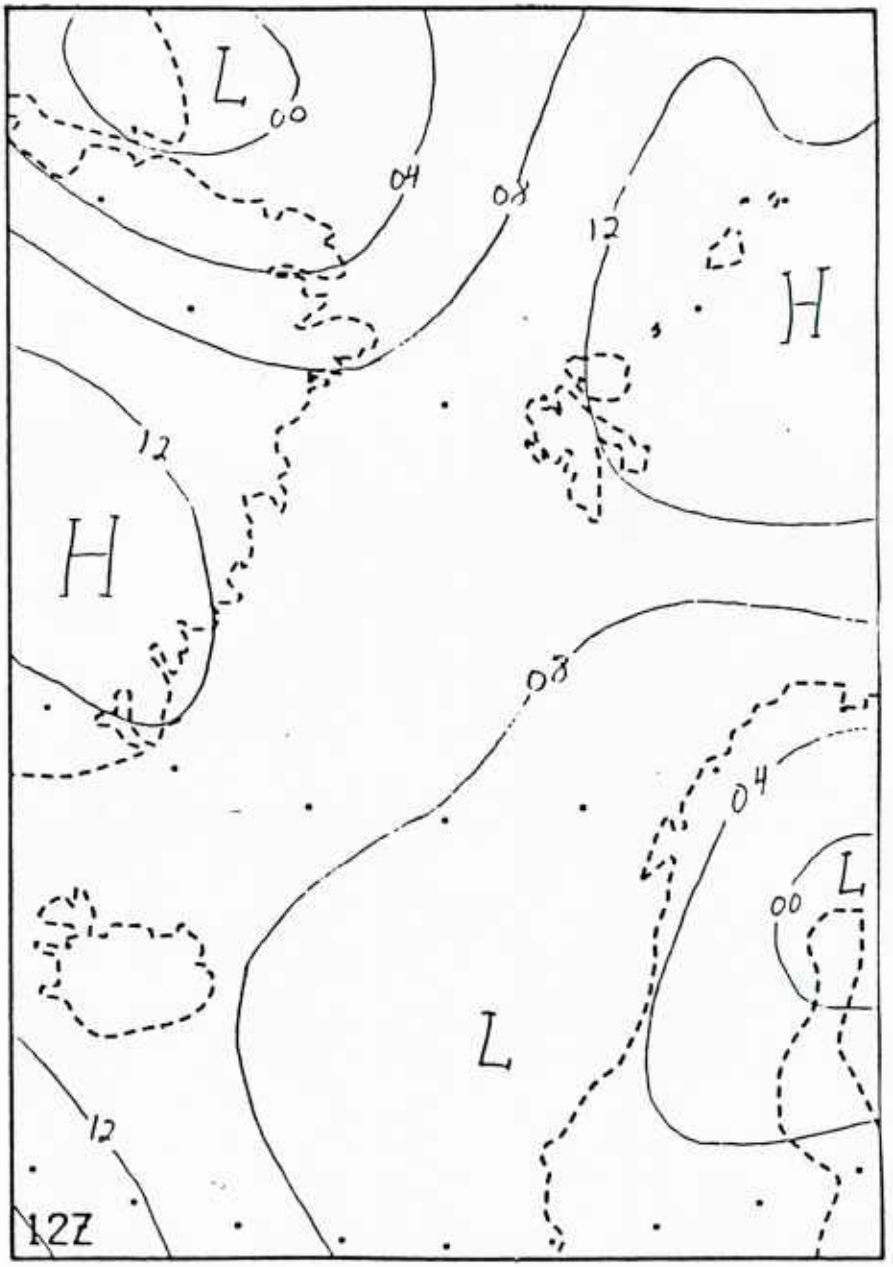

Figure 38b: Surface pressure chart 14 July 1984 1200 GMT.

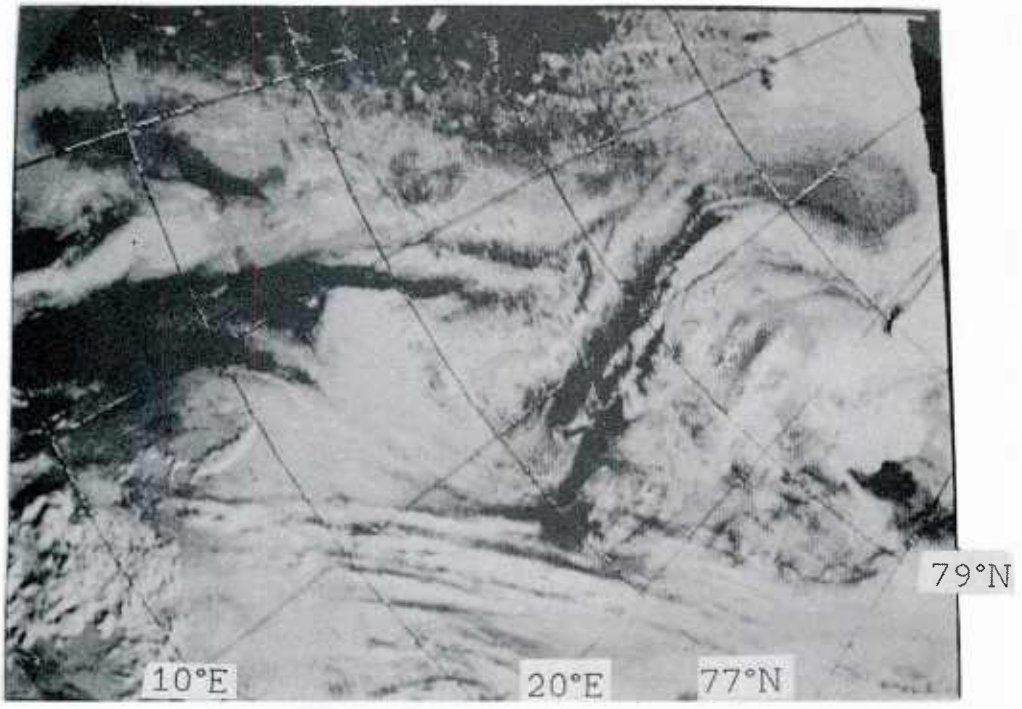

Figure 38c: NOAA-7 visual image 14 July 1984 0529 GMT. Stratiform clouds in different layers cover the Fram Strait area.

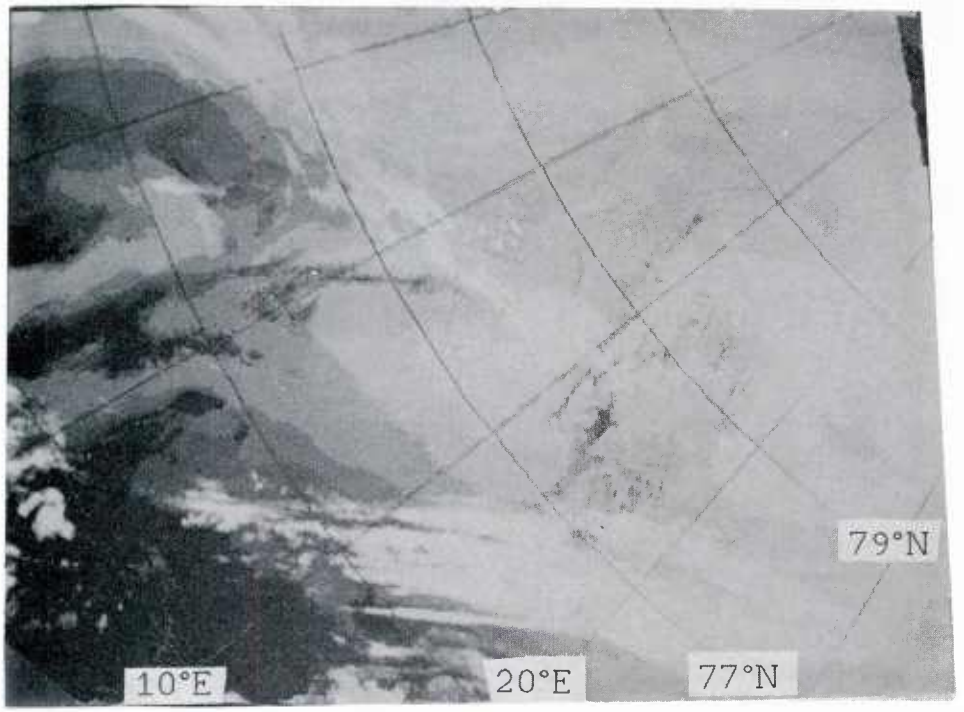

Figure 38d: NOAA-7 IR image 14 July 1984 0529 GMT. The thermal image indicates that there are different types of layer clouds ranging from colder than -20°C (white) to 0°C (black). The small temperature difference between the ground and the lowest clouds implies that the lowest clouds can be fog.

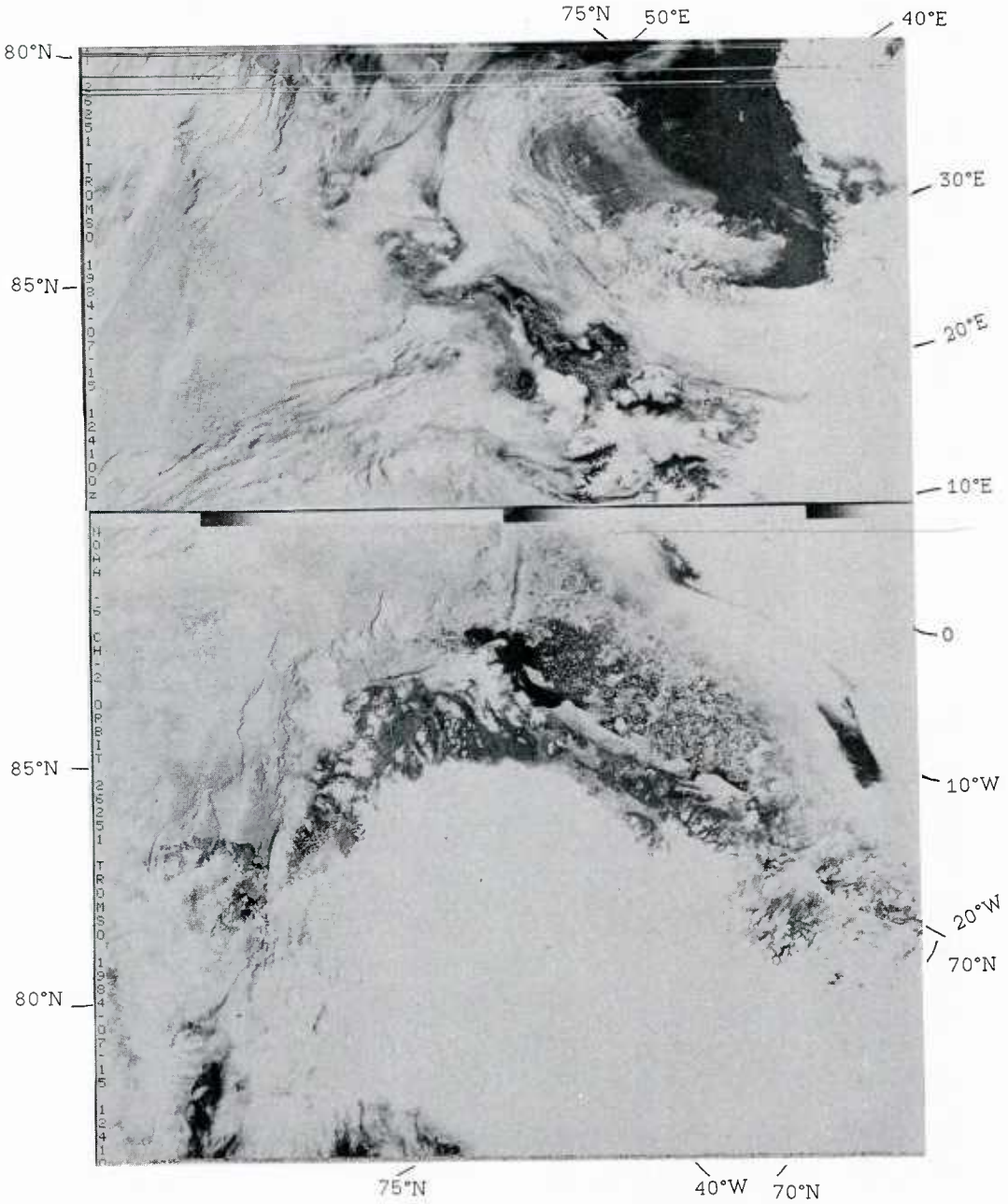

Figure 39a: NOAA-6 visual image 15 July 1984 1241 GMT.
The synoptic pressure pattern is showing a col over the MIZ area. High level clouds cover the eastern part of the area, while the western part is influenced by the subsidence on the lee-side of Greenland, and has clear sky. Easterly winds over Spitzbergen give lee subsidence along western slopes. Note also the ice-free waters along the northeast Greenland shore.

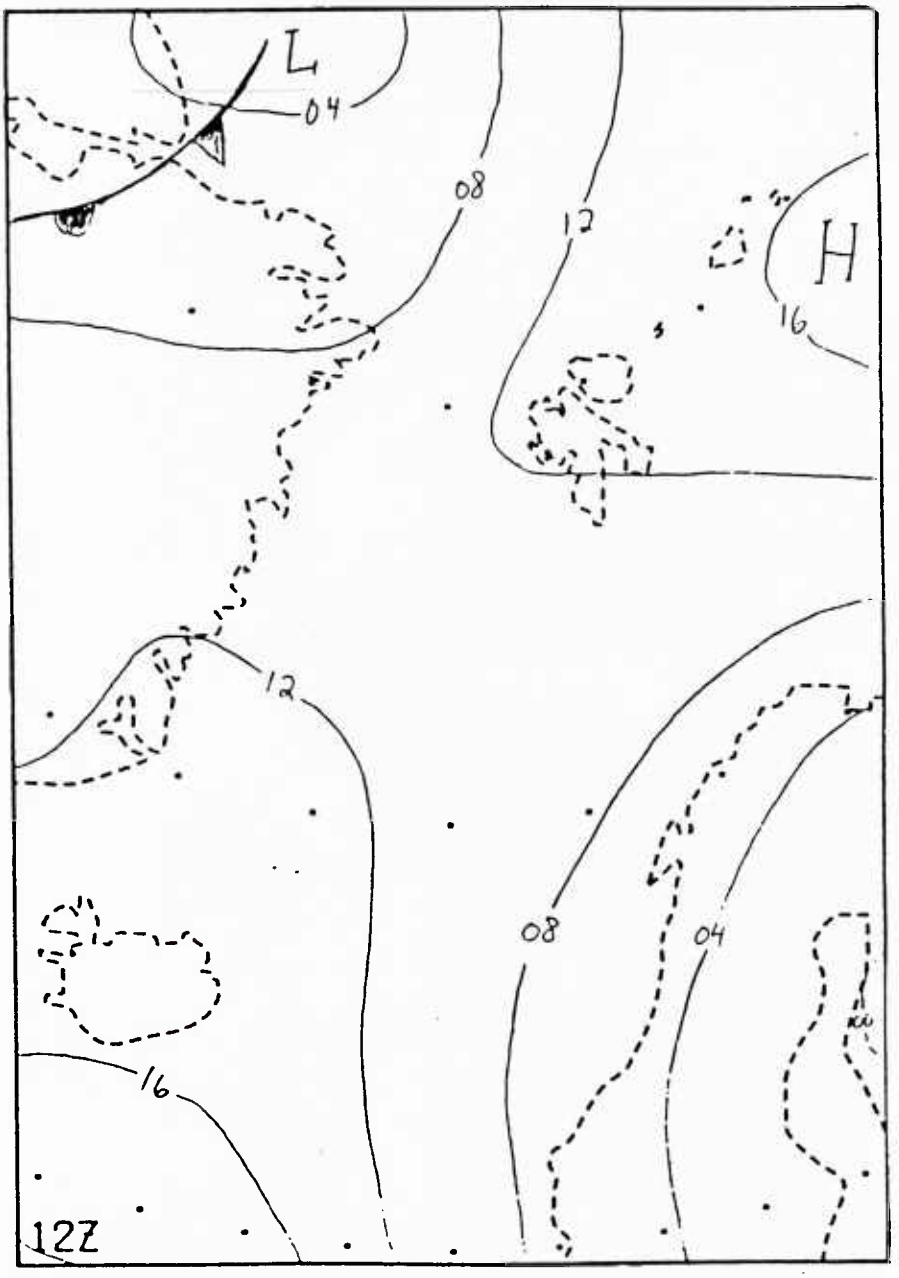

Figure 39b: Surface pressure chart 15 July 1984 1200 GMT.

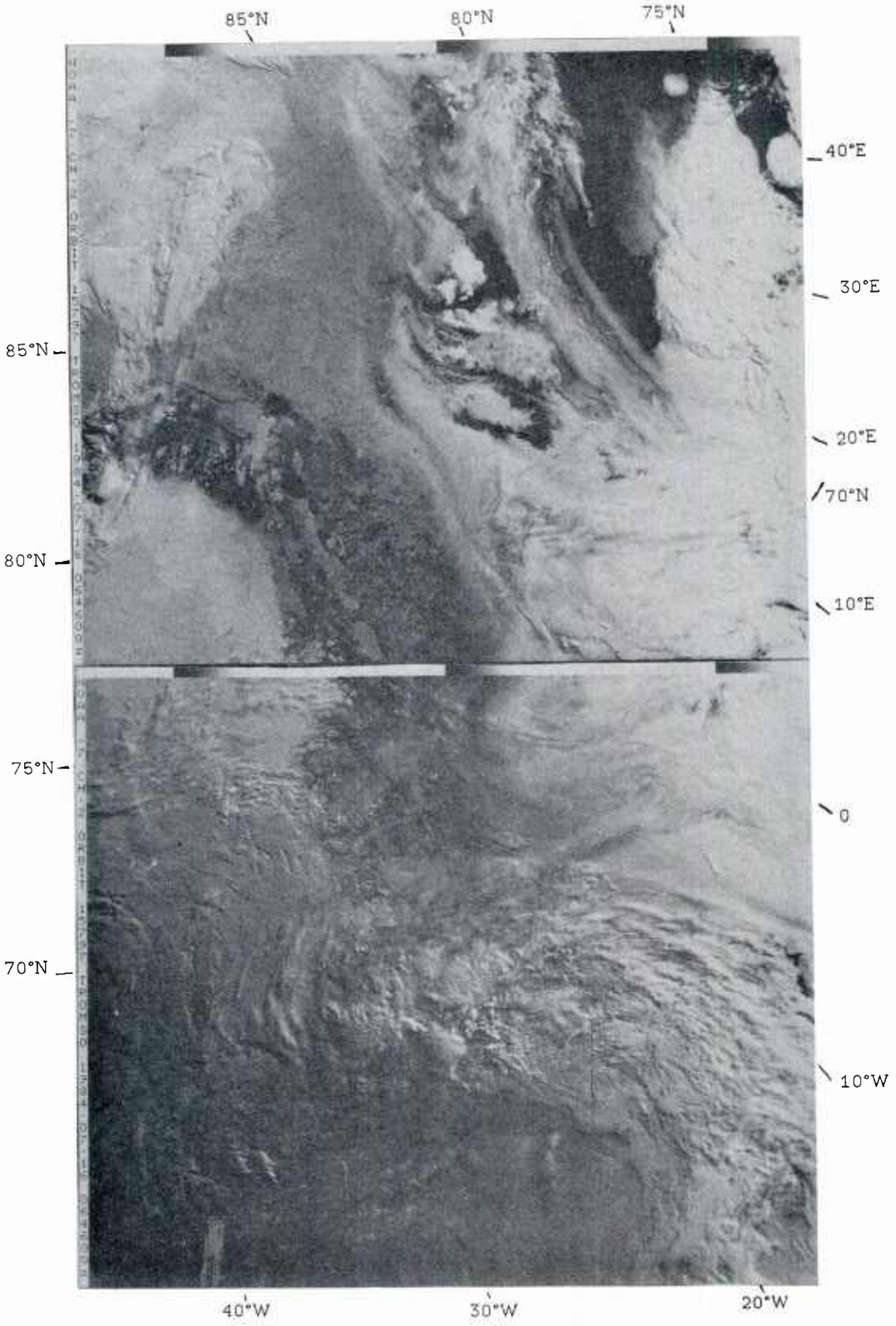

Figure 40a: NOAA-7 visual image 16 July 1984 0646 GMT. Southwesterly winds blow over the MIZ area, and stratiform cloud masses cover the eastern part of the area.

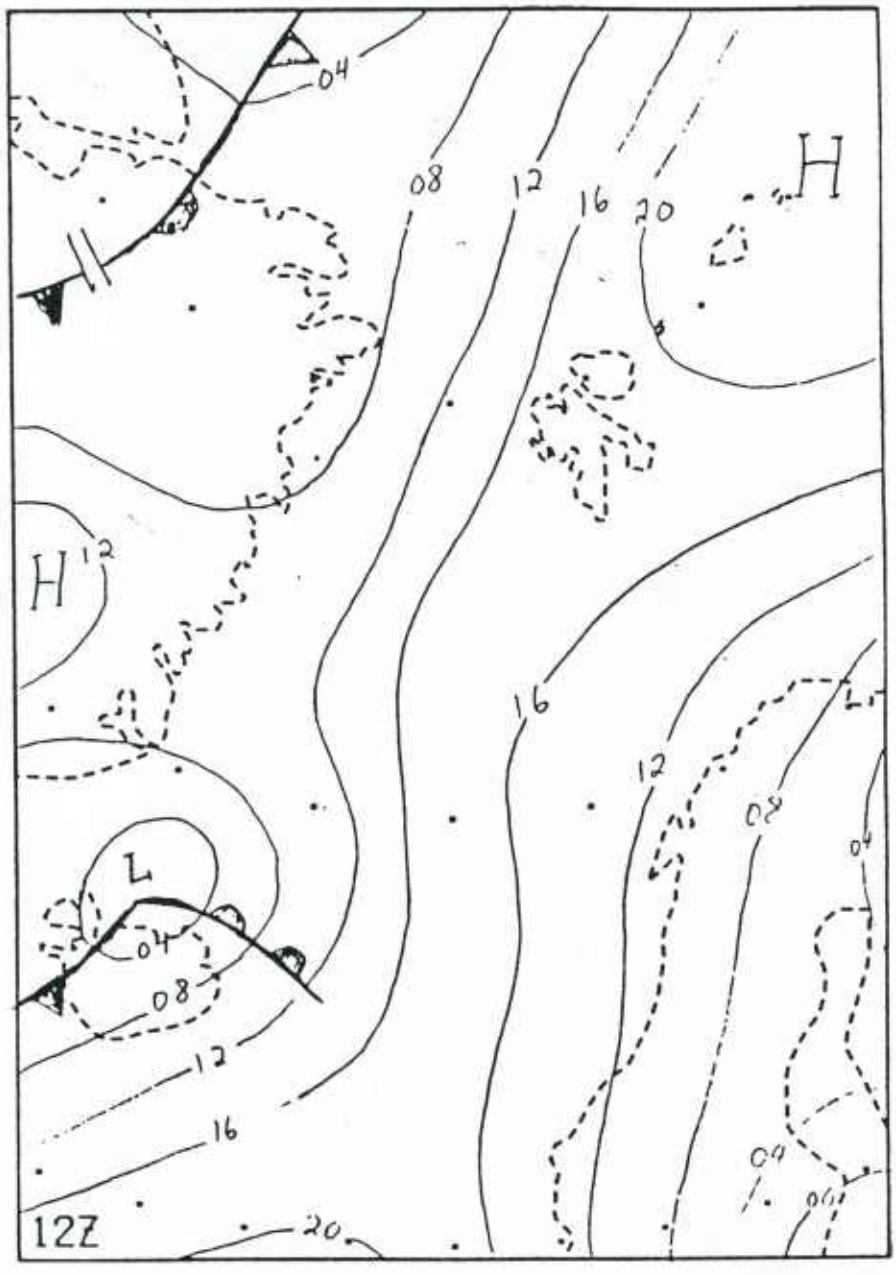

Figure 40b: Surface pressure chart 16 July 1984 1200 GMT.

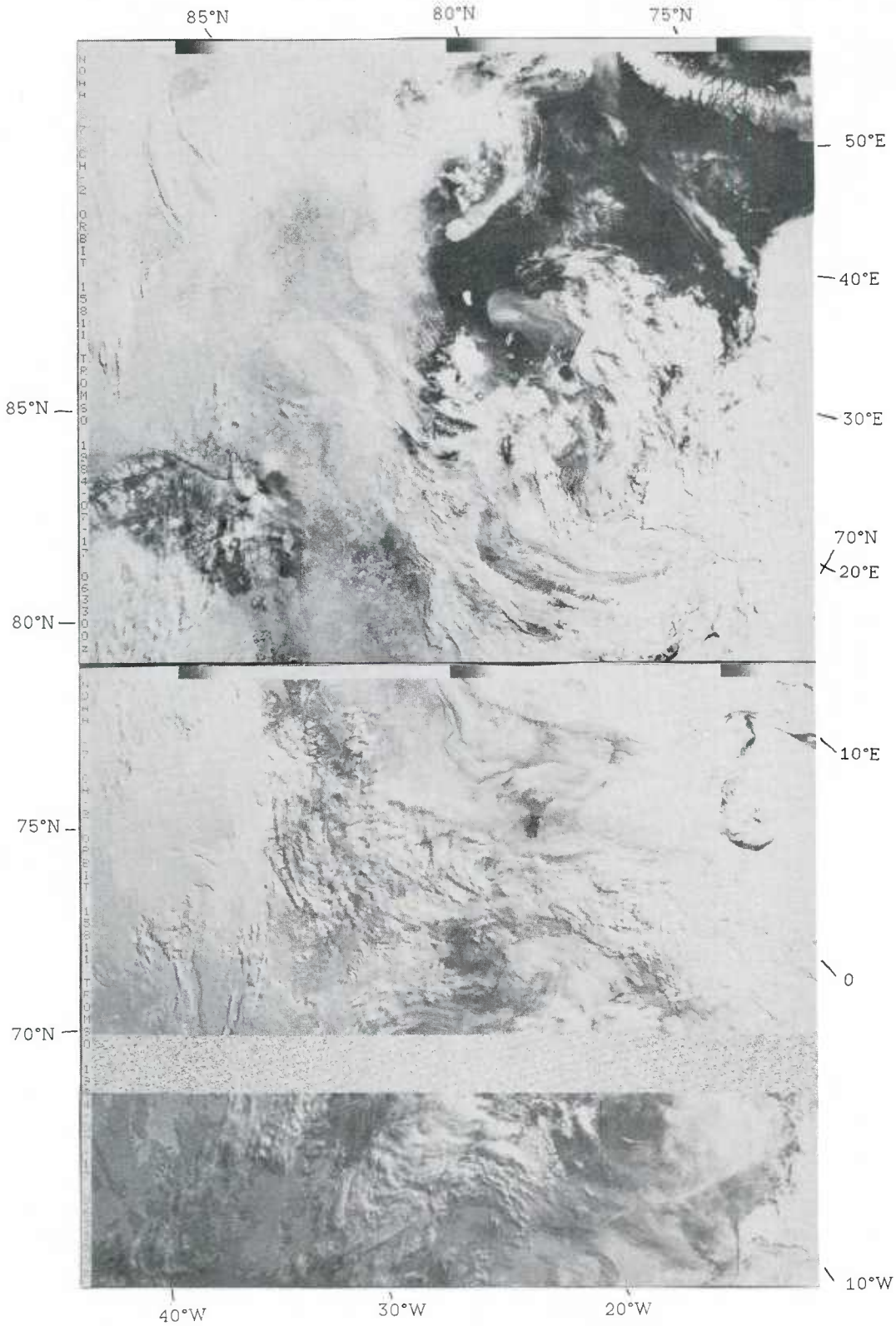

Figure 41a: NOAA-7 visual image 17 July 1984 0633 GMT.
Airflows from southeast and southwest converge in the MIZ area, and give thick cloud covers over the eastern part of the area. Over the western part there is thin cirrus. Note the small, but intense subsidence area at Jan Mayen.

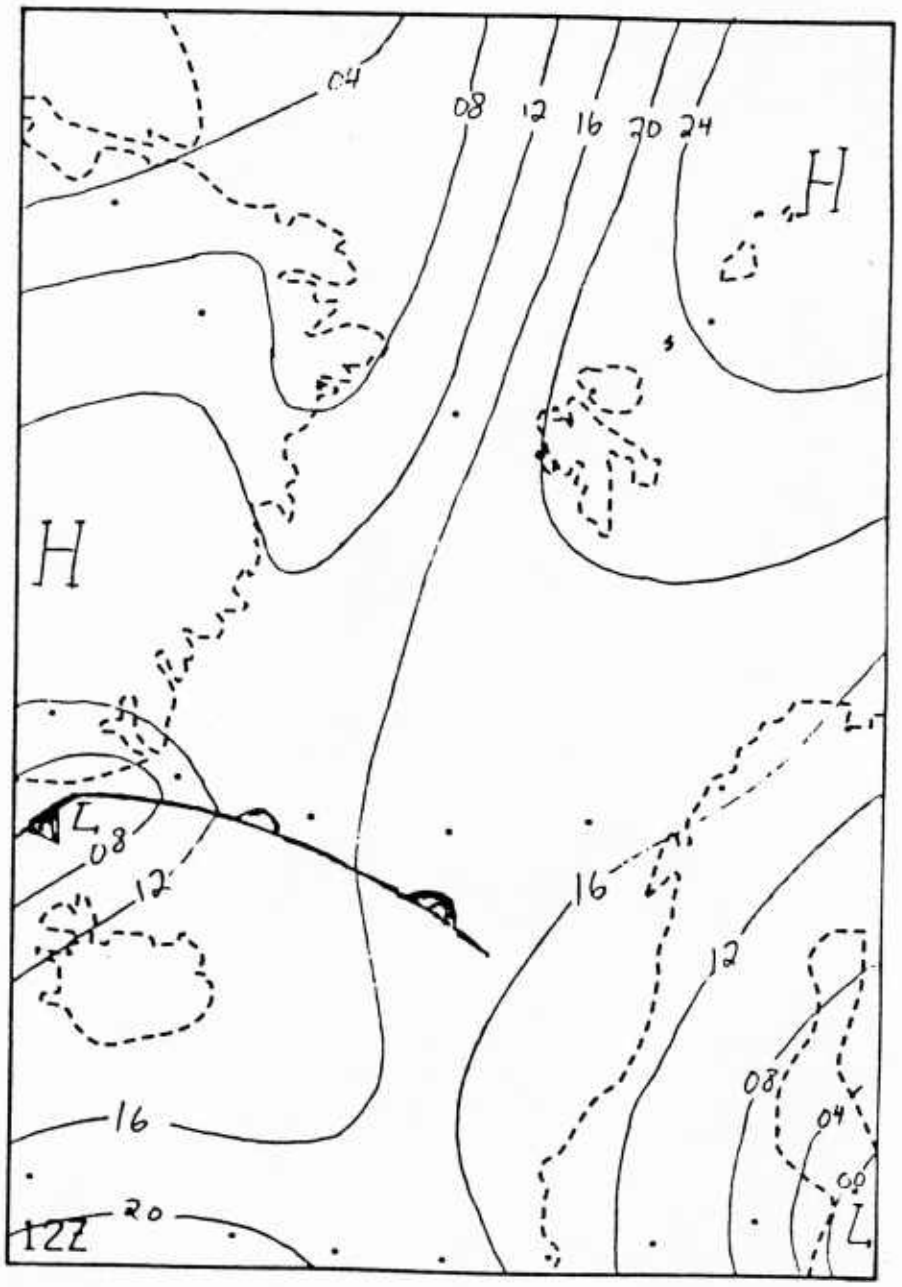

Figure 41b: Surface pressure chart 17 July 1984 1200 GMT.

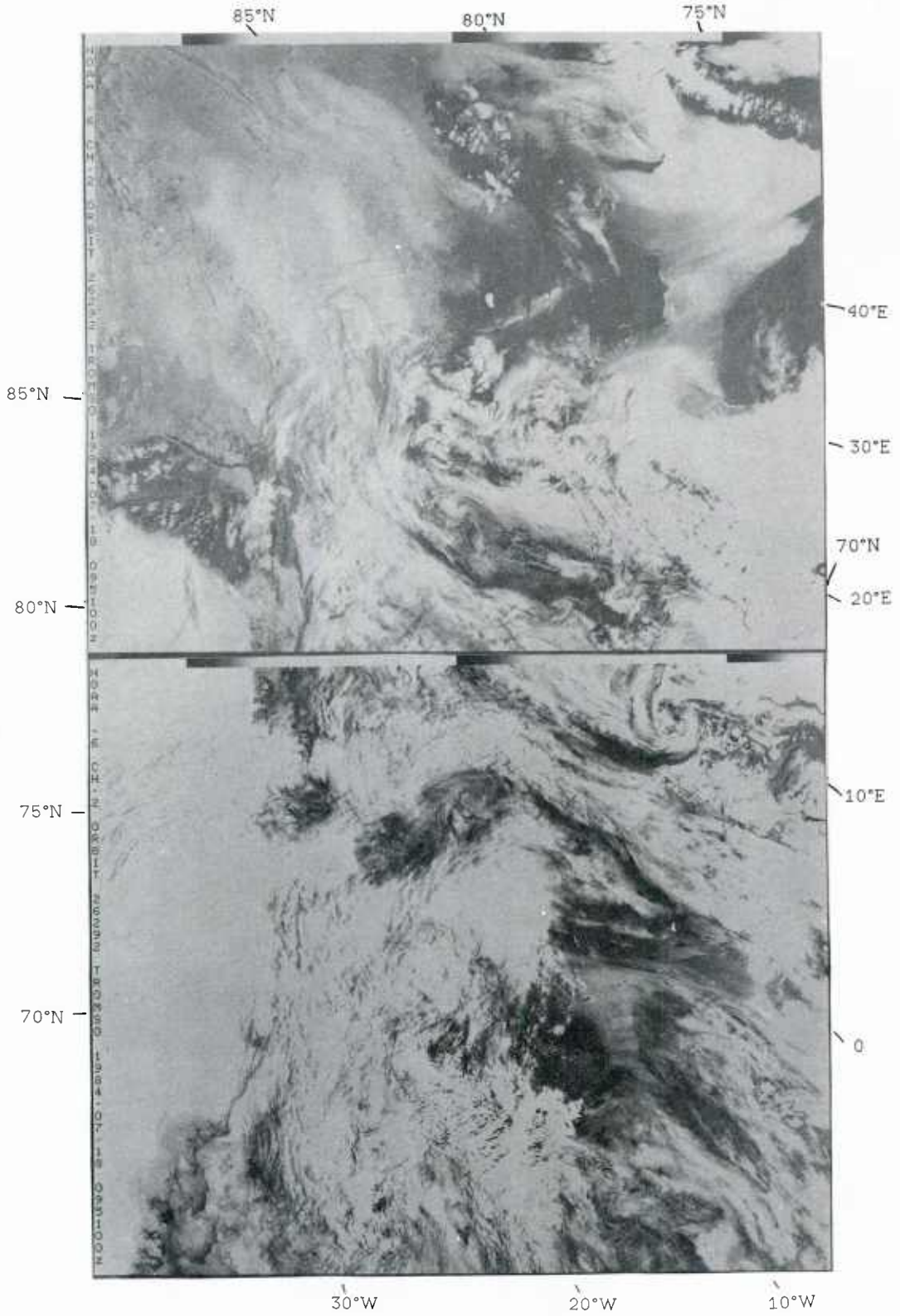

Figure 42a: NOAA-6 visual image 18 July 1984 0951 GMT.
In the MIZ area southerly winds with heavy cloud masses dominate the weather. Several mesoscale vortices are seen.

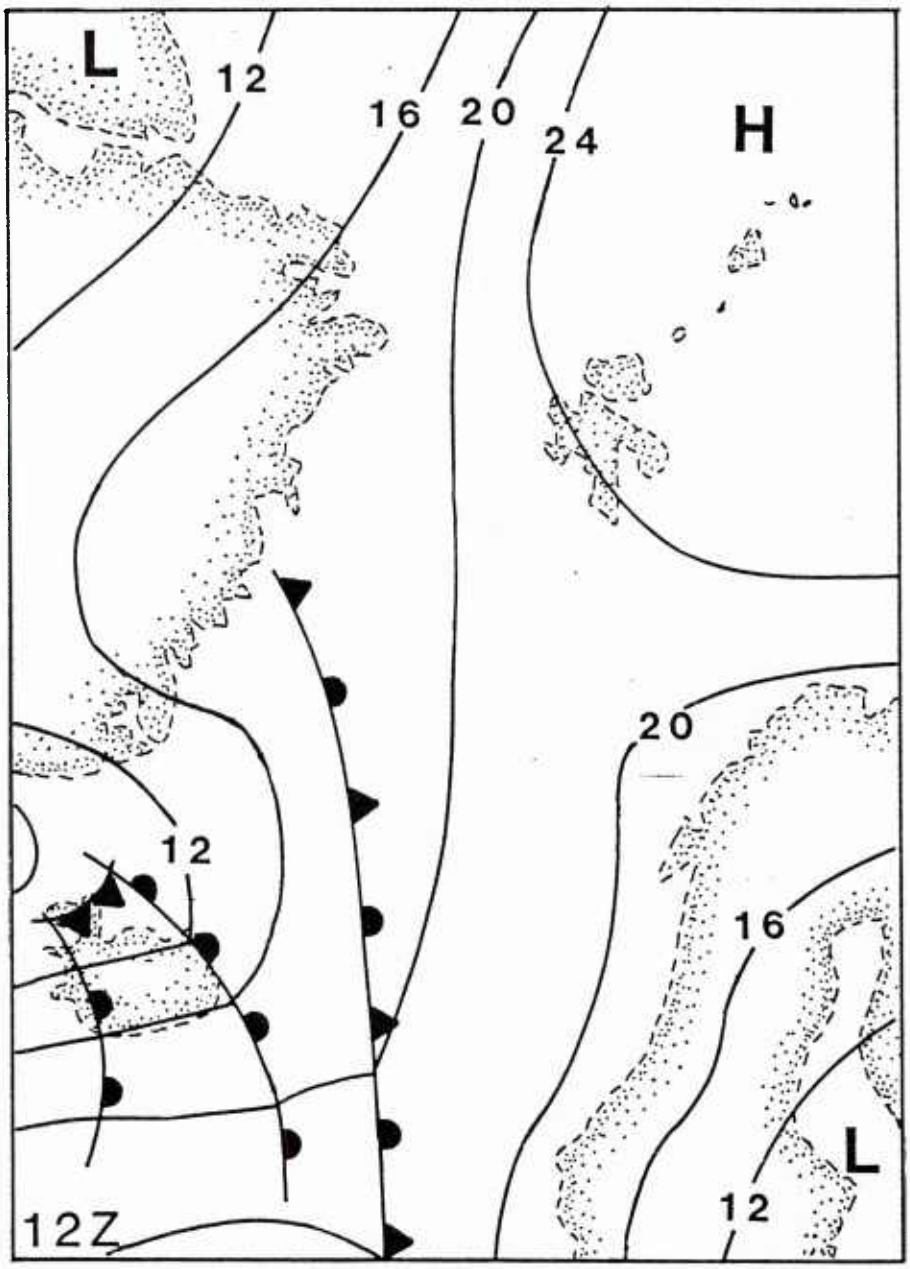

Figure 42b: Surface pressure chart 18 July 1984 1200 GMT.

This page intentionally left blank.

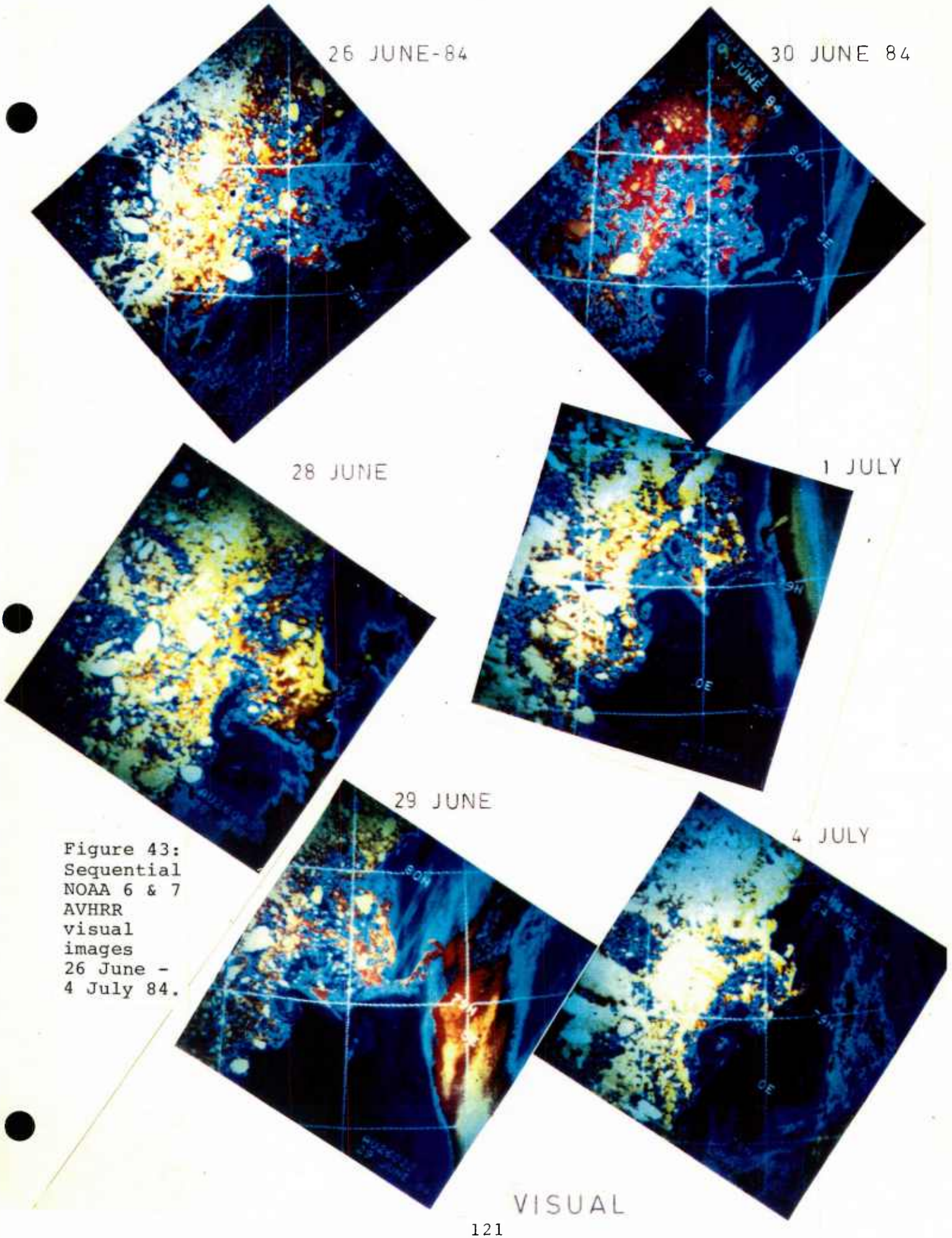

Figure 43: Sequential NOAA 6 & 7 AVHRR visual images 26 June - 4 July 84.

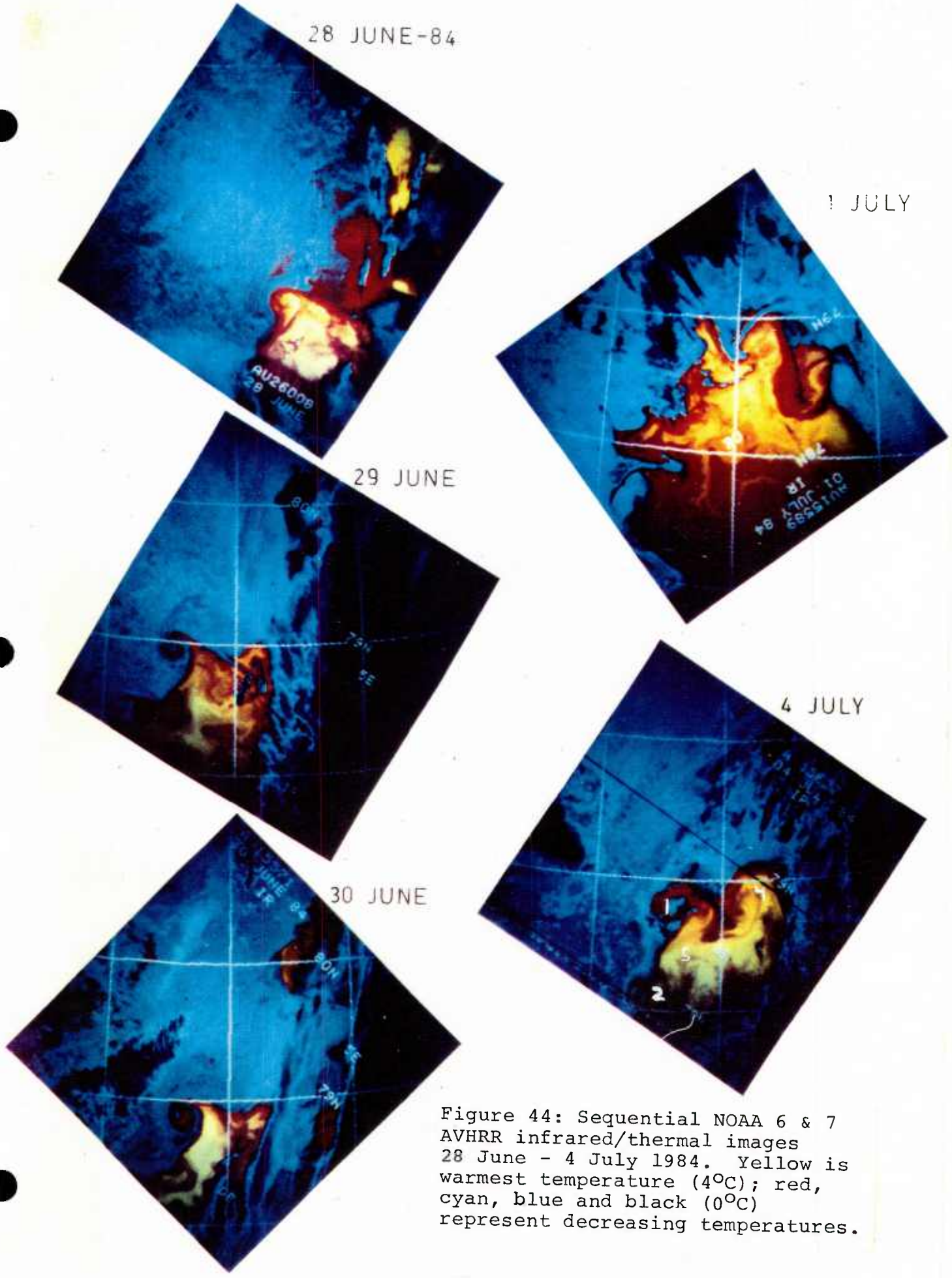

Figure 44: Sequential NOAA 6 & 7 AVHRR infrared/thermal images 28 June - 4 July 1984. Yellow is warmest temperature (4°C); red, cyan, blue and black (0°C) represent decreasing temperatures.

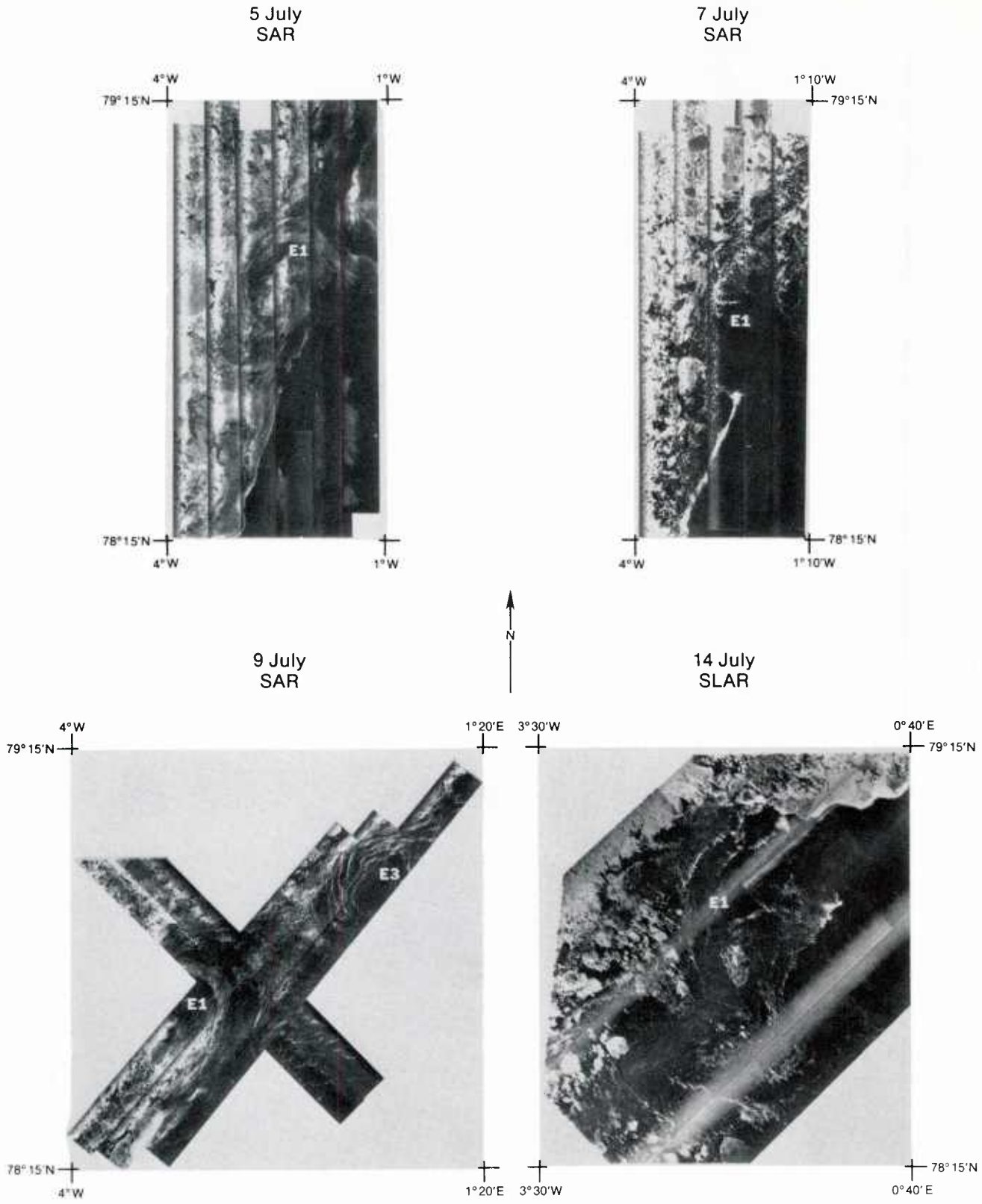

Figure 45: A sequence of aircraft SAR images from 5 July to 14 July. During this period cloudiness precluded the continued use of the NOAA satellite for monitoring the eddies. In the image bright zones represent ice and the dark zones are ice-free water.

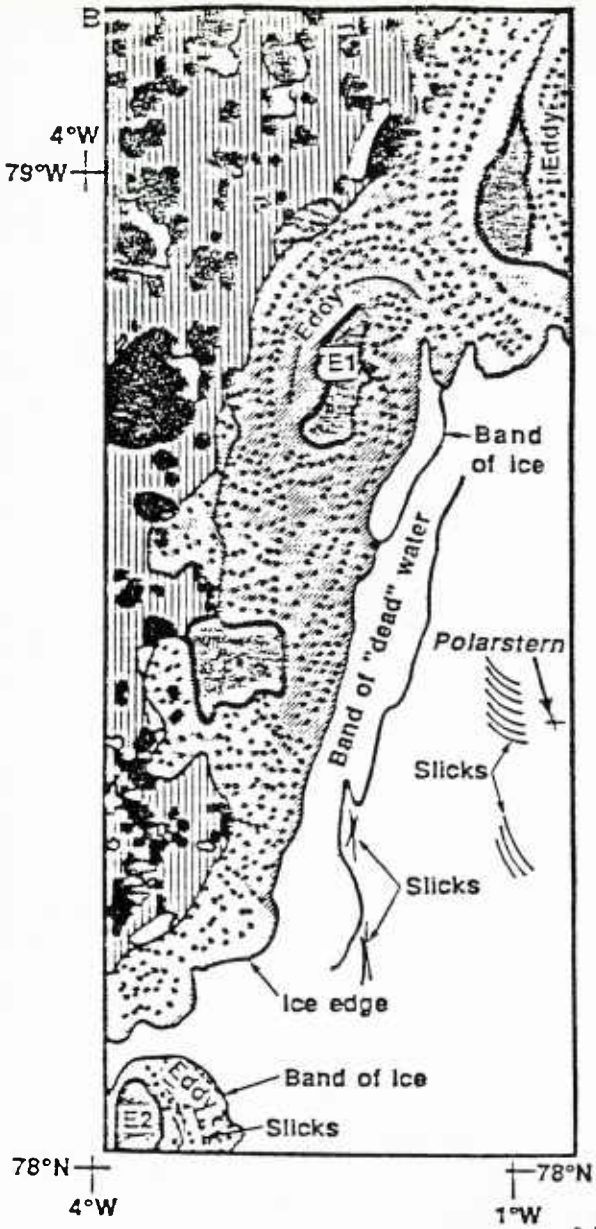

Figure 46: This figure is an interpretation of the SAR image for 5 July 1984. The SAR mosaic reveals that large individual floes (a), polynyas and ice-free ocean areas (b), 30%ice concentration areas with 10- to 500-m floes (c), 80% ice concentration areas with 10-m to 1.5-km floes (d), and 80% ice concentration areas with 10- to 6-km floes (e) are clearly delineated in the image. The median floe size for the points marked c, d and e is 125, 150 and 1000m, respectively. The dots in (c) indicate increased ice concentration due to surface currents.

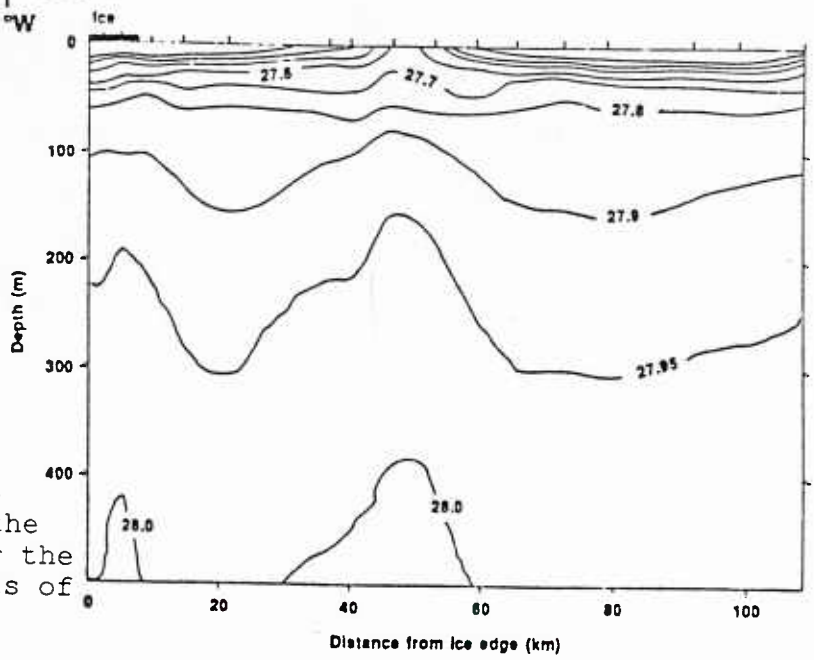

Figure 47:Vertical density structure in the east-west direction perpendicular to the ice edge across eddy E1 near the center of the eddy. The units of the isopycnals are in $\Delta\sigma_T$.

DISTRIBUTION

COMMANDER IN CHIEF
U.S. ATLANTIC FLEET
ATTN: FLT METEOROLOGIST
NORFOLK, VA 23511-6001

COMMANDER IN CHIEF
U.S. ATLANTIC FLEET
ATTN: NSAP SCIENCE ADVISOR
NORFOLK, VA 23511-6001

COMMANDER IN CHIEF
U.S. NAVAL FORCES, EUROPE
ATTN: METEOROLOGICAL OFFICER
FPO NEW YORK 09510

CINCUSNAVEUR
ATTN: NSAP SCIENCE ADVISOR
BOX 5
FPO NEW YORK 09510-0151

COMMANDER SECOND FLEET
ATTN: METEOROLOGICAL OFFICER
FPO NEW YORK 09501-6000

COMSECONDFLT
ATTN: NSAP SCIENCE ADVISOR
FPO NEW YORK 09501-6000

COMSIXTHFLT/COMFAIRMED
ATTN: NSAP SCIENCE ADVISOR
FPO NEW YORK 09501-6002

COMMANDER
U.S. NAVAL FORCES, AZORES
APO NEW YORK 09406

COMMANDER
U.S. NAVAL FORCES, ICELAND
FPO NEW YORK 09571

COMMANDER NAVAL AIR FORCE
U.S. ATLANTIC FLEET
NORFOLK, VA 23511-5188

COMMANDER NAVAL AIR FORCE
U.S. ATLANTIC FLEET
ATTN: NSAP SCIENCE ADVISOR
NORFOLK, VA 23511-5188

COMMANDER
NAVAL SURFACE FORCE
U.S. ATLANTIC FLEET
NORFOLK, VA 23511-6292

COMNAVSURFLANT
ATTN: NSAP SCIENCE ADVISOR
NORFOLK, VA 23511

COMSUBFORLANT
ATTN: CODE 014
NORFOLK, VA 23511-6296

COMMANDER
AMPHIBIOUS GROUP 2
ATTN: METEOROLOGICAL OFFICER
FPO NEW YORK 09501-6007

COMMANDER
OPTEVFOR
NAVAL BASE
NORFOLK, VA 23511-6388

COMMANDER
OPTEVFOR
ATTN: NSAP SCIENCE ADVISOR
NORFOLK, VA 23511-6388

COMMANDING OFFICER
OCEANOGRAPHIC UNIT FIVE
USNS HARKNESS (T-AGS 32)
FPO NEW YORK 09573-7105

COMMANDER
CRUISER-DESTROYER GROUP 8
ATTN: STAFF OCEANOG. (N35)
FPO NEW YORK 09501-4704

COMMANDER
SURFACE WARFARE DEV. GROUP
NAVAMPHIB BASE, LITTLE CREEK
NORFOLK, VA 23521

COMMANDING OFFICER
31 OCEANO. DEV. SQDN 8-VXN-8
NAVAL AIR STATION
PATUXENT RIVER, MD 20670-5109

USCINCLANT
NAVAL BASE
NORFOLK, VA 23511

ASST. FOR ENV. SCIENCES
ASST. SEC. OF THE NAVY (R&D)
ROOM 5E731, THE PENTAGON
WASHINGTON, DC 20350

CHIEF OF NAVAL RESEARCH (2)
LIBRARY SERVICES, CODE 784
BALLSTON TOWER #1
800 QUINCY ST.
ARLINGTON, VA 22217-5000

OFFICE OF NAVAL RESEARCH
CODE 1122AT, ATMOS. SCIENCES
ARLINGTON, VA 22217-5000

OFFICE OF NAVAL RESEARCH
ENV. SCI. PROGRAM, CODE 112
ARLINGTON, VA 22217-5000

OFFICE OF NAVAL RESEARCH
ATTN: PROGRAM MANAGER, 1122CS
ARLINGTON, VA 22217-5000

OFFICE OF NAVAL RESEARCH
ATTN: HEAD, OCEAN SCIENCES DIV
CODE 1122
ARLINGTON, VA 22217-5000

OFFICE OF NAVAL RESEARCH
CODE 1122 PO, PHYSICAL OCEANO.
ARLINGTON, VA 22217-5000

OFFICE OF NAVAL RESEARCH
CODE 1122 MM, MARINE METEO.
ARLINGTON, VA 22217-5000

OFFICE OF NAVAL TECHNOLOGY
ONR (CODE 22)
800 N. QUINCY ST.
ARLINGTON, VA 22217-5000

CHIEF OF NAVAL OPERATIONS
NAVY DEPT., OP-622C
WASHINGTON, DC 20350

CHIEF OF NAVAL OPERATIONS
NAVY DEPT. OP-986G
WASHINGTON, DC 20350

CHIEF OF NAVAL OPERATIONS
OP-962
U.S. NAVAL OBSERVATORY
WASHINGTON, DC 20390

CHIEF OF NAVAL OPERATIONS
OP-953
NAVY DEPARTMENT
WASHINGTON, DC 20350

DIRECTOR
NATIONAL SECURITY AGENCY
ATTN: LIBRARY (2C029)
FT. MEADE, MD 20755

OJCS/J3/ESD
THE PENTAGON, ROOM 2B887
WASHINGTON, DC 20301-5000

NAVAL DEPUTY TO THE
ADMINISTRATOR, NOAA
ROOM 200, PAGE BLDG. #1
3300 WHITEHAVEN ST. NW
WASHINGTON, DC 20235

LIBRARY
NAVAL ARCTIC RESEARCH LAB
BARROW, AK 99723

COMMANDING OFFICER
OFFICE OF NAVAL RESEARCH
1030 E. GREEN ST.
PASADENA, CA 91101

COMMANDING OFFICER
NAVAL OCEAN RSCH & DEV ACT
NSTL, MS 39529-5004

COMMANDING OFFICER
FLEET INTELLIGENCE CENTER
(EUROPE & ATLANTIC)
NORFOLK, VA 23511

COMMANDER
NAVAL OCEANOGRAPHY COMMAND
NSTL, MS 39529-5000

COMNAVOCEANCOM
ATTN: CODE N5
NSTL, MS 39529-5000

COMMANDING OFFICER
FLENUMOCEANCEN
MONTEREY, CA 93943-5005

COMMANDING OFFICER
NAVPOLAROCEANCEN, NAVY DEPT.
4301 SUITLAND RD
WASHINGTON, DC 20395-5180

COMMANDING OFFICER
U.S. NAVOCEANCOMFAC
FPO NEW YORK 09571-0926

COMMANDING OFFICER
NAVOCEANCOMFAC
NAVAL AIR STATION
BRUNSWICK, ME 04011-5000

SUPERINTENDENT
LIBRARY REPORTS
U.S. NAVAL ACADEMY
ANNAPOLIS, MD 21402

CHAIRMAN
OCEANOGRAPHY DEPT.
U.S. NAVAL ACADEMY
ANNAPOLIS, MD 21402

DIRECTOR OF RESEARCH
U.S. NAVAL ACADEMY
ANNAPOLIS, MD 21402

SUPERINTENDENT
NAVPGSCOL
MONTEREY, CA 93943-5000

NAVAL POSTGRADUATE SCHOOL
METEOROLOGY DEPT.
MONTEREY, CA 93943-5000

NAVAL POSTGRADUATE SCHOOL
OCEANOGRAPHY DEPT.
MONTEREY, CA 93943-5000

LIBRARY
NAVAL POSTGRADUATE SCHOOL
MONTEREY, CA 93943-5002

PRESIDENT
NAVAL WAR COLLEGE
GEOPHYS. OFFICER, NAVOPS DEPT.
NEWPORT, RI 02841

COMMANDER (2)
NAVAIRSYSCOM
ATTN: LIBRARY (AIR-723D)
WASHINGTON, DC 20361-0001

COMMANDER
NAVAIRSYSCOM (AIR-03)
WASHINGTON, DC 20361-0001

COMMANDER
NAVAIRSYSCOM (AIR-07)
WASHINGTON, DC 20361-0001

COMMANDER
NAVAIRSYSCOM, CODE 526W
WASHINGTON, DC 20361-0001

COMSPAWARSYSCOM
ATTN: CAPT. R. PLANTE
CODE 3213, NAVY DEPT.
WASHINGTON, DC 20363-5100

COMSPAWARSYSCOM
ATTN: CODE PMW 141-B1
WASHINGTON, DC 20363-5100

COMSPAWARSYSCOM
ATTN: CODE PWM 141
NAVY DEPT, BLDG NC1, ROOM 2E18
WASHINGTON, DC 20363-5100

NAVAL SPACE SYSTEMS ACTIVITY
CODE 60
P.O. BOX 92960
WORLDWAY POSTAL CENTER
LOS ANGELES, CA 90009

COMMANDER
NAVOCEANSYSCEN
SAN DIEGO, CA 92152-5000

COMMANDER
DAVID TAYLOR RESEARCH CENTER
ATTN: CODE 5220
BETHESDA, MD 20084-5000

COMMANDER
DAVID TAYLOR RESEARCH CENTER
SURFACE SHIP DYNAMICS BRANCH
ATTN: S. BALES
BETHESDA, MD 20084-5000

COMMANDER
NAVAL SURFACE WEAPONS CENTER
DAHLGREN,VA 22448-5000

COMMANDER
NAVSURFWEACEN, CODE R42
WHITE OAKS LAB
SILVER SPRING, MD 20903-5000

DIRECTOR
NAVSURFWEACEN, WHITE OAKS
NAVY SCIENCE ASSIST. PROGRAM
SILVER SPRING, MD 20903-5000

COMMANDING OFFICER
NAVAL UNDERWATER SYSTEMS CEN
NEWPORT, RI 02841-5047

CHIEF OF NAVAL EDUCATION &
TRAINING
NAVAL AIR STATION
PENSACOLA, FL 32508

COMMANDING OFFICER
FLEASWTRACENLANT
NAVAL STATION
NORFOLK, VA 23511-6495

COMMANDER
AWS/DNXS
SCOTT AFB, IL 62225

USAFETAC/TS
SCOTT AFB, IL 62225

SUPERINTENDENT
ATTN: USAFA (DEG)
USAF ACADEMY, CO 80840

3350TH TECH. TRNG GROUP
TTGU/2/STOP 623
CHANUTE AFB, IL 61868

AFGWC/DAPL
OFFUTT AFB, NE 68113

AFGL/LY
HANSCOM AFB, MA 01731

AFGL/OPI
HANSCOM AFB, MA 01731

OFFICER IN CHARGE
SERVICE SCHOOL COMMAND
DET. CHANUTE/STOP 62
CHANUTE AFB, IL 61868

COMMANDING OFFICER
US ARMY RESEARCH OFFICE
ATTN: GEOPHYSICS DIVISION
RESEARCH TRIANGLE PARK, NC
27709

LIBRARY, U.S. ARMY COLD REGION
RESEARCH & ENGINEERING LAB.
HANOVER, NH 03755

DIRECTOR (12)
DEFENSE TECH. INFORMATION
CENTER, CAMERON STATION
ALEXANDRIA, VA 22314

DIRECTOR, ENV. & LIFE SCI.
OFFICE OF UNDERSECRETARY OF
DEFENSE FOR RSCH & ENG E&LS
RM. 3D129, THE PENTAGON
WASHINGTON, DC 20505

CENTRAL INTELLIGENCE AGENCY
ATTN: OCR STANDARD DIST.
WASHINGTON, DC 20505

DIRECTOR, TECH. INFORMATION
DEFENSE ADV. RSCH PROJECTS
1400 WILSON BLVD.
ARLINGTON, VA 22209

COMMANDANT
U.S. COAST GUARD
WASHINGTON, DC 20226

CHIEF, MARINE SCI. SECTION
U.S. COAST GUARD ACADEMY
NEW LONDON, CT 06320

COMMANDING OFFICER
USCGC GLACIER (WAGB-4)
FPO SAN FRANCISCO 96601

COMMANDING OFFICER
USCG RSCH & DEV. CENTER
GROTON, CT 06340

NOAA-NESDIS LIAISON
ATTN: CODE SC2
NASA-JOHNSON SPACE CENTER
HOUSTON, TX 77058

DIRECTOR
NATIONAL EARTH SAT. SERV/SEL
FB-4, S321B
SUITLAND, MD 20233

CHIEF
MARINE & EARTH SCI. LIBRARY
NOAA, DEPT. OF COMMERCE
ROCKVILLE, MD 20852

FEDERAL COORD. FOR METEORO.
SERVS. & SUP. RSCH. (OFCM)
11426 ROCKVILLE PIKE
SUITE 300
ROCKVILLE, MD 20852

NATIONAL WEATHER SERVICE
WORLD WEATHER BLDG., RM 307
5200 AUTH ROAD
CAMP SPRINGS, MD 20023

NATIONAL CLIMATIC CENTER
ATTN: L. PRESTON D542X2
FEDERAL BLDG. - LIBRARY
ASHEVILLE, NC 28801

LABORATORY DIRECTOR
NATIONAL MARINE FISH. SERV
NOAA, P.O. BOX 6
WOODS HOLE, MA 92543

CHIEF
MESOSCALE APPLICATIONS BRANCH
NATIONAL EARTH SAT. SERV.
1225 W. DAYTON
MADISON, WI 53562

DIRECTOR
NATIONAL WEATHER SERVICE
GRAMAX BLDG.
8060 13TH ST.
SILVER SPRING, MD 20910

WAVE PROPAGATION LAB
NOAA, R/E/WP5
CHIEF, SEA STATE STUDIES
325 S. BROADWAY
BOULDER, CO 80303

HEAD, ATMOS. SCIENCES DIV.
NATIONAL SCIENCE FOUNDATION
1800 G STREET, NW
WASHINGTON, DC 20550

HEAD
OFFICE OF OCEANO. & LIMNOLOGY
SMITHSONIAN INSTITUTION
WASHINGTON, DC 20560

EXECUTIVE SECRETARY, CAO
SUBCOMMITTEE ON ATMOS. SCI.
NATIONAL SCIENCE FOUNDATION
RM. 510, 1800 G. STREET, NW
WASHINGTON, DC 20550

SPACE FLIGHT METEORO. GROUP
ATTN: STEVE SOKOL, CODE Z8
JOHNSON SPACE CENTER
HOUSTON, TX 77058

SCRIPPS INSTITUTION OF
OCEANOGRAPHY, LIBRARY
DOCUMENTS/REPORTS SECTION
LA JOLLA, CA 92037

WOODS HOLE OCEANO. INST.
DOCUMENT LIBRARY LO-206
WOODS HOLE, MA 02543

UNIVERSITY OF WASHINGTON
ATMOSPHERIC SCIENCES DEPT.
SEATTLE, WA 98195

DIRECTOR
COASTAL STUDIES INSTITUTE
LOUISIANA STATE UNIVERSITY
ATTN: O. HUH
BATON ROUGE, LA 70803

MR. W. G. SCHRAMM/WWW
WORLD METEOROLOGICAL
ORGANIZATION
CASE POSTALE #5, CH-1211
GENEVA, SWITZERLAND

LIBRARY/BIBLIOTHEQUE
ATMOSPHERIC ENVIRON. SERV.
4905 RUE DUFFERIN STREET
DOWNSVIEW, ONTARIO CANADA
M3H 5T4

CANADIAN COMMITTEE ON OCEANO.
OFFICE OF THE SECRETARY
DEPT. OF THE ENVIRONMENT
FONTAINE BLDG 11TH FLOOR
OTTAWA, ONTARIO K1A OH3
CANADA

METOC CENTRE
MARITIME FORCES PACIFIC HDQ
FORCES MAIL OFFICE
VICTORIA, BRITISH COLUMBIA
V0S-180, CANADA

DIRECTOR, INSTITUTE OF
PHYSICAL OCEANOGRAPHY
HARALDSGADE 6
2200 COPENHAGEN N.
DENMARK

DIRECTOR OF NAVAL
OCEANOGRAPHY & METEOROLOGY
LACON HOUSE, THEOBOLD ROAD
LONDON WC1X8RY, ENGLAND

METEORO. OFFICE LIBRARY
LONDON ROAD
BRACKNELL, BERKSHIRE
RG 12 1SZ, ENGLAND

MINISTRY OF DEFENCE
NAVY DEPARTMENT
ADMIRALTY RESEARCH LAB
TEDDINGTON, MIDDX
ENGLAND

COMMANDER IN CHIEF FLEET
ATTN: STAFF METEOROLOGIST &
OCEANOGRAPHY OFFICER
NORTHWOOD, MIDDLESEX HA6 3HP
ENGLAND

LIBRARY
FINNISH METEORO. INSTI.
BOX 503
SF-00101 HELSINKI 10
FINLAND

SERVICE HYDROGRAPHIQUE ET
OCEANOGRAPHIQUE DE LA MARINE
ESTABLISSEMENT PRINCIPAL
RUE DU CHATELLIER, B.P. 426
29275 - BREST CEDEX, FRANCE

DIRECTION DE LA METEOROLOGIE
ATTN: J. DETTWILLER, MN/RE
77 RUE DE SEVRES
92106 BOULOGNE-BILLANCOURT
CEDEX, FRANCE

EUROPEAN SPACE AGENCY
18, AVENUE EDOUARD BELIN
31055 TOULOUSE, CEDEX
FRANCE

DIRECTOR, METEOROLOGIE INST.
ZENTRALEINRICHTUNG 2 DER
FREIEN UNIVERSITAT BERLIN
BIBLIOTHEK, PODBIELSKIALLE 62
1000 BERLIN 33
FEDERAL REPUBLIC OF GERMANY

EUROPEAN SPACE OPERATIONS
ATTN: DR. J. MORGAN, METEO.
SAT. DATA, MANAGEMENT DEPT.
R. BOSCH STR 5 D61 DARMSTADT
FEDERAL REPUBLIC OF GERMANY

ICELANDIC MET. OFFICE
BUSTAOAVEGUR 9
105 REYKJAVIK, ICELAND

DIRECTOR, SWEDISH METEORO. &
HYDROLOGICAL INSTITUTE
P.O. BOX 923
S-601, 19 NORRKOPING
SWEDEN

DR. OLA JOHANNESSEN (3)
NANSEN REMOTE SENSING CENTER
EDVARD GRIEGSVEI 3A
5037 SOLHEIMSVIK, NORWAY